UNIVERSIDADE DE LISBOA

FACULDADE DE MEDICINA VETERINÁRIA

# DEVELOPMENT OF NOVEL ANTIBODY-DRUG CONJUGATED MOLECULES FOR TREATMENT OF B-CELL MALIGNANCIES

ANA FILIPA SANTOS ANDRÉ

Orientadores: Professor Doutor Frederico Nuno Castanheira Aires da Silva

Professor Doutor Luis Manuel Morgado Tavares
Professor Doutor João Manuel Braz Gonçalves

Tese especialmente elaborada para obtenção do grau de Doutor em Ciências Veterinárias na especialidade de Ciências Biológicas e Biomédicas

2023

UNIVERSIDADE DE LISBOA

FACULDADE DE MEDICINA VETERINÁRIA

# DEVELOPMENT OF NOVEL ANTIBODY-DRUG CONJUGATED MOLECULES FOR TREATMENT OF B-CELL MALIGNANCIES

ANA FILIPA SANTOS ANDRÉ

Orientadores: Professor Doutor Frederico Nuno Castanheira Aires da Silva

Professor Doutor Luis Manuel Morgado Tavares

Professor Doutor João Manuel Braz Gonçalves

Tese especialmente elaborada para obtenção do grau de Doutor em Ciências Veterinárias na especialidade de Ciências Biológicas e Biomédicas

Júri

Presidente: Professor Doutor Luís Filipe Lopes da Costa
Vogais:
- Professora Doutora Ana Colette Pereira de Castro Osório Maurício
- Professor Doutor João Nuno Sereno de Almeida Moreira
- Professor Doutor António José de Freitas Duarte
- Professor Doutor Frederico Nuno Castanheira Aires da Silva

2023

## DECLARAÇÃO RELATIVA ÀS CONDIÇÕES DE REPRODUÇÃO DA TESE

Nome: Ana Filipa Santos André

Título da Tese ou Dissertação: Development of novel antibody-drug conjugated molecules for treatment of B-cell maligancies

Ano de conclusão (indicar o da data da realização das provas públicas): 2023

Designação do curso de Mestrado ou de Doutoramento: Doutoramento em Ciências Veterinárias

Área científica em que melhor se enquadra (assinale uma):

☐ Clínica ☐ Produção Animal e Segurança Alimentar

☐ Morfologia e Função ☒ Sanidade Animal

Declaro sobre compromisso de honra que a tese ou dissertação agora entregue corresponde à que foi aprovada pelo júri constituído pela Faculdade de Medicina Veterinária da ULISBOA.

Declaro que concedo à Faculdade de Medicina Veterinária e aos seus agentes uma licença não-exclusiva para arquivar e tornar acessível, nomeadamente através do seu repositório institucional, nas condições abaixo indicadas, a minha tese ou dissertação, no todo ou em parte, em suporte digital.

Declaro que autorizo a Faculdade de Medicina Veterinária a arquivar mais de uma cópia da tese ou dissertação e a, sem alterar o seu conteúdo, converter o documento entregue, para qualquer formato de ficheiro, meio ou suporte, para efeitos de preservação e acesso.

Retenho todos os direitos de autor relativos à tese ou dissertação, e o direito de a usar em trabalhos futuros (como artigos ou livros).

Concordo que a minha tese ou dissertação seja colocada no repositório da Faculdade de Medicina Veterinária com o seguinte estatuto (assinale um):

1. ☐ Disponibilização imediata do conjunto do trabalho para acesso mundial;
2. ☒ Disponibilização do conjunto do trabalho para acesso exclusivo na Faculdade de Medicina Veterinária durante o período de ☒ 6 meses, ☐ 12 meses, sendo que após o tempo assinalado autorizo o acesso mundial*;

*Motivo: Proteção de propriedade industrial.

Nos exemplares das dissertações de mestrado ou teses de doutoramento entregues para a prestação de provas na Universidade e dos quais é obrigatoriamente enviado um exemplar para depósito na Biblioteca da Faculdade de Medicina Veterinária da Universidade de Lisboa deve constar uma das seguintes declarações (incluir apenas uma das três):

1. É AUTORIZADA A REPRODUÇÃO INTEGRAL DESTA TESE/TRABALHO APENAS PARA EFEITOS DE INVESTIGAÇÃO, MEDIANTE DECLARAÇÃO ESCRITA DO INTERESSADO, QUE A TAL SE COMPROMETE.
2. É AUTORIZADA A REPRODUÇÃO PARCIAL DESTA TESE/TRABALHO (indicar, caso tal seja necessário, nº máximo de páginas, ilustrações, gráficos, etc.) APENAS PARA EFEITOS DE INVESTIGAÇÃO, MEDIANTE DECLARAÇÃO ESCRITA DO INTERESSADO, QUE A TAL SE COMPROMETE.
3. DE ACORDO COM A LEGISLAÇÃO EM VIGOR, (indicar, caso tal seja necessário, nº máximo de páginas, ilustrações, gráficos, etc.) NÃO É PERMITIDA A REPRODUÇÃO DE QUALQUER PARTE DESTA TESE/TRABALHO.

Faculdade de Medicina Veterinária da Universidade de Lisboa, 3 de novembro de 2023

Assinatura: Ana Filipa Santos André Aires da Silva

*O caminho mais fácil pode ser mais rápido.*

*Ainda assim, não te levará onde realmente mereces estar.*

## Acknowledgements

Agradece a quem te faz bem.
Muitas vezes, basta um sorriso, um raio de sol e um vai correr tudo bem.
Obrigada a todos os que para mim foram um raio de sol nesta jornada. Por vezes, as nuvens teimavam em espreitar, mas havia sempre uma luz que espreitava e gritava “vai tudo correr bem”. Obrigada a todas essas vozes, que se tornaram essenciais para o término desta etapa e que muitas delas vou levar para a vida.

Ao meu orientador, o Prof. Doutor Frederico Aires da Silva, por tornar possível toda esta jornada, por acreditar em mim e por nunca desistir. Por me ter mostrado que podemos ir sempre mais longe, que nos podemos desafiar e sair da nossa zona de conforto. Acredite, levo tudo o que aprendi não só para a ciência, mas também para a vida. Obrigada por tudo.

Ao Prof. Doutor Luís Tavares, por me acompanhar nesta jornada. Obrigada por demonstrar sempre interesse pelo meu trabalho, pelas suas palavras sempre simpáticas e encorajadoras, por ser sempre alguém em que pude confiar e pelo seu conhecimento valioso que enriqueceu em muito o meu trabalho.

Ao Prof. Doutor João Gonçalves por me acompanhar nesta jornada, pelas suas contribuições e partilha de conhecimentos.

À Doutora Joana Dias, a minha companheira no linfoma. Obrigada por confiares em mim para entregares o teu trabalho e por todo o teu apoio para que chegássemos ao fim. Obrigada pela tua amizade, pelo teu suporte nos momentos mais difíceis e por me compreenderes tão bem. Muito também é teu. Foste essencial, não só para o trabalho, mas como uma colega e amiga que todos gostariam de ter. Obrigada por tanto.

À Doutora Sandra Aguiar, a colega e amiga que todos merecem ter. Obrigada por cada palavra e por cada incentivo. Obrigada por me teres acompanhado ao longo destes anos, como muito mais do que uma colega, uma amiga. Irei sempre lembrar todas as conversas e momentos em que me empurraste para a frente, quando tudo parecia que não tinha solução. Obrigada por teres cruzado meu caminho.

Às minhas colegas e amigas que me acompanharam dia após dia no laboratório: Isa, Magda, Sara, Marta, Ana Leonardo.

À Isa. Sabes bem o quanto foste e continuas a ser importante nesta caminhada. Guardo comigo todas as conversas e desabafos ao longo destes anos. Tenho um orgulho imenso na pessoa em que te tornaste e mais orgulho ainda porque crescemos juntas. Tenho a certeza que te levarei para a vida. Ficarei ansiosamente à espera pela tua vez de brilhar, mereces muito.
À Magda, obrigada sempre pela tua boa disposição e por todas as partilhas que tivemos nestes anos. Sem dúvida que os meus dias ficaram melhores contigo.
À Sara, a minha eterna colega e amiga de biotério. Obrigada por toda a ajuda, pela tua companhia e palavras de incentivo sempre certeiras.
À Marta e Ana, obrigada por todos os momentos que passámos juntas, por toda a entreajuda e partilha.

A todos os alunos que passaram pelo laboratório e que contribuíram, não só para o meu trabalho, mas também para o meu crescimento: Isabel Parreira, Joana Loureiro, Fabiana Marques, entre outros – obrigada pelo vosso empenho e dedicação.

Aos professores e colaboradores da FMV, obrigada a todos que se cruzaram comigo nos últimos anos. Todos fizeram parte dos meus dias e, com certeza, conseguiram torná-los melhores. Em especial à Prof. Doutora Berta São Braz, à Andreia Grilo, à Inês Dias e ao Doutor Pedro Bule, por terem facilitado o meu trabalho e ajudado sempre que necessário.
A todos os meus colegas de doutoramento, por todo o apoio, palavras amigas e por acreditarem sempre que chegaríamos a bom porto. Obrigada por me acompanharem e mostrarem que não estava sozinha.

A todos os colaboradores no ITN, à Doutora Lurdes e Doutor João Galamba, por toda a dedicação e empenho em ajudar em todos os trabalhos e por terem contribuído com o vosso melhor conhecimento, sempre com uma palavra de incentivo. A todos os colaboradores no IMM, obrigada por todo o apoio nos ensaios. Marco, obrigada por todas as tuas palavras e empenho. Aos colaboradores da faculdade de farmácia: Joana Carvalho, Manuela Gaspar, Cecília Rodrigues, Joana Amaral – obrigada pela vossa contribuição. Joana Carvalho, obrigada pelas tuas partilhas e pelo teu empenho para conseguirmos juntas desenvolver uma nova molécula. Aos colaboradores na FCUL, obrigada por todo o vosso conhecimento e trabalho.

Para terminar, aqueles que me acompanham desde sempre: família e amigos que também são família.

À Ana Cachucho e Liliana, de colegas de praxe a amigas de sempre. Ana, sabes que agora é até velhinhas e por muitos agradecimentos que escrevesse ias sempre lá estar. Obrigada por nunca me deixares baixar os braços. Sei que me compreendes e isso faz-me sentir que não estou sozinha. Obrigada por seres a amiga que és. E que as nossas aventuras continuem para além de muitos PhDs. Obrigada por estares sempre lá, na ciência e na vida. Liliana, obrigada por todas as conversas filosóficas pela noite dentro. Por seres sempre uma pessoa tão apaixonada por aquilo que faz e por, com isso, me motivares também a ser sempre melhor. Continua no teu caminho, a ciência precisa de ti e nós também. Meninas, nem a distância nos separa, no Algarve, na Suiça ou em Lisboa, levo-vos para a vida.
À Margarida, a minha amiga de sempre. Que me viu crescer e que sei que tem tanto orgulho em mim como eu tenho nela. Obrigada por me mostrares diferentes perspetivas da vida e que o mais importante é sermos felizes.

À minha mãe, por seres tudo e ainda mais. Foi por mim que o fiz, mas também por Ti. Obrigada por seres um exemplo de força e determinação. Por nunca desistires apesar das adversidades e que, com o teu exemplo, me ensinares a fazer o mesmo. Serás sempre uma inspiração e irei continuar sempre, por mim, mas também por Ti. Obrigada por seres assim como és.

À minha irmã, por tudo o que és. És a minha inspiração, que me faz querer sempre superar tudo e fazer sempre um pouco mais. Obrigada por estares sempre ao meu lado, mesmo nos dias menos bons. Sem ti, não teria conseguido. Foste muitas vezes o meu chão e, com isso, consegui manter os pés firmes. És um raio de sol na minha vida. Obrigada por seres luz e iluminares sempre o meu caminho.

Ao meu Filipe, por tudo o que me dás, sem querer nada em troca. Obrigada por seres amor, por seres amigo, por estares sempre lá, mesmo nos momentos mais difíceis. Obrigada por seres o meu Irish man. Sei que sem ti não teria chegado ao fim. Obrigada por permaneceres sempre e por teres esperado por mim, mesmo quando para ti isso exigia um esforço sobre-humano. Sei que contigo ao lado podemos vencer o mundo, por isso isto será apenas o início do que o universo tem reservado para nós. Vamos juntos?

Aos meus avós Zea e Fernando, exemplos de força, determinação e persistência. Avó, obrigada por sempre me incentivares a ir mais longe e por acreditares em mim. Avô, obrigada por seres um grande exemplo e por tudo o que construíste.

Aos meus tios e ao meu primo, por serem a minha família em Lisboa. Por estarem sempre lá em cada conversa, em cada jantar. Por me fazerem sentir em casa. Por me fazerem sentir

que teria sempre um sítio para onde voltar. Obrigada e voltarei sempre para vos ver e para jantar sempre mais uma vez.

Ao meu pai e família, por me incentivar a ser sempre melhor e a não desistir, apesar de todas as adversidades. Sei que queres o meu melhor e agradeço-te por isso. Obrigada por me ensinares o melhor que sabias e por, com isso, me fazeres crescer.

Não olhes para trás.
Porque o passado já lá foi.
E o futuro depende de ti agora.
Por isso, sê o teu presente.

## Funding

This work was supported by the Portuguese Funding Agency, Fundacão para a Ciência e Tecnologia, FCT IP (SAICT/2017/32085, PTDC/QUI-OUT/3989/2021 and Ph.D. fellowship SFRH/BD/131468/2017.

Gilead has provided support through Project Gilead GÉNESE PGG-050-2019.

CIISA has provided support through Project UIDB/00276/2020, funded by FCT and AL4Animals provided support through project LA/P/0059/2020, funded by FCT.

**Resumo: Desenvolvimento de novos anticorpos conjugados a fármacos para o tratamento de tumores de células B**

O cancro é umas das principais causas de morte e espera-se que os números continuem a crescer. Os cães são também muito afetados pelo cancro, sendo o linfoma não-Hodgkin um dos tipos de tumores hematológicos mais comuns em ambas as espécies. Devido às suas semelhanças, os cães são considerados um excelente modelo para acelerar a translação dos tratamentos para os humanos. Nas últimas décadas, os anticorpos monoclonais modificaram o tratamento na área do cancro trazendo-lhe especificidade. Contudo, a maioria dos anticorpos monoclonais não possuem por si só eficácia clínica e são atualmente utilizados em combinação com a quimioterapia. Assim, existe uma urgente necessidade de melhorar os tratamentos convencionais, que têm inúmeros efeitos adversos. Tendo isto em conta, e usando as vantagens promissoras dos anticorpos de pequeno domínio de coelho, tínhamos como objetivo criar uma plataforma para desenvolver novos sistemas de entrega de fármacos usando estes anticorpos para o tratamento de linfoma não-Hodgkin, usando o cão como modelo. Para isso, explorámos três tipos diferentes de sistemas: os anticorpos conjugados a fármacos, as imunotoxinas e os imunolipossomas. Para o desenvolvimento do anticorpo conjugado a fármaco, explorámos o potencial dos anticorpos de pequeno domínio de coelho para conjugar seletivamente com o fármaco através da cisteína 80. Para isso, selecionámos uma biblioteca de anticorpos contra recetores de linfoma canino de células B através de Phage display. Depois, o anticorpo VL que apresentava melhores características foi conjugado seletivamente com o fármaco SN-38 através da cisteína 80, obtendo a molécula C5-DAB-SN-38. Este trabalho validou uma plataforma para o desenvolvimento de novos anticorpos conjugados a fármacos que combinam os benefícios dos anticorpos de pequeno domínio de coelho com as vantagens do modelo canino de linfoma. Para além disso, este anticorpo foi também utilizado para desenvolver uma nova imunotoxina para o tratamento de linfoma canino de células B. Para isso, o anticorpo VL foi conjugado com a toxina PE38 e foi testado em células de linfoma canino de células B e no modelo murino xenografo. Este estudo validou as imunotoxinas como um potencial tratamento para o linfoma canino. Por fim, tínhamos como objetivo desenvolver um lipossoma para linfoma canino usando o Panobinostat, utilizando uma formulação com e sem folato. Ambas as formulações foram avaliadas em células de linfoma canino, validando os lipossomas como um tratamento eficaz para o linfoma canino. No futuro, o nosso objetivo é conjugar o anticorpo VL com o lipossoma para obter um imunolipossoma para linfoma canino de células B. Concluindo, todo o trabalho desenvolvido contribuiu para compreender a importância do uso do cão como modelo, e como estes animais podem contribuir para a translação clínica na área da imuno-oncologia.

**Palavras-chave:** anticorpos de pequeno domínio, linfoma, anticorpos conjugados a fármacos, imunotoxinas, imunolipossomas.

**Abstract: Development of novel antibody-drug conjugated molecules for treatment of B-cell malignancies**

Cancer is one of the leading causes of death worldwide, and is expected to continue increasing, with a projected 28.4 million cases by 2040. Dogs are also significantly affected by cancer, including NHL, which is one of the most common hematological malignancies in both species. Dogs are considered excellent models to accelerate the translation of treatments for human patients due to their similarities with humans. While immunotherapies, particularly monoclonal antibodies (mAbs), have brought specificity to cancer therapies, they are still mostly used in combination with conventional chemotherapy, which remains the standard of care for both species. However, conventional treatments still do not fully cure and have numerous adverse effects, highlighting the need for further improvement. To address this need, using the promising advantages of rabbit-derived sdAbs, we aimed to develop a platform for a novel sdAb drug delivery system for NHL treatment using the dog as an animal model. For this purpose, we explored three different drug delivery methods: ADCs, immunotoxins and immunoliposomes. For the development of ADC, we explored the potential of rabbit derived single-domain antibodies (sdAb) to selectively conjugate a payload towards cysteine at position 80. First, a rabbit-derived sdAb library against canine B-cell lymphoma receptors was subjected to *in vitro* and *in vivo* phage display. Then, VL sdAb that specifically targeted canine lymphoma cells *in vitro* and presented a good tumor uptake was selected for SN-38 site-selective payload conjugation via its Cys80 and generated a stable and homogeneous C5-DAB-SN-38. This study validated a platform to develop novel ADCs that combine rabbit sdAbs benefits with the advantages of canine lymphoma model. Furthermore, this previously characterized and validated VL sdAb was also used to develop a new immunotoxin for the treatment of canine B-cell lymphoma. For that purpose, VL sdAb was conjugated with the PE38 toxin truncated form and tested *in vitro* in a canine B-cell lymphoma cells and in *in vivo* in a xenograft mouse model of canine lymphoma. This study validated immunotoxins as a potential treatment for canine lymphoma. Lastly, to validate a new liposome for canine lymphoma, we aimed to develop a liposome-based nanocarrier for panobinostat, using folate-targeted and non-targeted formulations. Both formulations were evaluated in canine lymphoma cells, validating liposomes as an effective treatment for canine lymphoma. In the future, our goal is to conjugate our VL sdAb to the liposome to obtain an immunoliposome for canine B-cell lymphoma. In conclusion, all the work developed contributed to the understanding of the importance of using the dog as a model and how these animals can contribute for clinical translation in the immune-oncology field.

**Keywords:** single-domain antibodies, lymphoma, antibody-drug conjugates, immunotoxins, immunoliposomes

## Resumo alargado: Desenvolvimento de novos anticorpos conjugados a fármacos para o tratamento de tumores de células B

O cancro é umas das principais causas de morte, sendo já considerado um grave problema de saúde pública. Apesar dos números parecerem bastante elevados, espera-se que nos próximos anos continuem a aumentar. Os cães são também muito afetados pelo cancro, sendo o linfoma não-Hodgkin um dos tipos de tumores hematológicos mais comuns em ambas as espécies. Devido às semelhanças histopatológicas, genéticas, moleculares e clínicas desta doença em ambas as espécies, os cães são considerados um excelente modelo para acelerar a translação dos tratamentos para os humanos. Estas semelhanças, fazem com que as modalidades de tratamentos utilizadas e a sua resposta também seja bastante idêntica em ambas as espécies. Atualmente o tratamento mais recorrente é a quimioterapia, com toda a toxicidade que lhe está associada, provocando severos efeitos secundários nos pacientes. No entanto, nas últimas décadas, os anticorpos monoclonais modificaram o tratamento na área do cancro trazendo-lhe especificidade. Contudo, a maioria dos anticorpos monoclonais não possuem por si só eficácia clínica e são atualmente utilizados em combinação com a quimioterapia. Assim, existe uma urgente necessidade de melhorar os tratamentos convencionais, que têm inúmeros efeitos adversos. Tendo isto em conta, e usando as vantagens promissoras dos anticorpos de pequeno domínio de coelho, tínhamos como objetivo criar uma plataforma para desenvolver novos sistemas de entrega de fármacos usando estes anticorpos para o tratamento de linfoma não-Hodgkin, usando o cão como modelo. Para isso, explorámos três tipos diferentes de sistemas: os anticorpos conjugados a fármacos, as imunotoxinas e os imunolipossomas. Para o desenvolvimento do anticorpo conjugado a fármaco, explorámos o potencial dos anticorpos de pequeno domínio de coelho para conjugar seletivamente com o fármaco através da cisteína 80. Para isso, começámos por imunizar um coelho branco fêmea New Zealand, com células primárias de linfonodo de cães com linfoma canino muticêntrico, pertencentes ao biobanco anteriormente construído. Ao longo do tempo, fomos monitorizando a resposta imune do coelho através de ELISA e citometria de fluxo. Quando atingimos um título de anticorpos adequado, procedemos à eutanásia do coelho e à extração da medula óssea e do baço. A partir desses órgãos, fomos extrair o RNA, sintetizar cDNA e utilizá-lo para amplificar as cadeias variáveis leves (VL) com primers específicos para o efeito. Isto levou à construção de uma biblioteca imune altamente específica para linfoma canino. Posto isto, fomos selecionar esta biblioteca imune de anticorpos contra recetores de linfoma canino de células B através de Phage display. Para isto, utilizámos como alvo as células de linfoma canino (CLBL-1) e um modelo murino xenografo de linfoma canino. Ao longo das rondas de seleção, vimos um enriquecimento da população de fagos, demonstrando a especificidade da seleção efetuada. Em paralelo, fomos ainda efetuar uma análise por *next generation sequencing,* por forma a comparar as

populações de clones da biblioteca inicial com a população recolhida depois do phage display no modelo animal. Com esta análise foi possível comprovar que cada sequência de clones aparecia mais vezes representada no conjunto recolhido depois da seleção no modelo animal, comprovando, mais uma vez, o enriquecimento da população de clones que foi feito ao longo das rondas de seleção. Em seguida, fomos avaliar as características dos clones através de ELISA e de sequenciação, levando assim à escolha dos 3 melhores clones. Desses 3, o C5 VL foi o que apresentou as características mais vantajosas, principalmente em termos de produção, sendo o selecionado para prosseguir com a conjugação com o fármaco SN-38. Antes mesmo dessa conjugação, fomos avaliar as suas características específicas de ligação e internalização nas células de linfoma canino e ainda a sua biodistribuição no modelo xenografo de linfoma canino, comprovando a ligação e internalização nas células de linfoma canino e a captação tumoral de cerca de 1.5% aos 15 min. Em seguida, prosseguimos com a conjugação com o fármaco SN-38 através da cisteína 80, que comprovámos estar livre através da predição da estrutura tridimensional do C5. Esta conjugação foi feita utilizando uma sequência de diazaborinas altamente sensível à presença de espécies reativas de oxigénio, obtendo a molécula C5-DAB-SN-38 com um rácio de anticorpo e composto de 1. Por fim, o C5-DAB-SN-38 demonstrou ter um efeito citotóxico nas células de linfoma canino, através da inibição da enzima Topoisomerase I, tal como o SN-38 isolado. Este trabalho permitiu validar uma plataforma para o desenvolvimento de novos anticorpos conjugados a fármacos que combinam os benefícios dos anticorpos de pequeno domínio de coelho com as vantagens do modelo canino de linfoma. Para além disso, este anticorpo foi também utilizado para desenvolver uma nova imunotoxina para o tratamento de linfoma canino de células B. Para isso, o anticorpo C5 VL foi conjugado com a toxina PE38 utilizando métodos de fusão genética, através de uma sequência peptídica composta por serinas e glicinas conferindo flexibilidade à molécula. Em seguida, depois de expressar e purificar a imunotoxina C5-PE38, fomos avaliar as suas propriedades de ligação e internalização nas células, através de imunofluorescência e citometria de fluxo. Isto permitiu-nos comprovar a ligação da imunotoxina C5-PE38 às células CLBL-1 e ainda a internalização no seu citoplasma. Posto isto, prosseguimos com a avaliação da atividade citotóxica nas células de linfoma canino, permitindo comprovar essa atividade que atua de forma dose dependente com um IC50 de $9.5 \pm 0.04$ µg/mol. Em paralelo, fomos ainda comprovar o mecanismo de morte celular, através da inibição da síntese proteica por parte da imunotoxina C5-PE38. Por fim, efetuámos ensaios de biodistribuição, captação tumoral e de eficácia no modelo murino xenografo de linfoma canino. A imunotoxina C5-PE38 demonstrou uma captação tumoral de cerca de 2% aos 15 min e levou ainda à diminuição dos tumores em cerca de 76.2% e 92.3% com as doses 0.5 mg/kg e 1.5 mg/Kg, respetivamente. Estes resultados demonstraram a forte atividade anti tumoral da immunotoxina C5-PE38 no modelo murino xenografo de linfoma canino. Este

estudo permitiu ainda validar as imunotoxinas como um potencial tratamento para o linfoma canino. Por fim, tínhamos como objetivo desenvolver um lipossoma para linfoma canino usando o panobinostat, uma vez que esta é uma molécula muito promissora para o tratamento desta doença, mas apresenta uma elevada toxicidade. Para isso, utilizámos uma formulação com e sem folato. Em primeiro lugar, fomos avaliar as propriedades físico-químicas das formulações lipossomais, concluindo que todas possuíam as propriedades adequadas para serem utilizadas no nosso estudo. Em seguida, comprovámos a presença do recetor do folato nas células de linfoma canino através de *Western Blot*, utilizando extratos celulares, podendo assim ser usado como alvo neste estudo. Posto isto, fomos avaliar a citotoxicidade das formulações lipossomais nas células de linfoma canino e vimos que todas as formulações com folato apresentavam um efeito citotóxico nas células alvo, sendo que a formulação com folato apresentava uma citotoxicidade ligeiramente mais elevada. No sentido de avaliar o mecanismo de ação dos lipossomas com panobinostat na morte das células de linfoma canino, fomos avaliar o estado de acetilação das histonas dos extratos celulares na presença dos lipossomas com o panobinostat. Através de *Western Blot*, conseguimos verificar que todas as formulações lipossomais contendo o panobinostat induziam a acetilação das histonas nos extratos celulares. De forma a comprovar a apoptose como mecanismo principal de morte celular, fizemos ainda a análise da atividade das caspases 3/7, sendo esta atividade promovida de uma forma dose dependente na presença das formulações com panobinostat, o que comprova a apoptose na presença dos lipossomas com panobinostat. Seguidamente, a captação das formulações lipossomais pelas células de linfoma canino foi também testada através de citometria de fluxo e imunofluorescência. Estes dados permitiram-nos provar a ligação dos lipossomas às células de linfoma canino e ainda a sua internalização no citoplasma destas mesmas células. A ligação e a internalização nas células de linfoma canino provou-se que era mais elevada na presença dos lipossomas com o folato. Por fim, estudos de biodistribuição e de captação tumoral foram efetuados em ratinhos CD1 e SCID, respetivamente. Ambas as formulações lipossomais, com e sem folato, apresentaram um perfil de biodistribruição bastante idêntico com a sua eliminação dos principais órgãos rapidamente. Relativamente à captação tumoral, vimos que a formulação lipossomal com o folato acumulava mais nos tumores do que a formulação sem o folato, sendo que essa acumulação foi 1.6 vezes mais elevada às 24 h (2.2 ± 0.9% ID/g de tumor) do que na formulação sem folato (1.32 ± 0.2% ID/g de tumor). No futuro, o nosso objetivo é conjugar o anticorpo C5 VL com o lipossoma para obter um imunolipossoma para linfoma canino de células B. Para concluir, este trabalho contribuiu para o desenvolvimento de nanotransportadores com panobinostat para o tratamento de linfoma canino.

Em suma, todo o trabalho desenvolvido contribuiu com três novas moléculas para o tratamento de linfoma canino. Isto demonstra, mais uma vez, a importância do uso do cão

como modelo, e como estes animais podem contribuir para a translação clínica na área da imuno-oncologia. Este trabalho é mais um exemplo de como o conceito de uma só saúde pode contribuir de forma eficaz para o tratamento não só do cancro, mas também de outras doenças que possam vir a ser graves problemas de saúde pública.

**Palavras-chave:** anticorpos de pequeno domínio, linfoma, anticorpos conjugados a fármacos, imunotoxinas, imunolipossomas.

This thesis was based on the following manuscripts and patents:

**Chapter 1:**

André AS, Moutinho I, Dias JNR, Aires-da-Silva F. 2022. In vivo Phage Display: A promising selection strategy for the improvement of antibody targeting and drug delivery properties. Frontiers in Microbiology. 13:962124. doi:10.3389/fmicb.2022.962124.

**Chapter 2:**

André AS, Dias JNR, Aguiar S, Nogueira S, Bule P, Carvalho JI, António JPM, Cavaco M, Neves V, Oliveira S, et al. 2023. Rabbit derived VL single-domains as promising scaffolds to generate antibody–drug conjugates. Scientific Reports. 13(1):4837. doi:10.1038/s41598-023-31568-x.

Aires-da-Silva F, Andre AS, Dias JNR, Aguiar SI, Oliveira S, Tavares L. Rabbit derived single-domain antibodies as promising scaffolds for the development of highly specific and potent antibody drug conjugates. Patente nacional submetida a 13/09/2021 com o No. 117461 V.

Aires-da-Silva F, Andre AS, Dias JNR. Aguiar SI, Oliveira S, Tavares L. Highly specific rabbit single-domain antibodies for drug delivery in immunotherapy applications. International Patent, PCT/IB2022/056303, 07 July 2022.

**Chapter 3:**

Ana S. André, Joana N.R. Dias, Isa Moutinho, Joana Loureiro, Sara Nogueira, Pedro Bule, Luís Marques, Rui Malhó, Lurdes Gano, João D.G. Correia, Jorge Correia, Solange Gil, João Gonçaves, Ira Pastan, Luís Tavares, Frederico Aires-da-Silva. Novel pseudomonas exotoxin A based rabbit-derived single-domain antibody immunotoxin for canine B-cell lymphoma treatment. (Manuscript under preparation)

**Chapter 4:**

André AS, Dias JNR, Aguiar SI, Leonardo A, Nogueira S, Amaral JD, Fernandes C, Gano L, Correia JDG, Cavaco M, et al. 2023. Panobinostat-loaded folate targeted liposomes as a promising drug delivery system for treatment of canine B-cell lymphoma. Frontiers in Veterinary Science. 10:1236136. doi:10.3389/fvets.2023.1236136.

## Index

Acknowledgements ..... iv

Funding ..... viii

Resumo: Desenvolvimento de novos anticorpos conjugados a fármacos para o tratamento de tumores de células B ..... ix

Abstract: Development of novel antibody-drug conjugated molecules for treatment of B-cell malignancies ..... x

Resumo alargado: Desenvolvimento de novos anticorpos conjugados a fármacos para o tratamento de tumores de células B ..... xi

List of figures and tables ..... xx

List of abreviations ..... xxii

Chapter 1: Bibliographic review and objectives ..... 1

1.1. Cancer: a public health problem ..... 1

1.2. Non-Hodgkin lymphoma: the most spread lymphoma ..... 4

1.3. Canine model of lymphoma as a tool of comparative medicine ..... 5

1.4. Canine lymphoma ..... 7

1.4.1. Etiology ..... 8

1.4.2. Diagnosis ..... 8

1.4.3. Staging ..... 9

1.4.4. Conventional treatment: Chemotherapy ..... 9

1.4.4.1. Radiation therapy ..... 10

1.5. Immunotherapies and drug delivery systems ..... 10

1.5.1. Antibodies ..... 12

1.5.1.1. Conventional Antibodies ..... 12

1.5.1.2. Antibody fragments and single-domain antibodies as promising scaffolds ..... 13

1.5.1.3. Selection and screening of recombinant antibodies ..... 17

1.5.1.3.1. Phage display: a powerful technique for antibody selection ..... 18

1.5.1.3.2. Antibody libraries: a tool to increase the odds ..... 20
1.5.1.3.3. *In vivo* phage display ..... 21
1.5.2. Antibody-drug conjugates as a promising therapeutic molecule for cancer ..... 22
1.5.3. Immunotoxins ..... 26
1.5.4. Immunoliposomes: a new approach for cancer drug delivery ..... 29
1.6. Aims and outline ..... 34
Chapter 2: Rabbit derived VL single-domains as promising scaffolds to generate antibody-drug conjugates ..... 36
2.1. Introduction ..... 37
2.2. Results ..... 40
2.2.1. Rabbit immunization, antibody library construction and phage display selection ..... 40
2.2.2. Screening for VL sdAb towards cNHL targeting ..... 42
2.2.3. Binding and internalization characterization of C5 VL sdAb ..... 44
2.2.4. Biodistribution studies of C5 VL sdAb ..... 46
2.2.5. Development of C5-DAB-SN-38 and evaluation of its activity on cNHL cells ..... 47
2.3. Discussion ..... 50
2.4. Materials and Methods ..... 54
2.4.1. Cell lines and culture ..... 54
2.4.2. Rabbit immunization and antibody library construction ..... 54
2.4.3. Characterization of rabbit immune response ..... 55
2.4.4. Phage display selection of VL sdAbs targeting cNHL ..... 55
2.4.5. Analysis of phage display enrichment by next generation sequencing and VL sdAb lead selection by ELISA ..... 56
2.4.6. Production and purification of VL sdAbs ..... 56
2.4.7. Immunofluorescence microscopy and Flow Cytometry of C5 ..... 57
2.4.8. Biodistribution studies and tumor targeting ..... 57
2.4.9. 3D VL sdAb structure prediction ..... 58
2.4.10. Synthesis and characterization of the Linker-Payload (DAB-SN-38) ..... 58
2.4.11. Bioconjugation of C5 with SN-38 ..... 58

2.4.12. Cytotoxic assay ..... 59
2.4.13. DNA-Topo I Activity Assay ..... 59
Chapter 3: Novel pseudomonas exotoxin A based rabbit-derived single-domain antibody immunotoxin for canine B cell lymphoma treatment ..... 60
3.1. Introduction ..... 61
3.2. Results ..... 63
3.2.1. Construction and expression of recombinant C5-PE38 immunotoxin ..... 63
3.2.2. Evaluation of binding and internalization of recombinant C5-PE38 immunotoxin ..... 63
3.2.2. Evaluation of cytotoxic activity on canine B-cell lymphoma cells ..... 64
3.2.3. Assessment of protein synthesis inhibition ..... 66
3.2.4. Biodistribution studies on CLBL-1 canine B-cell lymphoma xenograft model ..... 67
3.2.5. Assesment of *in vivo* effects on canine B-cell lymphoma ..... 68
3.3. Discussion ..... 69
3.4. Conclusions ..... 72
3.5. Material and Methods ..... 73
3.5.1. Cell culture ..... 73
3.5.2. Structure prediction, construction and expression of C5-PE38 ..... 73
3.5.3. Cell Elisa ..... 73
3.5.4. Immunofluorescence ..... 74
3.5.5. Cytotoxic Assay ..... 74
3.5.6. Evaluation of Protein Synthesis ..... 74
3.5.7. Biodistribution studies ..... 75
3.5.8. *In vivo* efficacy ..... 76
3.5.9. Histopathological analysis ..... 76
3.5.10. Immunohistochemistry analysis ..... 76
Chapter 4: Panobinostat-loaded folate targeted liposomes as a promising drug delivery system for treatment of canine B-cell Lymphoma ..... 77
4.1. Introduction ..... 78
4.3. Results ..... 81

4.3.1. Physicochemical properties of panobinostat loaded liposomes are suitable for drug delivery ..... 81
4.3.2. Folate receptor is expressed in canine lymphoma cells ..... 82
4.3.3. Panobinostat-loaded liposomes present cytotoxicity in canine B-cell lymphoma ..... 83
4.3.4. Panobinostat-loaded liposomes induce H3 histone acetylation and apoptosis 84
4.3.6. Uptake of liposome formulations in CLBL-1 cells ..... 85
4.3.7. Biodistribution studies in CD1 mice and xenograft mice model of canine B-cell lymphoma ..... 87
4.4. Discussion ..... 89
4.5. Materials and Methods ..... 93
4.5.1. Materials ..... 93
4.5.2. Liposome preparation ..... 93
4.5.3. Characterization of panobinostat liposomal formulations ..... 94
4.5.4. Cell line and culture ..... 95
4.5.5. Immunoblotting ..... 95
4.5.6. Cytotoxic Assay ..... 95
4.5.7. Evaluation of apoptotic cell death ..... 96
4.5.8. Cellular uptake by Immunofluorescence and flow cytometry ..... 96
4.5.9. Animals ..... 97
4.5.10. Preparation of $^{111}$In-Lipossomes ..... 97
4.5.11. Biodistribution Studies in CD1 mice ..... 98
4.5.12. Tumor induction, biodistribution and tumor targeting in SCID mice ..... 98
4.5.13. Histopathological analysis ..... 98
4.5.14 Immunohistochemistry analysis ..... 99
4.5.15. Statistical Analysis ..... 99
Chapter 5: Final Conclusions and Future Perspectives ..... 100
References ..... 107

## List of figures and tables

Figure 1 - Map ranking of cancer as a cause of death at ages under 70 years in 2019. ..... 1
Figure 2 - Distribution of cancer cases A) and deaths B) by World area in 2020 for both sexes. ..... 2
Figure 3 - Distribution of the number of new cases and deaths of cancer in 2020, for both sexes in Portugal. ..... 3
Figure 4 - Incidence and mortality of the 15th most common cancers in the world in 2020. ... 4
Figure 5 – Schematic representation of an IgG structure including CDRs and function.. .....13
Figure 6 - Schematic representation of conventional IgG antibody and different antibody fragments. .....15
Figure 7 - Representation of a rabbit IgG antibody. .....16
Figure 10 - Schematic representation of an ADC and its mechanism. .....23
Figure 11- Generations of immunotoxins. .....26
Figure 12 - Pseudomonas Exotoxin Structure. .....27
Figure 13 - Mechanism of action of IT with PE38. .....28
Figure 14 - Schematic representation of different types of liposomes. .....30
Figure 15 - Schematic representation of an immunoliposome and its mechanism. .....33
Figure 16- Goals of the thesis.....35
Figure 17- A) Representation of a rabbit IgG antibody. B) Representation of the antibody selection process.....40
Figure 18 - Characterization of rabbit immune response. .....42
Figure 19 - Phage display selection and screening for sdAb for cNHL targeting. .....44
Figure 20 - Binding and internalization characterization of C5 VL sdAb. .....45
Figure 21 - Biodistribution profile of $^{99Tm}$Tc-C5. .....46
Figure 22 - A) Ribbon representation of C5 sdAb's predicted 3D structure. B) a) High-resolution mass spectra of conjugate C5-DAB-SN-38. C) Bioconjugation of C5-DAB-SN-38. D) Oxidation and self-immolative mechanism of ROS-responsive diazaborine linker. .....48
Figure 23 - Evaluation of the DAR of C5-DAB-SN-38 by HPLC-MS.....49
Figure 24 - Cytotoxic effects of C5-DAB-SN-38. .....50
Figure 25 - Expression and Purification of C5-PE38. .....64
Figure 26 - Binding and internalization characterization of C5-PE38. .....65
Figure 27 - Evaluation of cytotoxic activity on canine B-cell lymphoma cells. .....66
Figure 28 - Assessment of protein synthesis inhibition. .....67
Figure 29 - Biodistribution studies. .....68
Figure 30 - Anti-tumoral activity of C5-PE38 on xenograft canine lymphoma models. .....69

Table 1 - Characterization of target and nontargeted liposomes loaded with and without panobinostat. ..... 82
Figure 31 - Evaluation of folate receptor expression and cytotoxic activity of folate-targeted and nontargeted liposomes loaded with panobinostat was evaluated in CLBL-1 cells. ..... 83
Figure 32 - Assessment of H3 Histone Acetylation. ..... 84
Figure 33 - Evaluation of Apoptotic cell death. ..... 85
Figure 34 - Evaluation of cellular uptake by flow cytometry and immunofluorescence. ..... 86
Figure 35 - Xenograft tumor section presenting a neoplasia, classified as high grade centroblastic diffuse malignant lymphoma. ..... 87
Table 2 - Biodistribution profiles of radiolabeled FA-PEG-Pan-Lip and PEG-Pan-Lip in healthy mice. ..... 88
Table 3 - Biodistribution of radiolabeled folate-targeted and nontargeted liposomes in xenograft mice model of cNHL. ..... 88

## List of abreviations

ADC Antibody Drug Conjugates

ADCC Antibody-dependent cytotoxicity

ADE Antibody-dependent enhancement

ADP Adenosine diphosphate

aTTP Acquired thrombotic thrombocytopenic purpura

CDC Complement-dependent cytotoxicity

CDR Complementary determining regions

cL Canine Lymphoma

DT Diphteria toxin

eEF2 Eukaryotic elongation factor 2

EMA European Medicines Agency

ER Endoplasmic reticulum

Fab Antigen-binding fragment

Fc Crystallizable Fragment

FcRn Neonatal Fc receptor

FDA Food and drug administration

HAMA Human anti-mouse antibody

HL Hodgkin Lymphoma

Igs Immunoglobulins

LUV large unilamellar vesicles

mAb Monoclonal Antibody

MLV Multilamellar vesicles

NHL Non- Hodgkin Lymphoma

PA Phosphatic acid

PC Phosphatidylcholine

PE Phosphatidylethanolamine

PE Pseudomonas Exotoxin

PEG Polyethylene glycol

PG Phosphatidylglycerol

PI Phosphatidylinositol

PS Phosphatidylserine

RES Reticuloendothelial system

scFv Single-chain variable fragment

sdAb Single-domain antibody

SUV Small unilamellar vesicles

ULV Unilamellar vesicles

USDA United States Department of Agriculture

VWF Von Willebrand factor

# Chapter 1

Bibliographic review and objectives

## 1.1. Cancer: a public health problem

Cancer is undoubtedly a huge public health problem worldwide, with millions of cases and deaths occurring annually. Nowadays, cancer is an important obstacle in increasing life expectancy in every country. Cancer is already considered, in 112 out of 183 countries, the second or even the leading cause of death under 70 years of age (Figure 1).

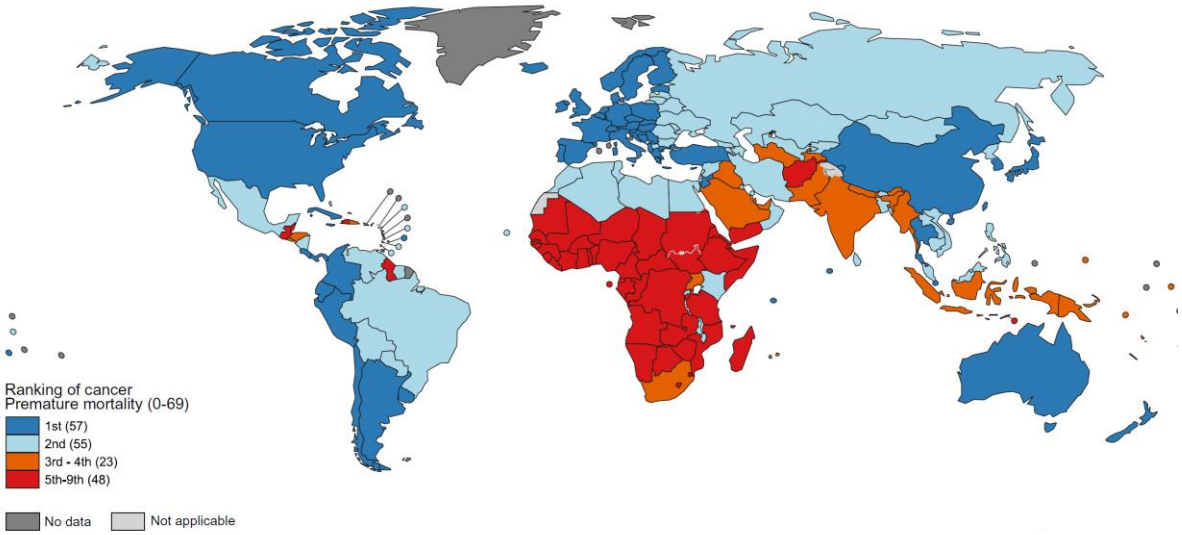


**Figure 1 - Map ranking of cancer as a cause of death at ages under 70 years in 2019.** Source: World Health Organization. Adapted from (Sung et al. 2021a).

Only in 2020, the estimated number of new cases worldwide was 19.3 million and almost 10 million of deaths caused by cancer (Figure 2). In many countries, cancer is already the leading cause of death, surpassing the mortality rates of stroke and coronary heart disease (Sung et al. 2021a).

Taking these numbers into account, today there is a 20% risk of getting cancer in a lifetime (under 75 years of age), and a 10% risk of dying from it. This means that 1 in 5 people will get cancer, and 1 in 10 will die from it (Ferlay et al. 2021).

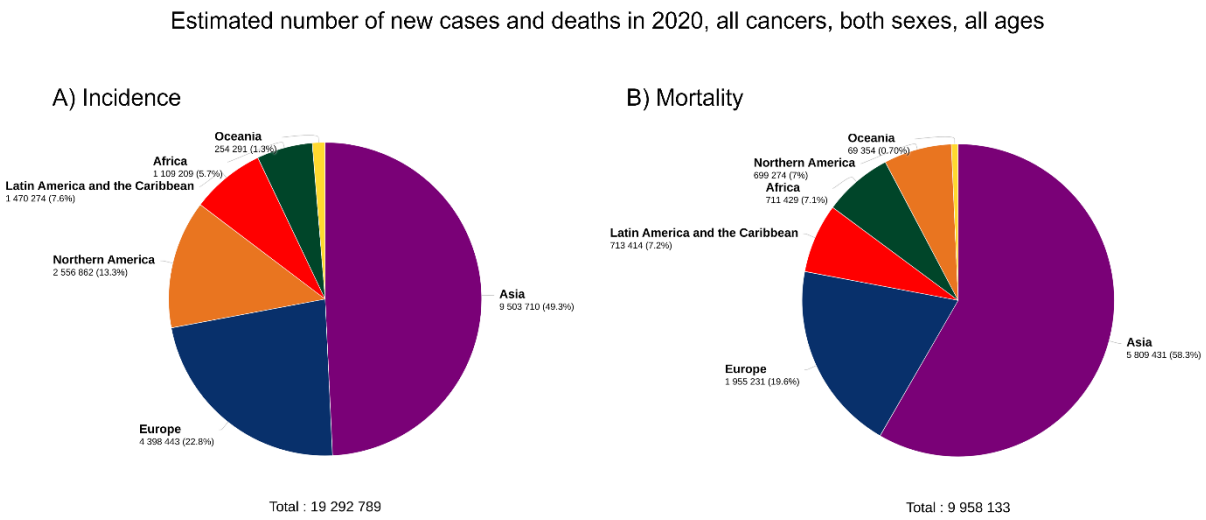


**Figure 2 - Distribution of cancer cases A) and deaths B) by World area in 2020 for both sexes.** Source: GLOBOCAN 2020. Graph production: Global cancer Observatory (http://gco.iarc.fr). Adapted from (Global Cancer Observatory: Cancer Today).

Globally, human breast cancer is nowadays the most commonly diagnosed type of cancer with around 2.3 million new cases (11.7%), followed by lung, colorectal, prostate and stomach cancers. Conversely, the most lethal is lung cancer with about 1.8 million deaths (18%). Lung cancer is followed by colorectal (9.4%), liver (8.3%), stomach and female breast (6.9%) cancers.

In Portugal, the numbers are also worrying with approximately 60.467 new cases of cancer and 30.168 deaths due to cancer in 2020 (Figure 3). The risk of developing cancer before 75 years of age is higher than the worldwide estimated risk of 25.7% for both sexes.

The risk of dying from cancer before 75 years of age is approximately 10.7%, which is very similar to the risk worldwide (Global Cancer Observatory: Cancer Today). Regarding cancer types incidences, colorectum cancer is the most common with around 10.501 cases (17.4%) followed by breast (11.6%), prostate (11.2%), lung (9%), and stomach (4.9%) cancers. In terms of mortality, the deathliest cancer is lung cancer with 4.797 deaths (15.9%) followed by colorectum (14.3%), stomach (7.7%), prostate (6.4%) and breast (6.2%) cancers.

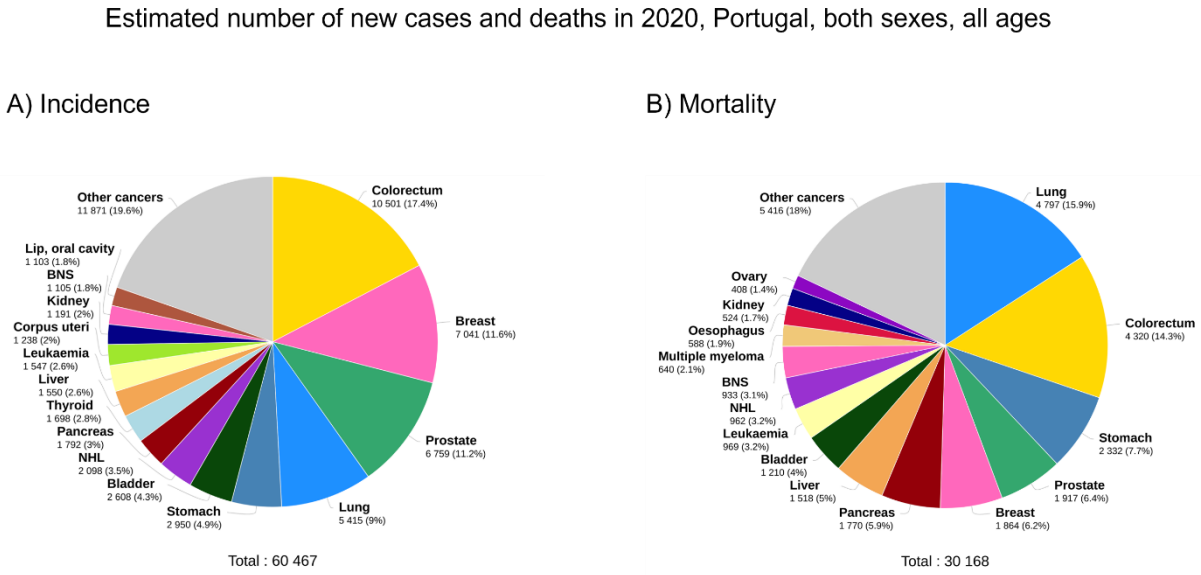


**Figure 3 - Distribution of the number of new cases and deaths of cancer in 2020, for both sexes in Portugal.** Source: GLOBOCAN 2020. Graph production: Global cancer Observatory (http://gco.iarc.fr). Adapted from (Global Cancer Observatory: Cancer Today).

Within all human cancer types worldwide, hematologic malignancies have two types represented in the top 15 of most common: non-Hodgkin lymphoma (NHL) and leukemia (Figure 4). In 2020, in terms of incidence of new cases, NHL was ranked eleventh, and leukemia, thirteenth. In Portugal, the numbers are similar but slightly higher. NHL and leukemia rank eighth and thirteenth in incidence, respectively. Regarding mortality, both worldwide as well as in Portugal, NHL and leukemia are part of the top 15.

Unfortunately, it is expected that the global cancer burden will continue to increase worldwide, rising to 28.4 million cases by 2040, representing an increase of 47% compared to 2020.

Overall, these numbers demonstrate that much needs to be done in order to improve treatments already on the market to diminish mortality rates mainly for cancers for which prevention strategies remain limited or unknown.

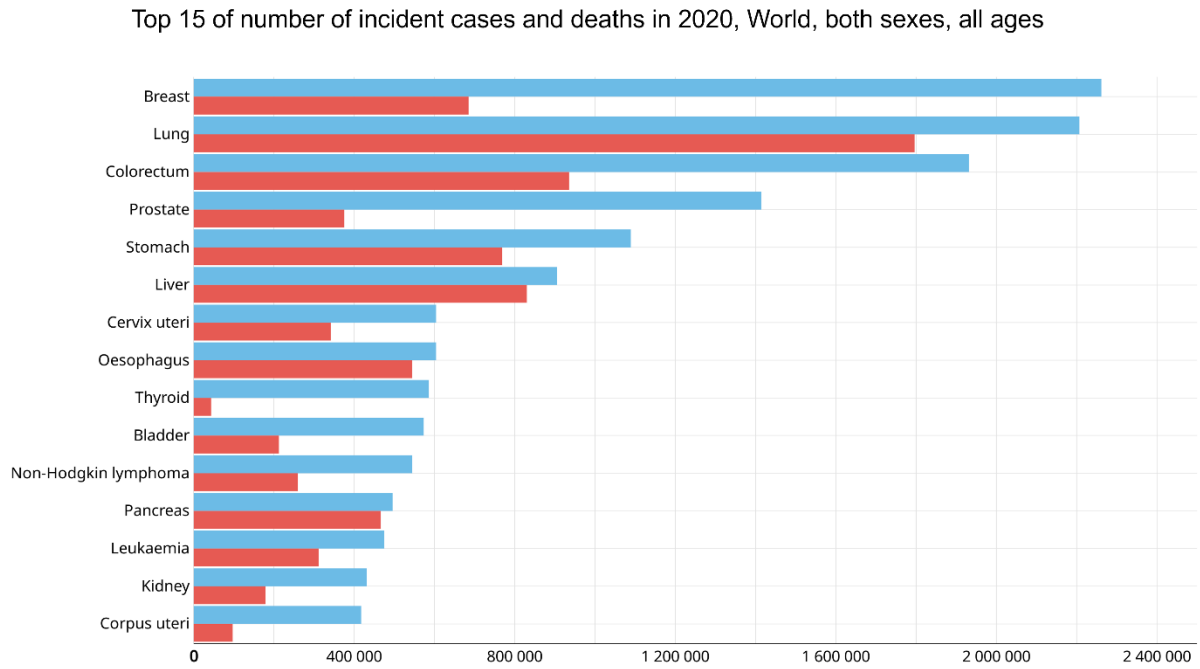


**Figure 4 - Incidence and mortality of the 15th most common cancers in the world in 2020.** Source: GLOBOCAN 2020. Graph production: Global cancer Observatory (http://gco.iarc.fr). Adapted from (Global Cancer Observatory: Cancer Today)

## 1.2. Non-Hodgkin lymphoma: the most spread lymphoma

Lymphomas are one of the most common malignancies arising from the lymphoreticular system. The two major subtypes of lymphomas are: Hodgkin lymphoma (HL) and non-Hodgkin lymphoma (NHL), which comprise approximately 90% of all lymphomas. Histologically, NHL can be differentiated from HL through the absence of Reed-Sternberg cells, that typically present CD15 and CD30 staining (Thandra et al. 2021). NHL include a vast range of cancers that arise from the clonal proliferation of lymphocytes subsets at different stages of maturation. About 85-90% arise from mature B lymphocytes; however, it can also arise from T or NK cells (Armitage et al. 2017).

There are almost 50 different types of human NHL. The most common are the follicular lymphoma (FL) and diffuse B-cell lymphoma (Thandra et al. 2021).

Genetic, epigenetic and other molecular alterations can be observed in the gene-expression profiles of nearly all non-Hodgkin lymphomas. In B-cell NHL, deregulated gene expression occurs due to balanced translocations that place key genes under the influence of active lineage-specific promoters or enhancers (Armitage et al. 2017).

Most of NHL's human patients present lymphadenopathy, and can present systemic symptoms such as fevers, drenching night sweats, weight loss, pruritis and fatigue. Since NHL can involve any organ, a wide range of symptoms is possible. Regarding diagnosis, it should be based on a biopsy sample, analyzed by an haematopathologist (Armitage et al. 2017).

In humans, B-cell lymphoma treatment has remained with the R-CHOP (Rituximab, Cyclophosphamide, Doxorubicin, Vincristine and Prednisone) protocol for decades. However, most of the patients experience high levels of toxicity with 30-40% of them still unresponsive or relapsing thereafter. Over the last 20 years, efforts have been made to improve the R-CHOP protocol, modifying the interval between cycles and adding new drugs, however without any success. More recently, new options have been considered in order to enhance the therapeutic outcome for relapsed and refractory B-cell lymphoma. One of them is the anti-CD19 chimeric antigen receptor T-cells (CAR-T) that is already being used as third-line therapy and second-line after R-CHOP. Other therapies such as the immunomodulator lenalidomide, the antibody-drug conjugate brentuximab and the BTK inhibitor ibrutinib have been improving the outcomes of patients, however, they still demonstrate high toxicity (Ayyappan and Maddocks 2019; Poletto et al. 2022).

### 1.3. Canine model of lymphoma as a tool of comparative medicine

In the last few years, comparative medicine has exploited the comparison of cancer for human and dog with the goal of advancing both human and animal health. This new field has been providing the opportunity for learning more about cancer as a whole disease across species. All of this benefits human and veterinary medicine by combining the findings in veterinary models to be used in novel therapies in humans. For B-cell lymphoma, the dog is one of the best models, surpassing many of the issues of rodent models.

Only a very small percentage of therapeutics that demonstrated to be efficacious in murine models displayed good results when applied to humans. This represents a huge and expensive waste of investment resources. Furthermore, murine models have many characteristics that are not appropriate for testing therapeutic potential candidates, such as insensitivity to chemotherapy-induced toxicity or even differences in the tumoral microenvironment that condition the responses to chemotherapy, radiotherapy and immunotherapy (Garden et al. 2018). Despite the mouse model being genetically homogeneous, which is critical and essential for the execution of the studies, it could also be a limitation of this animal model to study human diseases. Other issues include the differences in the environmental and microbiome factors between species that can affect the responses to cancer treatments, including immunotherapy. The use of laboratory models, such as the mouse, constitute a great drawback for translational immunotherapy. This is related with the fact that most models use immunocompromised mice for the xenograft's cells. This constitutes a huge disadvantage, as the elements of the immune system are not fully represented in these animals, making the study incomplete in terms of representing tumor-host interactions. One way to overcome this problem is to use humanized mice, since they share some components of the human hematopoietic and immune system. However, some essential components

continue to be missing, mainly the ones related with mimicking the ability to develop spontaneous cancers as in humans. The limitations of conventional models have uncovered a need for new animal models that could help to understand the responses in terms of efficacy and toxicity observed in human cancer patients (Park et al. 2016; Garden et al. 2018).

Numerous advantages are pointed out to spontaneous animal models such as dogs. Dogs are good pre-clinical models because they are larger than rodents, outbred, immunocompetent and can develop spontaneous tumors. Dogs are exposed to external and environmental factors, making them susceptible to various diseases that influence carcinogenesis and treatment efficacy of therapeutic agents. The heterogeneity of dogs makes them a closer model to study heterogeneity in human patients. The size of dogs is another important advantage that allows repeated biological sampling and imaging. Moreover, all biological processes are similar to those in humans.

Canine B-cell lymphoma and human NHL share many similarities in their clinical features, presentation and pathophysiology, making dogs an excellent model for studying disease progression and therapy (Marconato et al. 2013). The incidence of canine B-cell lymphoma of 15-30 / 100 000 is very similar to that of humans (Dias et al. 2021). Furthermore, dogs live in direct contact with humans, share similar environments, and are exposed to the same environment. In terms of disease, dogs spontaneously develop B-cell lymphoma like humans and have a heterogeneous genome comparable to humans. This spontaneously occurring cancer in dogs offers genetic diversity similar to that of human lymphoma, allowing the study of biological mechanisms, such as tumor initiation and promotion. Furthermore, the dog model allows for the recognition of many similarities between canine and human lymphomagenesis, for example, in identifying gene mutations common to both species (Richards and Suter 2015).

In terms of drug development, dogs have a longer life and are evolutionary closer to humans than murine models (Lindblad-Toh et al. 2005; Richards and Suter 2015). All of this, combined with fast disease progression, allows for earlier conclusions from clinical trials. Actually, only 1 to 3 years are required for clinical trials in pet dogs, in contrast to human clinical trials, which take about 15 years. This short period allows the integration of conclusions from dog clinical trials onto human trials, such as toxicity, response, pharmacodynamics, dose regimen, schedule, biomarkers and responding histology assessment (Marconato et al. 2013).

The final and most important reason for using dogs with lymphoma as animal model is the concept of a comparative research approach. This approach benefits both species, leading to representative advances in the treatment of B-cell lymphoma in humans and dogs. The culture of care and social status of dogs as companion animals, as well as being part of a family, allows them to benefit from a high-quality health care, promoting an increase in lifespan. This has created a new way of promoting the exploration of translational approaches, as well

as the need for novel cancer therapies in the veterinary field (Porrello et al. 2006; Henry and Bryan 2013; Richards and Suter 2015; Gardner et al. 2016).

However, some disadvantages can be listed, such as the difficulty in controlling variables and standardizing treatments, breed variability, limited standardized reagents, heterogeneous tumor biology and immune responses (Park et al. 2016).

Overall, comparative medicine and, in particular, the use of the dog as a model, offers a new perspective of developing new therapeutics in the veterinary field. This is especially important for pet dogs affected by lymphoma, as its incidence is largely high, and the existing treatments are rarely curative, increasing economic and emotional costs for the owners, as well as a lot of suffering for the pet dogs. In order to better understand, the next section will outline the characteristics of canine lymphoma (cL) and treatments already in use in more detail.

### 1.4. Canine lymphoma

Cancer is one of the deadliest diseases in companion animals, particularly dogs. Lymphomas comprise 7-24% of all canine neoplasias and are the most common hematopoietic malignancy in dogs, accounting for approximately 83% of the cases. The annual incidence is estimated to be between 13 and 114 per 100000 dogs at risk. The incidence of canine lymphoma has been increasing over the years.

Lymphoma can occur at any age, however, affects predominantly middle-aged to older dogs (median age of 6-9 years), with 1.5 per 100000 for dogs under 1 year of age, and 84 per 100000 for dogs 10 to 11 years old (Dorn et al. 1970; Merlo et al. 2008; Boerkamp et al. 2014; Vail et al. 2019).

It seemed that intact female dogs have a reduced risk of developing the disease, however, there is no apparent sex predisposition (Villamil et al. 2009; Zandvliet 2016).

Some breeds could have a higher incidence, such as boxers, bullmastiffs, basset hounds, St. Bernards, Scottish terriers, Airedales, Pitbulls, Briards, Irish setters, Rottweilers, and Bulldogs. With lower risk are included Dachshunds and Pomeranians (Priester and McKay 1980; Edwards et al. 2003; Ernst et al. 2016).

Canine lymphoma can present various clinical forms with different types, grades and sites. In the particular case of canine lymphoma, the most common form is the multicentric lymphoma. In this type of presentation, lymphoma affects the peripheral nodes. However, extra nodal forms can also exist, such as mediastinal, abdominal (gastrointestinal, hepatic, splenic, renal), cutaneous, ocular, central nervous system and pulmonary. About 75% of all canine lymphomas are multicentric, and according to the WHO, are classified into five stages (Ponce et al. 2010; Vezzali et al. 2010). Stages I and II are related with the lymph node infiltration: when limited to a single lymph node (stage I), or several lymph nodes (stage II). Stage III is

considered when a generalized, but non-painful, lymphadenopathy occurs. When the liver or spleen are involved, it represents stage IV, whereas blood and/or bone marrow involvement represent stage V. Moreover, a substage could be added using the suffix *a* and *b* indicating the absence or the presence of systemic signs such as fever, weight loss, or hypercalcemia (Zandvliet 2016).

### 1.4.1. Etiology

The etiology of canine lymphoma, although considered multifactorial, is widely unknown. However, it is known that some factors can contribute to increasing the risk of developing canine lymphoma.

In humans, some types of endemic lymphomas are associated with viral infections. For example, Burkitt lymphoma is associated with Epstein Barr Virus (EBV) infection. However, an infection with the malarial parasite *Plasmodium falciparum* is also necessary in order to develop lymphoma (Ferry 2006). The human T-lymphotropic viruses (HTLV) HTLV-I and HTLV-II were associated with forms of T-cell lymphoma (Müller et al. 2005).

In dogs, there are a few reports of a gamma herpes (Epstein Barr-like) virus associated with leukemia and lymphomas. Some reverse-transcriptase activity in supernatants of lymph node culture from dogs with lymphoma was also detected (Tomley et al. 1983; Chiou et al. 2005; Milman et al. 2011; Huang et al. 2012). Other studies using helicobacter infections in beagles also did not result in gastric lymphoma (Rossi et al. 1999). Nonetheless, due to the fact that experimental transmission was not verified and no evidence of transmissibility in canine lymphomas was shown, no significant viral etiology was associated with canine lymphomas.

In humans, immunosuppression or other immune disorders could influence the risk of developing lymphoma. With dogs, some cases of autoimmune diseases have been reported in dogs with lymphoma (Keller 1992). Moreover, there was a case reported of the development of lymphoma after a cyclosporine treatment (Blackwood et al. 2004). Alterations of the immune systems, like immune-mediated thrombocytopenia, can be also associated with higher risk of developing lymphoma in comparison to normal dogs (Keller 1992).

### 1.4.2. Diagnosis

Diagnosis of canine lymphoma routinely involves a complete physical examination, hematological and clinical chemistry profile, and in some cases, urinalysis is also performed (Gavazza et al. 2008). Bone marrow involvement is frequent, around 55%, and cannot be predicted from peripheral blood counts (Raskin and Krehbiel 1989; Martini et al. 2015). Bone marrow is analyzed through cytological examination of a single aspiration sample. The bone marrow involvement could also be detected by flow cytometry or core biopsy, however, these

techniques are not routinely performed in veterinary medicine (Aubry et al. 2014). Nevertheless, as the outcome of biopsy has limited effects on prognosis or treatment, and since it is a very invasive procedure, it is not recommended to perform it routinely (Vail et al. 2010).

Thoracic and abdominal radiographs are uniquely used as a possible differential diagnosis, however, they can display abnormalities (Blackwood et al. 1997).

### 1.4.3. Staging

To stage multicentric lymphoma it is essential to obtain a complete patient history, known as the substage. Physical examination (stages I-IV) and evaluation of peripheral blood and bone marrow are also required (stage V). Many other laboratory tests and diagnostic images can be used to improve staging. The more tests and techniques used, the better and more precise the staging will be, making it a better indicator for prognosis (Flory et al. 2007).

### 1.4.4. Conventional treatment: Chemotherapy

As canine lymphoma is naturally a systemic disease, chemotherapy is the treatment of choice. The majority of studies related with therapy use intermediate to high multicentric canine lymphoma, so this will be our focus. With chemotherapy, the goal is to obtain the maximum effect with minimal discomfort, drug administration and toxicity, and to reduce the stress caused on both animal and owner, as well as drug excretion in the owner's environment (Zandvliet 2016).

Contrary to humans, rituximab is not effective in dogs, thus the CHOP protocol is the standard for the treatment of high-grade canine lymphoma (Zandvliet 2016). Around 80% of the dogs have a complete response with CHOP protocol, however, the remission only lasts 6-11 months (Vail et al. 2019). Since it was noticed that remissions were frequent, protocols were adopted in two phases. Initially, a more intensive protocol was adopted to induce a complete remission called the induction phase, followed by a lifelong less intensive protocol with the aim of maintaining remission (maintenance phase). Later, it was verified that this kind of protocol does not offer treatment benefits, and the maintenance phase was diminished. A 6 month protocol is considered the standard care (Piek et al. 1999; Chun et al. 2000; Garrett et al. 2002), however, 12 (Simon et al. 2006) and 15 week protocols (Burton et al. 2013) have also been used and seemed to be effective. Other adjustments have been made such as increasing treatment intensity by increasing the number of drugs or drug doses, however, it only amplified adverse effects (Vaughan et al. 2007; Rassnick et al. 2010; Sorenmo et al. 2010).

The rescue protocol is implemented when the first-line protocol fails or when a subsequent relapse occurs. If the relapse occurs during the first-line protocol treatment, usually

it requires the use of an alternative drug. If the relapse occurs after the first-line protocol, the drug used before can also be included in the rescue protocol. These rescue protocols typically have worse outcomes, resulting in lower response rates, with shorter response times (2-3 months), and are more toxic than first-line protocols (Zandvliet 2016).

#### 1.4.4.1. Radiation therapy

Despite lymphoid cells being radiosensitive, the use of radiation therapy in the treatment of canine lymphoma is limited in the routine treatment also due to high costs and limitations related with equipment access.

Nevertheless, the use of radiation therapy in dogs with drug resistance lymphoma has been reported. In these cases, all peripheral lymph nodes were irradiated and the outcome was a complete remission with a median survival of 143 days (Zandvliet 2016).

To treat multicentric canine lymphoma, irradiation of the whole body is required, and can be performed in only one session, or in two separate sessions. Splitting in two separate sessions has less side effects and is preferable. Monotherapy with radiotherapy has also been described, however, the results were poor and adverse effects were common and severe in dogs in an advanced stage of the disease (Laing et al. 1989).

These poor outcomes highlight a common need for more specific and efficacious molecules for both species.

## 1.5. Immunotherapies and drug delivery systems

Regardless of all the advances achieved by chemotherapeutic protocols, they seem to have reached a plateau, where now it is mandatory to improve survival rates and the development of new methods of delivering or targeting traditional chemotherapeutic drugs, particularly the development of targeted immunotherapies.

Within immunotherapies, monoclonal antibodies (mAbs) emerged as a promising therapeutic tool to be used in a wide range of diseases. Since the approval of the first monoclonal antibody for human applications, the Orthoclone OKT3, by Emmons and Hunsicker in 1987 (Emmons and Hunsicker 1987), the use of mAbs have been widely spread in a wide variety of diseases and conditions. With personalized medicine rising, mAbs are positioned at the core of this forefront, paving the way for each patient's needs. Based on their success, the market size of mAbs has been continually growing, making them one of the top-selling drugs in the world.

For cancer, mAbs are the most commonly used and approved immunotherapies. The discovery of Rituximab, an antibody targeting the human surface antigen known as CD20, revolutionized the treatment of B-cell lymphoma (Motta et al. 2011; Ito et al. 2015). Rituximab

was the first FDA approved mAb for the treatment of human cancer, being used for B-cell NHL and acute lymphocytic leukemia subtypes (Maloney et al. 1994; Waldmann 2003; Chames et al. 2009). Regardless of Rituximab's crucial role in the treatment of B-cell malignancies in humans, its efficacy remains limited in canine lymphoma. It is known that CD20 is present in canine lymphoma, however Rituximab and other anti-human and anti-mouse antibodies able to recognize CD20 extracellular domains, failed to bind canine CD20, even though reported epitopes are conserved between human and canine CD20 (Jubala et al. 2005; Kano et al. 2005; Impellizeri et al. 2006).

Nowadays, there are more than 100 mAbs approved on the market for humans, but this number is expected to increase given the thousands of candidates that are under preclinical and clinical trials (Parray et al. 2020).

In the veterinary field, two monoclonal antibodies have been already approved. Lokivetmab was the first mAb to be approved for animals. In December 2016 the United States Department of Agriculture (USDA) approved Lokivetmab and a year later, in 2017, European Medicines Agency (EMA) approved it for the use in the European Union. Lokivetmab, also called Cytopoint, was developed for the treatment of atopic dermatitis in dogs. Frunevetmab, a felinized anti-nerve growth factor monoclonal antibody was the second monoclonal antibody approved by the EMA, in 2021. Later, in January of 2022, Frunevetmab, also called Solensia, was approved by the FDA for the treatment of pain from osteoarthritis in cats.

The approval of these molecules means that there is interest in investing in monoclonal antibodies in the veterinary field, making animals benefiting patients for this kind of therapeutics. All these advances raised other issues related with the fact that we are working in the veterinary field. Unfortunately, investment in the development of new treatment strategies for animals is limited when compared with humans, stimulating more affordable and easier to produce alternatives to the conventional ones. It is known that a conventional IgG, due to its structure and development, can achieve high economical costs, as well as time resources. Alternatively, antibody fragments, particularly single-domain antibodies, can be produced with significantly lower time and production costs. These fragments are the small portions that can be isolated from a full IgG and due to its reduced size, they are easily produced, with a lower economic cost associated. Single domain antibodies represent not only a possible alternative to the drawbacks of the conventional Antibody Drug Conjugates (ADCs), but also a promising scaffold to be used for the benefit of both humans and animals. The development of these recombinant antibody fragments and their applications will be described in detail in the next section.

### 1.5.1. Antibodies

#### 1.5.1.1. Conventional Antibodies

Antibodies, often known as immunoglobulins (Igs), are heterodimeric glycoproteins produced during the adaptive immune response by B cells. In mammals, antibodies are made up of two identical heavy chains (H) and two identical light chains (L) in a Y-shaped format. The L chain can be of the kappa (κ) or lamba (λ) subtypes and the H chain of the α, δ, ε,γ or μ isotypes. There are five different classes or isotypes of antibodies: IgA, IgD, IgE, IgG, and IgM. The different classes vary in sequence and length of the heavy-chain constant domains, each presenting a specific structure and role in immunological processes. Due to their characteristics, such as their prevalence in serum, importance for immune response and specificity, IgGs represent the most common isotype used in immunotherapy. In IgGs, the light chains are composed of a single constant (CL) and a variable domain (VL), whereas each heavy chain is made of three constant domains (CH1, CH2, and CH3) and one variable domain (VH). The variable domains located in the antibody N-terminus and the CL and CH1 regions constitute the antigen-binding fragment (Fab). The CH2 and CH3 domains are linked to the Fab region by a flexible sequence (hinge region), and forms the crystallizable fragment (Fc). The variable domains are essential for antibody specificity and affinity towards antigen, particularly through the three hypervariable loops known as complementary determining regions (CDRs). The antibody binding site is the result of the conformation of the VH and VL chain CDRs in six hypervariable loop structures (H1, H2, H3, L1, L2, L3) (Figure 5A). Four relatively conserved beta-sheet strands are also present on these domains, named framework sequences, that act as scaffolds for the support of CDR loops. In contrast, the Fc region is composed by constant domains and is related with the mediating antibody effector functions, namely antibody-dependent cytotoxicity (ADCC) and complement-dependent cytotoxicity (CDC) (Figure 5B) as well as binding to different Fc receptors in cells. Moreover, the antibody half-life is also related with the FC region via a recycling mechanism dependent on neonatal Fc receptor binding (FcRn) (Aires da Silva et al. 2008).

Monoclonal antibodies use different mechanisms to eliminate or neutralize the pathogenic disease or disease target. Two major types of actions can be developed by mAbs: they can directly and effectively block the activity of pathogens such as viruses neutralizing their entry into the target cells, or block the receptors expressed on tumor cells. They can also recruit a more general immune response via the boosting of the effector functions, such as ADCC and CDC responses (Aires da Silva et al. 2008; Chi et al. 2020).

In the ADCC response, after the antibody has recognized and attached to an antigen, the Fc domain engages Fc receptors (FcγRs) on the surface of effector cells such as macrophages and natural killer cells that mediate phagocytosis or lysis of the target antigen.

In CDC responses, cell death is directly promoted by antibodies via the development of a complement chain membrane attack complex (Figure 5B).

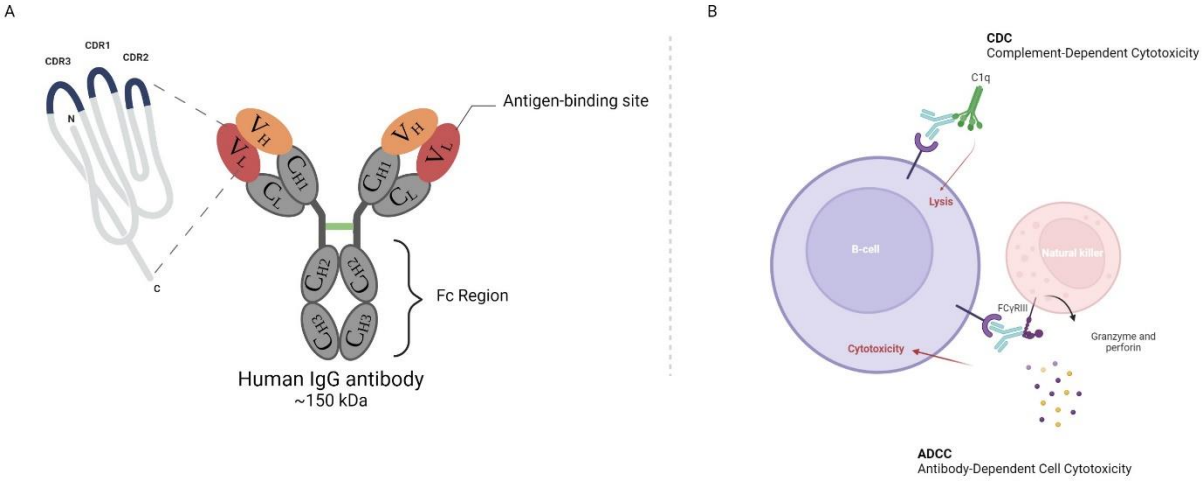


**Figure 5 – Schematic representation of an IgG structure including CDRs and function.** A) The variable domains (VL and VH) are responsible for the specificity and affinity towards the antigen via three hypervariable loops known as complementary determining regions (CDRs), present in VL and VH domains. The antibody-binding site is the result of the combination of the VL and VH chain CDRs in six hypervariable loop structures, three of which for VH and VL domains. The remaining portion, known as the framework region, works as a structural scaffold for supporting the CDR. B) The Fc region, composed by constant region domains, is related with the mediating antibody effector functions by Antibody-Dependent Cell Cytotoxicity (ADCC) and Complement-Dependent Cytotoxicity (CDC). In ADCC, Fc domain engages FC receptors on the surface of effector cells, such as natural killer cells that mediate cell death. In CDC, Fc region interacts with complement component 1 (C1q) triggering the complement cascade that leads to cell death. Images were created with BioRender.com.

#### 1.5.1.2. Antibody fragments and single-domain antibodies as promising scaffolds

Owing to its properties of a prolonged half-life and the capability to induce effector functions, full IgGs are the most approved Ig format on the market. Despite that, a full IgG may have some drawbacks that might compromise its translation to a clinical use and the range of its therapeutic applications. These limitations are mainly related with the high molecular weight of these molecules. It is well known that full IgGs have limited penetration into solid tumors, making them inappropriate for challenging targets. Furthermore, these conventional antibody formats also present a slow clearance rate and high production costs. Moreover, due to inappropriate activation of the Fc receptor-expressing cells, they frequently result in the release of high amounts of cytokine, leading to subsequent toxic effects.

In order to overcome these problems, in the past years, different antibody fragments have been explored (Figure 6). The development and use of antibody fragments is associated

with many advantages. Antibody fragments can maintain the specificity of the original Ig, with the advantage of having a smaller size that could be helpful to access hidden epitopes (Figure 6B). Moreover, production is also facilitated due to the lack of glycosylation that allows its production on prokaryotic expression systems, reducing overall costs. A lower immunogenicity, no antibody-dependent enhancement (ADE) effect stimulation and lower nonspecific uptake in tissues that highly express Fc receptors are also described due to the lack of the Fc domain (Holliger and Hudson 2005). To handle the limitations and take advantage of all these benefits, fragments as the antigen-binding fragment (Fab) or the single-chain variable fragment (scFv) have been produced. The Fab fragment consists of two constant domains ($CH_1$ and CL) and two variable domains (VH and VL) and single chain fragment variable (scFv) composed only of variable regions, one from the heavy chain (VH) and the other from the light chain (VL) (Figure 6B). This was possible mainly due to the development of recombinant DNA technologies and protein engineering methods that allowed the cloning of the variable and the constant domain genes of the light (L) and heavy (H) chain, instead of using the proteolytic cleavage of antibodies. These new methods also permitted cloning the VH and VL variable genes of an IgG to produce an scFv. These developments allowed the construction of more stable and effective molecules that have been approved in the last decade. At present, several Fab and scFv format molecules have the approval and are on the market, such as Abciximab, Ranibizuman, Certolizumab pegol and Idarucizumab in the Fab format, and Blinatumomab and Brolucizumab in the scFv format (Jin et al. 2022).

The approval of these new formats opened new perspectives for the use and development of small fragment antibodies, demonstrating the great importance for their clinical use. With these spotlights, new classes of fragments have emerged, in particular, single-domain antibodies (sdAbs).

SdAbs are the smallest fragments that can be isolated from a conventional IgG. These fragments can also be obtained naturally from antibodies devoid of light chains derived from two different organisms: the camelids, in particular, camels and llamas (VHH), and cartilaginous fish, such as wobbegong and nurse shark ($V_{NAR}$) (Hamers-Casterman et al. 1993; Greenberg et al. 1995; Muyldermans et al. 2001; Holt et al. 2003; Silva et al. 2004; Holliger and Hudson 2005).

Due to their smaller size, sdAbs in all the forms (VH, VL, VHH and $V_{NAR}$) (Figure 6B) display improved tissue penetration and are able to reach difficult-to-access targets such as enzyme active sites, hidden epitopes, or canyons in receptor molecules. Additionally, just as with the Fab and scFvs fragments, sdAbs also lacks the Fc domain, exhibiting a low nonspecific uptake in tissues that highly express Fc receptors. Moreover, other important advantages can be pointed out to the sdAbs, such as its high stability, low immunogenicity and lower manufacturing costs (Holliger and Hudson 2005).

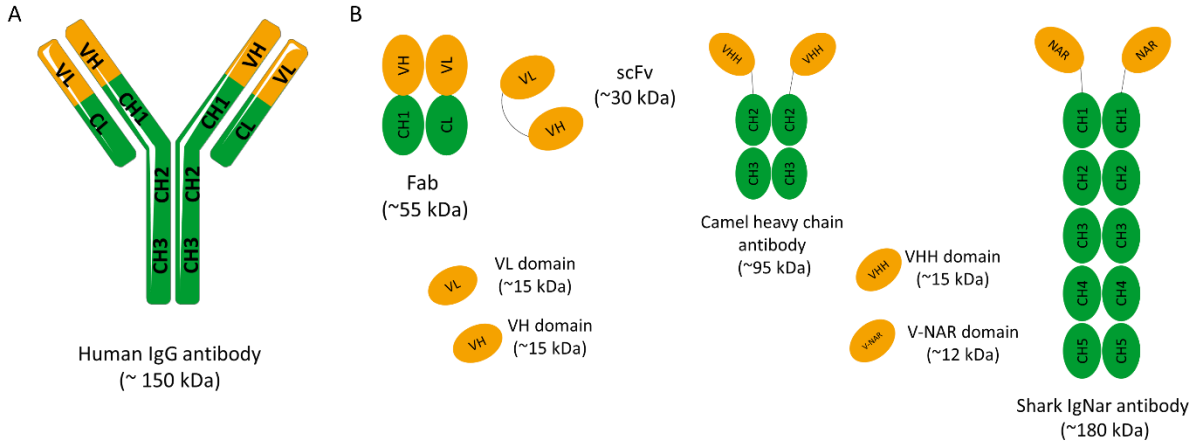


**Figure 6 - Schematic representation of conventional IgG antibody and different antibody fragments.** A) Schematic representation of a conventional IgG antibody. Immunoglobulin G (IgG) has approximately 150 kDa and consist of two identical light chains (L) and two identical heavy chains (H) connected by disulfide bonds. Light chains are made up of a variable domain (VL) and a constant domain (CL). Heavy chains are made up of a variable domain (VH) and three constant domains (CH1, CH2 e CH3). The IgG molecule can also be divided into two main fragments: the antigen-binding-domain (Fab) and the fragment crystallizable (Fc) domain. The Fab fragment consists of two constant domains (CH1 and CL) and two variable domains (VH and VL). B) Schematic representation of different antibody fragments. Fragment of antigen binding (Fab) composed of VL and a constant domain of the light chain (CL) linked to VH and a constant domain of the heavy chain (CH1) by a disulfide bond between the CL and CH1 domains. Single chain fragment variable (scFv) composed only of variable regions, one from the heavy chain (VH) and the other from the light chain (VL). The two variable regions are linked by a flexible glycine-serine linker (Gly4Ser)3. Camelid and shark immunoglobulin composed of only heavy chains. They present no light chain, and the displayed V domains bind their targets separately. Camelid heavy-chain antibodies composed a homodimer of one variable domain (VHH) and two C-like constant domains (CH). Shark new antigen receptor antibodies (IgNARs) composed of one variable domain (V-NAR) and five C-like constant domains (CH). Images were created with BioRender.com.

Due to sdAbs excellent characteristics, several molecules have entered clinical trials, with one of them having already been approved. Caplacizumab was the first sdAb approved, and is now being used for the treatment of acquired thrombotic thrombocytopenic purpura (aTTP), a rare disease characterized by excessive blood clotting in small blood vessels

(Morrison 2019). Caplacizumab has a VHH format and binds to the A1 domain of von Willebrand factor (VWF), blocking platelets from binding and aggregating to VWF.

Over the past years we have been showing the promising potential of rabbit derived sdAbs for several therapeutic applications (Silva et al. 2004; Goncalves and Silva 2008 Nov 13; Aires-Da-Silva et al. 2014 May 8; Cunha-Santos et al. 2016; Gouveia et al. 2017; Aguiar et al. 2021; Dias et al. 2022). In addition to the promising properties of single-domains, rabbit sdAbs have a unique characteristic in their light chain variable domain (VL) that makes them promising scaffolds for the development of antibody-drug-conjugates (ADCs). The rabbit kappa light chains have an unusual disulfide bridge that joins variable and constant domains, usually via cysteine residues at positions 80 and 171. This disulfide bridge links framework region 3 of the variable kappa light chain domain with the constant kappa light chain domain, a linkage not seen in mouse or human antibodies. Therefore, when the VL sdAb is isolated, the conserved cysteine at position 80 (normally paired with Cys171 in an IgG) becomes exposed on the protein's surface and its sulfhydryl group becomes free to be explored to selectively conjugate a chemical payload, without requiring further genetic engineering manipulation (Figure 7). Furthermore, rabbit sdAbs also display other advantages in terms of manufacturing costs and downstream processes, since it can be expressed in bacteria and purified by protein L (McCartney-Francis et al. 1984; Popkov et al. 2003; Goncalves and Silva 2008 Nov 13; Weber et al. 2017). Furthermore, since rabbits are evolutionarily distant from mice and rats, epitopes that are not immunogenic in rodents can be recognized by rabbit mAbs, increasing targetable epitopes and facilitating the generation of mAbs that cross react with other species.

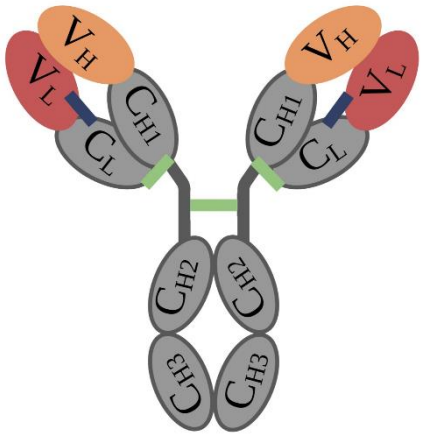


**Figure 7 - Representation of a rabbit IgG antibody.** In the present study, we aimed to explore the potential of rabbit-derived VL-sdAbs to develop a new generation of ADCs. Rabbit IgG contains two identical light chains paired with two identical heavy chains. The light chain is composed of an N-terminal variable domain (VL) (red), followed by one constant domain ($C_L$). The heavy chain consists of an N-terminal variable domain ($V_H$) (orange), followed by three constant domains ($C_{H1}$, $C_{H2}$ and $C_{H3}$). $C_{H1}$ and $C_{H2}$ are linked via a flexible hinge region and contains three disulfide-bridges (green). Most rabbit kappa light chains of the K1 isotype have an unusual disulfide bridge (blue) that joins the variable and constant domains, usually through cysteine residues at positions 80 and

171. This disulfide bridge links framework region 3 of the variable kappa light chain domain with the constant kappa light chain domain, a linkage not seen in mouse or human antibodies. Thus, when the VL-sdAb is isolated the conserved cysteine at position 80 (Cys80, normally paired with Cys171 in an IgG format) becomes exposed at the protein surface and its sulfhydryl group becomes free to be explored to selectively conjugate a chemical payload, without requiring further genetic engineering manipulation. Images were created with BioRender.com.

These unique characteristics of sdAbs makes them excellent scaffolds to be easily attached to other proteins, peptides, small molecules or even nanoparticles by simple molecular biology or chemical procedures.

In order to better reach the great potential of these scaffolds, it is important to select them using the adequate techniques. In the next section, a description of the most recent selection techniques is summarized.

#### 1.5.1.3. Selection and screening of recombinant antibodies

The Nobel-prize winning hybridoma technology opened new doors for the use of mouse antibodies as human therapeutics (Köhler and Milstein 1975). Hybridoma, particularly mouse hybridoma, was one of the first techniques to develop mAbs. A mouse hybridoma is a hybrid cell produced by injecting a specific antigen into a mouse, collecting the antibody producing cell from the mouse's spleen, and fusing it with a long-lived neoplastic cell (myeloma). The resulting hybrid cell can be isolated and expanded, producing many identical offspring. Each of these daughters' clones will secrete, over a long period of time, the immune cell product, the antibody. A B-cell hybridoma secretes a single specific antibody known as a monoclonal antibody. Regardless of the success of hybridoma, it is known that murine antibodies present several properties that restrict their clinical use. One of the most important drawbacks is the high immunogenicity of the mouse mAbs that result in the generation of human anti-mouse antibody response (HAMA). Moreover, murine mAbs presented diminished serum half-life and incapability to induce human effector responses (Khazaeli et al. 1994; Hwang and Foote 2005; Presta 2006). More recently, new hybridoma technologies have been developed using transgenic mice models that have integrated into their germline human immunoglobulin, such as HuMabMouse and XenoMouse platforms (Aires da Silva et al. 2008). Regardless, new antibody screening methods have been explored, in particular, platforms consisting of display technologies. Among display technologies, there is phage display, ribosome display, yeast display, bacterial display and mammalian cell surface display, all of which are transgenic mice platforms that express human immunoglobulin genes. Among them, phage display is by far the most used to generate recombinant therapeutic antibodies from different sources and antibody formats. Nowadays, there are 14 therapeutic antibodies approved by the FDA and EMA that were developed via phage display, including one of the most sold antibodies: Adalimumab (Alfaleh et al. 2020).

#### 1.5.1.3.1. Phage display: a powerful technique for antibody selection

Phage display was firstly described by George P. Smith in 1985, when it was demonstrated that a filamentous bacteriophage f1 was capable of displaying a fusion protein on the virion surface, after the insertion of a foreign DNA fragment into the phage's coat protein gene (Smith 1985). In the early 90s, phage display went through great improvements, mainly by the groups of Winter and McCafferty at the laboratory of molecular biology (Cambridge, United Kingdom), and by Lerner and Barbas at The Scripps Research Institute (La Jolla, United States) (McCafferty et al. 1990; Barbas et al. 1991). In phage display, antibody genes are linked to the amino-terminus region of the phage's minor coat protein pIII. As a result, when expressed, during normal phage biogenesis, mature phage particles incorporate the encoded fusion product, linking the antibody genotype and phenotype. During the process, phages expressing antibodies on their surface are produced, while possessing in their genome the antibody encoding gene. This allows the enrichment of antigen-specific phage antibodies using immobilized or labeled antigens (Winter et al. 1994; Hoogenboom 2002). Phage display is composed by four main steps: coating of the antigen; incubation of phage repertoire with the antigen; washing to remove non-specific phages; elution and reamplification of antigen-specific phages (Hoogenboom 1997; Griffiths and Duncan 1998; Hoogenboom 2005). To avoid the selection of non-specific binders, the washing step is crucial after incubation of the library with the antigen, eliminating unbound phages. Stringency can be incremented in each round by increasing the number of washing steps, leading to high-affinity phages. Stringency can be also achieved by the modification of the washing buffer by adding detergents, for example (Smith and Petrenko 1997). Different conditions can be used for the elution step, such as changing pH level, proteolytic cleavage or competition with free antigens. To simplify cleavage, some libraries possess a cleavage site, such as trypsin, between the antibody and the pIII protein (Ward et al. 1996; Kristensen and Winter 1998). Broadly speaking, three to six rounds of binding, elution and amplification are enough to recover highly specific antibodies and affinity (Figure 8) (Hoogenboom 1997; Griffiths and Duncan 1998; Hoogenboom 2005). The same principles described can be applied to select antibodies expressed on whole cells, liposomes, virus-like particles or other systems (Kirsch et al. 2008; Lipes et al. 2008; Dominik and Kossiakoff 2015; Jones et al. 2016; Stark et al. 2017).

The systems can be classified according to the type of phage used: filamentous M13, T7, bacteriophage lambda (λ phage) or T4 phage display systems. The most used are the filamentous phages, such as M13, since they do not lyse cells during their lifecycle. M13 consists of a circular ssDNA and five coat proteins (pVIII, pIX, pVII, pVI, pIII). M13 libraries are based on the peptide or antibody fusing positions. There are two types: pIII and pVIII libraries. Both contain a N-terminal signal sequence that directs them to the inner bacterial membrane

before phage assembly. The pIII coat protein is involved in phage-host interaction during infection and is about 406 amino acids long. The pIII phage library is the most commonly used in phage display, greatly due to the characteristic of displaying one to five copies of large foreign proteins on its surface. Moreover, this phagemid system has the advantage of its small size and ease of cloning (Bábíčková et al. 2013; Tan et al. 2016).

The urge of antibody fragments and single domain antibodies ushers the necessity of improving phage display systems. Thus, a new type of phages that can present a higher number of scFvs on filamentous phage particles have emerged, known as hyperphages. Hyperphages have a pIII phenotype and are able to infect *E. coli*, however, the functional pIII gene is missing, meaning that the phagemid-encoded pIII-antibody fusion is the source of pIII in phage assembly. This unique property of hyperphages increases antigen-binding activity by more than 50%, in comparison with the 3% of conventional phages, by simply increasing phage particles that are carried with the antibodies on their surface (Rondot et al. 2001; Pande et al. 2010).

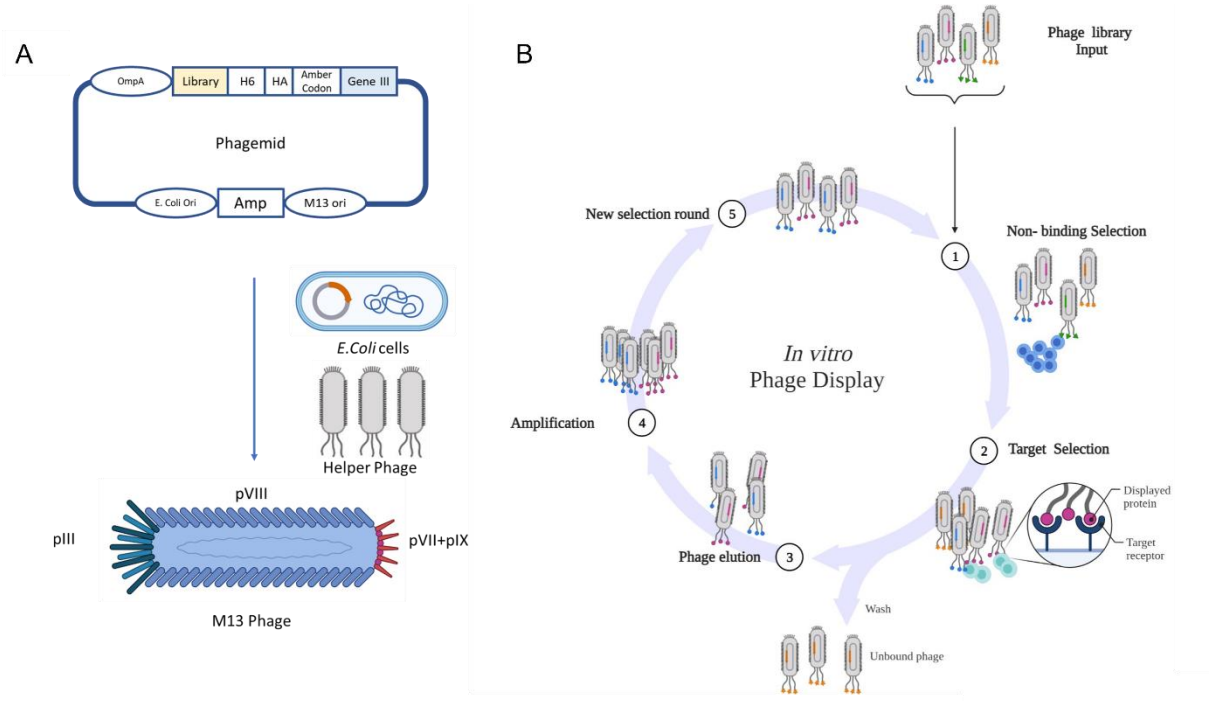


**Figure 8 - Schematic representation of *in vitro* Phage Display Technology.** (A) In phage display systems, antibody genes are linked to the amino terminus region of the phage minor coat protein pIII, as shown in the phagemid. When expressed, mature phages will incorporate the encoded fusion product, creating a link between antibody genotype and phenotype. B) *In vitro* phage display, selection is composed of several steps: coating of the antigen or preparation of the cells; incubation of phage repertoire with antigen; washing to remove non-specific phages; and elution and reamplification of antigen-specific phages. The stringency of selection could be increased by the increase in the number of washing steps. Images were created with BioRender.com.

#### 1.5.1.3.2. Antibody libraries: a tool to increase the odds

To increase the odds of discovering a good antibody, a high-quality antibody source is crucial, known as an antibody library. In general, there are three main types of antibody libraries: immune, naïve and synthetic (Winter et al. 1994; Hoogenboom 2002; Kügler et al. 2018). In immune libraries, the used antibody source is the lymphoid tissue of a donor that was previously immunized with a specific antigen, or, even individuals with a specific disease, such as cancer or a particular infection. Immune libraries have the advantage to generate higher affinity antibodies than those generated from hybridomas and naïve libraries due to the *in vivo* maturation that the gene fragments are going through (Winter et al. 1994; Griffiths and Duncan 1998; Hoogenboom 2002; Bradbury and Marks 2004). However, immune libraries have some disadvantages. The most obvious one is the time spent in immunizing animals. Other disadvantages are related with the unpredictability of the immune response to the target antigen, lack of immune response to the target antigen and the fact that a new library has to be constructed for each antigen. In terms of human libraries, due to ethical requirements, they can only be generated from patients B cells.

Immunization issues are not present in naïve libraries. Naïve libraries are recovered from large naïve repertoires of antibody fragments from non-immunized donors and represent the germline diversity of the antibody repertoire. Naïve libraries have some advantages over immune libraries, such as not needing immunization and being able to produce antibodies against itself, and non-immunogenic or toxic antigens. Furthermore, contrary to immune libraries, naïve can be used for all antigens, if large enough. The generation of the antibody is much quicker in naïve libraries, with the antibody isolated in less than two weeks (Winter et al. 1994; Hoogenboom 2002). However, the main disadvantage is the large size of the library that makes the exact nature of V-gene repertoire largely unknown and uncontrollable (Maynard and Georgiou 2000). Furthermore, it is reported that antibodies isolated from naïve libraries have a poor expression and are toxic to the host bacteria, due to the fact that antibody genes are representative of the human immunological repertoire, and that there is no guarantee that the clone obtained can be expressed in bacteria (Maynard and Georgiou 2000).

Synthetic libraries emerged to overcome the problems reported. Synthetic libraries are *in vitro* developed using oligonucleotides that introduce areas of complete or tailored degeneracy into the CDRs of one or more V genes. The degeneracy introduced into specific codon positions of synthetic oligonucleotides allows the control of the degree of randomization. Marks et al.(Marks et al. 1991) constructed the first synthetic library. To this end, a synthetic CDR3 of five to eight residues was developed with a repertoire of human VH genes from 49 human germline VH-gene segments rearranged *in vitro*. Subsequently, diversity was expanded from 4 to 12 residues to cover the natural length diversity of the CDR3 loop (Nissim et al. 1994). This demonstrated the importance of diversity in a longer CDR-H3 loop.

### 1.5.1.3.3. *In vivo* phage display

With the emergence of new classes of therapeutics and novel targets, the need for generating better molecules against challenging targets becomes more evident. To fulfill these needs, and in order to select the best-in-class antibodies against antigens in their native conformation, novel ways to perform phage display have been developed, in particular, the *in vivo* phage display.

Briefly, *in vivo* phage display consists in the selection of phage libraries using biopannings in living animals. This approach is very similar to the *in vitro* phage display, the differences being that the phage library is directly intravenously injected into animals and the phages allowed to circulate in order to permit the antibodies expressed at the phage surface to bind directly to a specific target, organ or tissue. Finally, animals are perfused to wash the unbound/unspecific phages, euthanized, and desired organs collected to recover the phages. This strategy allows the selection of antibodies based on desired pharmacokinetic and targeting specificity properties (Figure 9) (André et al. 2022).

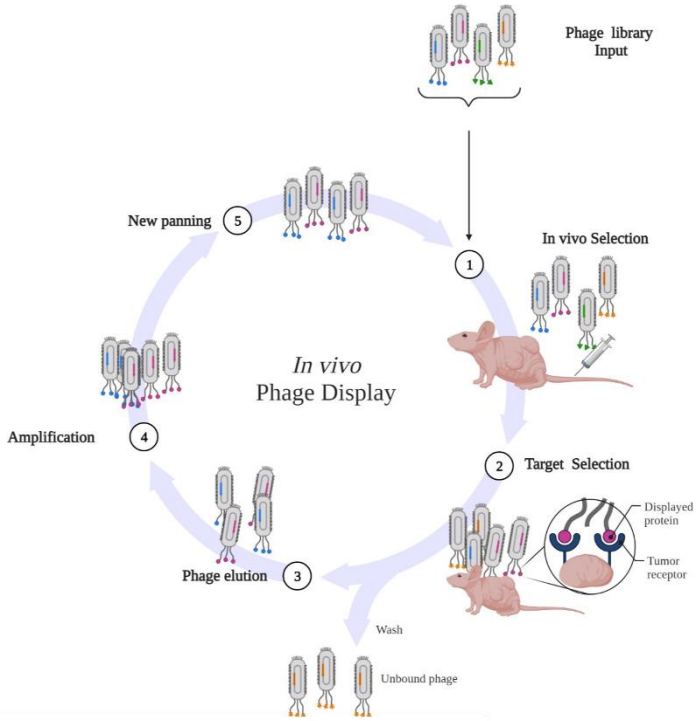


**Figure 9 - Schematic representation of *in vivo* Phage Display.** *In vivo* phage display selects phage libraries using a living animal. In this methodology, the library is directly injected into animals and antibodies are allowed to bind directly to the specific organ or tissues. Non-binding phages are washed and, in the end, animals are euthanized, and the desired organs collected to recover the phages. This scheme contains a representation of an *in vivo* experiment performed on a xenograft mouse model where the phages are recovered from the tumor. Adapted from (André et al. 2022). Images were created with BioRender.com.

To better perform *in vivo* phage display, it is mandatory to be aware of some parameters that can modulate the expected results. One of them is phage survival. As known, the immune

system, and, in particular, the reticuloendothelial system (RES), has a significant role in phage uptake. This can be observed by the high uptake in the liver and spleen. To better understand this issue, various studies have been comparing the survival time of phages in different mice models. Overall, these studies concluded that it is recommended to perform a phage library circulation time optimization study for each type of phage and animal model before starting the *in vivo* phage display experiment (Molenaar et al. 2002).

Another parameter to have in consideration with *in vivo* phage display is the route of administration. Many different routes can be considered for phage library administration. However, it is necessary to take into account that each route may influence uptake to the target tissue or organ. Due to the rapid systemic exposure of the phage's particles, intravenous injection is the most common route chosen. Before choosing the route, it is advisable to consider the targeted organ or tissue, as the findings show that the administration route near the target tissue may have some advantages, such as reduced uptake by other tissues. (Bábíčková et al. 2013).

Over the years, *in vivo* phage display has been proving itself to be an effective and powerful technique to select antibody fragments and peptides. This is evident in many studies in the literature where new molecules have been identified for several purposes, such as biomarkers and drug delivery. Moreover, *in vivo* phage display is being part of the new generation of emerging therapeutics antibodies, making it crucial in the antibody development field. Furthermore, to develop novel drug delivery systems, such as ADCs, it becomes necessary to have the best antibody candidates with the best characteristics of specificity, pharmacokinetics and stability (André et al. 2022). Thus, nowadays these kind of techniques play a crucial role in the journey of creating a new delivery system such as ADCs.

### 1.5.2. Antibody-drug conjugates as a promising therapeutic molecule for cancer

As aforementioned, monoclonal antibodies are one of the fastest growing classes of immunotherapies, since they offer an alternative tumor-selective treatment approach. Nevertheless, most mAbs are not sufficiently potent to be therapeutically active on their own. On the other hand, chemotherapy is at the core of current cancer therapy, however, it is often accompanied by high toxicity levels for patients. To overcome these challenges, antibody-drug conjugates (ADCs) have emerged as a class of promising therapeutic molecules in the oncological field that aims to solve the drawbacks of monoclonal antibodies and chemotherapy toxicity.

ADCs comprise an antibody conjugated to a highly cytotoxic compound via a chemical linker that is directed towards a target antigen expressed on the cancer's surface, reducing systemic exposure and, therefore, toxicity (Sievers and Senter 2013). Ideally, the optimal ADC requires a highly selective mAb for a specific tumor antigen, a linker that can be stable in circulation and cleavable at the target site, and a payload with high toxicity induced after its release (Figure 10A) (Chau et al. 2019). Briefly, upon treatment with an ADC, the antibody binds to the target antigen on the cell's surface, and the ADC is then internalized via receptor-mediated endocytosis. After endocytosis, an endosome is formed and the ADC is transported to the lysosome, after which the payload is released leading to cell death (Figure 10B) (Wu and Senter 2005).

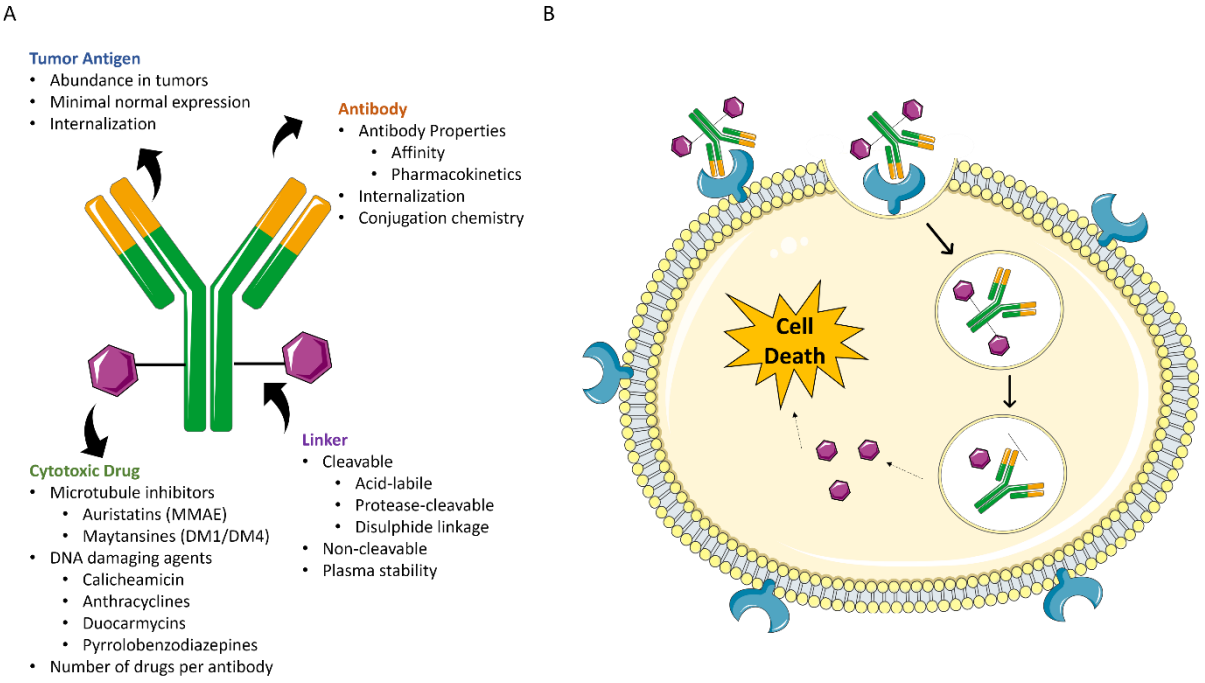


**Figure 10 - Schematic representation of an ADC and its mechanism.** A) ADC comprise an antibody conjugated to a highly cytotoxic compound via a linker that directed toward a target antigen expressed on the cancer cell surface. B) Upon treatment with an ADC, the antibody binds to the target antigen on the cell's surface, and the ADC is internalized via receptor-mediated endocytosis. After, an endosome is formed, and the payload is released leading to cell death. Images were created with BioRender.com.

As mentioned before, internalization is crucial for ADC efficacy, thus, it is important that the target epitope is at the cell surface. Another important issue for the target is its homogeneous expression at the surface of targeted cells and low expression on healthy cells, avoiding the off-target toxicity for neighboring cells. Regardless, the influence of antigen density on a cell's surface remains unclear because of the differential binding affinity and ADC

internalization, which affects drug uptake and release on the target cell (Ritchie et al. 2013; Staudacher and Brown 2017).

Regarding the payload, it needs to be highly potent, with IC50 in the subnanomolar range, as it is the ultimate effector element of the ADC. Adding to the potency, there is some molecular and physicochemical properties of the payload that are essential for the success of the ADC. The basic properties to take into account when a payload is chosen are the accessibility for conjugation, solubility and stability. It is important that the molecular structure of the payload enables the conjugation with the linker, as well as water solubility and prolonged stability in the blood, since the majority of ADCs are prepared in water and administered intravenously (Chau et al. 2019).

There are several classes of payloads. Payloads can either target DNA, in the case of duocarmycins, calicheamicins, pyrrolobenzodiazepines and SN-38, or tubulin, in the case of maytansines and auristatins. Drugs that damage DNA target DNA minor grooves, inducing double-strand breaks, such as calicheamicins and DNA alkylation by binding specifically to A-T-rich regions, such as PBDs (Thorson et al. 2000; Damle and Frost 2003; MacMillan and Boger 2009). Tubulin inhibitors, such as monomethyl auristatin E (MMAE) and monomethyl auristatin F (MMAF), inhibit microtubule polymerization, resulting in G2/M phase cell-cycle arrest (Francisco et al. 2003).

The linker is the component that maintains the connection between the payload and the antibody and is essential for the stability of the ADC in circulation. The ideal linker should be sufficiently stable in order to allow ADC systemic circulation and its access to the target site without cleavage, as well as its rapid cleavage after internalization to release the payload (Beck et al. 2017). Linkers can be divided into two categories regarding payload release mechanism: cleavable or non-cleavable. Cleavable linkers are linkers that release its payload in the presence of certain environmental conditions, such as low pH, proteolysis or high intracellular glutathione concentrations (Lu et al. 2016). Among cleavable linkers, one kind that has been explored for cancer therapies are linkers with chemical functions that are sensitive to the disease chemical environment, such as the presence of reactive oxygen species, due to the fact that high levels of ROS are one of the hallmarks of cancer. Diazaborines are one of these ROS-responsive type of linkers that have been emerging in the ADC field. This linker was the one used for the development of our ADC described under chapter 2 (António et al. 2021 Nov 5). Non-cleavable linkers are more stable in circulation due to nonreducible bonds formed with mAbs amino acid residues. This type of linker is dependent on lysosomal degradation of the mAb for the payload release. Thus, it is important for non-cleavable linkers to have an efficient internalization process and optimal trafficking to lysosomes (Frigerio and Kyle 2017).

The method and the site of conjugation are two essential aspects that can affect the therapeutic window and pharmacology of the ADC. The potency and toxicity of the ADC is determined by the number of payload molecules attached to the mAb, briefly called drug-to-antibody ratio (DAR). This conjugation occurs normally on the mAb, via lysine sidechains exposed or cysteine residues used to make interchain disulphide bonds in the hinge regions. DAR can have a high variability, varying from 0 to 8. It is important to take into account that higher doses increase the potency of the ADC, but also increase the undesirable off-target effects, as well as the drug clearance, leading to the decrease of the circulating half-life (Hamblett et al. 2004; Nagayama et al. 2017).

Currently, there are 12 ADCs approved by the FDA and EMA with more than 100 under clinical trials worldwide.

Despite the success, the manufacture of ADCs has been challenged with some engineering issues and drawbacks that range from the design itself to production (Perez et al. 2014). Furthermore, ADCs on the market used bioconjugation methods that are not specific, and therefore, result in the manufacturing of heterogeneous products that contain a mixture of species with different drug-to-antibody ratios, leading to different pharmacokinetic and therapeutic properties. Moreover, a low number of compound molecules can be attached to the antibody. As mentioned before, payload conjugation is typically made via multiple lysine modifications or by functionalization of thiols generated by reduction of interchain disulfide bonds, which is the main problem of ADC construction due to neither of these methods being ideal. The reason behind is related with the abundance of lysines and cysteines in conventional mAbs (> 80 lysine residues and 16 cysteine pairs in a typical IgG antibody). Also, conserved cysteines act as an important player in the antibody structure and its use for conjugation can lead to improper folding and aggregation problems (Wang et al. 2005; Shen et al. 2012; Panowski et al. 2014; Perez et al. 2014). Nowadays, to overcome this DAR heterogeneity, novel approaches focused on site-specific conjugations, such as engineered cysteine residues, unnatural amino acids or enzymatic conjugation via glycotransferases, are being used. These novel approaches involve genetic engineering of the mAb to introduce free cysteines or be based on modifying natural or engineered amino acid or carbohydrate residues in the antibody component by chemical or enzymatic reactions. In fact, some of these approaches resulted in more homogeneous ADCs and in allowing control of the site of drug attachment. However, the majority of these methods are not able to be implemented to scale-up the manufacturing of the ADC, as most of them are time consuming, require reengineering the antibody, and the chemical and enzymatic reactions are difficult to replicate (Doronina et al. 2003; McDonagh et al. 2006; Junutula et al. 2008; Kim et al. 2013; Cal et al. 2014; Dennler et al. 2014; Li et al. 2014; Panowski et al. 2014; Zhou et al. 2014; Maruani et al. 2015). Thus, there is a pressing need to identify and develop more stable, homogeneous and effective

ADCs. In this thesis we explored the potential of rabbit sdAbs and their free Cys80 for the development of a novel class of ADCs.

### 1.5.3. Immunotoxins

One of the main issues of ADCs, as aforementioned, are the bioconjugation methods, mainly when we are dealing with chemical payloads. This is related with the properties of the payload molecule that can difficult the bioconjugation process. To overcome this problem, a new class of antibody-drug conjugate (ADC) molecules have emerged, the immunotoxins that combine the antibodies with proteins or peptides, usually toxins derived from several organisms, such as bacteria. Bacterial toxins are highly toxic, and for this reason, one single molecule is enough to kill a cell. The combination of the toxin with an antibody results in an immunotoxin (IT) (Akbari et al. 2017). The first generation of immunotoxin was first proposed by Thrope et al (Thorpe et al. 1978). The first generation of ITs were constructed by chemical conjugation using a toxin derived from a bacteria and plant, as well as a murine antibody. This resulted in an unstable molecule, with low specificity, poor linker stability, high immunogenicity and a high heterogeneity of conjugation productions. In order to overcome the non-specific binding to normal tissues, the second generation of ITs appeared using the truncated forms of the bacterial toxin so that binding of the toxin is replaced by the antibody.

All over the years, immunotoxins have gone through some improvements in order to generate molecules with better efficacies and lower levels of toxicity. The greatest achievement was made with the 3$^{rd}$ generation of ITs with the use of genetic fusion methods, instead of chemical conjugation, improving IT stability by a great deal (Figure 11) (Kim et al. 2020). Moreover, because ITs promote cell death through protein synthesis inhibition, while not causing DNA damage, it is considered as an advantage over conventional molecules. Due to their properties, ITs have been rising as a class of promising molecules to treat cancer and are already being used to treat leukemias and lymphomas.

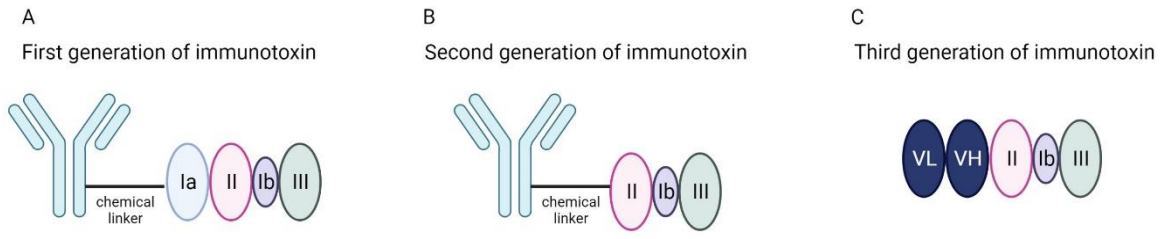


**Figure 11- Generations of immunotoxins.** A) The first generation of ITs were constructed by chemical conjugation of a toxin to an antibody. B) The second generation of ITs were constructed using truncated forms lacking the cell-binding domain chemically conjugated to an antibody. C) In the third generation, the IT was designed by genetic fusion of truncated forms of toxins with antibody fragments (scFv, dsFV, Fab, sdAb). Images were created with BioRender.com.

At present, there are three approved immunotoxins on the market. Denileukin difitox (Ontak) was the first IT approved by the FDA, in 1999, for the treatment of relapsed or refractory cutaneous T-cell lymphoma. In 2018, moxetumumab pasudotox (LUMOXITI) and tagraxofusp (Elzoris) were approved for the treatment of relapsed and refractory hairy cell leukemia and blastic plasmacytoid dendritic cell neoplasm, respectively. Ontak and Elzoris uses a truncated form of diphteria toxin (DT) known as DAB389, as a payload fused with IL2 and IL3, respectively. On the other hand, LUMOXITI uses a Pseudomonas Exotoxin (PE) truncated form linked to an anti-CD22 dsFv (Akbari et al. 2017). PE is a toxin derived from the bacteria Pseudomonas Aeruginosa and is one of the most common toxins used. PE consists of a single polypeptide chain with 638 residues (69 kDa), reduced to 613 residues (608 +REDLK) (66 kDa) after the removal of the signal peptide. Before PE enters the cell, the C-terminal lysine is removed by extracellular carboxypeptidase leaving the modified PE (608 + REDL). REDL sequence (Arg-Glu-Asp-Leu) in the C-terminal end is essential for the cytotoxic activity (Weldon and Pastan 2011). PE is composed of three functional domains: I, II and III (Figure 11). Domain I consists of amino acids 1-252 (Ia) and amino acids 365-404 (Ib), domain II of amino acids 253-364, and domain III of amino acids 405-613. Domain I subunits are separated after intracellular processing. Both subunits have different roles: subunit A (amino acids 280-613) has enzymatic activity (37 kDa), whereas subunit B (amino acids 1-279) has receptor binding activity (28 kDa). Domain III is known as a catalytic domain and is responsible for inhibiting protein synthesis. There are five amino acids of domain Ib (amino acids 400-404) that are required for full activity of the catalytic domain. When alone, toxin entrance is mediated by domain Ia that acts as a binding domain, binding the toxin to its receptor, known as alpha-2-macroglobulin, LRP1 or CD91. Domain II is responsible for the internalization of the toxin into the cell and contains a Furin cleavage site (amino-acids 274-280, RHRQPRG), a type of serine endoprotease site where proteolytic cleavage occurred between amino acids R279 and G280.

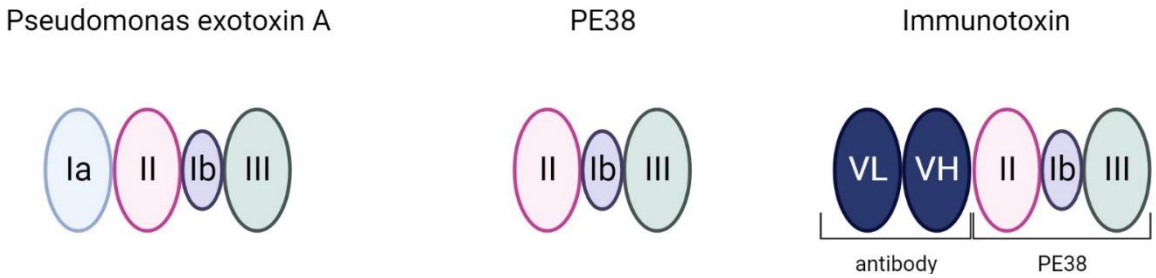


**Figure 12 - Pseudomonas Exotoxin Structure.** Pseudomonas Exotoxin is a toxin derived from Pseudomonas Aeruginosa, and one of the most widely used toxins. PE is composed by three domains: I, II and III. Domain I is composed by a subunit a with enzymatic activity, and a subunit b with receptor binding activity. In the immunotoxin format, cell-binding domain is replaced by the antibody and linked to PE38. Domain II is responsible for the internalization of the toxin and contains a furin clavage site. Domain III has a catalytic function that is responsible for inhibiting of protein synthesis. Images were created with BioRender.com.

Briefly, when in IT format, the cell-binding domain of PE38 is removed and replaced by a specific antibody to the target cell. The antibody specifically delivers the PE38 to the tumor cell. The IT is internalized via receptor mediated endocytosis and is routed to endosomes. In the endosomal lumen acidified by an ATPase proton pump, the toxin portion is cleaved by a protease named furin. The cleaved toxin (PE38) active (catalytic) domain goes to the trans-Golgi and then endoplasmic reticulum (ER) by retrograde trafficking and then is released into the cytosol. Then, PE38 inactivates eukaryotic elongation factor 2 (eEF2) by catalyzing adenosine diphosphate (ADP) ribosylation, causing inhibition of protein synthesis and cell death (Figure 13) (Kim et al. 2020).

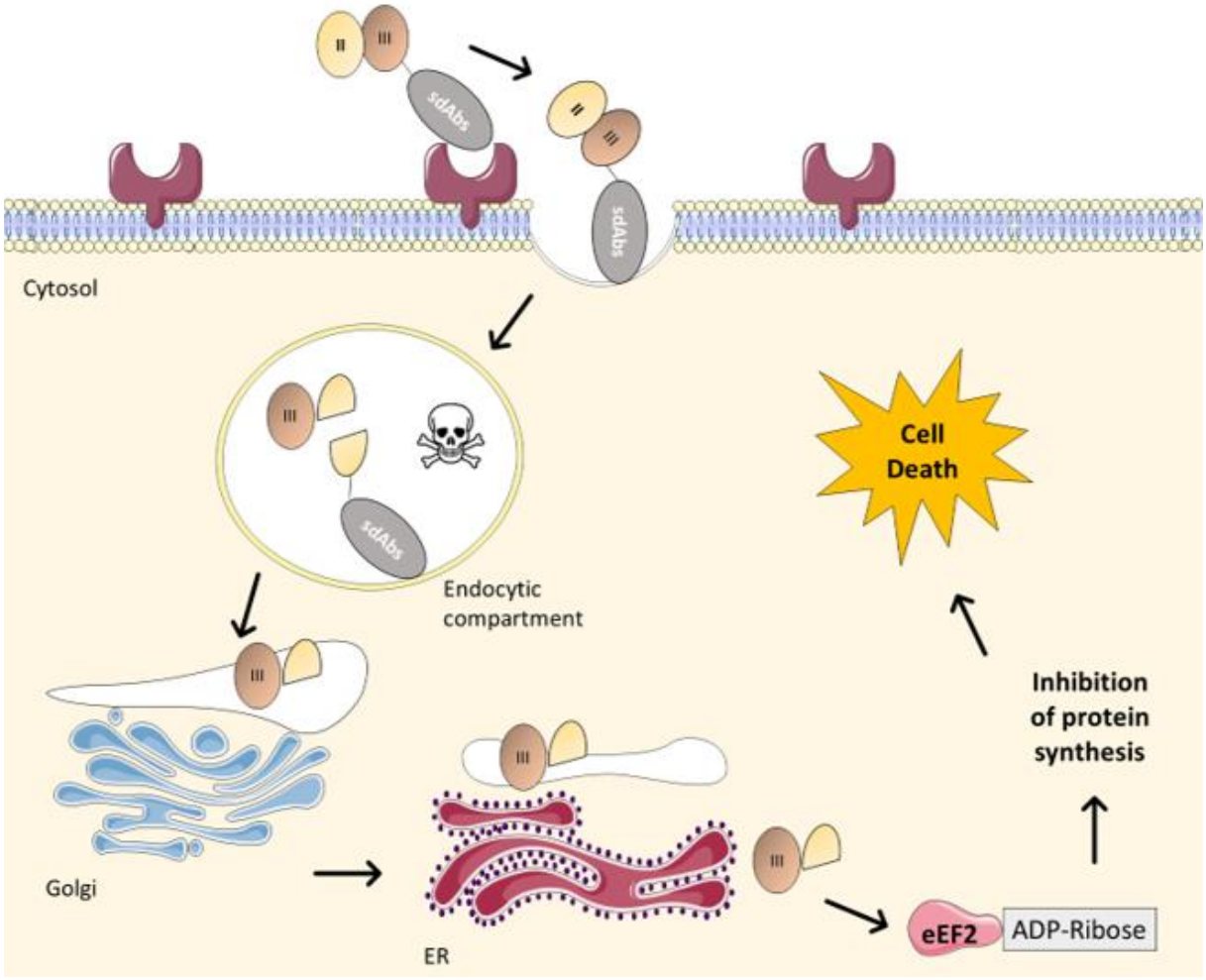


**Figure 13 - Mechanism of action of IT with PE38.** Immunotoxin enters the cell by receptor- mediated endocytosis and is routed to endosomes. In the endosome, the toxin moiety is cleaved by furin. The cleaved PE38 active domain is next routed to Golgi and endoplasmic reticulum, via retrograde trafficking before being released into the cytosol. Then, PE38 inactive eukaryotic elongation factor 2 (eEF2) by catalyzing adenosine diphosphate (ADP) ribosylation, causing inhibition of protein synthesis and cell death. Images were created with BioRender.com.

With all the potential mentioned above regarding rabbit sdAbs, we believe that they are also excellent scaffolds for immunotoxin development, which was also one of the goals of this thesis as described under chapter 3.

The versatility of sdAbs does not cease in ADCs and immunotoxins, as they can be very useful in other types of drug delivery systems. Despite ADCs and immunotoxins being promising approaches for delivering specific drugs to the tumor's cells, other classes of nanocarriers have been in use for the last few decades. One of the best studied nanocarriers for highly toxic drugs delivery are liposomes. The main advantage of liposomes, besides being able to protect the drug inside, is the capability of incorporating antibodies on the surface, turning regular liposomes into immunoliposomes.

### 1.5.4. Immunoliposomes: a new approach for cancer drug delivery

Over the years, multiple nano-sized vesicles have been discovered in order to enhance the therapeutic properties of the drugs already studied. Among these nano approaches, lipid-based systems have emerged as one with the best physicochemical properties and safety issues (Ferreira et al. 2021). Liposomes are spherical vesicles composed by one or more concentric lipid bilayers, entrapping the drug according to its characteristics. Encapsulation depends on the drugs' solubility. Briefly, hydrophobic drugs have affinity to the phospholipid bilayer, while hydrophilic drugs are entrapped in the aqueous center. As drug delivery vehicles, liposomes have exceptional properties. Liposome confers protection to the drug against physiologically occurring events, such as enzymatic degradation, chemical and immunologic inactivation and fast plasma clearance. Moreover, as the drug is protected, there is a minimization of the exposure to healthy tissue, reducing off-target effects (Bozzuto and Molinari 2015). The great characteristics of liposomes give them numerous advantages, such as their biodegradability, biocompatibility, excellent pharmacokinetic profiles, low cytotoxicity and the ability to be modified to induce pH and temperature sensitive release (Sercombe et al. 2015; Bulbake et al. 2017).

Liposomes are generally classified according to compartment structure and bilayer number, such as unilamellar vesicles (ULVs) or multilamellar vesicles (MLVs) (Pattni et al. 2015); according to particle size, into small unilamellar vesicles (SUVs, <100 nm) and large unilamellar vesicles (LUVs, >100 nm) (Fan et al. 2021); number of lamellae (unilammellar or multilamellar vesicles); lipid composition; charge of the bilayer (anionic, cationic or neutral); and surface functionalization (Figure 14) (Ferreira et al. 2021).

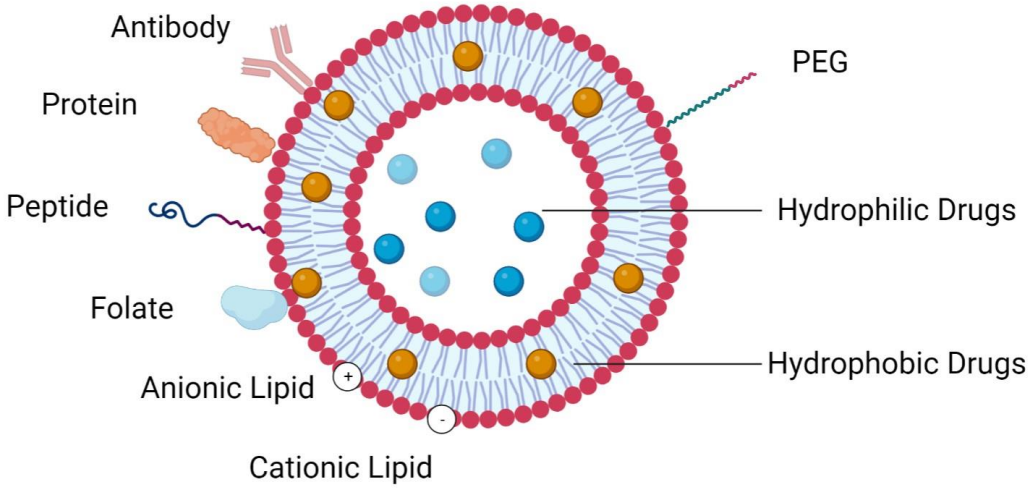


**Figure 14 – Schematic representation of different types of liposomes.** Adapted from (Ferreira et al. 2021). Images were created with BioRender.com.

The first generation of liposomes were known as conventional liposomes. These liposomes consisted of a lipid bilayer composed of cationic, anionic, or neutral (phosphor) lipids and cholesterol which surrounded an aqueous volume. The clinical potential of conventional liposomes was unveiled in 1980 with studies proving the improved therapeutic index of encapsulated drug, such as doxorubicin and amphotericin, when included in liposomal delivery formulation (Gabizon et al. 1982; Koning and Storm 2003; Metselaar and Storm 2005; Ding et al. 2006; Hua and Wu 2013). In comparison to the free drug, conventional liposomes reduce the toxicity of *in vivo* compounds, modifying pharmacokinetics and biodistribution, causing drug delivery to be more specific to the target tissue. However, it was seen that conventional liposomes were largely susceptible to rapid elimination from the bloodstream, diminishing therapeutic efficacy (Gabizon et al. 1991; Gabizon et al. 1994). The reported fast clearance was mainly due to the reticuloendothelial system promoting plasma components opsonization and uptake by macrophages (Hua and Wu 2013).

To overcome this problem, a new generation of sterically stabilized liposomes was developed. With the addition of hydrophilic polymer and polyethylene glycol (PEG), liposome

efficacy was greatly improved and opsonization by reticuloendothelial system (RES) was greatly reduced (Torchilin et al. 1992; Northfelt et al. 1996; Ishida et al. 2001).

The ideal liposomal formulation can be attained by choosing an adequate liposome composition. To establish safety, stability and efficiency of liposomes, the selection of phospholipids, head group and chain length, as well as liposome ratio, is crucial (Kapoor et al. 2017). Glycerophospholipids, which are amphiphilic lipids, composed by a glycerol molecule, bond to a phosphate group and to two fatty acid chains that may be saturated or unsaturated (Pinot et al. 2014). This phosphate group can be attached to another organic molecule (Monteiro et al. 2014; Beltrán-Gracia et al. 2019). According to this organic group, there are several types of natural phospholipids: phosphatic acid (PA), phosphatidylcholine (PC), phosphatidylethanolamine (PE), phosphatidylinositol (PI), phosphatidylglycerol (PG) and phosphatidylserine (PS). The most commonly used phospholipids are PC and PE. Additionally to phospholipids, there are more components that can be added to the liposomes in order to promote stability, such as cholesterol (CH), glycols and polyethylene glycol (PEG) (Inglut et al. 2020).

As mentioned before, liposomes are excellent drug delivery systems due to their ability to incorporate drugs with different characteristics. The selection method for drug loading depends on several factors, such as EE, drug/lipid ratio, drug leakage and retention, sterility, facility of production and scale-up, cost efficiency and liposome stability (Mayer et al. 1986; Maherani et al. 2011). Two primary techniques are used for drug loading, such as passive and active drug loading procedures. In some cases, the passive and active methods can be combined as in drug-lipid chemical conjugates. It is important to have a high drug loading in order to minimize the amount of excipient, attain therapeutic concentration, decrease volume dose and reduce dose number. With the passive method, drug encapsulation occurs during the preparation of liposomes. In this method, the drug can be encapsulated within the inner aqueous space, or embedded in the bilayer of liposomes by means of covalent, ionic, electrostatic, non-covalent or steric interactions between drug molecules and lipids. The main disadvantage of the passive drug loading method is its low encapsulating efficiency, with the need for an additional step for free drug removal (Liu et al. 2022).

The active drug loading method has a high efficiency of loading (above 90%), and is also known as remote drug loading. This method consists of loading the drug after empty liposomes are produced (Liu et al. 2022).

The first liposomal formulation used in human medicine was Doxil, a doxorubicin liposome, approved for the treatment of ovarian cancer, multiple myeloma and HIV-associated Kaposi's sarcoma. Nowadays, 14 different types of liposomes have been approved by the EMA and FDA. The majority are for cancer therapy, but there is liposomal formulation also for infections, anesthesia, vaccines, lung disease and photodynamic therapy (Liu et al. 2022).

There are two different strategies for liposome targeting: passive and active. Passive targeting is related with the properties and microenvironment of the disease, for example, the properties of cancer vasculature. This kind of targeting delivers liposomes to tissues or cells by transport, delivering them to the tumor's interstitium via leaky tumor vasculature through molecular drive within fluids (Lehner et al. 2013; Guimarães et al. 2021). One of the requirements of the liposomes used in passive targeting is a formulation that can avoid their rapid elimination by the body's defense mechanisms, such as phagocytic uptake or clearance by mononuclear phagocyte system (MPS) cells (Kraft et al. 2014). Thus, liposomes with PEG on the surface can be a good example of liposomes used in passive targeting, as PEGs increase the circulation time of the entire liposome (Zylberberg and Matosevic 2016).

More recently, ligand-targeted liposomes have emerged offering the promise of a site-specific delivery of drugs to targeted cell types or organs, that selectively express specific ligands at disease site (Hua and Wu 2013). This liposome targeting method is known as active targeting.

Several components can be attached to the liposomes surface, such as antibodies, peptides/proteins and carbohydrates. There are certain aspects to take into account in the selection of target ligands, such as the expression on the target, target cell uptake of the ligand-targeted formulation, and degree of target molecule coverage (Sawant and Torchilin 2012; Noble et al. 2014). It is also crucial that the selected ligand allows binding to target cells while also minimizing binding to healthy cells.

One of the most popular strategies of active targeting for cancer treatment with liposomes is targeting tumors with folate-modified liposomes. The history of folate and its receptors began in 1941 with the isolation of folic acid from spinach and with the discovery of the growth factor function in *Streptococus lactis R*. (Mitchell et al. 1941; Hoffbrand and Weir 2001; Cao et al. 2010). Since the beginning, the folate family has been closely associated with the development of anticancer drugs. Curiously, aminopterin was the first antagonist directed towards human cancer patients (Farber et al. 1948). The use of folates as targets offers many advantages, such as functional stability during manufacturing, biocompatibility and lack of an immunogenic response (Chaudhury and Das 2015). Liposomes conjugated with folates have been used with different therapeutic compounds, including daunorubicin in a murine model of leukemia (Pan and Lee 2005), carboplatin for human ovarian cancer xenograft (Chaudhury et al. 2012), MTX (Nogueira et al. 2015), irinotecan (Zhang and Yao 2012), docetaxel (Li et al. 2012), cytosine arabinoside (Sudimack et al. 2002), paclitaxel (Wu et al. 2006), imatinib (Ye et al. 2014), photosensitizers (Stevens et al. 2004), genes (Reddy et al. 2002), small interfering RNA (siRNA) and antisense oligonucleotides (Leamon et al. 2003).

Another strategy for active targeting is coupling mAbs to liposomes, creating immunoliposomes. Immunoliposomes are created by chemically coupling mAbs to the

liposomal surface. One of the main advantages of using monoclonal antibodies is their stability. However, due to their large size, entire antibodies have gone through some problems when conjugated with liposomes, mainly due to the presence of the Fc fragment that increases the uptake by circulating or liver macrophages or opsonization of the complex. Moreover, entire antibodies can also activate CDC and ADCC, causing a reduction of time spent in the blood stream and formulation specificity of the targeted liposomes. To overcome these problems, antibody fragments seem to be a solution for this targeting approach (Figure 15) (Torchilin 2010). Despite accelerated clearance, as seen with antibody fragments, the results showed that antibody fragments-liposomes circulate meaningly longer than full antibody-liposomes. Curiously, in the tumor, the accumulation of antibody-long circulation liposomes is similar with the accumulation of long-circulating liposomes without any antibody. The difference lies on the therapeutic activity that is much higher for antibody-targeted liposomes (Park et al. 1997; Moreira et al. 2001; Park et al. 2001; Park et al. 2002). A lower weight of mAb fragments, such scFV, single domain antibodies and nanobodies, allows the conjugation of a higher number of molecules conjugated per liposome (Torchilin 2010). Moreover, it has been seen that only 10 to 20 molecules of antibody per liposome are sufficient to attain an efficient targeting effect (Sapra and Allen 2003).

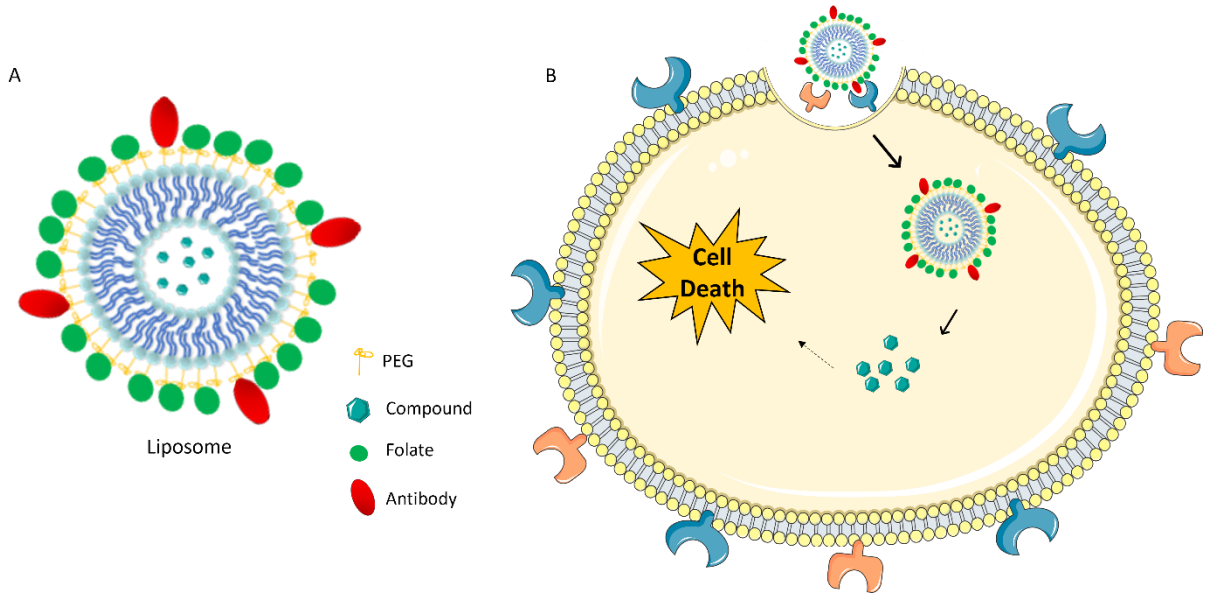


**Figure 15 - Schematic representation of an immunoliposome and its mechanism.** A) Immunoliposomes are created by coupling sdAbs to the liposomal surface. B) Upon treatment with an immunoliposome, the sdAb binds to the target antigen on the cell's surface, and the immunoliposome is internalized. After the payload is released leading to cell death. Images were created with BioRender.com.

With all these expansions in the therapeutic field, novel and promising scaffolds are being introduced with promising features. This opens new perspectives towards the

development of new drug delivery systems using the advantages of these innovative scaffolds, such as sdAbs. As a result, an sdAb can be applied in a wide range of drug delivery systems, such as ADCs, immunotoxins and liposomes, as will be described in this thesis.

## 1.6. Aims and outline

Considering the promising advantages of rabbit derived sdAbs, in the present thesis we aimed to develop a platform for novel sdAb drug delivery system for NHL treatment using the dog as an animal model of human NHL. For this purpose, we explored the development of different drug delivery methods, such as ADCs, immunotoxins and immunoliposomes.

The main goals (Figure 16) of this thesis can be summarized as:

1- Rabbit derived VL single-domains as promising scaffolds to generate antibody-drug conjugates (Chapter 2)

For the development of a new generation of ADCs, we explored the potential of rabbit-derived VL-single domain antibody scaffolds to selectively conjugate a payload towards cysteine at position 80. Firstly, a rabbit sdAb library directed towards canine B-cell lymphoma was subjected to *in vitro* and *in vivo* phage display. This allowed the identification of several highly specific VL-sdAbs, which specifically target canine lymphoma cells *in vitro* and present promising *in vivo* tumor uptake. Then, VL sdAb was selected for SN-38 site-selective payload conjugation via its exposed free Cys80 in order to generate a stable and homogenous C5-DAB-SN-38. Our strategy validated a platform to develop a novel class of ADCs that combine rabbit VL-sdAbs benefits with the advantages of the canine lymphoma model.

2- A novel single-domain antibody immunotoxin for canine B-cell lymphoma treatment (Chapter 3)

Using the potential of rabbit-derived sdAbs, we aimed to develop a new immunotoxin for the treatment of canine B-cell lymphoma. For this purpose, we used the previously characterized and validated sdAb, described in chapter 2. The sdAb was conjugated with the PE38 toxin truncated form and tested in canine B-cell lymphoma. This study validated immunotoxins as a potential treatment for canine lymphoma.

3- Panobinostat loaded liposomes as a drug delivery system for the treatment of canine B-cell lymphoma (Chapter 4)

In order to validate a new drug delivery method for canine lymphoma, we aimed to develop a liposome-based nanocarrier for panobinostat, using a folate-targeted and non-targeted formulation. Both formulations were evaluated in canine lymphoma cells. This work validates liposomes as a potentially effective treatment for canine lymphoma. In the future, our

goal is to conjugate the folate-liposome with our VL sdAb to obtain an immunoliposome with a dual targeting for canine B-cell lymphoma.

This thesis is divided into five Chapters to address and discuss the objectives mentioned above. The first chapter consists of a detailed review of the state-of-the-art literature. Chapters 2 to 4 are based on scientific manuscripts that were either published in international peer-reviewed journals or are currently in revision. The last chapter integrates a discussion, final conclusions and future perspectives.

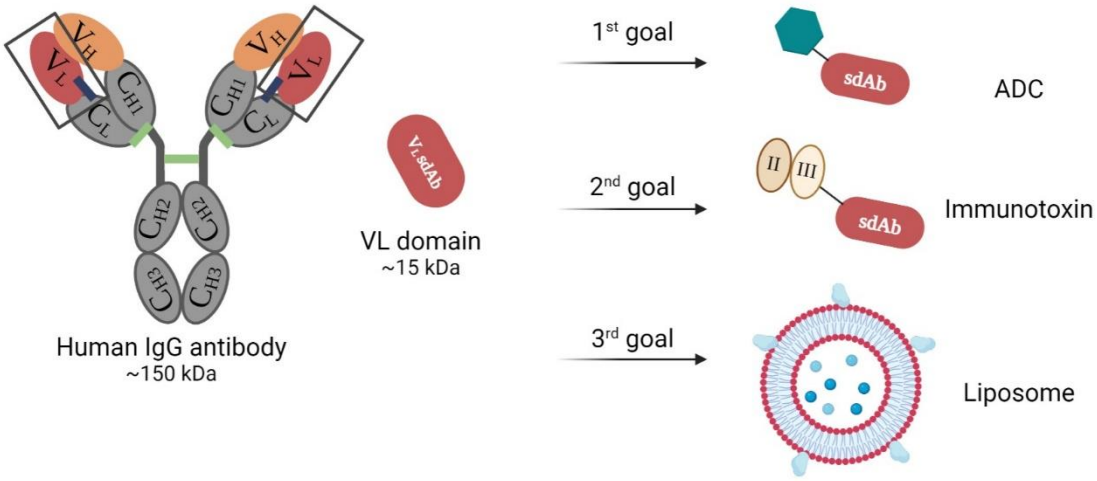


**Figure 16- Goals of the thesis.**

# Chapter 2

## Rabbit derived VL single-domains as promising scaffolds to generate antibody-drug conjugates

Ana S. André[1,2,9], Joana N. R. Dias[1,2,9], Sandra Aguiar[1,2], Sara Nogueira[1,2], Pedro Bule[1,2], Joana Inês Carvalho[3], João P. M. António[3], Marco Cavaco[4], Vera Neves[4], Soraia Oliveira[5], Gonçalo Vicente[6], Belmira Carrapiço[1,2], Berta São Braz[1,2], Barbara Rutgen[7], Lurdes Gano[8], João D. G. Correia[8], Miguel Castanho[4], João Gonçalves[3], Pedro M. P. Gois[3], Solange Gil[1,2], Luís Tavares[1,2] & Frederico Aires-da-Silva[1,2]

[1]CIISA-Centre for Interdisciplinary Research in Animal Health, Faculty of Veterinary Medicine, University of Lisbon, Avenida da Universidade Técnica, 1300-477 Lisbon, Portugal.
[2]Associate Laboratory for Animal and Veterinary Sciences (AL4AnimalS), 1300-477 Lisbon, Portugal.
[3]Research Institute for Medicines (iMed.ULisboa), Faculdade de Farmácia, Universidade de Lisboa, Lisbon, Portugal.
[4]Instituto de Medicina Molecular-João Lobo Antunes, Faculdade de Medicina, Universidade de Lisboa, Avenida Professor Egas Moniz, 1649-028 Lisboa, Portugal.
[5]Technophage SA, Avenida Professor Egas Moniz, 1649-028 Lisboa, Portugal.
[6]Veterinary Teaching Hospital, Faculty of Veterinary Medicine, Universidade de Lisboa, Av. da Universidade Técnica, 1300-477 Lisboa, Portugal.
[7]Department of Pathobiology, Clinical Pathology Unit, University of Veterinary Medicine, Vienna, Austria.
[8]Centro de Ciências e Tecnologias Nucleares, Departamento de Engenharia e Ciências Nucleares, IST, Universidade de Lisboa, Estrada Nacional 10, 2695-066 Bobadela LRS, Portugal.
[9]These authors contributed equally: Ana S. André and Joana N. R. Dias.

Adapted from André AS, Dias JNR, Aguiar S, Nogueira S, Bule P, Carvalho JI, António JPM, Cavaco M, Neves V, Oliveira S, et al. 2023. Rabbit derived VL single-domains as promising scaffolds to generate antibody–drug conjugates. Scientific Reports. 13(1):4837. doi:10.1038/s41598-023-31568-x.

## Abstract

Antibody–drug conjugates (ADCs) are among the fastest-growing classes of therapeutics in oncology. Although ADCs are in the spotlight, they still present significant engineering challenges. Therefore, there is an urgent need to develop more stable and effective ADCs. Most rabbit light chains have an extra disulfide bridge, that links the variable and constant domains, between Cys80 and Cys171, which is not found in the human or mouse. Thus, to develop a new generation of ADCs, we explored the potential of rabbit-derived VL-single-domain antibody scaffolds (sdAbs) to selectively conjugate a payload to Cys80. Hence, a rabbit sdAb library directed towards canine non-Hodgkin lymphoma (cNHL) was subjected to *in vitro* and *in vivo* phage display. This allowed the identification of several highly specific VL-sdAbs, including C5, which specifically target cNHL cells *in vitro* and present promising *in vivo* tumor uptake. C5 was selected for SN-38 site-selective payload conjugation through its exposed free Cys80 to generate a stable and homogenous C5-DAB-SN-38. C5-DAB-SN-38 exhibited potent cytotoxicity activity against cNHL cells while inhibiting DNA-TopoI activity. Overall, our strategy validates a platform to develop a novel class of ADCs that combines the benefits of rabbit VL-sdAb scaffolds and the canine lymphoma model as a powerful framework for clinically translation of novel therapeutics for cancer.

## 2.1. Introduction

The emergence of monoclonal antibodies (mAbs)-based therapies revolutionized cancer treatment by specifically targeting cancer cells. To date, approximately thirty mAbs have been approved for cancer treatment by the US Food and Drug Administration (FDA), however most mAbs do not possess clinical efficacy as single agents and are currently used in combination with conventional chemotherapy (DeVita and Chu 2008; Carter 2016; Sung et al. 2021a). The advances of chemical biology over the last decades allowed progress in a diversity of antitumor molecules (e.g., antibody–drug conjugates, radiopharmaceuticals and immunotoxins) (Weiner 2015). One of the emerging class of mAb-based targeted therapies are a novel class of anticancer treatment agents called antibody–drug conjugates (ADCs). Broadly, an ADC consists of an antibody attached by a linker to a cytotoxic compound. Due to its components, ADCs combine the targeting, pharmacokinetics and biodistribution properties of antibodies with the cytotoxic potency of small molecules (Sievers and Senter 2013). Nevertheless, the journey towards the development of an effective ADC revealed itself to be long and remarkably challenging.

The main challenges in ADC development, including those already on the market, consist of engineering issues that vary from design to production. These problems often lead to heterogeneous products containing a mixture of species with different drug-to-antibody

ratios (DARs) (Joubert et al. 2020; Matsuda and Mendelsohn 2021). This heterogeneity results in variable pharmacokinetic and therapeutic profiles, leading to CMCs (Chemistry, Manufacturing and Controls) challenges (Hamblett et al. 2004; Wang et al. 2005; Joubert et al. 2020). This issue is mostly associated with conventional drug bioconjugation methods that rely on multiple lysine modifications, or on the functionalization of thiols generated by the reduction of interchain disulfide bonds (Hamblett et al. 2004; Wang et al. 2005; Joubert et al. 2020). Conventional mAbs display more than 80 lysine residues, but only 30–40 are accessible to solvent modifications and only 8 cysteines can be modified in a conventional IgG. Moreover, conserved cysteines play a fundamental role in the antibody structure and its use in conjugation often leads to aggregation issues and misfolding (Hamblett et al. 2004; Wang et al. 2005; Shen et al. 2012; Panowski et al. 2014; Joubert et al. 2020). New approaches have been used to overcome these drawbacks, including site-specific conjugation methods, which have resulted in a new generation of more uniform ADCs. Yet, most of these methodologies are not compatible with the scale-up of the manufacturing process required for ADC production. Therefore, further improvements to ADC design and development are required to allow the synthesis of more homogeneous and stable molecules with higher therapeutic indexes (Beck et al. 2017; Tang et al. 2019; Coumans et al. 2020; Boschanski et al. 2021; Zhou et al. 2021). Most ADCs currently in development and on the market consist of a complete IgG antibody. However, the clinical use of these IgG-based products has been hampered by the low penetration in tumor tissues due to their high molecular weight, and by the high manufacturing costs in mammalian cells (Kim and Kim 2015; Joubert et al. 2020). Moreover, there is now evidence that the Fc domain of an IgG may be redundant or even unfavorable for ADCs efficacy (Kim and Kim 2015). In fact, ADCs prolonged half-life promoted by the neonatal Fc receptor (FcRn) increases exposure to healthy tissues, while FcγR cross-reacts with endothelial and immune cells, both of which are biological processes related to off-target toxicity (Joubert et al. 2020). A promising alternative to the conventional immunoglobulin (IgG) to produce ADCs are smaller formats, such as single-domain antibodies (sdAbs), single-chain antibody fragments (scFvs) and minibodies (Gébleux et al. 2015; Jolivet et al. 2022). sdAbs are presently the smallest functional antigen-binding fragments, only consisting of a VH or VL, that can be obtained from conventional IgGs. These small-size scaffolds of about 15 kDa present higher tumor penetration and accessibility to targets not easily reached by large-size conventional mAbs (Iezzi et al. 2018; Chen et al. 2020; Nessler et al. 2020). Furthermore, their faster clearance rate compared to the intact IgG, may be advantageous in cases where the risk of toxicity in healthy tissues increases with prolonged exposure (Hamblett et al. 2004). In addition to their reduced size, sdAbs also present higher stability and solubility, while decreasing the number of potentially immunogenic epitopes (Aires da Silva et al. 2008). Over the past years, we have been showing the great potential of rabbit-derived sdAbs for several

therapeutic applications (Silva et al. 2004; Goncalves and Silva 2008 Nov 13; Aires-Da-Silva et al. 2014 May 8; Cunha-Santos et al. 2016; Gouveia et al. 2017; Aguiar et al. 2021; Dias et al. 2022). Rabbit-derived sdAbs have all the promising properties of smaller antibody fragments and, in addition, have a unique characteristic in their light chain variable domains (VL) that make them promising scaffolds to develop ADCs (Figure 17A).

Most rabbit kappa light chains have an unusual disulfide bridge that joins the variable and constant domains, usually through cysteine residues at positions 80 and 171 (Figure 17A). This disulfide bridge links framework region 3 of the variable kappa light chain domain with the constant kappa light chain domain, a linkage not seen in mouse or human antibodies. Therefore, when the VL sdAb is isolated the conserved cysteine at position 80 (Cys80, normally paired with Cys171 in an IgG format) becomes exposed at the protein surface and its sulfhydryl group becomes free to be explored to selectively conjugate a chemical payload, without requiring further genetic engineering manipulation (McCartney-Francis et al. 1984; Popkov et al. 2003; Goncalves and Silva 2008 Nov 13; Weber et al. 2017). Furthermore, rabbit derived VL sdAbs present promising advantages in terms of manufacturing costs and downstream process since they can be expressed in bacterial systems and purified by protein L. Within this context, the present study aimed to explore the properties of rabbit-derived VL sdAbs to develop a new generation of ADCs for cancer treatment. For this purpose, we developed a VL sdAb ADC with a potent cytotoxic payload, SN-38, that was conjugated to the free Cys80. As illustrated in Figure 17B, to validate our strategy, we developed an ADC against canine non-Hodgkin lymphoma (cNHL), an animal model recently proposed as a powerful framework for clinically relevant translation of novel therapeutic molecules and approaches.

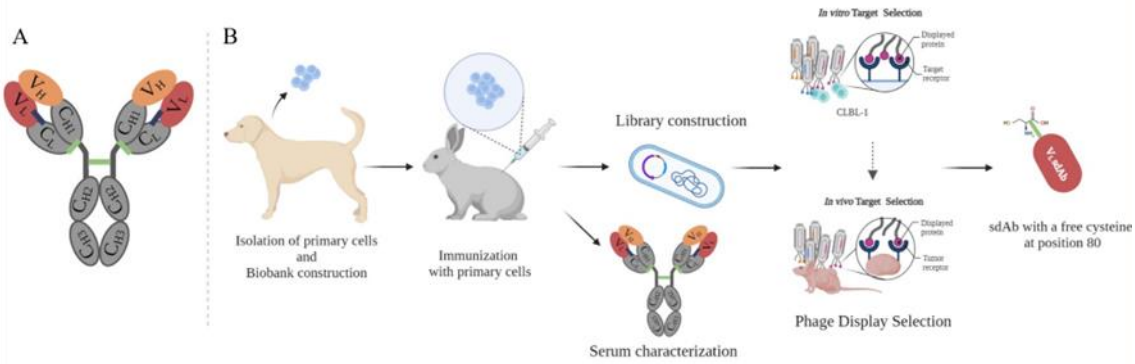


**Figure 17- A) Representation of a rabbit IgG antibody.** In the present study, we aimed to explore the potential of rabbit-derived VL-sdAbs to develop a new generation of ADCs. Rabbit IgG contains two identical light chains paired with two identical heavy chains. The light chain is composed of an N-terminal variable domain (VL) (red), followed by one constant domain ($C_L$). The heavy chain consists of an N-terminal variable domain ($V_H$) (orange), followed by three constant domains ($C_{H1}$, $C_{H2}$ and $C_{H3}$). $C_{H1}$ and $C_{H2}$ are linked via a flexible hinge region and contains three disulfide-bridges (green). Most rabbit kappa light chains of the K1 isotype have an unusual disulfide bridge (blue) that joins the variable and constant domains, usually through cysteine residues at positions 80 and 171. This disulfide bridge links framework region 3 of the variable kappa light chain domain with the constant kappa light chain domain, a linkage not seen in mouse or human antibodies. Thus, when the VL-sdAb is isolated the conserved cysteine at position 80 (Cys80, normally paired with Cys171 in an IgG format) becomes exposed at the protein surface and its sulfhydryl group becomes free to be explored to selectively conjugate a chemical payload, without requiring further genetic engineering manipulation. **B) Representation of the antibody selection process**. Aiming to develop a new ADC molecule, we firstly immunized one female New Zealand white rabbit with lymph node primary cells derived from a canine multicentric lymphoma biobank previously established[34]. To induce a strong immune response, the rabbit was immunized and boosted with $1x10^7$ of cNHL of primary cells isolated from the lymph node of ID5 and ID6 patients diagnosed with Diffuse Large B Cell Lymphoma (DLBCL). Tumor cells isolated from the patients were thawed, washed and resuspended in PBS. Lymph nodes cNHL primary cells were administered subcutaneously at 2-3 weeks for 3 months. Following the rabbit immunization and validation of the immune response, an immune VL-sdAb library was constructed. To select the best antibodies for NHL targeting, sdAb library was used for an in vitro whole cell and in vivo phage display in a xenograft CLBL-1 murine model. After, the phage display, NGS and sanger sequencing analysis a panel of VL-sdAbs were selected. The three most promising VL-sdAbs were characterized by flow cytometry and immunofluorescence microscopy and then the most promising VL sdAb was chosen to be conjugated to the SN-38 using the free exposed Cys80.

## 2.2. Results

### 2.2.1. Rabbit immunization, antibody library construction and phage display selection

Aiming to develop a highly specific rabbit-derived VL sdAb against cNHL, a whole-cell rabbit immunization strategy, antibody library construction, and phage display selection were performed, as depicted in Figure 17B. To induce a strong and specific immune response against cNHL receptors one female New Zealand rabbit was immunized with a poll of two

isolated cNHL primary cells (ID5 and ID6) from a canine multicentric lymphoma biobank previously established and characterized by our group (Dias et al. 2019a). The immunization response, antibody titers and specificity were monitored by cell ELISA and flow cytometry. As shown in Figure 18A, the results showed that the rabbit presented a final bleed serum with a high specificity against both cNHL primary cells (ID5 and ID6) and a canine B-cell lymphoma stable cell line (CLBL-1) (Rütgen et al. 2010; Rütgen et al. 2012). Furthermore, these data demonstrated that immunizations resulted in a strong immune response with a high serum titer (1/64,000), contrarily to the pre-bleed serum. The flow cytometry analysis confirmed the results obtained by ELISA (Figure 18B). Following the rabbit cell-immunization and validation of the immune response towards cNHL cells, our major goal was to select the most promising antibodies regarding cellular internalization and tumor uptake properties. For that purpose, an immune VL sdAb library was constructed as described in the methods sections and originating a phage displayed library with a diversity of $3.4 \times 10^8$. Selection of highly specific VL sdAbs with suitable properties for the development of ADCs was then performed using an *in vitro* and *in vivo* phage display screening (Fig. 19A). Firstly, a subtractive *in vitro* cell phage display was performed using the HEK293T cell line, which does not express the cNHL antigens. This cell phage display screening was based on previous Carlos Barbas' (Barbas III et al. 2001; Popkov et al. 2004) and our own studies (Dias et al. 2022) and consisted in a whole-cell selection protocol with negative and positive selection steps (subtractive phage display), implemented to remove antibodies reacting with common antigens. The CLBL-1 cell line was used for the positive selection due to its stable expression of cNHL antigens. Three pannings were performed and over the course of selection, stringency was incremented by increasing the number of washes in order to collect the VL-phages with greater target affinity and specificity. Two types of elution methods were used to select binders and internalized antibodies as described in the methods section. As shown in Figure 16B, and as expected, the three *in vitro* phage display pannings resulted in a lower number of VL phages in the output titers compared to the input titers (~ $10^{11–12}$ input to ~ $10^{3–4}$ output pfu). Furthermore, the biopannings profile indicates that the *in vitro* phage display successfully led to the enrichment for highly specific cNHL VL sdAbs with binding and cellular internalization properties. Following the *in vitro* phage display selection, a final *in vivo* phage display panning was performed in a murine xenograft cNHL model (Figure 19A). The output phages recovered from the 3$^{rd}$ *in vitro* panning was recovered, reamplified and tailed vein injected in a xenograft CLBL-1 murine model as previously described (Dias et al. 2018). The phages were recovered to retrieve sdAbs that specifically targeted and were uptaken by the grafted cNHL tumors. By allowing the enriched antibody panel to circulate in the mouse and collecting VL phages that targeted the xenograft tumor, we expected to select antibodies that met the defined biological effect, confirming the *in vivo* availability of the epitopes and tumor targeting. At the end, the phages recovered

presented a titer of 1.2 x $10^6$ of VL sdAb binders and 2.3 x $10^4$ of VL sdAb internalizers (phages/mL), which reflected a high enrichment towards phages that effectively target cNHL.

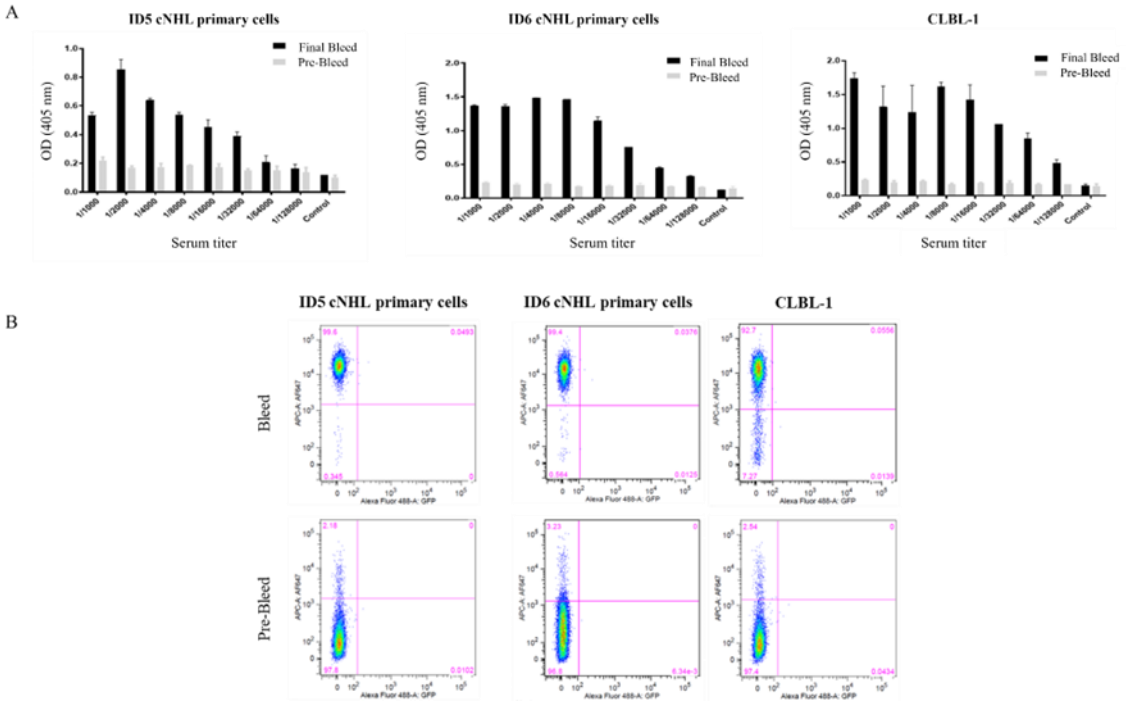


**Figure 18 - Characterization of rabbit immune response.** To evaluate the rabbit immune response, antibody titers were monitored by a cell ELISA and flow cytometry analysis using the cNHL primary cells and CLBL-1 cell line. Pre-bleed sera was used as control. A) Serum titration by ELISA. 5 × $10^4$ cells were incubated with serial dilutions of rabbit serum (from 1/1000 to 1/32000). Cells were incubated with secondary antibody goat-α anti-rabbit IgG-Fc specific HRP at 1/3000. The rabbit presented a high response against cNHL primary cells and CLBL-1 cell line with a high serum titer (1/64000), in opposition to the pre-bleed serum. B) Binding properties against cNHL cells were also analyzed by flow cytometry. Cells were incubated with the rabbit pre-bleed and final bleed (1/3000) and with the secondary antibody Alexa Fluor 647 Goat Anti-Rabbit IgG (1/10000). The flow cytometry analysis confirmed a high serum activity of the rabbit against the primary cNHL cells (ID5 and ID6 patient cells) and CLBL-1 cell line.

### 2.2.2. Screening for VL sdAb towards cNHL targeting

After the phage display selection, to express and select the best anti-cNHL VL sdAbs, phagemid DNA derived from the *in vivo* output selection was cloned and transformed as described in the methods section. Then, individual clones were auto-induced, and the supernatant tested in ELISA assays against CLBL-1 and Jurkat cell extracts. To select the best lead candidates, three parameters were evaluated: binding against cNHL, expression yields and unspecific binding. Several clones were screened and the VL sdAbs that revealed a stronger signal against CLBL-1 cells were selected (Figure 19C). After selection, to

characterize the selected clones, the eighteen best lead candidates were analyzed by sanger sequencing. The sequences were analyzed as described in the methods section. After the alignment of the eighteen sequences, we concluded that some of the clone sequences were identical, leading to six different clones (data not shown). To get further insights of the enriched sequences during the *in vivo* phage display selection, we performed next generation sequencing (NGS) of the biopanning repertoires. NGS allows massive sequence analysis of the panning population, enabling a genomic assessment of the library diversity and frequency of each clone. Two samples were sequenced: biopanning from the CLBL-1 tumor models and initial immune VL sdAb cNHL library (Figure 19D). Upon bioinformatic analysis of the NGS data, we were able to determine the diversity of each sample and identify the most represented clones. A total of 34880 and 48864 sequences were obtained for the biopanning from the CLBL-1 tumors and cNHL library, respectively. The number of singletons, consisting of the sequences with a single occurrence, varied between samples, ranging from 76.8% in the library, and 33.3% in the *in vivo* biopanning from the CLBL-1. Through the comparison of the sequence prevalence between the biopannings and the library, we were able to verify that the number of occurrences in each sequence was higher in the biopanning clones. These results evidenced the specificity of the phage display selection, which resulted in the enrichment of sdAb clones among the highly diverse library. The comparison of ELISA data, sanger sequencing and NGS analysis allowed to select the three best clones (A12, B12 and C5) that were produced and purified. Due to its binding characteristics and production properties (protein yields of 8-10 mg/L), C5 was chosen to be thoroughly characterized and used in the development of the ADC.

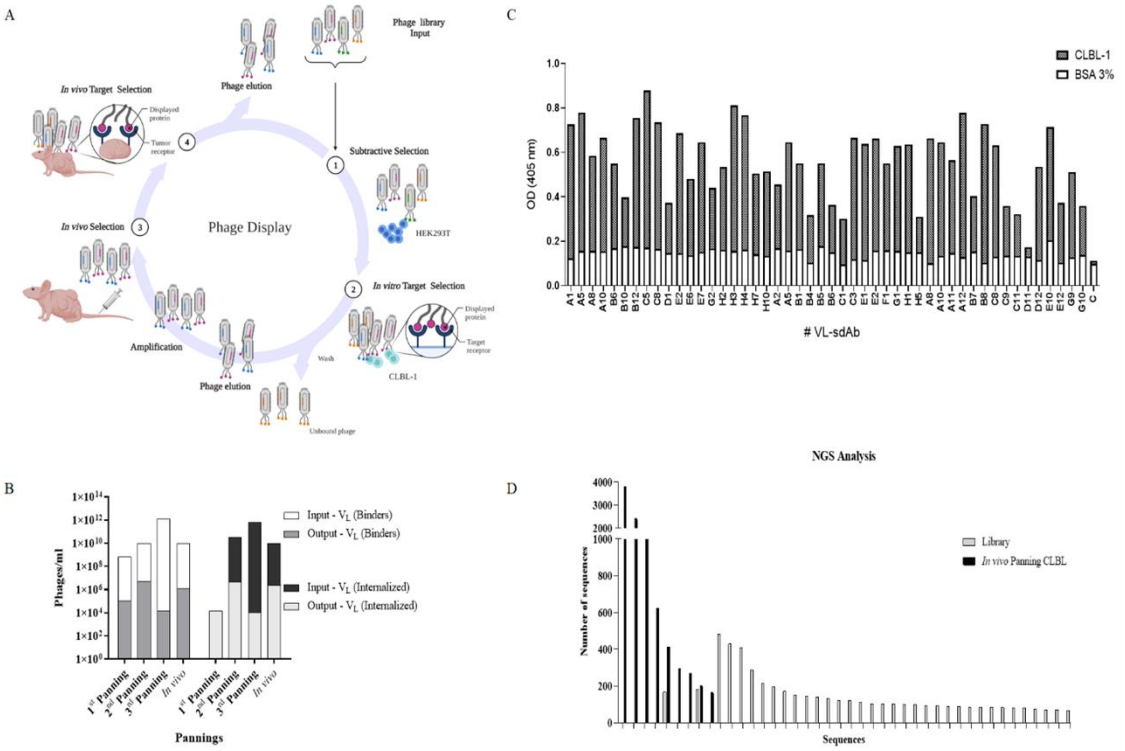


**Figure 19 - Phage display selection and screening for sdAb for cNHL targeting**. A and B) To select the best antibodies for NHL targeting, the constructed sdAb immune library with a diversity of $3.4 \times 10^8$ was used for an *in vitro* whole cell and *in vivo* phage display in a xenograft CLBL-1 murine model. A) Phage library was first panned using a subtractive cell phage display protocol on HEK293T cells followed by a positive selection on CLBL-1 cells. Three rounds of *in vitro* selections were performed, and an additional panning was performed *in vivo* in a xenograft CLBL-1 murine model. Briefly, the output phages from the 3rd *in vitro* panning were recovered, reamplified and tailed vein injected in a xenograft murine cNHL model. After 60 min, the mice were euthanized, and the phages recovered from the tumor. Two different elution methods were performed to recover binder and internalized antibodies. B) The three *in vitro* pannings resulted in a lower number of phages in the output titers compared to the input titers (~$10^{11\text{-}12}$ input pfu to ~$10^{3\text{-}4}$ output pfu). At the end, the *in vivo* panning presented a titer of $1.2 \times 10^6$ of VL sdAbs binders and $2.3 \times 10^4$ of VL sdAbs internalizers (phages/mL), indicating a high enrichment towards the phages to target cNHL. C) To select the most promising VL sdAbs, individual clones were autoinduced and the supernatant tested in ELISA assays against CLBL-1 extracts and 3% BSA. The clones that revealed a stronger signal against CLBL-1 were selected. D) To characterize in more detail the enriched sequences during the *in vivo* phage display, next generation sequencing was performed. Two samples were sequenced: biopanning from CLBL-1 tumor models and initial immune library. Upon bioinformatic analysis, we identified the diversity of each sample and the most represented clones. The number of occurrences was higher in biopannings compared with the initial library, supporting the specificity of the phage display selection that diminishes the high diversity of clones present in the library.

### 2.2.3. Binding and internalization characterization of C5 VL sdAb

The C5 binding and cellular internalization properties towards CLBL-1 cells were studied by flow cytometry and immunofluorescence. For flow cytometry, C5 was incubated with CLBL-1 cells as described in the methods section. As demonstrated in Figure 20A, C5

specifically binds to the CLBL-1 cells. On the contrary, no binding interaction of C5 with Jurkat cells, a leukemic T-cell line, was observed (Figure 20B). Live/dead reagent was used to exclude dead cells and the background noise was also evaluated in the control with the secondary antibody (data not shown). To better characterize the binding of the C5 to the CLBL-1 cells, we further evaluated C5 cellular internalization properties using an immunofluorescence assay. As shown in Figure 20C, a high density of Alexa Fluor-488 labeled C5 was observed in the perinuclear region. Conversely, there was no detectable fluorescence in the control sample image nor in Jurkat cells (Figure 20D). Thus, these data confirmed the C5 binding to the CLBL-1 cells and its internalization into the cytoplasm. This cellular internalization feature is essential to develop an efficacious ADC.

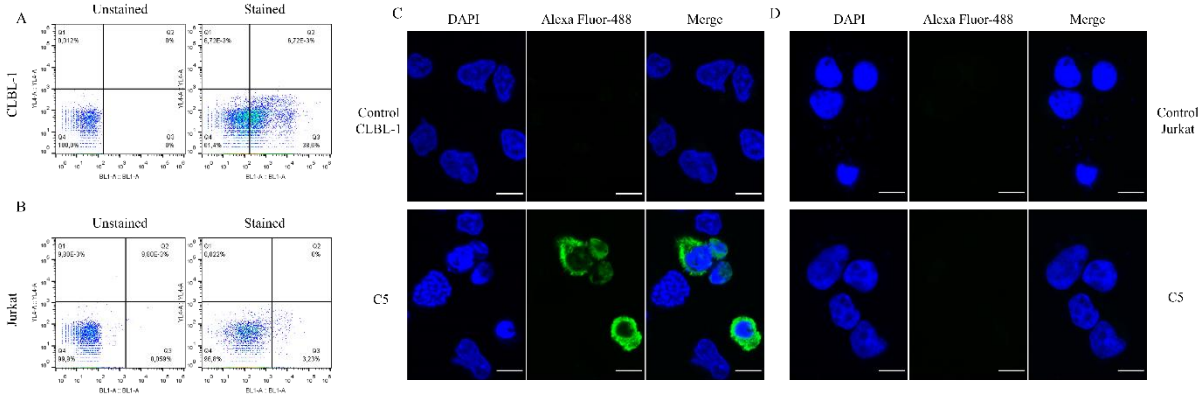


**Figure 20 - Binding and internalization characterization of C5 VL sdAb.** C5 binding and internalization properties against CLBL-1 and Jurkat cells were evaluated by flow cytometry and immunofluorescence. A) For flow cytometry analysis, 1 × $10^6$ of CLBL-1 cells were incubated with Live/Dead reagents for 30 min. Then, 3 µM of C5 were incubated with the cells for 90 min at 37° C. After, cells were washed, fixed with PFA, permeabilized and incubated for 30 min with anti-HA antibody (1/50), washed twice and incubated with anti-rat Alexa Fluor-488 (1/250). C5 has demonstrated to bind to the CLBL-1 cells. B) 1 × $10^6$ Jurkat cells were exposed to the same protocol as CLBL-1 cells. By contrast, no binding of C5 was detected with Jurkat cells. C) To confirm the binding of C5 to the CLBL-1 verified by flow cytometry, we evaluated its distribution on the cells by immunofluorescence assay. 1 × $10^6$ of CLBL-1 and Jurkat cells were plated on ibidi µ-Slide 8 Well Glass Bottom and incubated with 3 µM of C5 for 90 min. After incubation, cells were washed, fixed, permeabilized, blocked and incubated overnight with rat anti-HA (1/50). Next day, cells were washed and incubated with anti-rat Alexa Fluor-488 (1/500). At the end, DAPI Vectashield was added to the cells. It is possible to observe a high density of C5 labeled with Alexa Fluor-488 in the perinuclear region. D) In contrast, there is no detectable fluorescence in the control image, nor in the presence of the Jurkat cells. Representative microphotographs with C5 (green) and DAPI stained-nuclei (blue) are shown.

### 2.2.4. Biodistribution studies of C5 VL sdAb

To evaluate the tumor uptake and pharmacokinetic profile of the selected C5, a biodistribution assay was conducted as described in the methods section. The obtained biodistribution profile of the labeled 99mTc-C5, expressed as % ID/g, is presented in Figure 21A and B, showing that tumor uptake was around 1.5% ID/g at 15 min, decreasing to 1% at 3 h after injection. In addition, apart from the liver and spleen, the biodistribution data revealed a rapid elimination from blood and major organs, with low levels of activity. These results were also confirmed by western blot analysis that established the presence of the C5 in the CLBL-1 xenograft tumors (Figure 21C). Thus, the obtained data demonstrated that C5 VL sdAb presented a favorable tumor uptake and biodistribution profile, making it a promising candidate to develop our ADC.

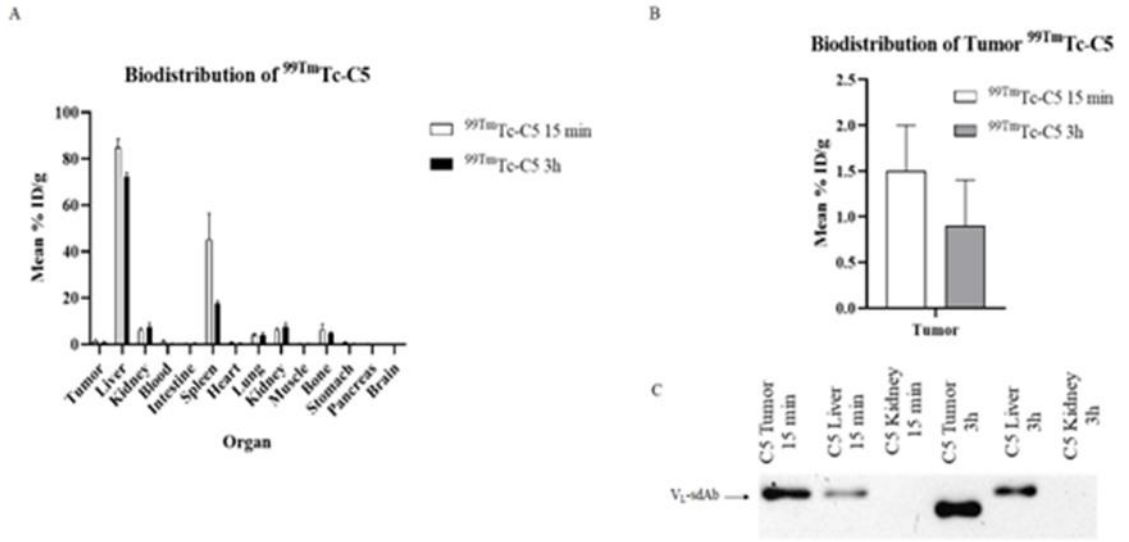


**Figure 21 - Biodistribution profile of $^{99Tm}$Tc-C5**. To evaluate the tumoral uptake and pharmacokinetic profile of the C5 VL sdAb, a biodistribution assay was performed on a xenograft model of cNHL at two different time points (15 min and 3 h). C5 was radiolabeled with $^{99m}Tc(CO)_3(H_2O)_3$ and intravenously injected in the tail vein of a xenograft mouse model of cNHL. Mice were sacrificed at 15 min and 3 h, and the radioactivity of each organ was measured. The activity in each organ was calculated and expressed as a percentage of injected radioactivity dose per gram of organ or tissue (% ID/g). A and B) The results show that the tumoral uptake was around 1.5±0.5 % ID/g at 15 min, diminishing to 1% at 3 h after injection. A fast elimination in the major organs was noticed, with exception of the liver and spleen. C) The results were also confirmed by western blot analysis. C5 was recovered from the mice organs by immunoprecipitation with His beads and analysed by western blot. Samples were loaded in a 15% SDS page acrylamide gel. Following gel transfer and blocking, the membrane was incubated with HRP-conjugated anti-His antibody (1/3000). This analysis confirmed the presence of the C5 VL sdAb in CLBL-1 xenograft tumors at 15 min and 3 h. Representative blots are shown.

### 2.2.5. Development of C5-DAB-SN-38 and evaluation of its activity on cNHL cells

Aiming to develop our ADC by exploring free cysteine residues, we started by modeling the tridimensional structure of C5 VL sdAb using a protein structure prediction software. The obtained structural model revealed a traditional immunoglobulin domain fold composed of eight antiparallel β-strands arranged into two β-sheets, which are connected by a single disulfide bond formed between Cys23 and Cys90, forming a β- sandwich (Figure 22A). The three complementarity-determining regions (CDRs) motifs are easily identifiable, with CDR3 having the largest area of exposed surface. Importantly, the structure shows the presence of a third cysteine (Cys80) on its surface with a free sulfhydryl group, which is normally involved in a rabbit-unique interdomain disulfide bond with another cysteine on the CL domain (McCartney-Francis et al. 1984; Popkov et al. 2003; Weber et al. 2017; Braz Gonçalves and Silva). As predicted, by isolating the VL domain, Cys80 becomes exposed at the protein surface and its sulfhydryl group becomes free to be used in cysteine-based conjugation strategies. As such, C5 single free cysteine was modified with DAB-SN-38, a molecule containing the cytotoxic drug SN-38 and a maleimide group, connected by a ROS-responsive diazaborine linker (Figure 22B-D). C5 was successfully converted in the homogenous targeting drug conjugate, C5-DAB-SN-38. The expected DAR of 1 was confirmed by reverse phase-HPLC and displayed >95% of single modified sdAb (Figure 23). The *in vitro* cytotoxicity of C5-DAB-SN-38 was evaluated on cNHL cells and on irrelevant cells. For that, a cell viability assay on CLBL-1 and Jurkat cells was conducted. C5-DAB-SN-38 exhibited a dose-dependent cytotoxicity on cNHL cells proliferation (Figure 24A). Importantly, the EC50 value of C5-DAB-SN-38 (10.2 nM; 95% CI 9.4-11.1) was similar to that of SN-38 (4.7 nM; 95% CI 4.2-5.2), showing that conjugation does not interfere with the cytotoxicity of SN-38 (Figure 24C). By contrast, C5-DAB-SN-38 had no effect in the proliferation of Jurkat cells, a leukemic T-cell line, which demonstrates the ability of C5-DAB-SN-38 to recognize selectively the target cells (Figure 24B). In addition, the C5 alone does not affect cell proliferation in both cell lines (Figure 24A and B). The primary mechanism of cell death induced by SN-38 is the inhibition of DNA-Topo I activity, preventing the conversion of supercoiled DNA into a relaxed DNA form. Thus, to confirm if the underlying mechanism of action responsible for the cytotoxic effects of C5-DAB-SN-38 on cNHL cells is maintained, we evaluated its activity on DNA-Topo I. As shown in Figure 24D, C5-DAB-SN-38 inhibits DNA-Topo I as evidenced by the presence of the supercoiled DNA form. In contrast, neither C5 nor the vehicle were able to alter the enzyme activity, suggesting that C5-DAB-SN-38 effects and its mechanism of action are related to SN-38 cytotoxicity.

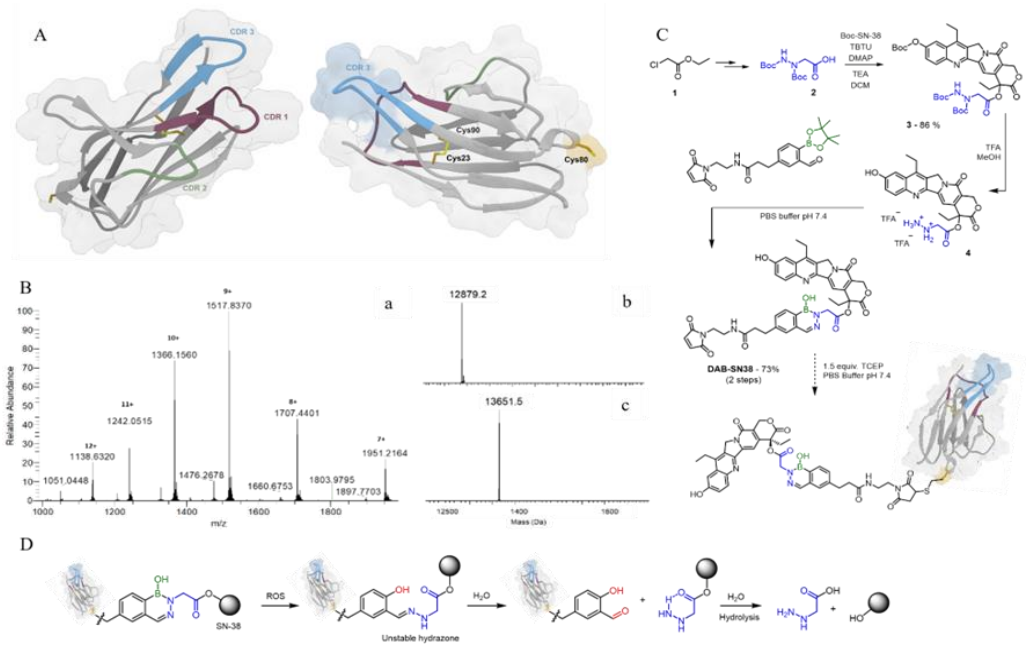


**Figure 22 - A) Ribbon representation of C5 sdAb's predicted 3D structure.** The complementarity-determining regions (CDRs) domains have been highlighted in purple (CDR1), green (CDR2) and blue (CDR3). The side chain atoms are shown in stick representation and colored in yellow. The van der Waals surface is depicted in transparent coloring. The surfaces of CDR3 and Cys80 have been highlighted with blue and yellow coloring, respectively. CDR and amino acid numbering were done according to Kabat et al. B) a) High-resolution mass spectra of conjugate C5-DAB-SN-38. To a PBS pH 7.4 solution containing C5 (10 µM) and TCEP (1.5 equiv., 3.5 mM), DAB (20 equiv., 9 mM, DMSO) was added and the solution was mixed during 1.5 h at 25 ºC. The expected conjugate was evaluated after 1.5 hours by High-Resolution Mass Spectrometry, recorded in a Thermo Scientific Q Exactive hybrid quadrupole-Orbitrap mass spectrometer (Thermo Scientific Q Exactive Plus). The final immunoconjugate VL-DAB-SN38 was detected. The mass spectra were deconvoluted using MagTran software. b) Deconvoluted high-resolution mass spectra of C5 (12879.2 Da). c) Deconvoluted high-resolution mass spectra of conjugate C5-DAB-SN-38 (13651.5 Da). C) Bioconjugation of C5-DAB-SN-38. Conjugate C5-DAB-SN-38 obtained from C5 cysteine modification at PBS buffer at pH 7.4 (10 µM) at room temperature. D) Oxidation and self-immolative mechanism of ROS-responsive diazaborine linker.

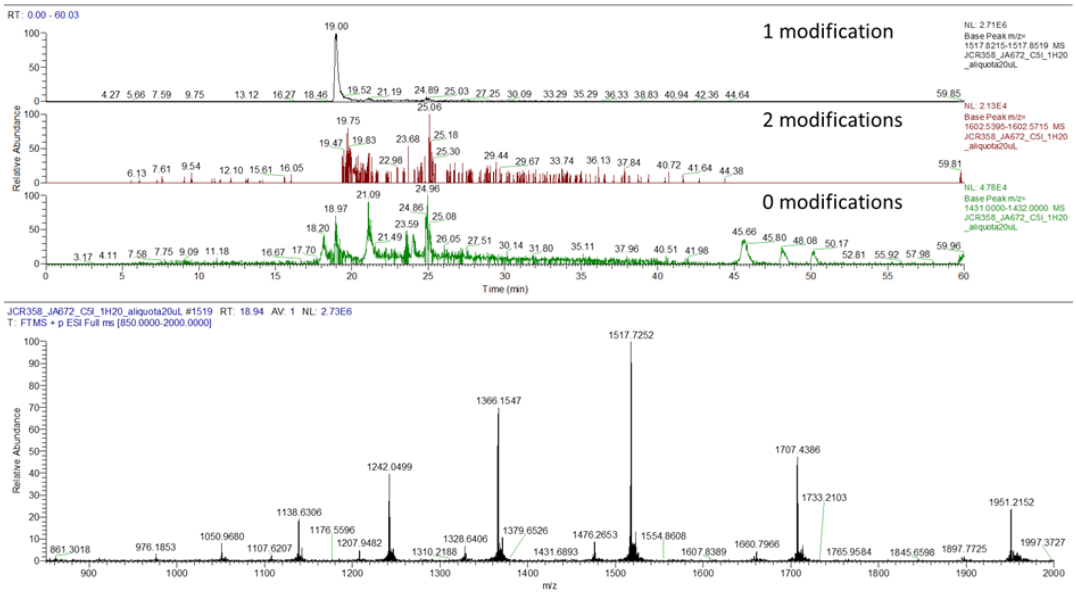


**Figure 23 - Evaluation of the DAR of C5-DAB-SN-38 by HPLC-MS.** Extracted Ion Current chromatogram of: (Top) Single-modified, (Middle) Double-modified and (Bottom) unmodified C5. EIC of the single modification displays an intensity of $2.71 \times 10^6$, compared to $10^4$ intensities of double-modified and unmodified C5. These numbers suggest >95% of single-modified C5, validating the presence of a homogenous conjugate.

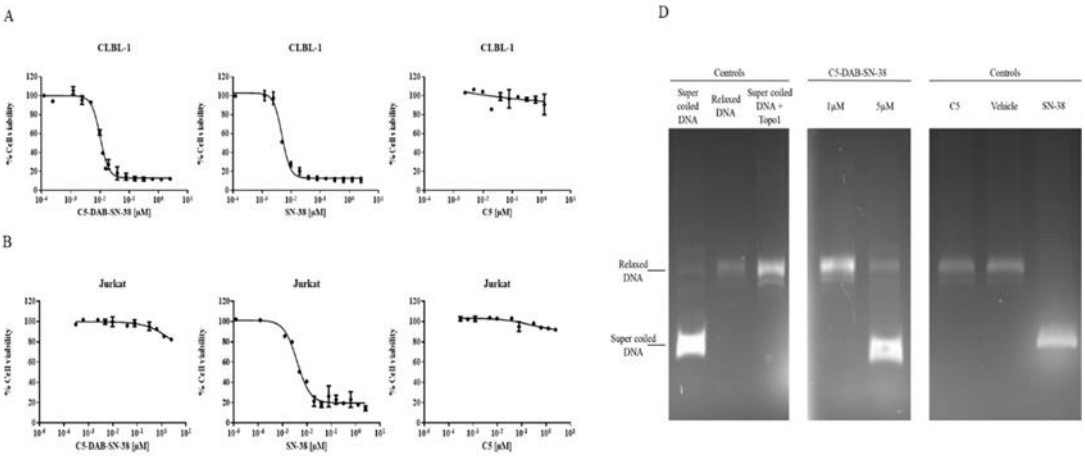


C

| $IC_{50}$ (nM) | CLBL-1 | Jurkat |
|---|---|---|
| C5-DAB-SN-38 | 10.2 (95% CI 9.4-11.1) | NA |
| SN-38 | 4.8 (95% CI 4.4-5.3) | 3.9 (95% CI 3.0-5.1) |
| C5 | NA | NA |

**Figure 24 - Cytotoxic effects of C5-DAB-SN-38.** To determine the effect of C5-DAB-SN-38 on CLBL-1 and Jurkat cells, a cell viability assay was performed using the WST-1 reagent. 6 × $10^4$ cells were seeded and treated with increasing amounts (2.5 μM to 12.5 nM) of each compound (C5, C5-DAB-SN-38 and SN-38). After 48 h treatment, cell viability was assessed. A) C5-DAB-SN-38 demonstrated a dose-dependent toxicity effect on cNHL cells. B) On the other hand, C5-DAB-SN-38 had no effect on Jurkat cells, proving the specificity of the ADC. C5 was used as control. C) Best-fit EC50 values of each formulation were calculated using GraphPad Prism software (version 9.2.0, San Diego, CA, USA) using the log (inhibitor) vs response (variable slope) function. D) Effects of C5-DAB-SN-38 on DNA TopoI activity. To evaluate the effects of C5-DAB-SN-38 on DNA Topo I, we evaluated its activity using the Human Topoisomerase I Assay Kit. After incubation of C5-DAB-SN-38 with 1× reaction buffer and 10 U of Topo I for 1 h at 37° C, the supercoiled DNA was added. To stop the reaction, stop loading buffer was added. DNA TopoI activity was visualized by 1% agarose gel electrophoresis attained with ethidium bromide. Relaxed DNA indicated TopoI activity, while supercoiled DNA indicated an inhibition. The presence of C5-DAB-SN-38 at higher concentrations inhibits DNA TopoI in a dose dependent manner, empathizing the effect of SN-38, present on the ADC, as a cause of cell death. Relaxed DNA and supercoiled DNA were used as positive/negative controls. C5 and SN-38 were also used as controls.

## 2.3. Discussion

Following decades of research and troubleshooting, several technological advances and a better understanding of the mechanisms underlying ADC activity have resulted in the development of multiple agents that provide significant therapeutic benefit to cancer patients. While advances in this area have been encouraging, the clinical translation of these innovative therapeutics has been hindered by several hurdles related to the complexity of their clinical development. The approval of eight new ADCs over the last five years provided a renewed interest in the potential of this class of drugs. However, the overall low approval rate continues to highlight the need for novel strategies to maximize the potential benefit that ADCs can

provide to cancer patients (Tong et al. 2021).Thus, several additional therapeutic candidates and new approaches on ADC development are being actively investigated, some of which have the potential to change cancer therapy strategies. One of the most promising approaches to improve the efficiency of ADC is exploring alternative antibody formats for targeted payload delivery. Over the past few years, we have shown the great potential of rabbit-derived sdAbs for several therapeutic applications, as an alternative to conventional mAbs (Silva et al. 2004; Goncalves and Silva 2008; Aires-Da-Silva et al. 2014; Cunha-Santos et al. 2016; Gouveia et al. 2017; Aguiar et al. 2021; Dias et al. 2022). Due to their reduced size and low complexity, as well as the lack of the Fc region, sdAbs have been able to achieve improved tumour penetration and *in vivo* tolerance compared to traditional ADCs (Shen et al. 2012; Nessler et al. 2020; Aguiar et al. 2021). Importantly, rabbit VL domains possess a unique intrachain disulfide bridge between cysteine 80 in VL and cysteine 171 in CL, that is not found in human or mouse VL domains. Thus, an isolated VL sdAb presents a free exposed cysteine at position 80 that can be used for payload conjugation without any modification (McCartney-Francis et al. 1984; Popkov et al. 2003; Goncalves and Silva 2008; Weber et al. 2017). This unique characteristic makes rabbit VL sdAbs promising scaffolds to integrate a homogeneous and stable ADC, overcoming the heterogeneity problems associated with conventional drug bioconjugation methods, while surpassing manufacturing costs associated with novel site-specific conjugation methods. Within this context, in the present study we aimed to explore the properties of rabbit-derived VL sdAbs to develop a new generation of highly selective and potent ADC for cancer treatment. To validate our antibody platform, we used the canine lymphoma as an animal model of human NHL. Owing to remarkable similarities with its human counterpart, the canine lymphoma model has been proposed as a powerful framework for rapid and clinically relevant translation of novel immunotherapies. Naturally occurring NHL in dogs present many clinical, pathological, immunologic, molecular, diagnostic and therapeutic similarities to those observed in humans, that are difficult to reproduce in conventional preclinical models. This allows studying the complex immune interactions during the course of treatment while also addressing long-term efficacy and toxicity of cancer immunotherapies (Park et al. 2016). Furthermore, the use of dogs as a model in cancer drug discovery can be mutually beneficial for all parties, since the therapeutics for cNHL are rarely curative and often limited (Marconato et al. 2013; Dias et al. 2021). Hence, in the present study, we aimed to develop a novel class of rabbit-derived VL sdAb-based ADC for the treatment of cNHL, that serves as an animal model for hNHL. To achieve this, a highly diverse immune library of rabbit VL sdAbs against primary canine NHL cells was successfully constructed to ensure the presence of antibodies against different targets in the disease setting. Due to their unique B-cell ontogeny, rabbit antibody-derived libraries present a highly distinctive and diverse antibody repertoire, rich in *in vivo* pruned binders of high diversity, specificity and affinity (Weber et al.

2017). Importantly, rabbits are evolutionarily distant from mice and rats, so epitopes that are not immunogenic in rodents can be recognized by rabbit mAbs, increasing the targetable epitopes and facilitating the generation of mAbs that cross react with other species - a key aspect for clinical translation. Our data showed that rabbit immunizations with intact B-cell canine non-Hodgkin lymphoma primary cells resulted in a specific and selective high-tittered antiserum against cNHL epitopes. The strong and specific response generated allowed the construction of an antibody library highly diverse and representative ($3.4 \times 10^8$). Thereafter, a strategy of an *in vitro* whole-cell phage display, followed by an *in vivo* phage display in a cNHL xenograft murine model, was used to select the best sdAbs targeting antigens in their natural conformation and tumor microenvironment. This methodology allowed the selection of both VL-phages that bind and internalize to the tumor cells. One of the main benefits of this *in vivo* selection is its innate negative selection feature. This enables the reduction of the off-target tissue and protein interactions by eliminating non-specific ligands, enriching the recovery of specific ligands that specifically target the tumor. Despite its advantages, *in vivo* phage display selection remains relatively unexplored (Gustafson et al. 2018; André et al. 2022). To date, few studies on cancer models have been reported. Soendergaard et al. used *in vivo* phage display selection to identify an ovarian cancer targeting peptide (Soendergaard et al. 2014). Another study of Veleva et al., applied a combination of *in vitro* and *in vivo* screening to isolate a peptide that is selective for circulating bone marrow derived cells from angiogenic Lewis Lung carcinoma tumors (Veleva et al. 2011). To the best of our knowledge, this is the first time that an *in vivo* selection has been applied in the selection of sdAbs against lymphoma and for ADC development. Overall, the obtained results reinforce *in vivo* phage display as a powerful technology that has the potential to expand the repertoire of targetable tumor receptors, while simultaneously confirms the availability of the *in vivo* epitope and generates highly specific antibodies for tumor targeting. After obtaining a specific pool of sdAbs for cNHL targets by phage display selection, we selected the best VL sdAb candidates based on their binding activity to cNHL targets and expression via ELISA screening. This study was complemented with a Sanger and NGS analysis of the recovered *in vivo* biopanning with the initial library. By investigating the prevalence of each sequence in each sample, NGS analysis revealed the specific enrichment attained by the phage display selection and reinforced the ELISA results proposing the selection of C5 VL-sdAb as the most promising clone. To confirm C5 suitability as our ADC targeting moiety, its binding and cellular internalization on cNHL cells was further characterized by flow cytometry and immunofluorescence. Overall, these results proved the specificity of the interaction between the sdAb and cNHL cells and the subsequent complex internalization, which are key attributes for the success of an ADC. Importantly, the biodistribution studies demonstrated that C5 exhibited a good tumor uptake with an accumulation percentage of around 1.5% ID/g after 15 min of injection, meaning that an

adequate amount of our sdAb is reaching the tumor. The biodistribution profiles of different antibody formats were already compared by different groups. Schneider et al. (Schneider et al. 2009), compared different antibody formats, including scFvs, and the percentages of tumor uptake obtained were between 1 and 1.5% for 25 min and 3h after injection. Another study conducted by Duray et al. (Duray et al. 2021) using sdAbs, revealed a tumor uptake of 2.22% and 0.79% for 48 h post-injection. The values obtained for small fragments are in the same range as those we obtained for our sdAb, C5, leading us to conclude that our data resulted in a good tumor uptake. Moreover, C5 biodistribution profile presents a rapid clearance from the major organs, except for the organs related with the excretory paths (liver and kidney) and in the spleen. This fast clearance from the systemic circulation is mostly advantageous given that it results in shorter effective circulation times, mitigating the possibility of off-target release. Finally, and importantly to proceed with ADC development, the presence of the free Cys80 at the surface of C5 was confirmed by modelling its tridimensional structure using a protein structure prediction software.

Once the target-specific antibody is selected, the choice of a potent payload becomes critical. To design our ADC, we explored the potent, well-characterized and clinically validated payload – SN-38. SN-38 acts as a Topo I inhibitor through binding and stabilization of the Topo I-DNA cleavage complexes, leading to accumulation of DNA damage and apoptosis (Pommier 2013; Jensen et al. 2016). Cancer cells express high yields of Topo I, making its expression 14-16 times higher than in normal cells. The increase of this enzyme yield is particularly observed in certain types of cancer, including NHL. Additionally, a recent study reported its use in the construction of a sdAb which suggests it possesses adequate physicochemical properties (hydrophobicity and potency) to build our new sdAb-drug conjugate (Wu et al. 2022). Moreover, SN-38 has already proven clinical efficacy, being used as payload in a recently FDA-approved ADC, Sacituzumab govitecan (Trodelvy), indicated for the treatment of metastatic triple negative breast cancer (Syed 2020). Therefore, considering its high activity, we envisioned the construction of an ADC featuring both C5 and SN-38, connected by a linker. The linker is another key component of the ADC as it governs the stability of the conjugate and avoids random release of the cytotoxic payload in circulation. In the new generation of ADCs, the linker evolved from a stable and inert spacer into a functional structure capable of responding to specific stimulus and releasing the payload selectively at the target tissues. This selectivity is achieved by taking advantage of the exquisite properties of tumoral microenvironment, which includes acidic pH, high concentration of glutathione and overexpression of proteolytic enzymes. In addition, high concentrations of reactive oxygen species (ROS) is also one of the hallmarks of cancer (Gorrini et al. 2013). Recently, we reported the development of a new bioconjugation linker (diazaborines) that is susceptible to oxidation in the presence of ROS (António et al. 2021) and is an excellent option for the

preparation of a tumor-targeted ADC. DAB-SN-38, a highly complex molecule featuring the SN-38 drug, a ROS-responsive diazaborine linker and a maleimide bioconjugation handle, was conjugated to C5 at the free Cys80 to generate the stable and homogenous C5-DAB-SN-38, with a drug-to-antibody ratio (DAR) 1. The expected DAR was confirmed by reverse phase-HPLC which displayed >95% of single modified sdAb. The obtained data showed that C5-DAB-SN-38 promoted cell death on the canine lymphoma cell line, CLBL-1. In addition, our results demonstrated that C5-DAB-SN-38 cytotoxicity is associated with DNA-Topo I inhibition, as expected. Noteworthy, these results indicate that the ADC C5-DAB-SN-38 was stable generated and presented a high cytotoxic activity against canine diffuse large B-cell lymphoma under the nM range, revealing the potential of these rabbit-derived sdAbs as ADC moieties.

In conclusion, the results presented herein validate a highly efficient approach for the discovery and generation of anti-tumor antibodies for ADC development. The combination of an immunized library using NHL cells from canine patients with an innovative *in vivo* phage display on a cNHL xenograft murine model enabled the selection of highly specific antibodies against NHL. Importantly, by exploring the promising properties and unique characteristics of rabbit derived VL sdAbs scaffolds we were able to engineer a potent ADC with a DAR 1 by conjugating the SN-38 payload into the free exposed Cys80 of the VL framework. Thus, this work creates a new research avenue in the development of ADCs for cancer treatment by urging the emergence of a novel class of rabbit-derived sdAb-based products with versatile properties for payload conjugation. In addition, the opportunity to carry clinical studies in pet dogs with naturally occurring canine B-cell lymphoma may also provide resources with realistic perspectives for clinical translation in the immune-oncology field.

## 2.4. Materials and Methods

### 2.4.1. Cell lines and culture

CLBL-1, Jurkat and HEK293T cell lines were obtained and maintained as previously described (Rütgen et al. 2010; Rütgen et al. 2012; Dias et al. 2018; Dias et al. 2018a; Dias et al. 2022).

### 2.4.2. Rabbit immunization and antibody library construction

All animal-handling procedures were performed according to EU recommendations for good practices and animal welfare and approved by the Animal Care and Ethical Committee of the Veterinary Medicine Faculty (Protocol_0050132016). All methods were performed in accordance with the relevant guidelines and regulations. The study was conducted according ARRIVE guidelines. One female New Zealand White rabbit (Charles River) was immunized with lymph node primary cells derived from a canine multicentric lymphoma biobank (cNHL)

previously established and characterized by our group (Dias et al. 2019a). To induce a strong and specific immune response against NHL receptors, rabbit was immunized and boosted with $1 \times 10^7$ of cNHL primary cells isolated from tumor affected lymph node from two patients (ID5 and ID6) (Dias et al. 2019a) diagnosed with Diffuse Large B Cell Lymphoma (DLBCL). For that purpose, tumor cells isolated from lymphoma-affected lymph nodes were thawed, washed in PBS and after confirmation of cell viability, resuspended in 1 mL of PBS. The injections were administered subcutaneously at 2-3 weeks intervals for 3 months. Before each immunization, blood was harvested from the marginal ear vein for serum isolation. Five days after the final boost, rabbit was sacrificed by cardiac puncture exsanguination, following propofol anesthesia, and spleen and bone marrow were harvested for total RNA isolation, cDNA synthesis and VL immune library was constructed as previously described (Aguiar et al. 2021; Dias et al. 2022; Braz Gonçalves and Silva).

### 2.4.3. Characterization of rabbit immune response

The rabbit immune response was monitored by cell ELISA sera testing using the cNHL cells (ID5 and ID6) (Dias et al. 2019b; Dias et al. 2022) used in the immunizations and CLBL-1 cells, a canine DLBCL stable cell line (Rütgen et al. 2010; Rütgen et al. 2012), as described previously (Dias et al. 2022). Pre-bleed sera was used as control. Each serum was also analyzed for its binding properties against cNHL cells by flow cytometry. For that, ID5 and ID6 cNHL cells and CLBL-1 cells were prepared. Cells were washed twice in 0.5% PBS-BSA and incubated with the rabbit pre-bleed and final bleed (1/3000) for 30 min at 4º C. Cells were then washed with cold 0.5% PBS-BSA three times and incubated with secondary antibody (Alexa Fluor-647 Goat Anti-Rabbit IgG) at 1/10000 in 0.5% PBS-BSA for 30 min at 4º C. Cells were washed with 0.5% PBS-BSA three times and submitted to flow cytometry analysis (FACSCalibur). Unstained cells were used as negative control for voltage settings. For multiple-color sorts, single color controls were used for compensation settings. Data was analyzed by FlowJo software version 10 (FlowJo LLC).

### 2.4.4. Phage display selection of VL sdAbs targeting cNHL

The phage library displaying VL sdAbs was first panned using a subtractive cell phage display protocol as previously described by Carlos Barbas (Barbas III et al. 2001; Popkov et al. 2004) and our studies (Dias et al. 2022), and that included a negative selection on HEK293T cells followed by a positive selection on CLBL-1 cells. Then, after three rounds of *in vitro* selections, an additional panning was performed *in vivo* in a xenograft CLBL-1 murine model (Dias et al. 2018). All animal-handling procedures were performed according to EU recommendations for good practices and animal welfare and approved by the Animal Care and Ethical Committee of the Veterinary Medicine Faculty (Protocol_0050132016). All

methods were performed in accordance with the relevant guidelines and regulations. The study was conducted according ARRIVE guidelines. Briefly, female 6–8-wk-old SOPF/SHO SCID mice (Charles River) were maintained as mentioned before (Dias et al. 2018). Then, the tumors were induced as established previously (Dias et al. 2018). When tumors reached a minimum volume of 100 $mm^3$, three SCID mice were intravenously injected into the tail vein with 100 µL of phage ($1 \times 10^{10}$ pfu/mL) freshly prepared from the third *in vitro* selection round. Phages were allowed to circulate for 60 min, then mice were sacrificed, perfused and xenograft tumors were removed and weighted. Following tumor homogenization in 70 µm cell strainers (VWR, Radnor, PA, USA) phages were recovered by incubating the homogenized tumor with trypsin, as described previously (Aguiar et al. 2021). To elute the internalizing phages, the cell pellet obtained after the trypsin elution was washed 3 × with PBS and centrifuged at 10,000 × g at 4 º C, 5 min. Then, the cell pellet was resuspended with 200 µL of 0.1 M triethylamine, incubated 10 min and neutralized with 50 µL of 1 M Tris 7.5. The eluted phages were treated as described before (Aguiar et al. 2021).

### 2.4.5. Analysis of phage display enrichment by next generation sequencing and VL sdAb lead selection by ELISA

To analyse the enrichment and profile obtained after the *in vivo* phage display selection, we performed a next generation sequencing (NGS) analysis as described previously (Aguiar et al. 2021). As control the initial immune VL sdAb library was sequenced and the data obtained compared with the selected library. To select the most promising VL sdAbs with ADC properties, phagemid DNA from the *in vivo* output selection (internalizers output) was cloned into the PT7-PL (PT7-peptide leader) vector, transformed into *Escherichia coli* BL21 (Lucigen) and autoinduced as previously reported (Aguiar et al. 2021; Dias et al. 2022). To evaluate the relative binding activity and specificity an ELISA was performed as previously mentioned (Dias et al. 2022). The best lead candidates in terms of binding and expression levels, were selected and sequenced at Eurofins company. Sequence analysis was performed as mentioned before (Kabat et al. 1991; Aguiar et al. 2021).

### 2.4.6. Production and purification of VL sdAbs

The three best VL sdAbs were selected according to cNHL cell binding activity and expression yields. C5 was chosen as the best lead candidate to be expressed and purified. For that, C5 was cloned into the pET21 expression vector (Sigma-Aldrich, St. Louis, MO, USA) and transformed in *E. coli* BL21 (Lucigen). C5 was expressed as described previously (Aguiar et al. 2021). After expression, bacteria were harvested by centrifugation (1500 x g, 15 min, 4° C), and resuspended in 50 mL of initial buffer (50 mM HEPES, 1 M NaCl, 10 mM Imidazole, 2

M Urea, 5 mM CaCl2, 1 mM β-mercaptoethanol, and pH=8) supplemented with protease inhibitors (Roche). Cells were lysed by sonication and the inclusion bodies were recovered by centrifugation (7500xg, 30 min, 4° C) as described previously (Gouveia et al. 2017). Refolding was performed by step wise dialysis, according to Gouveia et al, 2017 (Gouveia et al. 2017). After that, C5 was purified by size exclusion chromatography (SEC) as previously mentioned (Aguiar et al. 2021).

### 2.4.7. Immunofluorescence microscopy and Flow Cytometry of C5

$1.5 \times 10^5$ of CLBL-1 or Jurkat cells were plated on ibidi µ-Slide 8 Well Glass Bottom (Ibidi, Fitchburg, WI, USA) and incubated for 24 h at 37° C in a humidified atmosphere of 5% CO2. Then, 3 µM of C5 was added to the cells and incubated for 90 min at 37° C. After incubation, cells were washed twice with PBS, fixed with 4% PFA for 15 min at room temperature, permeabilized with 0.1% Triton X-100 for 10 min at RT, washed, blocked with 0.1% Triton X-100 and 3% PBS/ BSA and incubated overnight with rat anti-HA (Roche, 1/50) at 4° C. Next day, cells were washed twice with PBS and incubated with anti-rat Alexa Fluor-488 (1/500) for 1 h at RT. After washing, DAPI Vectashield (Vector Labs, Burlingame, CA, USA) was added to the cells. Image acquisition was performed on a confocal point-scanning Zeiss LSM 880 microscope (Carl Zeiss, Germany) equipped with a Plan-Apochromat DIC X63 oil objective (1.40 numerical aperture). Diode 405-30 laser was used to excite DAPI, and argon laser in the 488-nm line to excite Alexa Fluor-488. In the Airyscan acquisition mode, ×1.80 zoom images were recorded at 1024 × 1024 resolution. ZEN software was used for image acquisition and Fiji software was used for image processing. For Flow Cytometry analysis, $1 \times 10^6$ of CLBL-1 or Jurkat cells were treated as described previously (Dias et al. 2022). C5 was incubated for 90 min at 37° C.

### 2.4.8. Biodistribution studies and tumor targeting

To evaluate the biodistribution and tumor targeting in a xenograft CLBL-1 murine model (Dias et al. 2018), C5 was radiolabeled with the radioactive precursor $[^{99m}Tc(CO)_3(H_2O)_3]^+$ prepared from an IsoLink kit (Covidien, Ireland). Radiochemical purity (RP) was checked by Reversed-phase high-performance liquid chromatography (RP-HPLC) and instant thin-layer chromatography silica gel (ITLC-SG, Agilent Technologies, USA). In brief, fac-$[^{99m}Tc(CO)_3(H_2O)_3]^+$ solution was added to a nitrogen-purged closed glass vial containing a solution of His-tag with C5 to obtain a final concentration of 1 mg/mL. The mixture was incubated for 45–60 min at 37 ºC and then a ITLC-SG analysis using 5% HCL (6 M) solution in MeOH as eluent was performed to evaluate the RP of 99mTc(CO)3-C5. While $[^{99m}Tc(CO)_3(H_2O)_3]^+$ and $[^{99m}TcO_4]^-$ migrate in the front of the solvent (Rf = 1), the 99mTc(CO)3-C5 remains at origin (Rf = 0). Radioactivity distribution on the ITLC-SG strip was

evaluated using a miniGita Star scanning device (Elysia-Raytest, Germany) coupled with a Gamma BGO-V-Detector (Elysia Raytest). For purification and concentration of the 99mTc-labeled sdAb, a 3K Amicon (Merck Milipore) was used. 99mTc(CO)3- C5 diluted in PBS was used for the biodistribution studies after RP determination by ITLC-SG. For that, mice were intravenously injected in the tail vein with 100 µL of 99mTc(CO)3-C5 and sacrificed by cervical dislocation at 15 min, and 3 h after injection. Radioactivity was measured using a dose calibrator (Carpintec CRC- 15W). After the removal of the tumor and tissues of interest, their radioactivity was measured using a γ-counter (Berthold, Germany). The uptake was represented as a percentage of injected activity dose per gram of organ or tissue (%ID/g). To confirm the results and C5 tumor uptake, western blot analysis was performed as described previously (Aguiar et al. 2021). All animal-handling procedures were performed according to EU recommendations for good practices and animal welfare and approved by the Animal Care and Ethical Committee of the Veterinary Medicine Faculty (Protocol_0050132016). All methods were performed in accordance with the relevant guidelines and regulations. The study was conducted according ARRIVE guidelines.

### 2.4.9. 3D VL sdAb structure prediction

The tridimensional structure of C5 was predicted using the Phyre2 protein fold recognition server (http://www.sbg.bio.ic.ac.uk/phyre2) (Kelley et al. 2015). The best model was obtained using the structure of an immunoglobulin light chain as a template (PDB entry: 1BJM) with a level of confidence of 100% and a coverage of 98%. Visual representations of the obtained model were produced using the UCSF Chimera software (Pettersen et al. 2004).

### 2.4.10. Synthesis and characterization of the Linker-Payload (DAB-SN-38)

The synthesis of DAB-SN-38 was performed as previously reported (António et al. 2021).

### 2.4.11. Bioconjugation of C5 with SN-38

To conjugate the C5 with SN-38, a PBS pH 7.4 solution containing C5 (10 µM) and TCEP (1.5 equiv., 3.5 mM), DAB (20 equiv., 9 mM, DMSO) was added, and the solution was mixed during 90 min at 25º C. The expected conjugate was evaluated after 90 min by High-Resolution Mass Spectrometry, recorded in a Thermo Scientific Q Exactive Plus (Thermo Scientific). The final immunoconjugate C5-DAB-SN-38 was detected and purified by dialysis using a Pur–A–Lyzer™ Midi Dialysis Kit with a 3.5 kDa cut-off. The mass spectra were deconvoluted using MagTran software.

### 2.4.12. Cytotoxic assay

To determine the effect of C5-DAB-SN-38 on CLBL-1 and Jurkat cell proliferation, a cell viability assay was performed as described previously (Dias et al. 2018a). Briefly, cells were seeded at a density of $6 \times 10^4$ well in 200 µl of culture medium and subjected to increasing concentration (2.5 µM to 12.5 nM) of each compound (C5, C5-DAB-SN-38 and SN-38). After 48 h treatment, cell viability was assessed using WST-1, following the manufacturer's instructions. Absorbance at 450 nm was measured using the iMark microplate Reader (Bio-Rad). Two replicate wells were used to determine each data point and three independent experiments were carried out in different days. Best-fit EC50 values of each formulation were calculated using GraphPad Prism software (version 9.2.0, San Diego, CA, USA) using the log (inhibitor) vs response (variable slope) function.

### 2.4.13. DNA-Topo I Activity Assay

Topo I activity on C5-DAB-SN-38 was determined using the Human Topoisomerase I Assay Kit (Topogen, Buena Vista, CO, USA) according to the manufacturer's instructions. Samples were loaded on a 1% agarose gel and run in 1x TAE buffer. Gel was stained with ethidium bromide for 45 min and destained in distilled water. Relaxed DNA, SN-38 and C5 were used as controls.

# Chapter 3

## Novel pseudomonas exotoxin A based rabbit-derived single-domain antibody immunotoxin for canine B cell lymphoma treatment

Ana S. André[1,2], Joana N.R. Dias[1,2], Isa Moutinho[1,2], Joana Loureiro[1,2], Sara Nogueira[1,2], Pedro Bule[1,2], Luís Marques[3], Rui Malhó[3], Lurdes Gano[4], João D.G. Correia[4], Jorge Correia[1,2], Solange Gil[1,2], João Gonçaves[5], Ira Pastan[6], Luís Tavares[1,2], Frederico Aires-da-Silva[1,2]

[1]Centro de Investigação Interdisciplinar em Sanidade Animal (CIISA), Faculdade de Medicina Veterinária, Universidade de Lisboa, Avenida da Universidade Técnica, 1300-477 Lisboa, Portugal.

[2]Associate Laboratory for Animal and Veterinary Sciences (AL4AnimalS).

[3]Biosystems and Integrative Sciences Institute, Faculdade de Ciências, Universidade de Lisboa, Lisboa, Portugal.

[4]Centro de Ciências e Tecnologias Nucleares, Departamento de Engenharia e Ciências. Nucleares, IST, Universidade de Lisboa, Estrada Nacional 10, 2695-066 Bobadela LRS, Portugal.

[5]Research Institute for Medicines (iMed.ULisboa), Faculty of Pharmacy, Universidade de Lisboa, Portugal.

[6]Laboratory of Molecular Biology, Center for Cancer Research, National Cancer Institute, National Institutes of Health, 37 Convent Drive, Bldg 37, Bethesda, MD, 20892, USA.

### Abstract

Lymphoma and, in particular, non-Hodgkin lymphoma (NHL) is one of the most common lymphoma subtypes in humans and dogs. Despite the great advances made in treatments made lately, the lack of specificity as well as the side effects of the conventional chemotherapy have opened an opportunity for a novel class of molecules. Throughout the years, immunotoxins have been demonstrating their potential for hematopoietic malignancies. Within this context, in the present study our goal was to combine this potential with the advantages of rabbit single-derived domain antibodies in order to design a novel immunotoxin for NHL treatment using canine lymphoma as a model. For this purpose, we fused the Pseudomonas exotoxin PE38 domain with a specific single-domain antibody, C5, that was previously developed for canine B-cell lymphoma. This resulted in a stable C5-PE38 immunotoxin with potent cytotoxic activity (IC50= 9.5 ± 0.04 μg/mL) and protein synthesis

inhibition on canine lymphoma cells. In vivo results on a xenograft mouse model of canine lymphoma demonstrated a 2% of tumor uptake after 15 min post injection and an inhibition of tumor growth in the presence of the C5-PE38 immunotoxin. After two weeks of treatment, C5-PE38 at 0.5 mg/kg and 1.5 mg/kg doses inhibited tumor growth by 76.2% and 92.3%, respectively, when compared to vehicle control treated mice ($p < 0.05$). The results attained validate PE38 toxin as a promising therapeutic molecule for the treatment of dog-related tumors, and single-domain antibodies as a suitable scaffold for the development of new immunotoxins, strengthening the role of dogs as a clinical model for advancing the development of novel therapeutic molecules aimed at treating human lymphoma.

**Keywords:** sdAb, immunotoxins, PE38, lymphoma, cancer NHL

## 3.1. Introduction

Over the last years, cancer treatment has evolved and the options available for patients have gone through a huge improvement. However, cancer still remains as the leading cause of death, not only in humans but also in dogs. This unveiled an opportunity to bring together veterinary and human medicine for the comparative research of cancer.

One of the most common neoplasias, in both species, is lymphoma, in particularly, non-Hodgkin (NHL). In humans, NHL represents 90% of all lymphomas, representing 85-90% of cases from B-cells (Wang et al. 2020). This neoplasia usually develops in the lymph nodes and, in humans, the most aggressive form is diffuse large B-cell (DLBCL) and Burkitt's lymphoma. In dogs, the scenario is very similar to humans, with an incidence of 15-30 per 100 000 dogs. Canine lymphoma can display several histological subtypes, however, the multicentric form is the most common and is diagnosed with intermediate to high-grade lymphoma, in the majority of B-cell origins. Due to the shared molecular, genetic and histopathologic features, dogs, and in particular, canine lymphoma has been suggested as a comparative model for the development of novel therapeutics for human NHL. Regarding canine lymphoma treatment, despite the temporary remission achieved with conventional chemotherapy, the truth is that it rarely is curative with most of the patients relapsing with lethal, drug-resistant lymphoma. Within this context, there is an urgent need to improve conventional treatments that still do not fully cure and have numerous adverse effects.

In search for more specific and potent treatments, arming antibodies with toxic agents, such as toxins emerged as a promising alternative, which can overcome the specificity issue by using a specific antibody, and chemotherapy resistances by using a different class of molecules, known as bacterial toxins. Due to their promising characteristics, bacterial toxins have been showing their potential in the cancer field. Bacterial toxins are highly toxic, and for this reason, seem to be a promising alternative to chemical compounds, since one single

molecule is sufficient to kill a cell. The combination of the toxin with the antibody results in an immunotoxin (IT) (Akbari et al. 2017).

The use of bacterial toxins was firstly proposed by Thrope et al (Thorpe et al. 1978) with the creation of the first generation of immunotoxins (Kim et al. 2020). Over the years, immunotoxins have been improved to fulfill the needs of cancer treatments and so generate molecules with better efficacies. The use of truncated forms of toxins is one of the ways to reduce the non-specific binding of ITs since the binding of the toxin is replaced by the antibody. To avoid one of the major problems of heterogeneity, a new generation of ITs began to use methods of genetic fusion instead of the chemical conjugation, leading to an improvement in IT stability (Kim et al. 2020). Additionally, immunotoxins have the peculiarity that kills cells by inhibition of protein synthesis, a unique mechanism that does not damage DNA, making it an advantage over conventional treatments.

To date three approved immunotoxins are on the market. Denileukin difitox (Ontak) was the first approval by FDA in 1999, for the treatment of relapsed or refractory cutaneous T-cell lymphoma. More recently, in 2018, moxetumomab pasudotox (LUMOXITI) and tagraxofusp (Elzoris) were approved for the treatment of relapsed and refractory hairy cell leukemia and blastic plasmacytoid dendritic cell neoplasm, respectively. Ontak and Elzoris used a truncated Diphtheria Toxin (DT), named as DAB389, as a payload fused with IL2 and IL3, respectively. LUMOXITI consists of an anti-CD22 dsFv fused to a Pseudomonas Exotoxin (PE) truncated form (Akbari et al. 2017). PE is one of the most common toxins used in RIT and is derived from the bacteria *Pseudomonas aeruginosa*. The toxin is composed of three structural domains: a binding domain (I), a processing domain (II) and the catalytic domain (III). The most common portion of the PE used for IT construction, including in the moxetumomab pasudotox, is PE38, whose binding domain has been replaced by the antibody (Dieffenbach and Pastan 2020; Mazor and Pastan 2020). The mechanism of action of the immunotoxin is dependent on two keys factors: the target binding and the cellular internalization. Since the binding domain of the toxin is replaced, the antibody is responsible for the targeting and internalization of the whole immunotoxin. Thus, it is important to choose a highly specific antibody with the ideal characteristics to conjugate with the immunotoxin (Hamamichi et al. 2020; Kim et al. 2020).

Throughout recent years, we have been demonstrating the great potential of rabbit single-domain antibodies for a multitude of therapeutic implementations (Goncalves and Silva 2008; Silva et al. 2004; Aires-da-Silva et al. 2014; Cunha-Santos et al. 2016; Gouveia et al. 2017; Dias et al. 2022; Aguiar et al. 2021; André et al. 2023). These fragments represent the smallest portions derived from conventional IgGs responsible for antigen binding. Due to their reduced size, they reach difficult-to-access targets, show improved tumor penetration, high stabilities, reduced immunogenicity, and diminished manufacturing costs. Additionally, these

sdAbs can be facilely attached to other bioactive payloads, such as therapeutic peptides or proteins, through uncomplicated molecular biological methodologies (Aires-da-Silva 2008; Gonçalves and Silva 2008). These unique properties make them excellent frameworks for the construction of immunotoxins.

Thus, in this study, we aimed at exploring the versatile properties of rabbit derived sdAbs to develop a new immunotoxin using the PE truncated form, PE38, for cancer treatment. To this end, we fused the PE38 with a specific single-domain antibody, C5, that was previously developed by our group against canine B-cell lymphoma (André et al. 2023).

## 3.2. Results

### 3.2.1. Construction and expression of recombinant C5-PE38 immunotoxin

Aiming to develop our immunotoxin, we started by modeling the tridimensional structure of C5-PE38 (Figure 25A).

To construct the immunotoxin C5-PE38, we used a sdAb and the PE38 toxin (Figure 25B). C5-PE38 is composed of a C5, sdAb, C5, fused to a 38 kDa fragment of PE38 toxin. C5 is an sdAb previously selected by phage display against canine B-cell lymphoma. The PE38 toxin is made up of two domains: domain II contains a furin cleavage site, essential for toxin activation, and domain III contains the ADP ribosylation activity. The two sequences were joined using a flexible linker (SSGGGGSGGGGGGSSRSS) and a His-tag was introduced at the N-terminus for easier purification. The linked sequence was then inserted into the pET-21 vector, precisely within the NheI and NotI restriction digestion sites. The fusion of both molecules was successfully performed using a PCR overlap extension resulting in a single fragment that confirmed by sequencing.

Then, C5-PE38 was successfully expressed and purified (Figure 25C) using the inclusion bodies protocol described in the material and methods section. Immunotoxin was prepared from a 2 liter-culture of *E. Coli*. Refolding was performed by step-wise dialysis. The final yield was 5 mg/L of C5-PE38. Upon production, C5-PE38 was evaluated by SDS-PAGE. Figure 25D shows the SDS-Page gel of the purified C5-PE38 with a molecular weight of approximately 50 kDa. The data obtained confirmed the purity and integrity of the constructed immunotoxin.

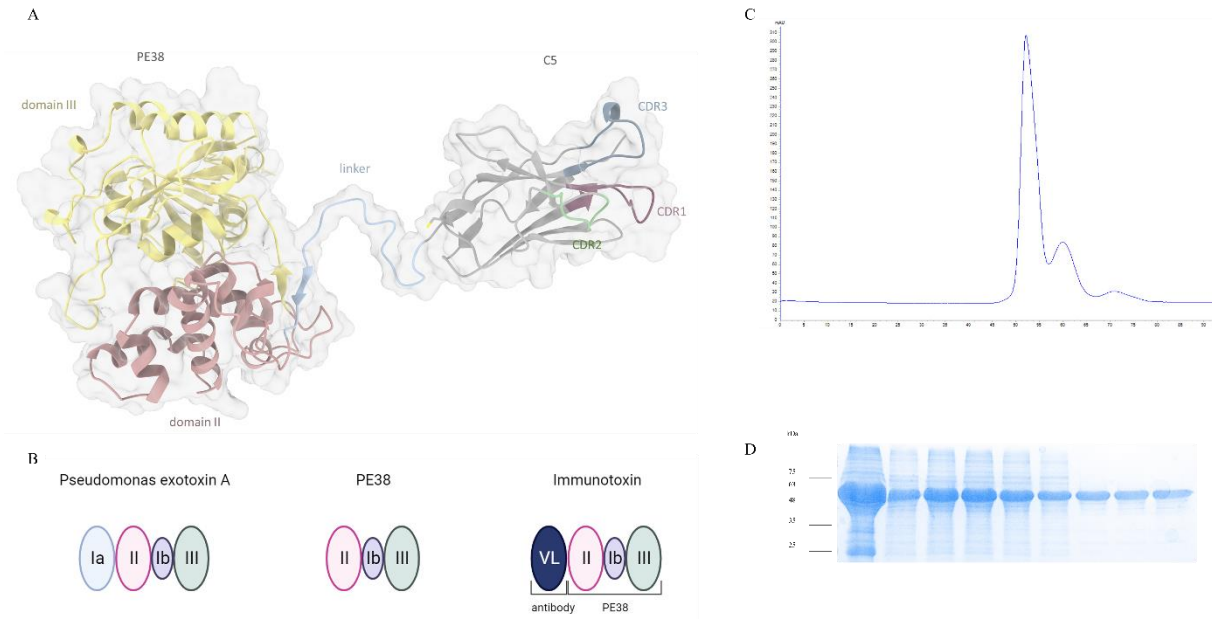


**Figure 25 - Expression and Purification of C5-PE38.** A) Ribbon representation of the 3D structure predicted for C5-PE38. The CDR domains of the C5 sdAb (grey) are highlighted in purple (CDR1), green (CDR2), and blue (CDR3). Domains II and III of the truncated PE38 are coloured red and yellow, respectively. The peptide linker is colored blue. The van der Waals surface is depicted in transparent coloring. CDR numbering was performed according to Kabat et al. B) To construct the immunotoxin C5-PE38, we used a sdAb and the PE38 toxin. C5-PE38 is composed of a C5, sdAb, C5, fused to a 38 kDa fragment of PE38 toxin. C and D) Expression and Purification of C5-PE38. B) C5-PE38 was produced using the inclusion bodies protocol. Immunotoxin was prepared from a 2 liter-culture of *E.coli*, purified and the refolding was performed by step-wise dialysis. C) C5-PE38 was evaluated by SDS-PAGE. SDS-Page gel of the immunotoxin confirmed the molecular weight of approximately 50 kDa and the purity and integrity of the immunotoxin.

### 3.2.2. Evaluation of binding and internalization of recombinant C5-PE38 immunotoxin

In order to confirm the binding and internalization of the recombinant C5-PE38 immunotoxin, a cell ELISA and an immunofluorescence assay were performed. As illustrated in Figure 26A, a high density of Alexa Fluor-488 labeled C5-PE38 was observed in the perinuclear region of CLBL-1 cells. In contrast, there was no detectable fluorescence in the control sample nor in Jurkat cells (Figure 26B). These findings confirmed the C5-PE38 binding to the CLBL-1 cells and its internalization into the cytoplasm.

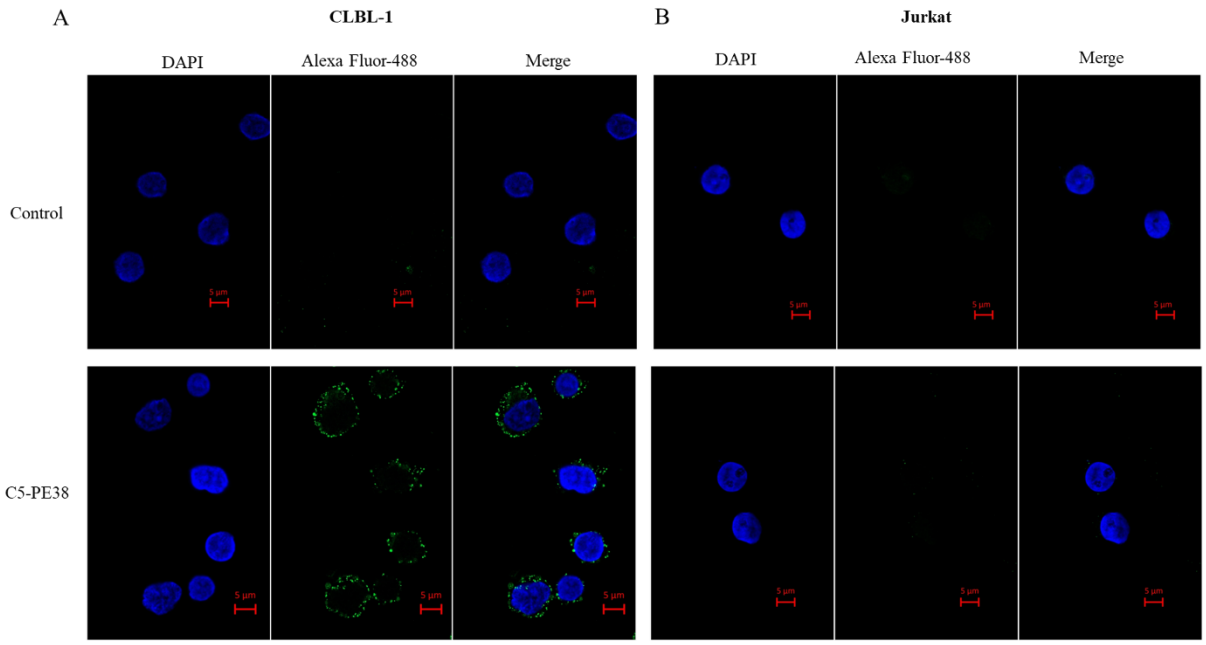


**Figure 26 - Binding and internalization characterization of C5-PE38.** C5-PE38 binding and internalization properties against CLBL-1 and Jurkat cells were evaluated by immunofluorescence. (**A**) 1 x $10^5$ of CLBL-1 and Jurkat cells were plated on ibidi µ-Slide 8 Well Glass Bottom and incubated with 3 µM of C5-PE38 for 90 min. After incubation, cells were washed, fixed, permeabilized, blocked and incubated for 1 h with anti-HA Alexa Fluor-488 (1/500). At the end, ibidi Mounting Medium with DAPI was added to the cells. It is possible to observe the C5-PE38 labeled with Alexa Fluor-488 in the perinuclear region. (**D**) In contrast, there is no detectable fluorescence in the control image, nor in the Jurkat cells. Representative microphotographs with C5-PE38 (green) and DAPI stained nuclei (blue) are shown.

### 3.2.3. Evaluation of cytotoxic activity on canine B-cell lymphoma cells

In order to assess the *in vitro* activity of the C5-PE38 immunotoxin, a cell viability assay on CLBL-1 canine B-cell lymphoma cells was performed using WST-1 reagent, as described in the Material and Methods Section. As shown in Figure 27, C5-PE38 demonstrated a potent cytotoxic activity on CLBL-1 cells. Furthermore, a dose-dependent toxicity on cNHL cell viability was observed in the presence of C5-PE38. The IC50 of C5-PE38 was 9.5 ± 0.04 µg/mL. On the other hand, cell viability was not affected by the presence of only the C5 sdAb or PE38.

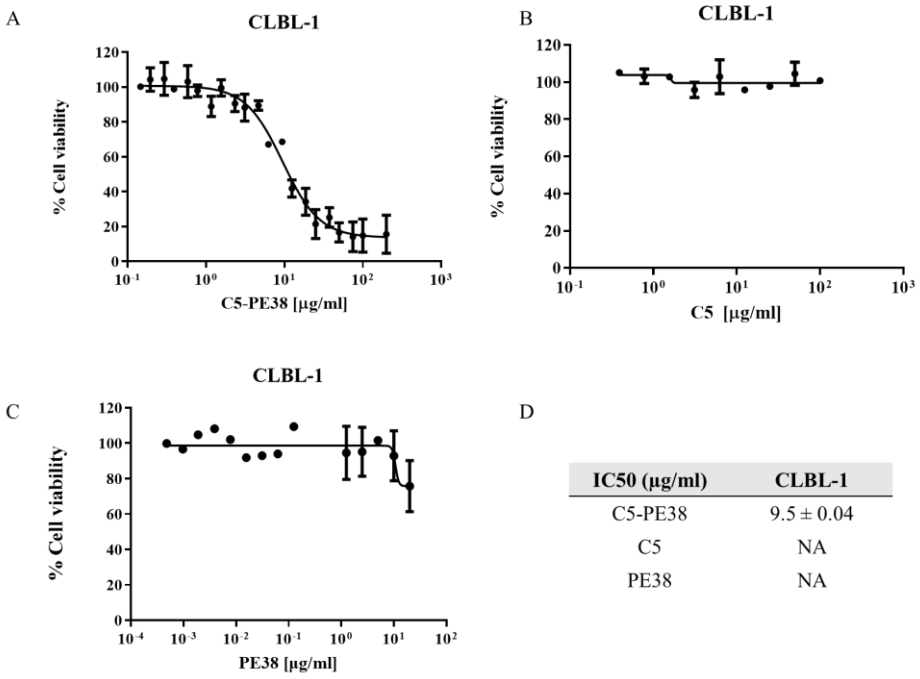


**Figure 27 - Evaluation of cytotoxic activity on canine B-cell lymphoma cells.** A) and D) To determine the effect of C5-PE38 on CLBL-1 cells, a cell viability assay using WST-1 reagent was performed. C5-PE38 demonstrated a dose-dependent cytotoxic effect on cNHL cell proliferation with an IC50 of 9.5 ± 0.04 µg/mL. B) and C) C5 and PE38 toxin were used as control demonstrating no effect on CLBL-1 cells. Best-fit EC50 values of each formulation were calculated using GraphPad Prism software (version 9.2.0, San Diego, CA, USA) using the log (inhibitor) vs response (variable slope) function.

### 3.2.4. Assessment of protein synthesis inhibition

The main cell death mechanism associated with the PE-38 toxin is via protein synthesis inhibition. To confirm that the cell death induced by C5-PE38 acts using the same mechanism, protein synthesis was evaluated as described in the material and methods section. Data shown in the Figure 28 confirms the inhibition of protein synthesis at high concentrations of C5-PE38. On the other hand, at lower concentrations inhibition of protein synthesis was not verified and hence cell death does not occur. These results prove a dose-dependent effect of C5-PE38 on inhibition of protein synthesis. The results displayed were also confirmed by immunofluorescence, shown in Figure 28, reinforcing the hypothesis of a dose-dependent effect and inhibition of protein synthesis.

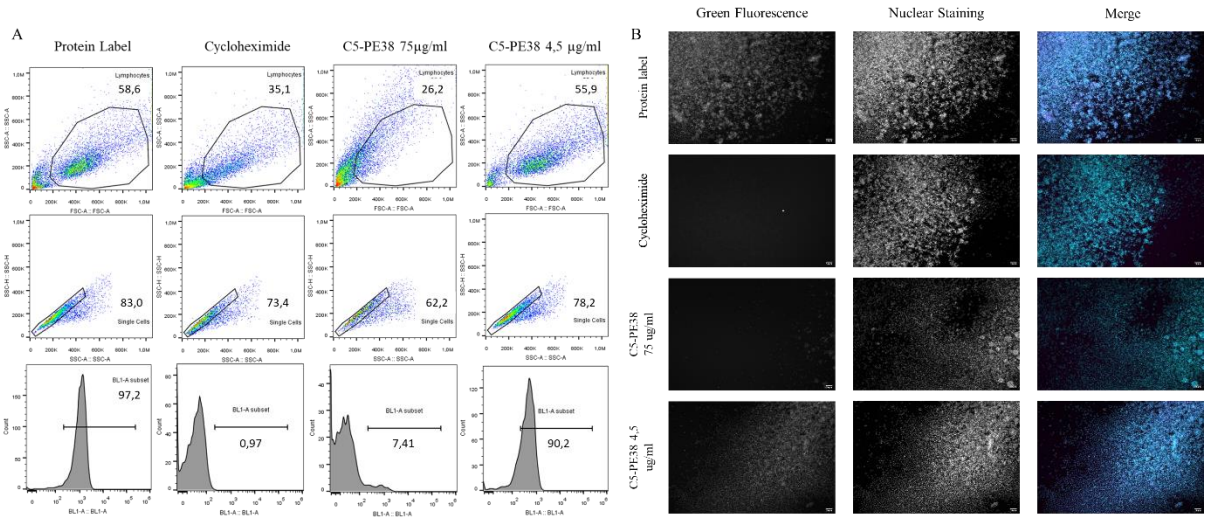


**Figure 28 - Assessment of protein synthesis inhibition**. In order to determine the C5-PE38 mechanism of action, the Protein Synthesis Assay kit was performed using two different analysis methods: A) flow cytometry and B) microscopy. CLBL-1 cells were treated with different concentrations of immunotoxin, 75 to 4.5 µg/ml and then kit instructions were followed. Data obtained confirmed the inhibition of the protein synthesis at high concentrations. On the contrary, at lower concentrations inhibition does not occur and cells do not die. According to the data, this effect seems to be dose-dependent and was confirmed by the two methods of analysis.

### 3.2.5. Biodistribution studies on CLBL-1 canine B-cell lymphoma xenograft model

To evaluate the distribution of the C5-PE38 immunotoxin in various organs, a biodistribution assay was performed using the radiolabeled C5-PE38. For that, radiolabeled C5-PE38 was intravenously injected in the mice tail of a xenograft model of CLBL-1 canine lymphoma as described in the material and methods section. The data obtained is shown in Figure 29 A and B and is expressed as the percentage of injected activity per gram of organ (% ID/g). The measured activity revealed an accumulation in the organs responsible for the excretory paths (liver and kidneys) and in the spleen, which is similar to the biodistribution profile of the non-conjugated C5 sdAb. Importantly, tumor uptake was similar to C5, with a percentage of activity around 2% at 15 min after injection, decreasing to around 1% after 3 h of injection. These findings were further validated through western blot analysis, which confirmed the presence of the C5-PE38 in the CLBL-1 xenograft tumors (Figure 29C).

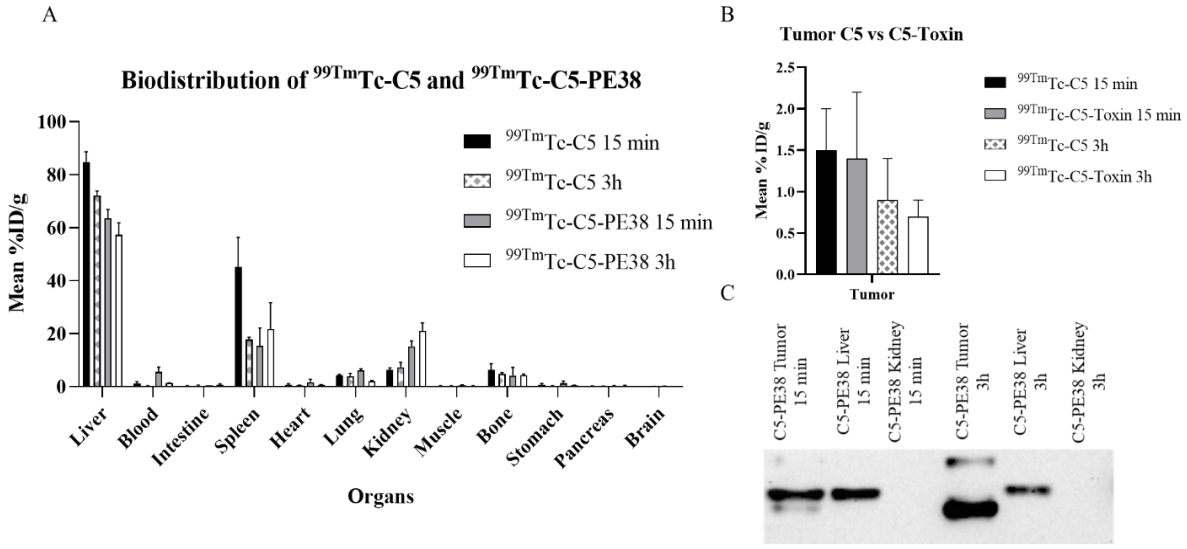


**Figure 29 - Biodistribution studies.** A) To evaluate tumor uptake and the organ distribution of the immunotoxin a biodistribution assay was performed using the C5-PE38 radiolabeled. C5-PE38 demonstrated an accumulation in the liver, kidney and spleen. B) Regarding tumor uptake, it was similar to C5, with a percentage of 2% of activity, decreasing to around 1% after 3 h. C) The presence of the immunotoxin in the mains organs and tumor was also confirmed by western blotting.

### 3.2.6. Assessment of *in vivo* effects on canine B-cell lymphoma

To evaluate the *in vivo* anti-tumor effectiveness of the C5-PE38, we conducted an efficacy study using a xenograft model of CLBL-1 canine B-cell lymphoma. Tumor volumes and body weights were measured every day as described in the material and methods section. As shown in Figure 30, after treatment with the dose of 0.5 mg/Kg, the tumor growth halted and began to regress upon the 3rd day of treatment. By increasing the dose to 1.5 mg/Kg, tumor volume and weight decreased significantly. Animals demonstrated a slight decrease in body weight, which is more pronounced at the highest dose of 1.5 mg/Kg. After three treatments, C5-PE38 at 0.5 mg/Kg and 1.5 mg/Kg doses inhibited tumor growth by 76.2% and 92.3%, respectively, when compared to vehicle control treated mice ($p < 0.05$). These results confirmed the strong antitumoral activity of the immunotoxin on canine lymphoma xenograft model.

To assess macroscopic and microscopic characteristics of the tumor, necropsy and histopathological analysis were performed.

Macroscopically, tumors were nodular, soft, hemorrhagic and highly adherent to surrounding tissues. Microscopically, infiltration of the dermis, hypodermis, muscular panniculus and muscle striated by large lymphoid cells of indistinct cytoplasm and nucleus containing several little evident nucleoli were observed in the tumors. Immunohistochemistry

analysis using CD20 and CD3 markers revealed that the tumors were positive for CD20 and negative for CD3. These features confirm the phenotype of the CLBL-1 cells.

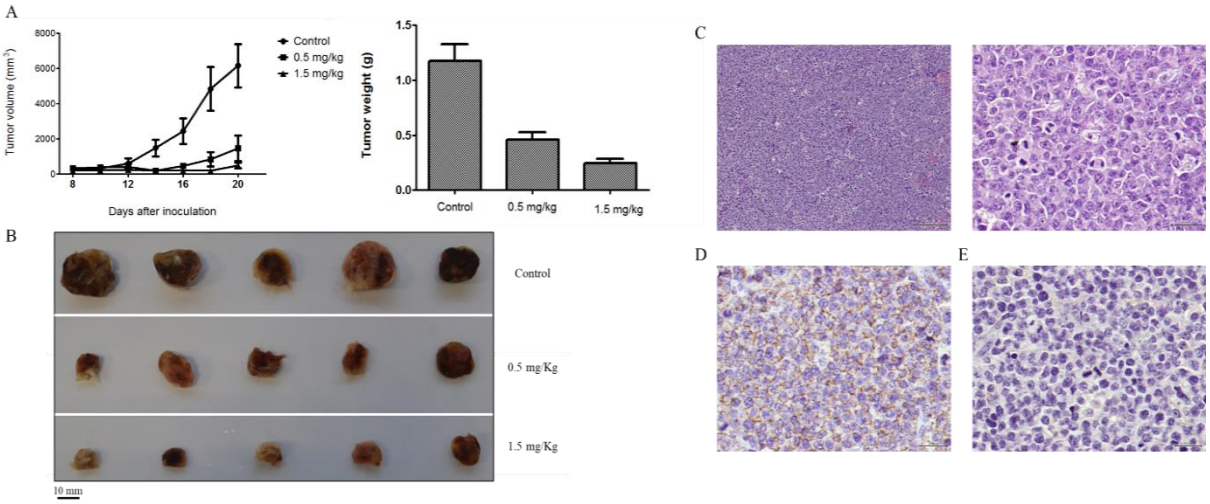


**Figure 30 - Anti-tumoral activity of C5-PE38 on xenograft canine lymphoma models.** A) Immunotoxin efficacy was *in vivo* evaluated on a xenograft model of canine lymphoma. Tumor volume was calculated using the formula $(width)^2$ x length. When the tumors reached a volume of 100 $mm^3$, mice were divided in 3 groups: control (n=5), 0.5 mg/Kg (n=5) and 1.5 mg/kg (n=5). Three treatments were intravenously administrated. Efficacy was determined by tumor growth inhibition that is determined as the percentage change in tumor volume of the treated over control animals (%T/C). B) Representative images of xenografted tumors were taken at the end of the treatment. Scale bar = 10 mm. C) Representative images of the hematoxylin and eosin (H&E) stained xenograft tumor sections. Malignant neoplasia lesion of round cells, namely, high grade lymphoma, with high cell density and a diffuse and starry-sky pattern. Left panel magnification = 100x - Right panel magnification = 400x. D) Representative images of immunohistochemistry for CD20 of xenograft tumor sections. High grade B-cell lymphoma showing positivity in virtually 100% of the tumor cells for CD20 on the cellular membrane level. E) Representative images of immunohistochemistry for CD3 of xenograft tumor sections. High grade B-cell lymphoma showing that tumor cells were negative for CD3.

## 3.3. Discussion

The remarkable similarities between canine lymphoma and human NHL prove that there is a great opportunity that benefits both species. To the best of our knowledge, this is the first attempt in developing an immunotoxin for canine lymphoma, representing a great opportunity for comparative oncology.

The urge of the immunotoxins on the market of the cancer treatment opened new perspectives for the patients, particularly for those with tumor drug resistance mechanisms acquired due to treatments with conventional cytotoxic molecules. Due to the cell death mechanism induced by immunotoxins that is related with the disruption of the process of protein synthesis and with the possibility of inducing cell death by activation of caspases, immunotoxins are able to be used in the treatment of apoptosis-resistant cancers. Moreover, the mechanism of action of novel immunotoxins allows the combination with standard agents,

and can kill nondividing cells, having less cross-resistance with conventional agents. Regarding target choice, the demand for differential expression of the target is essential for immunotoxins, making the choice of suitable targets essential. Thus, due to the high specificity of immunotoxins, the selection of the antibody is crucial in order to avoid some side effects as well as toxicities (M. Li et al. 2017).

Interestingly, the only three immunotoxins already approved by the FDA are for hematologic cancer and are made using a truncated form of the bacterial toxin that have a reduced immunogenicity and nonspecific binding property. The success of the immunotoxins for the treatment of hematologic malignancies is related with many characteristics of these tumor cells which make them tumors with the ideal conditions for increasing the therapeutic potential of immunotoxins. In fact, hematological cancer cells are easily reached in circulation, by contrast one of the major limitations of solid tumors is the poor penetration of the immunotoxins. This limitation is related with the physiological and physical properties of solid tumors, such as defective blood capillaries, a lack of functional lymphatics, increased extracellular matrix deposition and high interstitial fluid pressure, impairing the extravasation of agents from blood vessels and subsequent spreading within tumor tissues. Furthermore, the heterogeneous antigen expression and antigen shedding of the solid tumors also contribute to the restricted tumor penetration of the immunotoxins.

Taking this into account, in this work we aimed to develop a new immunotoxin for the treatment of canine lymphoma and its translation to human NHL. For that purpose, we used an already characterized and validated rabbit derived single domain antibody selected for its binding and internalization properties against canine lymphoma cells conjugated (André et al. 2023) with the PE38 toxin truncated form. This study relies on the use of the potentialities of the dog as an excellent animal model to validate potential treatments to be implemented to the human.

Various studies reported the use of the dog as a canine model for the study of immunotoxins. Henry et al used canine model of spontaneous invasive carcinomas to evaluate the efficacy of BR96 sFv-PE40 immunotoxin, obtaining great results in the treatment of certain carcinomas (Henry et al. 2005). Damle et al, used dog to study the immunogenicity of BMS-191352, a Pseudomonas Exotoxin immunoconjugate (Damle et al. 2010). More recently, dog was used to evaluate a novel EGF-anthrax toxin chimera developed to treat bladder cancer (Jack et al. 2020).

In 2018, the first immunotoxin using an antibody fragment was approved, proving the clinical efficacy of the immunotoxin concept based on these small scaffolds (Dhillon 2018). Moxetumomab pasudotox (Lumoxiti®), an Fv fragment of an anti-CD22 monoclonal antibody fused by a peptidic linker to a 38 kDa fragment of PE, PE38, gained FDA approval for the

treatment of Hairy-Cell Leukemia (HCL) (Kreitman and Pastan 2020). Nonetheless, to date there are no approved immunotoxins using single-domain antibodies as scaffold.

Regarding the bacterial toxin, PE is a potent toxin produced by Pseudomonas aeruginosa (Kreitman and Pastan 2020). Although its mechanism of action is complex and not fully understood, it is well known that PE catalyzes the transfer of ADP ribose from nicotinamide adenine dinucleotide to elongation factor 2 (EF2) (Kreitman and Pastan 2011). This modification irreversibly alters EF2 and inactivates it, leading to protein translation arrest and apoptosis. Recombinant immunotoxins are generated by replacing the binding domain of the toxin with the Fv portion of an antibody that directs the toxin to a cancer cell (Kreitman and Pastan 2020). A few clinical trials have evaluated PE based immunotoxins in humans. Of these, clinical success was best achieved with Moxetumomab pasudotox (Lumoxiti®) (Leshem and Pastan 2019). Apart from achieving complete responses in relapsed/refractory HCL, Lumoxiti® was also active in a phase I study in pediatric patients with relapsed or refractory childhood acute lymphoblastic leukemia. Thus, Lumoxiti® is currently being tested in combination with other agents for other $CD22^{+}$ malignancies.

Various studies have reported the use of nanobodies to deliver bacterial toxin pseudomonas exotoxin A (PE). PE and its derived fragments have been fused to anti-GPC3 (Wang et al. 2017; Fleming et al. 2020), anti-GPC2 (N. Li et al. 2017), anti-VEGFR2 (Behdani et al. 2013), anti-CD7 (Tang et al. 2016; Yu et al. 2017), anti-HER2 (Sokolova et al. 2017), and anti-CD38 (Li et al. 2016) nanobodies, improving cytotoxic activities in several tumor models. Importantly, Cao et al. optimized an anti-HER2-PE toxin that increased both efficacy and the maximum tolerated dose (Cao et al. 2020). Within this context, in the present study we developed our immunotoxin by using the C5 sdAb that was previously developed by our group against canine B-cell lymphoma. The selection of the C5 sdAb was performed using an *in vivo* phage display on a xenograft mouse model of canine B-cell lymphoma. This sdAb was already characterized and validated as a suitable scaffold to construct an ADC (André et al. 2023).

To build the immunotoxin, we used genetic methods to fuse the sdAb with the PE38 toxin. The use of genetic methods instead of chemical conjugation was introduced on the 3rd generation of immunotoxins revolutionizing the development of new immunotoxins. The evolution of the molecular methods allowed the fusion of antibody fragments to truncated and deimmunized toxins via peptide linker, which made possible the reduction in immunogenicity, elimination of heterogeneity and better tissue penetration due to the reduced size of the molecules. Furthermore, peptide linkers abundant in small or hydrophilic amino acids such as serine and glycine, offer enhanced structural flexibility that promotes interdomain interactions among the domains (Antignani and FitzGerald 2013; Kim et al. 2020).

Although the genetic engineering grafting of the toxic payload has surpassed major drug-antibody conjugation issues, the use of a bacterial toxin as a payload has hampered its

clinical use due to immunogenicity. The most common toxicity observed with immunotoxins, in particular with PE, is the vascular leak syndrome (VLS) that is characterized by weight gain, generalized edema, hypoalbuminemia and orthostatic hypotension. This effect occurs due to the damage caused by immunotoxins when it tries to transverse the endothelial cells to exit the blood vessels. Studies have reported that the truncated form of PE showed less VLS due to the requirement of a ligand that reacts with the endothelium as opposed to the non-truncated form which binds directly to the endothelium (Kuan et al. 1995; M. Li et al. 2017). For this reason, in this work we used the truncated form of PE38 to avoid these undesired effects. On the other hand, studies demonstrated that the PE38 toxin shows less immunogenicity in patients with hematologic malignancies where the immune system is suppressed (Mazor et al. 2016). In fact, immunosuppression present in Hairy-Cell leukemia patients is a critical feature of the therapeutic benefit of Lumoxiti®, as in patients with an intact immune system anti-drug antibody responses were extremely frequent and potentially inhibited its antitumoral activity (Mazor et al. 2018). Possibly, the immunosuppression present in the hematologic malignancies is the key for the success of the immunotoxins in this kind of tumors.

After the fusion of the immunotoxin, C5-PE38 activity was *in vitro* evaluated on canine lymphoma cells, demonstrating a potent effect on cell death mediated by inhibition of protein synthesis. To verify the tumor uptake and reinforce the specificity to the tumor cells of the immunotoxin, biodistribution studies were performed using the C5-PE38 radiolabeled with 99mTc(CO)3(H2O)$^3$. A fast elimination from the main organs was verified, however an accumulation in the liver, kidney and spleen was found. This accumulation could be justified by the excretory paths that occurs in those organs. In terms of tumor uptake, the activity values exhibit a time-dependent decrease, highlighting the rapid uptake of the immunotoxin by the tumor. The obtained biodistribution profile aligns notably with that acquired for the C5 sdAb, revealing that the conjugation with PE38 preserves the sdAbs's specificity. These findings underscore the promising potential of the developed C5-PE38 immunotoxin, both for the targeted elimination of tumor cells and as a potential treatment for canine B-cell lymphoma.

In order to assess *in vivo* efficacy of the C5-PE38 immunotoxin we performed a study on a xenograft model of CLBL-1 canine lymphoma. The data obtained confirmed the strong antitumoral activity of the immunotoxin on the canine lymphoma model.

## 3.4. Conclusions

In conclusion, we developed a new immunotoxin by fusing a rabbit single domain antibody as the targeting moiety with PE38 toxin used as payload. The results attained validate PE38 toxin as a possible molecule to treat dog-related tumor and sdAbs as a suitable scaffold to develop new immunotoxins. This opens new perspectives for the use of the immunotoxins

as a treatment for canine lymphoma, reinforcing the dog as a clinical model for the development of new therapeutic molecules to treat human lymphoma.

## 3.5. Material and Methods

### 3.5.1. Cell culture

The canine B-cell lymphoma cell line CLBL-1 was provided by Dr. Barbara Rutgen (University of Vienna, Austria). CLBL-1 was maintained in RPMI-1640 medium (Gibco) supplemented with 10% FCS (Gibco, Thermo Fisher Scientific, Waltham, MA, USA) and penicillin 100 U/mL/ streptomycin 0.1 mg/mL (Gibco) in a humidified atmosphere at 37º C with 5% $CO_2$ (T75-tissue culture flasks, Greiner Bio-One, Kremsmünster, Austria).

### 3.5.2. Structure prediction, construction and expression of C5-PE38

The tridimensional structure of the C5-PE38 conjugate was predicted using the rosettafold deep learning-based modelling method on Bakerlab's Robetta server (Baek et al. 2021). The best model obtained presented a confidence level of 0.77. Visual representations of the structure were produced using the UCSF ChimeraX software (Pettersen et al. 2021).

C5-PE38 immunotoxin is composed of the C5 clone ($V_L$) fused to PE38 toxin with a peptidic linker (SSGGGGSGGGGGGSSRSS). C5 DNA and PE38 toxin DNA were amplified individually using specific primers that added a C-terminal linker to the sdAb. Then, C5 and the toxin were fused using a PCR overlap extension. The resulting PCR product was purified and cloned into pET-21 plasmid. The sequence was confirmed by DNA sequencing. The expression, purification and refolding of the C5-PE38 was performed as described previously by us (André et al. 2023). Immunotoxin purity was analyzed by SDS/PAGE gel with 15% acrylamide gel under denaturing conditions.

### 3.5.3. Cell Elisa

To evaluate the specific binding to the canine B-lymphoma cells an ELISA was performed as previously reported (Dias et al. 2022).

### 3.5.4. Immunofluorescence

$1.5 \times 10^5$ of CLBL-1 or Jurkat cells were plated on ibidi µ-Slide 8 Well Glass Bottom (Ibidi, Fitchburg, WI, USA) and incubated for 24 h at 37° C in a humidified atmosphere of 5% CO2. Then, 3 µM of C5-PE38 was added to the cells and incubated for 90 min at 37° C. After, cells were treated as previously reported (André et al. 2023). Image acquisition was performed on a confocal point-scanning Zeiss LSM 880 microscope (Carl Zeiss, Germany) equipped with a Plan-Apochromat DIC X63 oil objective (1.40 numerical aperture). Diode 405-30 laser was

used to excite DAPI, and argon laser in the 488-nm line to excite Alexa Fluor-488. In the Airyscan acquisition mode, ×1.80 zoom images were recorded at 1024 × 1024 resolution. ZEN software was used for image acquisition and Fiji software was used for image processing.

### 3.5.5. Cytotoxic Assay

To determine the effect of C5-PE38 on CLBL-1 cells, a cell viability assay was performed using the Cell Proliferation Reagent WST-1 (Roche, Basel, Switzerland). Briefly, cells were seeded at a density of 6 x $10^4$ well in 200 µl of culture medium and subjected to increasing concentration (200 to 0.15 µg/mL) of each compound (C5, PE38 and C5-PE38). After 72 h treatment, cell viability was assessed using WST-1, following the manufacturer's instructions. Absorbance at 450 nm was measured using the iMark microplate Reader (Bio-Rad, Hercules, CA, USA). Two replicate wells were utilized to determine each data point and three independent experiments were carried out in different days. Best-fit EC50 values of each formulation were calculated using GraphPad Prism software (version 9.2.0, San Diego, CA, USA) using the log (inhibitor) vs response (variable slope) function.

### 3.5.6. Evaluation of Protein Synthesis

To determine C5-PE38 mechanism of action the Protein Synthesis Assay Kit (Green) (Abcam, Cambridge, UK) was used according to the manufacturer instructions. The protocol was adjusted according to the analysis method: flow cytometry or microscopy.

For the flow cytometry protocol, 6 x $10^4$ of CLBL-1 cells were seeded into 96-wells plates, resuspended in 100 µl of complete RPMI-1640. Then, increasing concentrations of C5-PE38 (75 to 4.5 µg/mL) were added to the respective wells and the plates incubated at 37° C in a humidified atmosphere containing 5% $CO_2$ for 24 h. Next day, cells were transferred to centrifuge tubes and resuspended in a final volume of 100 µl of the respective compound dilution. Cycloheximide (1:100) was added to the corresponding control and incubated for 45 min at 37° C. After incubation, protein label (2x) was added to all reactions, except for negative controls, and incubated for 2 h at 37° C. After incubation, cells were washed with PBS, fixated with fixative solution for 15 min at RT, permeabilized with permeabilization buffer for 10 min at RT, and then, reaction cocktail (93 µl of PBS, 1 µl of Cooper reagent, 1 µl of fluorescent azide and 5 µl of reducing agent) was added and incubated for 30 min at RT. A last wash with wash buffer was performed and cells resuspended in 100 µl of PBS. Finally, reactions were analyzed in Attune NxT flow cytometer (Thermo Scientific).

For microscopy assay, 96 wells-plate were coated with 100 µl of 0.01% poly-L-Lysine, for 1 h and washed with PBS. Then, 6 x $10^4$ of CLBL-1 cells were resuspended in complete RPMI 1640, added to each well, and incubated overnight at 37° C in a humidified atmosphere containing 5% $CO_2$. Next day, medium was removed, C5-PE38 dilutions were added to the

respective wells and incubated for 24 h at 37° C. Cycloheximide controls, fixation, permeabilization and reaction steps were performed as described above. In the end, cells were incubated with DNA Stain (1:1000) for 20 min, then the DNA stain was removed, and 100 µl of PBS was added. Image acquisition was performed on a confocal Leica SP-E microscope equipped with a Leica DFC365FX camera and a Plan-Apochromat x10, x20 and x40 objectives. 532 laser with an intensity of less than 20% and the I3 Leica filters were used to detect the green signal, and A Leica filter was used to detect the nuclear fluorescence. Fiji software was used for image processing.

### 3.5.7. Biodistribution studies

Biodistribution of VL-PE38 immunotoxin was evaluated on a xenograft model of cNHL, as described previously (André et al. 2023).

All procedures were approved by the Animal Care and Ethical Committee of the Veterinary Medicine Faculty and followed EU recommendations for good practices and animal welfare. Female 6-8-week-old SCID (CB17/Icr-Prkdcscid/IcrIcoCrl) mice were kept in microisolation cages individually ventilated under pathogen-free conditions and allowed to acclimatize for two weeks.

C5-PE38 was radiolabeled with the radioactive precursor $[^{99m}Tc(CO)_3(H_2O)_3]^+$ prepared by addition of a 0.9% saline solution of Na $[^{99m}TcO_4]$, eluted from a $^{99}Mo/^{99m}Tc$ generator, to an IsoLink® kit (Covidien, Dublin, Ireland). The radiochemical purity was assessed by Reversed-phase high-performance liquid chromatography (RP-HPLC) and instant thin-layer chromatography silica gel (ITLC-SG, Agilent Technologies, Santa Clara, CA, USA). An amount of *fac*-$[^{99m}Tc(CO)_3(H_2O)_3]^+$ solution was added to a nitrogen-purged closed glass vial containing a solution of His-tag with C5-PE38 to a final concentration of 1 mg/mL. Then, the mixture was incubated for 45-60 min at 37º C and the radiochemical purity of $^{99m}Tc(CO)_3$-C5-PE38 evaluated by ITLC-SG analysis using 5% HCL (6M) solution in MeOH as eluent. The radioactive $^{99m}Tc(CO)_3$-C5-PE38 remains at origin (Rf=0) and the precursors $[^{99m}Tc(CO)_3(H_2O)_3]^+$ and $[TcO_4]^-$ migrate in the front of the solvent (RF=1). Radioactivity distribution on the ITLC-SG strips was measured using a miniGita Star scanning device (Elysia-Raytest, Straubenhardt, Germany) coupled with a Gamma BGO-V-Detector (Elysia Raytest). Next, a 10K Amicon (Merck Milipore) was used for purification and concentration of the $^{99m}Tc$-labeled C5-PE38. For biodistribution studies, $^{99m}Tc(CO)_3$-C5-PE38 was diluted in PBS and intravenously injected into the tails vein. Mice were sacrificed by cervical dislocation and radioactivity measured using a dose calibrator (Carpintec CRC-15W). Tumor and tissues of interest were removed, and radioactivity measured using a γ-counter (Berthold, Bad Wildbad, Germany). The uptake was represented as a percentage of injected radioactivity

dose per gram of organ or tissue (% ID/g). To confirm the results and C5-PE38 tumor uptake, western blot analysis was performed as described previously (Aguiar et al. 2021).

### 3.5.8. *In vivo* efficacy

1 x $10^6$ suspension of cells in PBS with matrigel were subcutaneously injected in the dorsal intrascapular region to induce the tumor. When the tumors reached a minimum volume of 100 $mm^3$, mice were randomly divided in 3 groups: control (n=5), 0.5 mg/kg (n=5) C5-PE38 and 1.5 mg/kg (n=5) C5-PE38. Treatments were intravenously injected in three different days consecutively. Tumor volume was calculated using the formula $(width)^2 \times length$. Immunotoxin efficacy was determined by tumor growth inhibition that is determined as the percent change in tumor volume of treated over control animals (%T/C).

### 3.5.9. Histopathological analysis

Tumors were fixed in 10% buffered formalin and embedded in paraffin utilizing a Leica tissue processor. Sections were cut from paraffin blocks and stained with hematoxylin & eosin (H&E). sections were mounted onto superfrost ultra plus slides (Menzel-Glaser, Braunschweig, DE) for immunohistochemistry.

### 3.5.10. Immunohistochemistry analysis

A representative area of each tumor was selected and tissue sections of 3 µm thickness were mounted on glass slides (Superfrost glass slides, Thermo Scientific, Braunschweig, Germany), deparaffinized with xylene and hydrated in a graded ethanol series of distilled water. The Novolink Polymer Detection System (Noocastra, Leica Biosystems, Newcastle, UK) was used according to the manufacturer's instructions. The antigen retrieval treatment was achieved by microwave treatment (5 min at 900 watts plus 15 min at 650 watts) in Tris-EDTA buffer (pH 9.0). To block endogenous peroxidase and to prevent unspecific labelling, the system's Peroxidase Block Solution and Protein Block Solution were used sequentially. Sections were incubated 30 min at room temperature with polyclonal rabbit anti-human CD20 (Thermo Fisher Scientific), diluted 1:200 and rabbit polyclonal anti-human CD3 (Dako, Glostrup, Denmark), diluted 1:400. Labelling was developed by incubating the slides with system's chromogen, diaminobenzidine (DAB), and hydrogen peroxide as substrate. Nuclear background staining was performed with Gill's hematoxylin (30 sec). Labelling without the primary antibody was used as negative control, while dog lymph node sections were used as positive control.

# Chapter 4

## Panobinostat-loaded folate targeted liposomes as a promising drug delivery system for treatment of canine B-cell Lymphoma

Ana S. André[1,2], Joana N. R. Dias[1,2], Sandra I. Aguiar[1,2], Ana Leonardo[1,2], Sara Nogueira[1,2], Joana D. Amaral[3], Célia Fernandes[4], Lurdes Gano[4], João D. G. Correia[4], Marco Cavaco[5], Vera Neves[5], Jorge Correia[1,2], Miguel Castanho[5], Cecília M. P. Rodrigues[3], Maria Manuela Gaspar[3], Luís Tavares[1,2], Frederico Aires-da-Silva[1,2]

[1]CIISA-Centre for Interdisciplinary Research in Animal Health, Faculty of Veterinary Medicine, University of Lisbon, Avenida da Universidade Técnica, 1300-477, Lisbon, Portugal.

[2]Associate Laboratory for Animal and Veterinary Sciences (AL4AnimalS), 1300-477, Lisbon, Portugal.

[3]Research Institute for Medicines (iMed.ULisboa), Faculty of Pharmacy, Universidade de Lisboa, Portugal.

[4]Centro de Ciências e Tecnologias Nucleares and Departamento de Engenharia e Ciências Nucleares, Instituto Superior Técnico, Universidade de Lisboa, CTN, Estrada Nacional 10, (km 139,7), 2695 – 066 Bobadela LRS, Portugal.

[5]Instituto de Medicina Molecular-João Lobo Antunes, Faculdade de Medicina, Universidade de Lisboa, Avenida Professor Egas Moniz, 1649-028, Lisboa, Portugal.

Adapted from André AS, Dias JNR, Aguiar SI, Leonardo A, Nogueira S, Amaral JD, Fernandes C, Gano L, Correia JDG, Cavaco M, et al. 2023. Panobinostat-loaded folate targeted liposomes as a promising drug delivery system for treatment of canine B-cell lymphoma. Frontiers in Veterinary Science. 10:1236136. doi:10.3389/fvets.2023.1236136.

## Abstract

Cancer is a major public health problem with over 19 million cases reported in 2020. Similarly to humans, dogs are also largely affected by cancer, with non-Hodgkin´s lymphoma (NHL) among the most common cancers in both species. Comparative medicine has the potential to accelerate the development of new therapeutic options in oncology by leveraging commonalities between diseases affecting both humans and animals. Within this context, in the present study, we investigated the potential of panobinostat (Pan)-loaded folate-targeted PEGylated liposomes (FA-PEG-Pan-Lip) for the treatment of canine B-cell lymphoma, while contributing to new perspectives in comparative oncology. Two formulations were developed, namely: PEG-Pan-Lip and FA-PEG-Pan-Lip. Firstly, folate receptor expression in the CLBL-1 canine B-cell lymphoma cell line was assessed. After confirming receptor expression, both Pan-loaded formulations (PEG-Pan-Lip, FA-PEG-Pan-Lip) demonstrated dose-dependent inhibitory effects on CLBL-1 cell proliferation. The FA-PEG-Pan-Lip formulation ($IC_{50}$= 10.9 ± 0.03 nM) showed higher cytotoxicity than the non-targeted PEG-Pan-Lip formulation ($IC_{50}$= 12.9 ± 0.03 nM) and the free panobinostat (Pan) compound ($IC_{50}$= 18.32 ± 0.03 nM). Moreover, mechanistically, both Pan-containing formulations induced acetylation of H3 histone and apoptosis. Flow cytometry and immunofluorescence analysis of intracellular uptake of rhodamine-labelled liposome formulations in CLBL-1 cells confirmed cellular internalization of PEG-Lip and FA-PEG-Lip formulations and higher uptake profile for the latter. Biodistribution studies of both formulations in CD1 and SCID mice revealed a rapid clearance from the major organs and a 1.6-fold enhancement of tumor uptake at 24 h for $^{111}$In-FA-PEG-Pan-Lip (2.2 ± 0.1 % ID/g of tumor) compared to $^{111}$In-PEG-Pan-Lip formulation (1.2 ± 0.2 % ID/g of tumor). In summary, our results provide new data validating Pan-loaded folate liposomes as a promising targeted drug delivery system for the treatment of canine B-cell lymphoma and open innovative perspectives for comparative oncology.

**Keywords:** Non-Hodgkin Lymphoma, Canine B-cell Lymphoma, Liposome, Folate, Panobinostat, Drug Delivery.

## 4.1. Introduction

Cancer is a major public health and economic issue, and its burden continues to increase worldwide. With over 19 million cases in 2020, it is expected that there will be 29 million cases by 2040 due to the aging and growing population (Sung et al. 2021b). The past few decades have seen unprecedented advances in the development of new cancer treatments, particularly with the major advances in immunotherapy and the approval of emerging therapeutics, such as immune-checkpoint inhibitors, antibody-drug conjugates,

bispecific antibodies, and CAR-T cells. Nevertheless, although the landscape of cancer treatment has changed dramatically in recent years, new approaches to fight cancer need to be explored rapidly and effectively. Comparative medicine has the potential to accelerate the development of new therapeutic options in the field of oncology by leveraging commonalities between diseases that are common to humans and animals. In particular, the canine model provides a powerful resource for developing models of naturally occurring tumours, that share many clinical and pathophysiological features with their human counterparts (Schiffman and Breen 2015; Gardner et al. 2016). Domestic dogs are highly affected by cancer and approximately 4 million dogs die from cancer each year, making it the leading cause of death (Gardner et al. 2016). Thus, efforts are also being made in comparative research to provide quality cancer treatment options for dogs as caregivers are becoming increasingly demanding.

Non-Hodgkin´s lymphoma (NHL) is one of the most common cancers in both species (Schiffman and Breen 2015; Gardner et al. 2016; Bowzyk Al-Naeeb et al. 2018; Bray et al. 2018). NHL is a malignancy that originates from cells of the immune system, the vast majority of which are B lymphocytes (Bowzyk Al-Naeeb et al. 2018). In humans, NHL is among the 15 most prevalent and deadly malignancies worldwide (Sung et al. 2021b). The incidence in dogs is similar to that in humans, affecting 15-30 per 100 000 dogs (Gardner et al. 2016). Owing to the great similarity in pathologic presentation shared between canine and human NHL, the World Health Organization (WHO) classification criteria is also used for canine tumors (Ito et al. 2014; Schiffman and Breen 2015). Although NHL encompasses several subtypes, diffuse large B-cell lymphoma (DLBCL) accounts for one third of all NHL, making it the most common aggressive form in both humans and dogs (Ito et al. 2014; Ansell 2015; Gardner et al. 2016). Veterinary therapies have evolved with human therapies, and similar to humans, CHOP (cyclophosphamide, doxorubicin, vincristine, and prednisolone)-based chemotherapy is the standard treatment for canine lymphoma. Although treatment response and resistance also present (Torchilin, 2010; Gaspar et al., 2012; Chaudhury and Das, 2015; Aguiar et al., 2021) clinical patterns comparable to human NHL, the low-dose chemotherapeutic protocol used in dogs significantly reduces cure rates in veterinary medicine. In most cases disease relapse occurs after remission and the 2-year survival rate is only 20%, demonstrating the urgent need for novel treatment strategies (Paoloni and Khanna 2008; Ansell 2015; Bowzyk Al-Naeeb et al. 2018). Moreover, the toxicity of conventional chemotherapy often limits its efficacy. Therefore, interest in designing and developing more targeted and specific molecules has increased over recent years.

Cancer is highly associated with genetic alterations, with epigenetic processes playing a key role in carcinogenesis, namely influencing gene transcription, regulating anti-oncogenes and DNA repair genes. Therefore, new research and discoveries have been directed toward the development of agents that can regulate these epigenetic mechanisms. Among the

compounds targeting epigenetic regulators, histone deacetylase inhibitors (HDACis) have emerged as a promising new class of anticancer therapeutics (Eckschlager et al. 2017). Histone deacetylases are important naturally occurring enzymes that promote deacetylation of histones and alter gene transcription. HDACis act on a variety of proteins mainly involved in the control of cell growth, differentiation, and apoptosis. On the other hand, by inducing acetylation of histone and non-histone proteins, HDACis promote cell differentiation, cell cycle arrest, angiogenesis inhibition and apoptosis induction (Glozak and Seto 2007; Chun 2015; Eckschlager et al. 2017). The activity of HDACis has been demonstrated in a number of hematological malignancies, including lymphoblastic leukemia, cutaneous T-cell lymphoma, DLBCL, Hodgkin lymphoma and Burkitt lymphoma (Sermer et al. 2019). Currently, three HDACis are approved by the U.S. Food and Drug Administration (FDA) for clinical use in human cancer therapy: vorinostat, romidepsin, and belinostat. Only belinostat and panobinostat (Pan) have been approved by the European Medicines Agency (EMA) ( Mann et al., 2007; Bertino and Otterson, 2011; Lee et al., 2015; Shah, 2019). Considering the high efficacy of HDACis in human targeted cancer therapy, we recently conducted the first investigation on their antitumor properties using a canine B-cell lymphoma model. For this purpose, a panel of seven HDACis (CI-994, Pan, SBHA, SAHA, scriptaid, trichostatin A and tubacin) were initially tested on the well-characterized CLBL-1 canine B-cell lymphoma cell line, and Pan was identified as the most promising compound with strong *in vitro* and *in vivo* antitumor properties (Dias et al. 2018b). Our results have validated HDACis, and in particular, Pan as a novel anticancer therapy for veterinary medicine, while contributing to comparative oncology. Nevertheless, owing to their potent and broad-spectrum inhibition, HDACis have been associated with significant dose-limiting toxicities, which might lead to some limitations, clinical utility, and safety as a single/adjuvant agent. There are many ways to mitigate the toxicity presented by HDACi, such as the synthesis of more efficient and safer molecules, modification of existing molecules and exploration of drug delivery systems to specifically deliver the HADCi into cancer cells, such as liposomes.

Nanomedicine and drug delivery systems play a prominent role in modern medicine and can help to circumvent the current pitfalls of several anticancer drugs, including non-targeted HDACis. Lipid-based nanosystems, particularly liposomes, represent an attractive nanocarrier for drug delivery for cancer treatment (Co et al. 2019; De Souza et al. 2020; Ferreira et al. 2021; Luiz et al. 2023). Liposomes are lipid vesicles composed of one or more bilayers enclosing one or various internal aqueous compartments that are able to incorporate both hydrophilic and hydrophobic compounds. Liposomes have many advantages such as biodegradability, biocompatibility, improvement of pharmacokinetic profiles, low cytotoxicity and the ability to be modified to allow pH and temperature sensitive release (Sercombe et al. 2015; Bulbake et al. 2017; De Souza et al. 2020). Moreover, due to their unique properties,

liposomes can be designed to deliver active drugs to specific sites, through surface modification. In recent years, several ligands, such as monoclonal antibodies, antibody fragments, proteins, peptides, vitamins, carbohydrates, and glycoproteins, have been attached to the surface of liposomes to selectively target tumor cells overexpressing a specific cell surface receptor (Torchilin 2010; Gaspar et al. 2012; Chaudhury and Das 2015; Aguiar et al. 2021). The folate receptor (FR) has been identified as a promising target because it is highly overexpressed on the surface of a variety of tumor types, while its distribution in normal tissues and organs is limited. Some studies have shown that conjugation of folic acid (FA) is a promising approach for active targeting of liposomes to increase the amount of drug delivered to the target cell compared to free drugs or passively targeted liposomes (Chaudhury et al. 2012; Gaspar et al. 2012; Chaudhury and Das 2015). Within this context, in the present study we aimed to develop Pan-loaded folate targeted PEGylated liposomes with improved therapeutic outcomes for the treatment of canine B-cell lymphoma. For this purpose, non-targeted Pan-loaded and folate-targeted PEGylated liposomal formulations were prepared and their cytotoxic and targeting properties were thoroughly investigated.

## 4.3. Results

### 4.3.1. Physicochemical properties of panobinostat loaded liposomes are suitable for drug delivery

Owing to the potent anticancer activity of Pan on canine B-cell lymphoma demonstrated previously by our group (Dias et al. 2018), this HDACi was selected for the study described herein. Although Pan exhibited promising cytotoxicity and antitumor properties *in vitro* and *in vivo,* it has been associated with significant dose-limiting toxicities, which might lead to some limitations for its clinical translation and safety as a single/adjuvant agent. Therefore, there is an urgent need to mitigate the high toxicity of Pan, as well as other HDACis. One of the best strategies to overcome this issue is to explore drug delivery systems. Within this context, in the present study we aimed to develop a panobinostat loaded PEGylated liposome drug delivery system with improved therapeutic outcomes. For this purpose, unloaded and loaded folate-targeted (FA-PEG-Lip and FA-PEG-Pan-Lip) and non-targeted liposomal formulations (PEG-Lip and PEG-Pan-Lip) were prepared, characterized and their biological activity tested. All liposomal formulations were prepared using the dehydration-rehydration method followed by an extrusion step to reduce and homogenize the mean size of the liposomes. The physicochemical properties of the liposomes, namely particle size, zeta potential, and incorporation parameters, such as encapsulation efficiency and loading capacity, are listed in Table 1. All liposome formulations presented a mean size of 130 nm and a PI < 0.2, demonstrating the high homogeneity of the so developed liposomes. The Zeta potential

revealed a neutral surface charge under all the conditions being in accordance with the presence of DSPE-PEG at liposomal surface. Regarding Pan incorporation parameters, liposomes loaded with folate presented a higher encapsulation efficiency (94%), with a final loading capacity of 33 µg/µmoL than non-targeted liposomes (21 µg/µmoL). Nevertheless, all formulations were selected to study their cytotoxic and targeting properties against canine B-cell lymphoma.

**Table 1 - Characterization of target and nontargeted liposomes loaded with and without panobinostat.** Data are expressed as mean ± SD.

| Lipid Composition (molar ratio) | (PAN /Lip)i (µg/µmol) | (PAN /Lip)f (µg/µmol) | E.E. (%) | Mean size (nm) (P.I.) | Zeta Pot (mV) |
|---|---|---|---|---|---|
| **PEG-Pan-Lip** **DPPC:Chol:DSPE-PEG (1.85:1.0.15)** | **39 ± 1** | 21 ± 1 | 56 ± 2 | 130 (<0.050) | - 2 ± 1 |
| **FA-PEG-Pan-Lip** **DPPC:Chol:DSPE-PEG: DSPE-PEG-FA (1.85:1.0.12:0.03)** | 35 ± 1 | 33 ± 1 | 94 ± 2 | 130 (<0.050) | - 2 ± 1 |
| **PEG- Lip** **DPPC:Chol:DSPE-PEG (1.85:1.0.15)** | na | na | na | 130 (<0.070) | - 3 ± 1 |
| **FA-PEG-Lip** **DPPC:Chol:DSPE-PEG: DSPE-PEG-FA (1.85:1.0.12:0.03)** | na | na | na | 130 (<0.070) | - 3 ± 1 |

### 4.3.2. Folate receptor is expressed in canine lymphoma cells

The folate receptor is overexpressed in cancer cells, making it a suitable molecular target for specific drug delivery (Chaudhury and Das 2015). Therefore, to assess the feasibility of using the folate receptor as a target for canine B-cell lymphoma, we evaluated its expression by western blot analysis in the well-characterized CLBL-1 canine lymphoma cell line (Rütgen et al. 2010; Rütgen et al. 2012). Immunoblotting analysis (Figure 30A) confirmed folate receptor expression in the canine DLBCL cell line and demonstrated an increasing presence of the receptor, in agreement with the increasing amount of cellular extract. These results confirmed the presence of the folate receptor in CLBL-1, allowing us to explore it as a promising target and to evaluate the cytotoxic and targeting properties of the different liposome formulations prepared.

### 4.3.3. Panobinostat-loaded liposomes present cytotoxicity in canine B-cell lymphoma

To evaluate the potential cytotoxic activity of the different liposome formulations in canine B-cell lymphoma, we conducted a cell viability assay in the CLBL-1 cell line. Cell viability of lymphoma cells subjected to a 24 h treatment with non-targeted and folate-targeted liposomes loaded with Pan was evaluated using Alamar Blue reagent, as described in the Materials and Methods section. PEG-Lip, FA-PEG-Lip and free Pan were used as controls. As shown in Figure 31B, Pan liposome formulations (PEG-Pan-Lip and FA-PEG-Pan-Lip) exhibited a dose-dependent inhibitory effect on CLBL-1 cell proliferation. In contrast, no cytotoxicity was observed for the PEG-Lip and FA-PEG-Lip formulations (data not shown). The

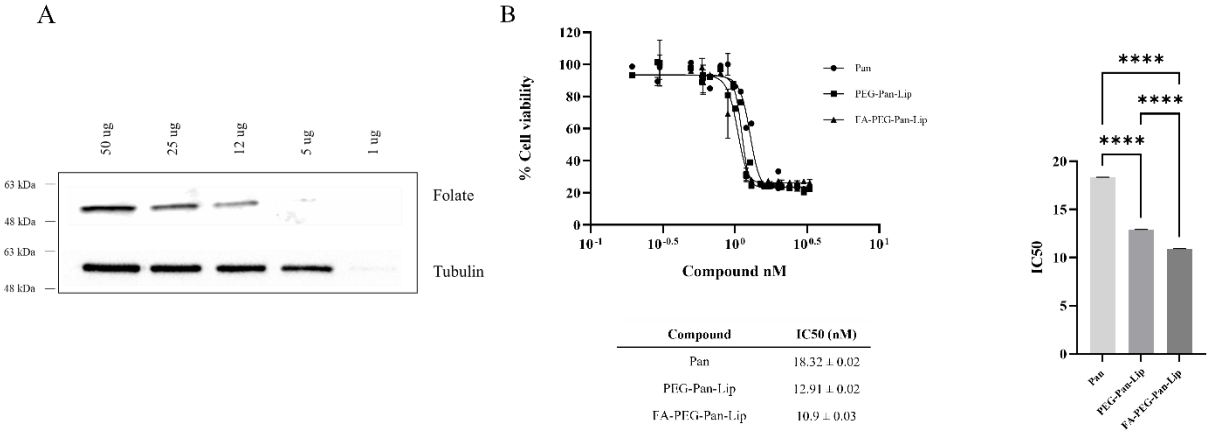


**Figure 31 - Evaluation of folate receptor expression and cytotoxic activity of folate-targeted and nontargeted liposomes loaded with panobinostat was evaluated in CLBL-1 cells.** A) Folate receptor expression was evaluated in total cell extracts from CLBL-1 cells using an anti-folate receptor antibody. Loading was controlled with an anti-tubulin antibody. Representative blots are shown. B) Cells were treated with increasing concentrations of liposomes. After 24 h treatment, cell viability was measured using Alamar Blue reagent. Two replicate wells were utilized to determine each data point and three independent experiments were carried out in different days. Best-fit IC50 values of each formulation were calculated using the log (inhibitor) vs response (variable slope) function. Statistical significance was determined with one-way ANOVA followed by a Tukey's test. Values of $p < 0.05$ were considered significant. **** $p < 0.0001$.

differences between the $IC_{50}$ values for each liposomal formulation and Pan-free were statistically significant. Moreover, the cytotoxicity of Pan was potentiated after incorporation in liposomes, probably due to a higher internalization in tumor cells. Importantly, the obtained data have shown that the $IC_{50}$ values were in the nM range and that the Pan folate-targeted liposomal formulation seems to exhibit a slightly higher cytotoxic effect than the non-target liposomal formulation and Pan-free (FA-PEG-Pan-Lip, $IC_{50}$ = 10.9 ± 0.03 nM, PEG-Pan-Lip, $IC_{50}$ = 12.91 ± 0.02 nM and Pan-free, $IC_{50}$ = 18.32 ± 0.024 nM).

### 4.3.4. Panobinostat-loaded liposomes induce H3 histone acetylation and apoptosis

Pan alters gene expression by inducing the acetylation of histones at an early stage, causing several effects on the cell cycle and resulting in cell death. Thus, to validate the mechanism of action of Pan-loaded liposomes in CLBL-1 cells, we evaluated the acetylation status of H3 histones by western blot. The acetylation status of cells treated with liposomes loaded with Pan were compared to unloaded liposome formulations. Immunoblotting analysis (Figure 32) demonstrated that CLBL-1 cells presented a hyperacetylation status, after 24 h of treatment with PEG-Pan-Lip, FA-PEG-Pan-Lip formulations, when compared with PEG-Lip and FA-PEG-Lip formulations and vehicle-/control-treated cells. Cell death occurred by apoptosis (Figure 33A, B). These results are in agreement with the cell viability and

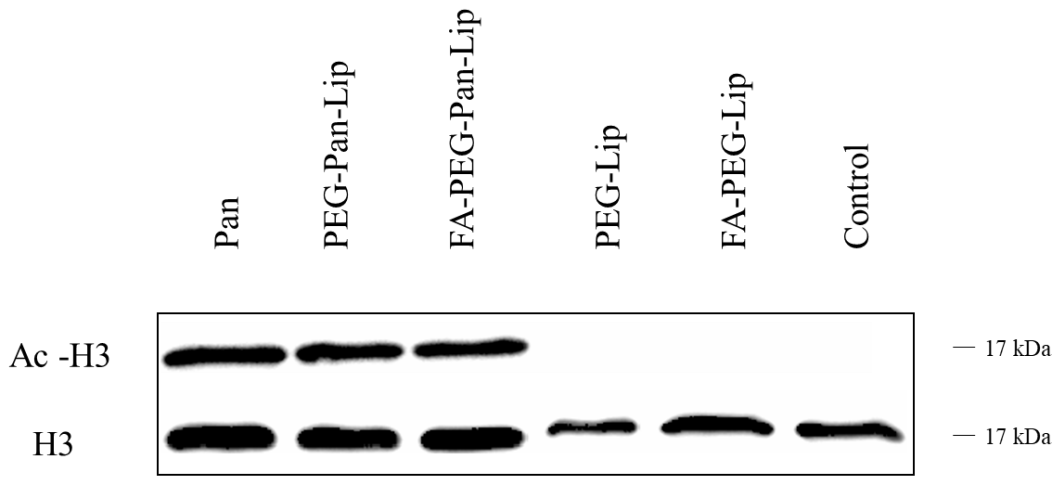


**Figure 32 - Assessment of H3 Histone Acetylation.** H3 histone acetylation was assessed in total cell extracts from CLBL-1 cells after 24 h treatment with 20 µM of folate-targeted liposomes and nontargeted liposomes loaded with Panobinostat. Acetylation of H3 histones was evaluated by western blotting with an anti-acetyl-histone H3 polyclonal antibody. As loading control, H3 histone was assessed using anti-histone H3 polyclonal antibody. Representative blots are presented.

proliferation data upon Pan treatment, indicating that the cytotoxic activity of Pan in the CLBL-1 cell line is consistent with the induction of apoptosis. To confirm that apoptosis is a central mechanism of Pan-loaded liposome-induced cell death, the caspase 3/7 activity levels and the percentage of apoptotic cells after 24 h of treatment were determined. The results shown in Figure 33C indicate that caspase 3/7 activity was promoted in a dose-dependent manner by the PEG-Pan-Lip and FA-PEG-Pan-Lip formulations and the maximum caspase-3/7 activity was seen at 20 nM.

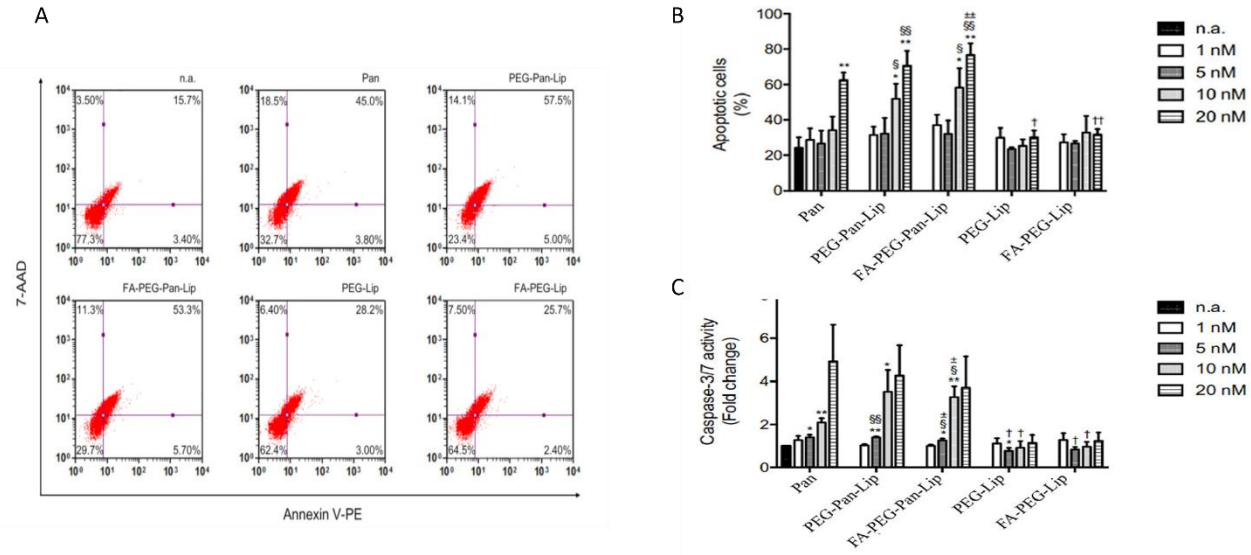


**Figure 33 - Evaluation of Apoptotic cell death**. A) CLBL-1 were treated with 20 nM folate-targeted and non-targeted liposomes loaded with panobinostat for 24 h and representative flow cytometry plots using Annexin V/7-AAD staining are shown. B) The percentage of apoptotic cells was determined in CLBL-1 cells subjected to a range of concentrations of folate-targeted and nontargeted liposomes loaded with panobinostat. After 24 h treatment, apoptotic cells were determined by flow cytometry using Guava Nexin Assay. C) Caspase 3/7 activity was evaluated in CLBL-1 cells subjected to increasing concentrations of folate-targeted and nontargeted liposomes loaded with panobinostat. After 24 h treatment, activity was determined using the Caspase-Glo 3/7 assay. Results are expressed as means ± SEM fold change to control cells. *p < 0.05 and **p < 0.01 from n.a.; †p < 0.05 and ††p < 0.005 from Pan Free; §p < 0.05 and §§p < 0.01 from PEG; ±p < 0.05 and ±±p < 0.001 from PEG Fol. Statistical analysis was performed using Student's t-test. Values of p < 0.05 were considered significant. n.a., no addition.

### 4.3.6. Uptake of liposome formulations in CLBL-1 cells

Intracellular uptake of rhodamine-labelled liposome formulation in CLBL-1 cells was evaluated by flow cytometry and immunofluorescence. For flow cytometry, labeled liposomes were incubated with CLBL-1 cells at different time points (90 min, 3 h and 6 h). The uptake of both formulations (FA-PEG-Pan-Lip and PEG-Pan-Lip) differed significantly, as shown in Figure 34A. The uptake was higher in the formulation containing folate at all time-points tested, demonstrating the importance of folate in facilitating cellular uptake. Additionally, the cellular uptake seemed to be time-dependent, since the amount of liposomes increased with time, reaching the highest value after 6 h incubation. Live/dead reagent was used to exclude dead cells, and background noise was evaluated in the control with the secondary antibody (data not shown). To better characterize the uptake efficiency of all liposomal formulations in CLBL-1 cells, we further evaluated the cellular internalization properties of the liposomes using confocal point-scanning microscopy after staining the nucleus with DAPI. As shown in Figure 34B, liposomes accumulated in the perinuclear area, confirming the internalization of both

formulations. Moreover, FA-PEG-Pan-Lip significantly increased the fluorescent signal in the perinuclear region, in comparison with the PEG-Pan-Lip.

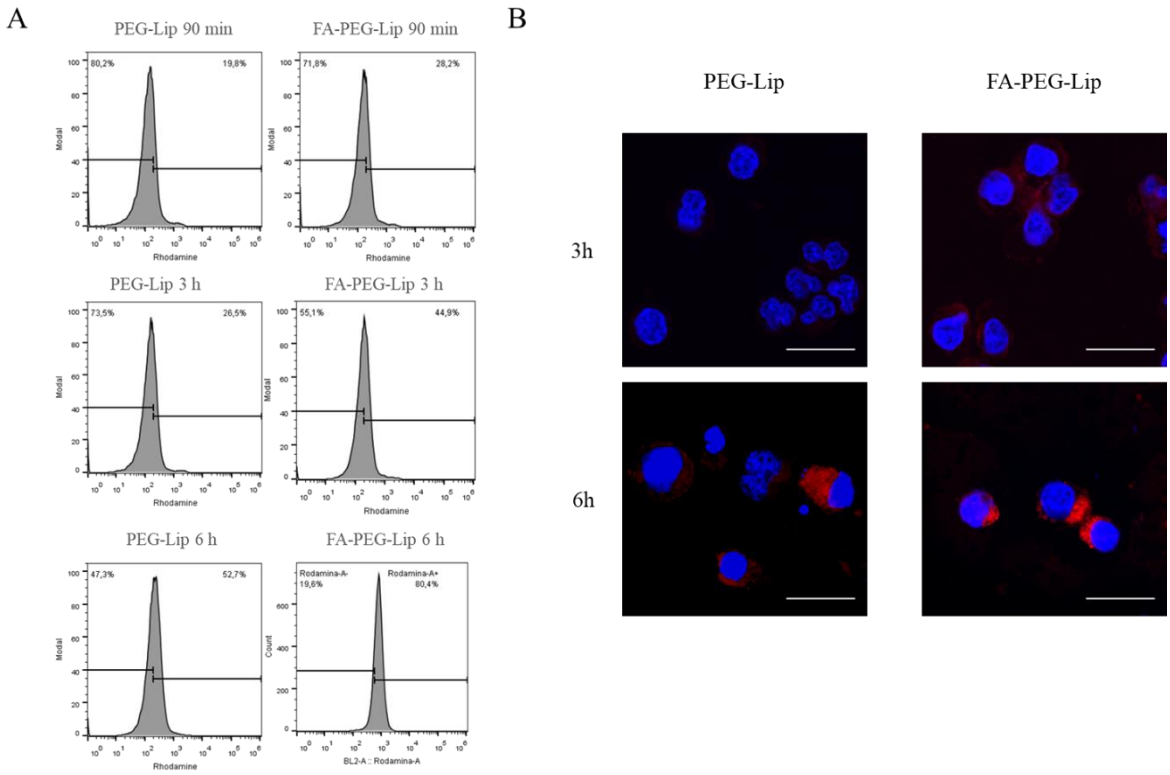


**Figure 34 - Evaluation of cellular uptake by flow cytometry and immunofluorescence.** A) To evaluate the quantitative cellular uptake of the liposomes, flow cytometry was performed. 1 x $10^6$ of CLBL-1 cells were incubated with 5 µmol/mL of PEG and PEG Folate labeled with phosphatidyl ethanolamine covalently linked to rhodamine for 90 min, 3 h and 6 h. Cellular uptake seems to be time dependent, achieving a high value after 6h of incubation. Moreover, the percentage of uptake was higher in the formulation containing folate. B) To determine the qualitative analysis, immunofluorescence was performed. 1 x $10^5$ of CLBL-1 cells were incubated for 3 h and 6 h with liposomes labeled with rhodamine. An accumulation of liposomes in the perinuclear area, confirmed the internalization of both formulations.

### 4.3.7. Biodistribution studies in CD1 mice and xenograft mice model of canine B-cell lymphoma

To assess the *in vivo* stability, pharmacokinetic and tumor uptake profile of non-targeted and folate-targeted liposome formulations, we performed a biodistribution study in CD1 mice and in SCID xenograft mouse model of CLBL-1, respectively. For that purpose, FA-PEG-Pan-Lip and PEG-Pan-Lip formulations were radiolabeled with $^{111}$In, according to a previously reported procedure (Gaspar et al. 2007; Pinho et al. 2023). Both $^{111}$In-lipossomes were intravenously administrated to CD1 or to SCID mice and the biodistribution was evaluated at different time points. The biodistribution data of $^{111}$In-labeled PEG-Pan-Lip and FA-PEG-Pan-Lip, expressed as % ID/g of the main tissues and tumors, are presented in Table 2 and Table 3. Analysis of the data, in the CD1 mouse model, revealed that both $^{111}$In-liposomal preparations presented a similar tissue distribution profile with a moderate blood clearance (12.7 ± 3.8, 3.5 ± 0.6, 0.67 ± 0.08% ID/g for $^{111}$In-PEG-Pan-Lip and 12.8 ± 0.7, 5.4 ± 0.7, 1.2 ± 0.6% ID/g for $^{111}$In-FA-PEG-Pan-Lip, at 1 h, 24 h and 48 h p.i., respectively). Moderate hepatic uptake was found (1.1 ± 0.6, 5.9 ± 0.5% ID/g of liver for $^{111}$In-PEG-Pan-Lip and 2.19 ± 0.05, 6.8 ± 1.4% ID/g for $^{111}$In-FA-PEG-Pan-Lip, at 1 h, 24 h, respectively) that slightly decreased at 48 h indicating the hepatobiliar path as the main elimination route. However, the involvement of the urinary excretory pathway is also evident in the kidney uptake and in the whole-body radioactivity excretion rate. In fact, the untargeted formulation ($^{111}$In-PEG-Pan-Lip) had a low kidney uptake (< 2.7 ± 0.3% ID/g of kidney) associated to a rapid total excretion (59.7 ± 6.6, 68.3 ± 0.4, 82.3 ± 4.2% ID/g, at 1 h, 24 h and 48 h p.i., respectively). The kidney uptake of the targeted formulation ($^{111}$In-FA-PEG-Pan-Lip) increased over time (1.7 ± 0.9, 5.6 ± 0.3, 4.1 ± 2.7% ID/g of kidney, at 1 h, 24 h and 48 h p.i., respectively) probably due to the presence of the folate moiety in the liposomes since the high expression of folate receptors in the renal proximal tubules is known. Consequently, the rate of total excretion is lower, approximately 30%, at 1 h p.i. The washout from major organs, except spleen was also rapid in both formulations. Liposomes were promptly eliminated from the heart, intestine, lungs and stomach. Radioactivity accumulation of radiolabeled liposomes was observed in the spleen (1.7 ± 0.4, 12.5 ± 4.2, 11.2 ± 3.9% ID/g for $^{111}$In-PEG-Pan-Lip and 2.6 ± 1.1, 7.8 ± 1.5, 8.2 ± 1.6% ID/g for $^{111}$In-FA-PEG-Pan-Lip, at 1 h, 24 h and 48 h p.i., respectively) reflecting the expected uptake from the mononuclear phagocyte system. Regarding the biodistribution and tumor uptake in the SCID xenograft mouse model of CLBL-1, the trend of the biodistribution profile is similar. Moderate blood clearance associated to hepatic and splenic uptake. Higher kidney uptake and lower rate of total excretion of $^{111}$In-FA-PEG-Pan-Lip than $^{111}$In-PEG-Pan-Lip. Moreover, and importantly, this preliminary biodistribution study demonstrated the ability of the targeted formulation ($^{111}$In-FA-PEG-Pan-Lip) to accumulate in FR-expressing tumors.

Indeed, the tumor uptake was 1.6-fold higher at 24 h p.i (2.2 ± 0.9% ID/g of tumor) than the $^{111}$In-PEG-Pan-Lip formulation (1.32 ± 0.2% ID/g of tumor), as shown in Table 3.

**Table 3- Biodistribution profiles of radiolabeled FA-PEG-Pan-Lip and PEG-Pan-Lip in healthy mice.** Radiolabeled liposomes were intravenous injected into CD1 mice. After sacrifice, the tissues were dissected and counted in a gamma counter, at different time points (1 h, 24 h and 48 h p.i.).

| Organ | $^{111}$In-$L_1$-PEG-Pan-Lip | | | $^{111}$In-$L_2$-FA-PEG-Pan-Lip | | |
|---|---|---|---|---|---|---|
| | 1 h | 24 h | 48 h | 1 h | 24 h | 48 h |
| **Blood** | **12.7 ± 3.8** | **3.5 ± 0.6** | **0.67 ± 0.08** | **12.8 ± 0.7** | **5.4 ± 0.7** | **1.2 ± 0.6** |
| **Liver** | 1.1 ± 0.6 | 5.9 ± 0.5 | 4.5 ± 1.4 | 2.19 ± 0.05 | 6.8 ± 1.4 | 6.3 ± 1.6 |
| **Intestine** | 0.55 ± 0.06 | 0.98 ± 0.07 | 0.6 ± 0.2 | 1.0 ± 0.4 | 1.2 ± 0.2 | 1.1 ± 0.2 |
| **Spleen** | 1.7 ± 0.4 | 12.5 ± 4.2 | 11.2 ± 3.9 | 2.6 ± 1.1 | 7.8 ± 1.5 | 8.2 ± 1.6 |
| **Heart** | 0.7 ± 0.2 | 1.3 ± 0.3 | 0.7 ± 0.2 | 0.7 ± 0.4 | 1.9 ± 0.7 | 0.9 ± 0.2 |
| **Lung** | 1.0 ± 0.5 | 1.6 ± 0.6 | 0.6 ± 0.2 | 1.4 ± 0.6 | 2.2 ± 0.4 | 0.5 ± 0.3 |
| **Kidney** | 1.3 ± 0.6 | 2.7 ± 0.3 | 2.2 ± 0.0 | 1.7 ± 0.9 | 5.6 ± 0.3 | 4.1 ± 2.7 |
| **Muscle** | 0.4 ± 0.1 | 1.3 ± 0.9 | 0.26 ± 0.02 | 1.5 ± 0.1 | 0.7 ± 0.5 | 0.6 ± 0.1 |
| **Bone** | 0.6 ± 0.3 | 0.7 ± 0.3 | 0.6 ± 0.1 | 0.8 ± 0.2 | 1.0 ± 0.2 | 0.63 ± 0.02 |
| **Stomach** | 1.7 ± 0.9 | 1.1 ± 0.2 | 0.7 ± 0.3 | 1.2 ± 0.8 | 1.3 ± 0.7 | 0.8 ± 0.4 |
| **Brain** | 0.13 ± 0.03 | 0.16 ± 0.07 | 0.07 ± 0.05 | 0.17 ± 0.01 | 0.13 ± 0.03 | 0.04 ± 0.01 |
| **Carcass (%ID)** | 18.0 ± 0.9 | 26.0 ± 2.3 | 13.4 ± 0.7 | 37.2 ± 5.6 | 33.5 ± 3.9 | 28.8 ± 3.9 |
| **Excretion (%ID)** | 59.7 ± 6.6 | 68.3 ± 0.4 | 82.3 ± 4.2 | 25.7 ± 3.9 | 54.3 ± 1.4 | 63.5 ± 0.4 |

**Table 2- Biodistribution of radiolabeled folate-targeted and nontargeted liposomes in xenograft mice model of cNHL.** Radiolabeled liposomes were intravenous injected into SCID mice. After sacrifice, the tissues were dissected and counted in a gamma counter, at different time points (24 h and 48 h p.i.).

| Organ | $^{111}$In-PEG-Pan-Lip | | $^{111}$In-FA-PEG-Pan-Lip | |
|---|---|---|---|---|
| | **24 h** | **48 h** | **24 h** | **48 h** |
| **Blood** | 1.8 ± 0.5 | 1.0 ± 0.3 | 4.6 ± 0.7 | 2.4 ± 0.4 |
| **Liver** | 5.0 ± 0.6 | 5.8 ± 1.6 | 11.9 ± 2.1 | 8.5 ± 2.0 |
| **Intestine** | 0.8 ± 0.2 | 0.73 ± 0.08 | 1.7 ± 0.1 | 1.6 ± 0.2 |
| **Spleen** | 20.6 ± 2.4 | 25.8 ± 0.5 | 16.8 ± 4.1 | 12.4 ± 4.4 |
| **Heart** | 0.32 ± 0.07 | 0.40 ± 0.02 | 1.2 ± 0.3 | 0.9 ± 0.2 |
| **Lung** | 0.68 ± 0.07 | 0.7 ± 0.2 | 2.3 ± 0.7 | 1.1 ± 0.6 |
| **Kidney** | 2.5 ± 0.3 | 1.9 ± 0.5 | 4.6 ± 0.9 | 4.4 ± 1.6 |
| **Muscle** | 0.12 ± 0.06 | 0.3 ± 0.2 | 0.7 ± 0.4 | 0.6 ± 0.4 |
| **Bone** | 0.3 ± 0.2 | 0.29 ± 0.07 | 0.8 ± 0.1 | 0.6 ± 0.1 |
| **Stomach** | 0.5 ± 0.2 | 0.40 ± 0.07 | 1.5 ± 0.7 | 1.0 ± 0.2 |
| **Brain** | 0.05 ± 0.02 | 0.04 ± 0.01 | 0.2 ± 0.1 | 0.05 ± 0.02 |
| **Tumor** | 1.3 ± 0.2 | 2.08 ± 0.09 | 2.2 ± 0.9 | 2.5 ± 0.8 |
| **Carcass (%ID)** | 14.5 ± 1.3 | 12.1 ± 1.2 | 34.4 ± 4.9 | 31.8 ± 3.5 |
| **Excretion (%ID)** | 69.8 ± 0.2 | 73.0 ± 1.1 | 27.8 ± 6.2 | 39.0 ± 9.1 |

Moreover, it is important to mention that histological and immunohistochemical analysis demonstrated that xenograft tumors maintained histological features and expression of B-cell markers were positive and expression of T-cell markers were negative, reflecting those of the original CLBL-1 cell line xenografts (Figure 35).

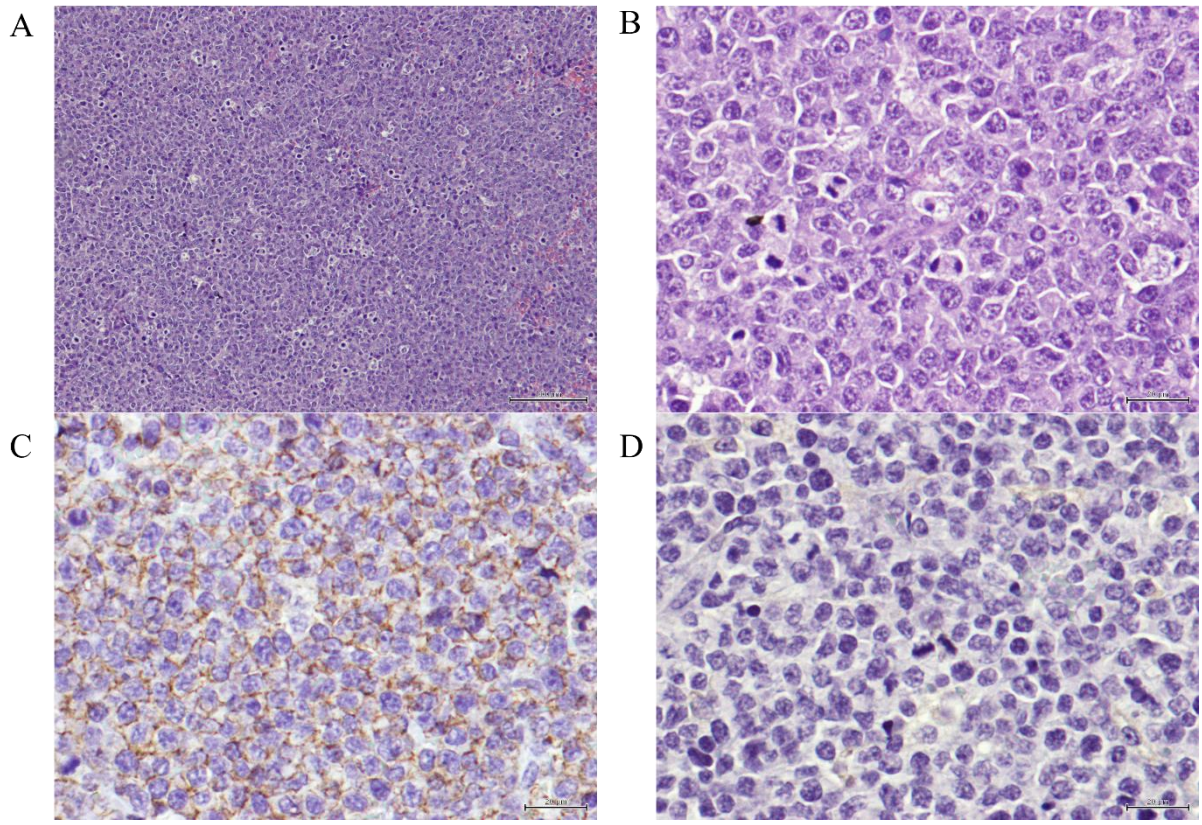


**Figure 35** - **A) Xenograft tumor section presenting a neoplasia, classified as high grade centroblastic diffuse malignant lymphoma.** The neoplasia consists of monomorphic large cells with a high cell density and a starry-sky pattern. Hematoxylin and eosin (H&E) stained. Magnification = 100×, scale bar = 100μm. (B) Xenograft tumor section presenting a lymphoma. The neoplastic is composed by monomorphic round cells, with several marginal and small nucleoli per cell and high mitotic index. Hematoxylin and eosin (H&E) stained. Magnification = 400×, scale bar = 20μm. (C) Xenograft tumor section presenting the immunohistochemistry technique for B-cells, exhibiting positive staining on the cellular membrane level in virtually 100% of the tumor. Anti-CD20 antibody, Gill's hematoxylin. Magnification = 400×, scale bar = 20μm. (D) Xenograft tumor section presenting the immunohistochemistry technique for T-cells, showing that the tumor cells are negative for this marker (anti-CD3, Gill's hematoxylin, 100x). Anti-CD3 antibody, Gill's hematoxylin. Magnification = 400×, scale bar = 20μm.

## 4.4. Discussion

Lymphoma and NHL, in particular, are responsible for millions of deaths worldwide, representing a disturbing global health problem. The similarities between human NHL and canine lymphoma make NHL a transversal disease for both species, opening new opportunities to explore the advantages of translational research. In the present study, we explored a novel liposome-based drug delivery system to enhance the therapeutic benefits of

Pan, a validated anticancer drug in comparative medicine (Dias et al. 2018). Pan is a cytotoxic compound belonging to the HDACi class that has shown great promise in relapsed DLBCL patients, inducing long-lasting durable responses in a phase 2 clinical study (Assouline et al. 2016). Recently, we demonstrated its anticancer activity against canine B-cell lymphoma (Dias et al. 2018). However, this study revealed some *in vivo* toxic effects that can limit its clinical progression as a treatment option for canine lymphoma. The primary goal of anticancer therapy in veterinary medicine is to provide the best quality of life for as long as possible, as such dogs are not good candidates for aggressive regimens independent of their curability potential. This is also a concern in human medicine, considering that the potential of these molecules as anticancer therapeutics has been hampered by toxicity- and specificity-related issues. Although a multitude of drugs acting via HDAC inhibition are currently in clinical trials or in the market, only HDACis, such as vorinostat, romidepsin, and belinostat have been approved for some T-cell lymphomas and Pan for multiple myeloma. In addition to its non-specificity, HDACis, including valproic acid, trichostatin A, sodium butyrate, and vorinostat, are associated with clinical toxic effects, such as thrombocytopenia, nausea, and fatigue. Furthermore, vorinostat and romidepsin, two FDA-approved HDACis, are reported to have no partial or complete response in solid tumors and are linked to severe cardiac toxicity. Thus, in the present study, we hypothesized that the encapsulation of Pan into liposome nanocarriers could improve their therapeutic index and further reduce associated systemic toxicity effects, extending their use in both human and veterinary clinical settings.

Due to their biological and technological advantages, liposomes have been considered in the past few years as promising drug delivery systems for cancer applications. Remarkable advances have been made and multiple biomedical applications of liposomes have been tested in clinical trials or have already been approved (Bozzuto and Molinari 2015; Beltrán-Gracia et al. 2019). The first liposomal formulation used in human medicine was Doxil, a doxorubicin liposomal formulation, approved for the treatment of ovarian cancer, multiple myeloma, and HIV-associated Kaposi's sarcoma (Barenholz 2012). Over the years, other formulations have been approved for cancer therapy, such as Myocet, Marqibo and Vyxeos (Liu et al. 2022). Many studies in veterinary medicine have reported the use of drugs encapsulated in liposomes. Doxorubicin liposomes have been tested in canine models to evaluate their pharmacokinetics, biodistribution, and safety profiles (Vail et al. 1997; Sorenmo et al. 2007; Teske et al. 2011). These studies confirmed that Doxil did not induce cardiotoxicity or myelosuppression in dogs, one of the most important side effects of free doxorubicin, making it a viable therapeutic option (Sorenmo et al. 2007; Teske et al. 2011). Another pilot study conducted by Hauck et al. reported results from a phase I clinical trial in dogs with spontaneous tumors, namely sarcomas and carcinomas, using low-temperature doxorubicin-loaded liposomes. Of the 21 patients enrolled in the study, 12 presented with stable disease

and 6 had a partial response to the treatment. This study showed favorable clinical responses, validating a novel approach of a liposome-based delivery system for veterinary use (Hauck 2006).

Within this context, in the present study we aimed to develop Pan-loaded folate-targeted PEGylated liposomes with improved therapeutic outcomes for the treatment of canine B-cell lymphoma. For this purpose, non-targeted and folate-targeted PEGylated liposomal formulations were prepared and their cytotoxic and targeting properties against canine diffuse large B-cell lymphoma were thoroughly investigated. While non-targeted liposomes rely on enhanced permeability and retention to deliver the therapeutic agent to the tumor site, targeted liposomes are functionalized with surface ligands to improve selective tumor targeting and facilitate intracellular uptake. Due to its overexpression in a wide range of tumors, folate receptor targeting has shown great potential in mediating the tumor uptake of a variety of drugs (Kumar et al. 2019). Several studies by Gabizon et al. demonstrated significant differences between non-targeted and folate-targeted liposomes in folate receptor-overexpressing tumors, including lymphoma (Gabizon et al. 2003; Gabizon et al. 2010). This study compared the *in vivo* distribution of folate-targeted and non-targeted liposomes and found that folate-targeted liposomes were more effective than non-targeted liposomes in a lymphoma tumor model (Gabizon et al. 2003). The conclusions of this study were further reinforced by Shmeeda et al., who demonstrated intracellular uptake of folate-targeted liposomes in lymphoma cells (Shmeeda 2006). In another study, Gabizon et al. proved that folate-targeted liposomes loaded with doxorubicin were more effective than the non-targeted liposomes in a lymphoma model (Gabizon et al. 2010). More recently, Qiu et al. demonstrated the application of this drug delivery system in NHL by using vincristine-loaded lipid-polymer hybrid liposomes (VCR-loaded LPNs). This study reported a targeted effect in the delivery of FA-VCR-loaded LPNs towards B-cell lymphoma cells, with an outstanding therapeutic effect in the treatment of lymphoma, reducing systemic toxicity (Qiu et al. 2018). Considering the high efficacy of drug-loaded folate-targeted liposomes in human lymphoma, we evaluated the folate receptor expression in canine diffuse large B-cell lymphoma and confirmed its overexpression in the CLBL-1 canine lymphoma B-cell line.

Pan liposomes were prepared using an active loading method and both formulations exhibited high incorporation parameters, particularly the one containing FA (PEG-Pan-Lip EE = 56 ± 2% and FA-PEG-Pan-Lip EE= 94 ± 2%). The methodology used in the present work, active loading, means that Pan was incorporated in pre-formed unloaded liposomes (Gaspar et al. 2012) in opposition to a passive loading where the compound is incorporated during liposome preparation (Gaspar et al. 2015). The active loading method presents several advantages over the passive methods namely stability and higher incorporation parameters as widely demonstrated in literature (Barenholz 2021; Nakhaei et al. 2021). The pH or salt

gradient differences between intra and extraliposomal membrane are the most known underlying mechanisms dictating the active drug loading. Moreover, active loading is based on the fact that uncharged drugs will cross the liposomal membrane and become protonated and entrapped inside the aqueous compartment of liposomes thus contributing to achieve high loadings and high stable liposomal formulations (Sur et al. 2014).

Liposomal formulations were further investigated *in vitro* to assess the suitability of their drug delivery properties. Firstly, cytotoxicity assays were performed to analyze the effect of the liposomal formulations on the viability of canine diffuse large B-cell lymphoma cells. The data demonstrated that encapsulated Pan in both formulations (FA-PEG-Pan-Lip and PEG-Pan-Lip) maintained its cytotoxicity in CLBL-1 cells, when compared with Pan-free. The $IC_{50}$ values determined for liposomal formulations were lower in comparison with Pan-free data, indicating that cytotoxic properties of the compound were not only preserved after incorporation in liposomes but potentiated. In addition, our data demonstrated that the cytotoxicity activity of the FA-PEG-Pan-Lip formulation was slightly higher than PEG-Pan-Lip formulation (FA-PEG-Pan-Lip $IC_{50}$ = 10.9 ± 0.03 nM *versus* PEG-Pan-Lip $IC_{50}$ = 12.91 ± 0.02 nM). These data are in accordance with those reported in the literature, where folate is expected to enhance tumor uptake (Kumar et al. 2019). Moreover, our data demonstrated that FA-PEG-Pan-Lip and PEG-Pan-Lip formulations were able to induce histone H3 acetylation in the CLBL-1 canine lymphoma cell line, the key molecular mechanism of HDACis.

HDAC inhibitors can induce multiple antitumor pathways. One of the main mechanisms of transformed cell death is the activation of apoptosis via intrinsic and extrinsic pathways (Xu et al. 2007). Activation of caspases-3 and 7 is an essential step during apoptosis and is used as a reliable marker for cells undergoing apoptosis (Shim et al. 2017). All liposomal formulations loaded with Pan at 20 nM demonstrated a high percentage of apoptotic cells and high levels of caspase-3 and 7 activation, similar to the data for the Pan-free formulation. Finally, to assess the *in vivo* stability and pharmacokinetic profile of each liposomal formulation, we performed biodistribution studies in CD1 mice and in a xenograft SCID mouse model of canine B-cell lymphoma. Biodistribution data demonstrated that FA-PEG-Pan-Lip formulation remained in circulation for a longer time, suggesting extended drug retention. In FA-PEG-Pan-Lip and PEG-Pan-Lip formulations, fast clearance from the major organs was observed, which is crucial to prevent systemic toxicity. However, a high accumulation of liposomal formulations was noted in the liver and spleen. Liposomes have specific clearance mechanisms from the bloodstream. The main mechanism is via recognition and uptake by macrophages of the reticuloendothelial system; consequently, the two main organs that present a major capacity for liposomal accumulation are the liver and the spleen (Ait-Oudhia et al. 2014). Thus, accumulation in the spleen and liver could be related to the elimination of liposomes. Importantly, the biodistribution data in the xenograft SCID mouse model of CLBL-

1 have shown that the tumor uptake was higher with the targeted formulation ($^{111}$In-FA-PEG-Pan-Lip) with a percentage of 2.2% and 2.5% ID/g of tumor at 24h and 48h, respectively. To the best of our knowledge, this is the first study to report the use of a liposome-based drug delivery system loaded with Pan in the treatment of canine B-cell lymphoma. Overall, these results validated that folate-targeted liposomes encapsulated with Pan can be a promising drug delivery system to be explored for a more effective and safer cancer treatment modality. Although this target-liposome-based drug delivery system showed strong cytotoxicity in canine lymphoma cells, additional preclinical studies in canine B-cell lymphoma xenograft murine models are needed to evaluate its *in vivo* efficacy and safety, to then allow its further progression to clinical studies in canine patients. In conclusion, this study contributes to the development of Pan nanocarriers for the treatment of canine B-cell lymphoma as a predictive preclinical surrogate for human NHL, mutually benefiting both species and opening up perspectives in comparative oncology.

## 4.5. Materials and Methods

### 4.5.1. Materials

Dipalmitoyl phosphatidyl choline (DPPC), poly(ethylene glycol) (PEG-2000) covalently linked to distearoyl phosphatidyl ethanolamine (DSPE-PEG), rhodamine covalently linked to phosphatidyl ethanolamine (Rho-PE) and the functionalized DSPE-PEG phospholipids with folate (DSPE-PEG-FA) were purchased from Avanti Polar Lipids (Alabaster, AL, USA). Cholesterol (Chol), and phosphate buffered saline (PBS) were obtained from Sigma-Aldrich (St. Louis, MO, USA). Pan was purchased from Selleckchem (Houston, TX USA, Cat # S1030). All other reagents were of analytical grade.

### 4.5.2. Liposome preparation

Encapsulation of Pan in liposomes was achieved by an active loading method with an ammonium sulphate gradient as previously described by us (Gaspar et al. 2012). Briefly, the relevant lipids, DPPC: Chol: DSPE-PEG in a molar ratio of 1.85: 1: 0.15 for non-targeted liposomes and DPPC: Chol: DSPE-PEG: DSPE-PEG-FA in a molar ratio of 1.85: 1: 0.12: 0.03 for targeted liposomes were dissolved in chloroform and the organic solvent was removed by rotary evaporation. The homogeneous lipid film formed was hydrated with water and the resulting suspension was frozen (-70° C) and lyophilized (Edwards, CO, USA) overnight. Rehydration of the lyophilized powder was performed with ammonium sulphate (135 mM, pH 5.4) at 45° C for 30 min. To produce a homogeneous liposome suspension, the unloaded liposomes were filtered under nitrogen pressure (10-500 lb/in2), through polycarbonate membranes of proper pore size (at 45° C), using a Lipex thermo-barrel extruder (Lipex:

Biomembranes Inc., Vancouver, BC, Canada) until the liposomes reached a mean size of 0.1 μm. An ammonium sulphate gradient was established by replacing the additional liposomal medium with PBS buffer (pH 7.4) using a desalting column (Econo-Pac 10 DG, Bio-Rad, Hercules, CA, USA). Pan was incubated with unloaded liposomes at a molar ratio of 1:16 μmol of lipid, previously diluted in PBS (from a stock solution at 67 mg/mL) for 1 h at 45° C. To separate the unencapsulated Pan an ultracentrifugation was performed at 250,000 g for 2 h at 15° C in a Beckman LM-80 ultracentrifuge (Beckman Instruments, Fullerton, CA, USA). The pellet was suspended in PBS (pH 7.4). Four different formulations were prepared: folate-targeted unloaded liposomes (FA-PEG-Lip), non-targeted unloaded liposomes (PEG-Lip), folate-targeted loaded with Pan liposomes (FA-PEG-Pan-Lip) and non-targeted loaded with Pan liposomes (PEG-Pan-Lip).

For flow cytometry studies unloaded liposomes and Pan liposomes were prepared as above described. The only difference was the inclusion in the lipid composition of Rho-PE at 0.2 mol% of total lipid.

For biodistribution studies, selected Pan liposomes were labelled with Indium-111 ($^{111}$In). For that, the chelating agent diethylenetriamine pentaacetic acid (DTPA) at a concentration of 6 μM was encapsulated during liposome preparation after achievement of the lipid film and before lyophilization (Gaspar et al. 2007). Then liposomes were prepared as above described. Pan liposomes co-loaded with DTPA were then labelled with $^{111}$In using the lipophilic complex $^{111}$In-oxine as precursor, as described below.

### 4.5.3. Characterization of panobinostat liposomal formulations

After disruption of liposomes with ethanol, Pan was quantified by spectrophotometry with the aid of a calibration curve (standards ranged from 2.5 to 20 μg/mL). The absorbance of all samples were read at 282 nm. The lipid content of liposomal formulation under study was determined using an enzyme-linked colorimetric method, Phospholipids Choline Oxidase-Peroxidase (Spinreact, Spain) (Pinho et al. 2019). Liposomes were characterized in terms of lipid composition and by the following encapsulation parameters: the initial and final Pan to lipid ratios ((Pan/Lip)i and (Pan/lip)f, respectively; and encapsulation efficiency defined as the percentage of [(Pan/Lip)f]/ [(Pan/Lip)i]. Pan liposomes mean size was determined by dynamic light scattering in a Zetasizer Nano S (Malvern Instruments Inc., Malvern, UK). As a measure of particle size distribution of the dispersion, the system reports the polydispersity index ranging from 0.0 for a completely monodisperse sample up to 1.0 for a polydisperse suspension. The zeta potential was determined by laser Doppler electrophoresis in a Zetasizer Nano Z (Malvern Instruments Inc, Malvern, UK).

### 4.5.4. Cell line and culture

The canine CLBL-1 B-cell lymphoma cell line (provided by Dr. Barbara Rütgen, Department of Pathobiology, University of Veterinary Medicine, Vienna, Austria) (Rütgen et al. 2010; Rütgen et al. 2012) was cultured in Roswell Park Memorial Institute-1640 (RPMI 1640) medium (Gibco, Thermo Fisher Scientifics, Waltham, MA, USA) supplemented with 10% heat inactivated fetal calf serum (FCS, Gibco) and penicillin 100 U/ mL/ streptomycin 0.1 mg/mL (Gibco) at 37° C in a humidified atmosphere of 5% $CO_2$ (T75-tissue culture flasks, Greiner Bio-One, Kremsmünster, Austria).

### 4.5.5. Immunoblotting

Cells were harvested, washed twice with PBS and lysed with RIPA lysis Buffer (25 mM TrisHCL pH 7.6, 150 mM NaCl, 1% NP-40, 1% sodiumdeoxycholate, 0.1% SDS) supplemented with protease inhibitor cocktail (Roche, Basel, Switzerland). An increasing amount of total protein cell extract was loaded onto 15% SDS – polyacrylamide gel electrophoresis (SDS-PAGE) and transferred to nitrocellulose membranes. The membranes were blocked in 5% non-fat milk in PBS containing 0.2% Tween-20. After blocking, the membranes were incubated with primary antibodies. To evaluate folate expression, membranes were incubated with folate receptor alpha antibody (1:500 dilution, 0.5 mg/mL, Invitrogen, Thermo Fisher scientific, Carlsbad, CA, USA) or anti-α-tubulin antibody (monoclonal, mouse, 1:1250 dilution, Sigma-Aldrich). To assess acetylation of H3 histone, membranes were incubated with anti-acetylhistone H3 (Lys9, Lys14) antibody (polyclonal, rabbit, 1:2500 dilution, Thermo Fisher Scientific, Rockford, IL, USA) or anti-histone H3 (polyclonal, rabbit, 1:1000 dilution, Thermo Fisher Scientific). Membranes were then incubated with secondary antibody: Peroxidase-AffiniPure anti-rabbit IgG antibody (polyclonal, goat, 1:10000 dilution, Jackson ImmunoResearch, PA, USA) or anti-mouse IgG HRP antibody (polyclonal, sheep, 1:7500 dilution, Jackson ImmunoResearch) to assess folate expression and Peroxidase-AffiniPure anti-rabbit IgG antibody (polyclonal, goat, 1:10000 dilution, Jackson ImmunoResearch, PA, USA), to evaluate H3 acetylation. Proteins were detected using Luminata Forte Western HRP (Merck Millipore, Billerica, MA, USA) and acquired using the ChemiDoc XRS+ imaging system (Bio-Rad, Hercules, CA, USA).

### 4.5.6. Cytotoxic Assay

To determine the effect of Pan loaded in non-targeted and FA-targeted liposomal formulations on CLBL-1 cell proliferation, a cell viability assay was performed using the Alamar blue cell viability (Invitrogen). Briefly, $6 \times 10^5$ of cells were seeded in 96-well plates in 200 µl of culture medium and subjected to increasing doses (0.4 - 2000 nM) of each PEG-Pan-Lip

and FA-PEG-Pan-Lip formulations. Free Pan was used as a control. After 24 h treatment, cell viability was determined using Alamar Blue reagent, according to the manufacturer's instructions. Absorbance at 570 nm and 600 nm was measured using the iMark microplate Reader (Bio-Rad). Cell viability was calculated using the formula provided by the manufacturer. Two replicate wells were used to determine each data point and two independent experiments were carried out in different days. Best-fit $EC_{50}$ values of each formulation were calculated using GraphPad Prism software (version 9.2.0, San Diego, CA, USA) using response vs. log (inhibitor) function with variable slope.

### 4.5.7. Evaluation of apoptotic cell death

The percentage of apoptotic cells after treatment with each liposomal formulation was determined by flow cytometry using the Guava Nexin Assay. Cells were seeded and treated with increasing concentrations (1-20 nM) of liposome formulations loaded with Pan for 24 h. After treatment, cells were recovered, centrifuged at 500 g for 5 min and resuspended in PBS containing 2% FBS. Then, an equal volume of Guava Nexin reagent was added to 50 µl of the cell suspension and incubated for 20 min, at room temperature, protected from light. Guava easyCyte 5HT flow cytometer using the Nexin software module was used for sample acquisition and analysis.

Caspase-3 and 7 activities were measured using Caspase Glo 3/7 Assay (Promega, Madison, WI, USA). For this purpose, CLBL-1 cells were seeded and treated with 1-20 nM of each liposomal formulation loaded with Pan for 24 h. After treatment, 100 µl of each cell suspension was transferred into a white 96-well plate and 75 µl of caspase-Glo 3/7 reagent was added. The mixture was mixed by orbital shaking for 30 seconds and then incubated at room temperature for 30 min. Incubation allowed complete cell lysis, stabilization of cleavage of the proluminescent substrate mediated by caspases and an increase in the luminescent signal. Luminescence was measured using the GloMax-Multi+ Detection System (Promega).

### 4.5.8. Cellular uptake by Immunofluorescence and flow cytometry

To perform the qualitative analysis, $1.5 \times 10^5$ of CLBL-1 cells were plated on ibidi µ-Slide 8 Well Glass Bottom (Ibidi, Fitchburg, WI, USA) and incubated for 24 h at 37° C in a humidified atmosphere of 5% $CO_2$. Then, the rhodamine-labeled PEG-Lip and FA-PEG-Lip was added to the cells and incubated at 37º C for 3 and 6 h, respectively. After incubation, cells were washed twice with PBS, fixed with PFA 4% for 15 min at RT and washed twice. After washing, DAPI Vectashield (Vector Labs, Burlingame, CA, USA) was added to the cells. Image acquisition was performed on a confocal point-scanning Zeiss LSM 880 microscope (Carl Zeiss, Germany) equipped with a Plan-Apochromat DIC X63 oil objective (1.40 numerical

aperture). Diode 405-30 laser was used to excite DAPI, and DPSS 561-20 laser to excite Rhodamine. In the Airyscan acquisition mode, ×1.80 zoom images were recorded at 1024 × 1024 resolution. ZEN software was used for image acquisition and Fiji software was used for image processing.

To determine the quantitative cellular uptake of PEG-Lip and FA-PEG-Lip formulations, flow cytometry was performed. Briefly, $1 \times 10^6$ of CLBL-1 cells were incubated with 5 µmol/mL or 7.5 µmol/mL of the rhodamine-labeled PEG-Lip and FA-PEG-Lip in a complete medium without phenol red for 90 min, 3 h and 6 h at 37° C. The cells were centrifuged and washed twice with PBS to remove unbound liposomes. Data were collected and analyzed using the Attune NxT flow cytometer (Thermo Scientific).

### 4.5.9. Animals

All animal-handling procedures were performed in accordance to EU recommendations for good practices and animal welfare and were approved by the Animal Care and Ethical Committee of the Faculty of Veterinary Medicine (Protocol_0050132016). All methods were performed in accordance with the relevant guidelines and regulations. Female 6-8-week-old SOPF/SHO SCID mice or CD1 mice were purchased from Charles River. Immunodeficient mice were maintained in microisolation cages under pathogen-free conditions. CD1 mice were maintained under standard conditions. Room conditions included a room temperature of 24-26° C and a cycle of 12 h light and 12 h of darkness. Food and water were sterilized and provided *ad libitum*.

### 4.5.10. Preparation of $^{111}$In-Lipossomes

The diethylenetriaminepentaacetic acid(DTPA)-containing liposomes were labeled with Indium-111 ($^{111}$In) upon incubation of the respective liposome with $^{111}$In-8-hydroxyquinoline (oxine) following a modified procedure of the literature (Yang et al. 2012). The radiolabeling of oxine involved, firstly, the preparation of an ethanolic solution of oxine (250 µL, 13.8 mM), which was diluted with 0.4 M acetate buffer pH 5.5 (1000 µL). The resulting oxine solution was added to indium ($^{111}$In) chloride (290 µL, 370 MBq/mL, Mallinckrodt / Curium, The Netherlands) and then incubated at room temperature for 15 min. The lipophilic components were extracted with dichloromethane (3×) and then evaporated to dryness under a gentle stream of nitrogen. The radiochemical yield was generally greater than 95% $^{111}$In-oxine as determined by instant thin-layer chromatography using glass microfiber chromatography paper impregnated with silica gel (iTLC-SG, Agilent Technologies) and ethanol as eluent. The obtained dry residue containing $^{111}$In-oxine was firstly dissolved in ethanol (30 µL) and phosphate-buffered saline (PBS) pH 7.4 (80 µL) was added. The resulting mixture was incubated with the DTPA-

containing liposomes (300 µL – 1.5 mL) for 45 min at 37° C. The $^{111}$In-liposomes were purified by ultrafiltration using a centrifugal concentrator - Amicon Ultra-0.5 Centrifugal Filter Unit (100 kDa MWCO, 0.5 mL sample volume, Merck) following the manufacturer´s instructions. The labeling efficiency, which varied between 51% and 80% depending on the type of liposome, was determined by dividing the radioactivity from the concentrate that corresponds to $^{111}$In-liposome by the total amount loaded onto the Amicon filter.

### 4.5.11. Biodistribution Studies in CD1 mice

To evaluate the biodistribution in healthy mice, targeted and non-targeted $^{111}$In-labeled liposomes diluted in PBS (100 µL) were injected intravenously via the tail vein into CD1 mice. At 1 h, 3 h and 24 h post-injection (p.i.), mice were sacrificed by cervical dislocation. The injected radioactivity dose and the radioactivity in the sacrificed animal were measured using a dose calibrator (Carpintec CRC-15W, Ramsey, USA). The difference between the radioactivity in the injected dose and the sacrificed animals was accepted to be due to excretion. After sacrificed, tissue samples were collected, rinsed with PBS, weighed, and counted in a gamma counter (Hidex AMG, Hidex, Turku, Finland). Results are expressed as the mean percentage of the injected dose (ID) per gram of tissue (% ID/g tissue) (mean ± SD) (n=3 per liposomal formulation).

### 4.5.12. Tumor induction, biodistribution and tumor targeting in SCID mice

For tumor induction, $1 \times 10^6$ CLBL-1 cells diluted in PBS and matrigel (1:1) (Corning, NY, USA, Cat) were subcutaneously injected into the dorsal interscapular region of SCID mice as previously described (Dias et al. 2018). Tumor volume was calculated using the formula $(\text{width})^2 \times \text{length}$. When the tumor reached a minimum volume of 100 $mm^3$, the mice were randomized and divided into two distinct groups (targeted and non-targeted $^{111}$In-labeled liposomal formulations). Subsequently, the radiolabeled liposomes were intravenous injected into SCID mice. After sacrifice, the tissues were dissected and counted in a gamma counter, at different time points (24 h and 48 h p.i.). Tumor and tissue uptake were expressed as percentage of the injected dose per gram of tissue (% ID/g).

### 4.5.13. Histopathological Analysis

Tumors were fixed in 10% buffered formalin and embedded in paraffin utilizing a Leica tissue processor. Sections were cut from paraffin blocks and stained with hematoxylin and eosin (H&E). Sections were mounted onto superfrost ultra plus slides (Menzel-Glaser, Braunschweig, DE) for immunohistochemistry.

### 4.5.14. Immunohistochemistry Analysis

A representative area of each tumor was selected and tissue sections of 3μm thickness were mounted on glass slides (Superfrost glass slides, Thermo Scientific, Braunschweig, Germany), deparaffinized with xylene and hydrated in a graded ethanol series of distilled water. The Novolink Polymer Detection System (Noocastra, Leica Biosystems, Newcastle, UK) was used according to the manufacturer's instructions. The antigen retrieval treatment was achieved by microwave treatment (5 min at 900 watts plus 15 min at 650 watts) in Tris-EDTA buffer (pH 9.0). To block endogenous peroxidase and to prevent unspecific labeling, the system's Peroxidase Block Solution and Protein Block Solution were used sequentially. Sections were incubated 30 min at room temperature with polyclonal rabbit anti-human CD20 (Thermo Fisher Scientific), diluted 1:200 and rabbit polyclonal anti-human CD3 (Dako, Glostrup, Denmark), diluted 1:400. Labeling was developed by incubating the slides with system's chromogen, diaminobenzidine (DAB), and hydrogen peroxide as substrate. Nuclear background staining was performed with Gill's hematoxylin (30 s). Labeling without the primary antibody was used as negative control, while dog lymph node sections were used as positive control.

### 4.5.15. Statistical Analysis

Results are expressed as mean ± standard deviation (SD) or mean ± standard error mean (SEM). Statistical analysis was performed using one-way ANOVA and two-tailed Student's t-test using GraphPad Prism® 9 (GraphPad Software, CA, USA). $p<0.05$ was considered statistically significant.

# Chapter 5

## Final Conclusions and Future Perspectives

In the last few decades, tremendous advances have been made in the treatment of cancer, with immunotherapies being the core of immune-oncology. However, it was only in the last few years that these therapies have gained the highlight needed to find their own space among cancer treatments, due to an unprecedented amount of approvals by regulatory agencies. In line with this, rapid drug development and groundbreaking clinical responses have been reported for cancer immunotherapies, establishing them as new hopes for cancer treatment. These great results are the culmination of all the efforts put into cancer research, and now we are reaping the fruits of many decades of painstaking research and development (Kelly 2018).

Cancer immunotherapy has been displaying impressive benefits for patients in different tumors and attention is now leaning towards immune-oncology. Regardless of this promising knowledge, many cancer types, have been treated with the same highly toxic treatments for decades, focusing only on effectiveness. An illustrative case is non-Hodgkin Lymphoma, particularly DLBCL. The R-CHOP protocol has remained the first-line standard of care for DLBCL for decades, and regardless of its 60% curative rate, most patients experience high levels of toxicity due to the high number of treatment cycles to which they were subjected. Often, when chemotherapy regimens are intensified, high efficacy occurs at the expense of high toxicity. In the last few years, several attempts have been made to resolve this issue unfortunately, without success. Moreover, an attempt to replace Rituximab by Obinutuzumab, a second generation of CD20 monoclonal antibody, failed (Stegemann et al. 2022).

As a result, standard treatments did not seem to meet the medical goals for patient care and the need to invest in different agents with higher efficacy and lower toxicity arose. This has unveiled an unmet need for novel molecules that combine high efficacy and low toxicity. More recently, an R-CHP regimen using the ADC Polatuzumab Vedotin, an anti-CD79b monoclonal antibody conjugated by a protease-cleavable linker to monomethyl auristatin E – a potent microtubule inhibitor, has demonstrated to be superior to R-CHOP in terms of progression-free survival in the POLARIX phase III trial. Polatuzumab Vedotin has shown efficacy in patients with relapsed or refractory DLBCL, singularly and in combination with rituximab. Indeed, the findings of the POLARIX study will have profound implications not only in future trials, but also in the first line of care for NHL. Moreover, this study opens new perspectives for the use of ADCs for NHL treatment (Tilly et al. 2022).

Within this context, one of the fastest growing areas of immunotherapies are monoclonal antibodies and in particular their conjugation with potent compounds, giving rise to antibody-drug conjugates and their derivates (eg. Immunotoxins). Indeed, eight ADCs have been approved in the past five years. However, considering that hundreds of molecules are starting clinical trials, with few approved, this highlights the need to improve and leverage the benefits of ADCs in patient care. Hence, new approaches for ADC development have been explored, including the use of different antibody formats and payload molecules.

One of the most promising antibody formats that has been showing its potential in the last few years is the sdAbs, that due to its reduced size and low complexity can achieve high tumor penetration compared with traditional IgGs present in ADCs. Moreover, and importantly, rabbit VL-sdAbs present a free exposed cysteine at position 80 that constitutes a huge advantage for payload conjugation over IgGs, surpassing the issues related with ADCs heterogeneity.

Regarding payload molecules, throughout the years, different types of molecules have been exploited. This raises a very important concern in cancer treatment: drug resistance. Unfortunately, drug resistance remains one of the biggest challenges in cancer treatment. Currently, it is the major limiting factor in attaining cure in cancer patients. To overcome this limitation, different types of molecules with distinct mechanisms of action have been used in ADCs and in other drug delivery systems.

Regardless of recent clinical breakthroughs in cancer immunotherapy, the reality is that all of them depend on preclinical testing with most making use of mouse models. For many years, mouse models have remained as the foundation for the development of cancer therapies, and there are no doubts that their importance remains nowadays. However, the inability of murine models in mimicking the characteristics of human tumors and the frequent failures of these models in phase I and II clinical trials generate an urgent need in developing better models. The conjugation of this unmet need with the rapid growth and success of immunotherapies created strong reasons for bringing veterinary species into the drug development field. This opportunity unveiled a huge potential of comparative oncology with recognized benefits to human and canine health. Dogs are natural cancer spontaneous models, meaning that they are able to develop tumors spontaneously in the presence of an intact immune system, providing a link between mice and pre-clinical models in humans. This feature can contribute to the discovery and development of new and promising therapies. Moreover, with biologic and histologic similarities shared between dogs and humans, new therapeutic targets and disease-associated genes can be identified. The shared environment is also a particular feature between humans and dogs and can help to determine some risk factors associated with certain cancer types.

Despite advances in the last few years, it is clear that the development of new therapeutics still has a long way ahead with many challenges to overcome. Nevertheless, studies in dogs with spontaneous cancers can shorten the journey for therapeutic development by providing critical new information that includes the assessment of drug interactions and resistance patterns, benefiting both species, but particularly the journey of drug development.

Within this context, the present study aimed to develop a novel platform for sdAb-based drug delivery system for the treatment of B-cell malignancies. To validate our system, canine lymphoma was used as an animal model of NHL. In addition, due to the challenges associated with the development of drug delivery systems, we defined complementary objectives with a multidisciplinary approach. In the first place, we aimed to develop a solid platform for the discovery of specific sdAbs and then use them for the development of different molecules for drug delivery. These resulted in three different approaches to develop three different methods of drug delivery: antibody-drug conjugates, immunotoxins and liposomes. Moreover, and due to the glaring problem of drug resistance in the cancer field, testing different drugs to be integrated in our drug delivery systems was imperative. In line with this, our drug delivery systems present three different drugs: SN-38, PE-38 and Panobinostat. This work is summarized in five chapters with specific goals for each of them that contributed to the accomplishment of the main goal, which consists in the development of a drug-delivery system platform for the treatment of B-cell malignancies.

The first chapter begins with an overview of cancer worldwide, incorporating the number of this disease in Portugal. We started with a general overview, and then set it to a more specific range. We also explored the state of the art of human and canine lymphoma, focusing on B-cell lymphoma, as well as the importance of using the dog as a model for human NHL. We then ran an overview of immunotherapies, departing from monoclonal antibodies as one of the most applied immunotherapies. All the antibodies crucial features and therapeutic potentials were mentioned, as well as the therapeutic options available on the market. In addition, to conventional antibodies, an overview of small fragments was described, particularly, single-domain antibodies (sdAbs). For sdAbs, we highlighted their advantages and potential for drug delivery in cancer therapy. Then, we also mentioned the selection method that was mostly used for sdAbs, as well as a phage display with an *in vitro* and *in vivo* approach. In the remaining sections, the following three drug delivery systems were briefly summarized: ADCs, immunotoxins and liposomes.

As mentioned previously, the main purpose of ADCs is to minimize systemic toxicity by specifically targeting tumor cells, thereby increasing drug efficacy. Therefore, the discovery of highly specific antibodies is crucial for successful development of ADCs. Considering the advantages of sdAbs and their potential as suitable scaffolds for drug delivery, we aimed to select a highly specific sdAb for NHL to generate a novel antibody-drug conjugate. For this

purpose, chapter 2 describes the study performed to accomplish our goal of developing a novel ADC. For that, we explored the properties of rabbit-derived VL sdAbs in order to develop a highly specific and potent ADC for cancer treatment. To validate our molecule, we used canine lymphoma as an animal model of human NHL. We first began by developing a platform to select a specific sdAb against NHL. Therefore, a highly diverse immune library of rabbit VL sdAb against cNHL was successfully constructed, ensuring the diversity of the sdAbs of the library. Therefore, in order to select the best sdAb in its natural conformation and tumoral microenvironment, an *in vitro* whole cell phage display followed by an *in vivo* phage display in a canine lymphoma xenograft murine model was performed. The strategy employed allowed the selection of VL-phages that bind and internalize into tumor cells. Nowadays, phage display is one of the most widespread and powerful display technology for antibody selection. This is mainly due to its advantages which allow the linkage between phenotype and encapsulated genotype. Furthermore, a single round of *in vivo* phage display can be performed in combination with *in vitro* phage display. Indeed, as selection is performed on an *in vivo* model, negative selection is naturally performed, excluding the non-specific phages resulting in the identification of a pool of specific sdAbs for canine lymphoma targets. Moreover, *in vivo* phage display allows the selection of the best sdAbs given their specificity, pharmacokinetics and stability characteristics, which are essential for the incorporation of the sdAb in a drug delivery system. This also helps in reducing the number of candidates to be tested further ahead in pre-clinical trials, making the development process quicker and more effective. Then, the best VL sdAb candidate according to its binding activity to cNHL targets and expression, were selected, and its characteristics evaluated. Due to its characteristics, sdAb C5 was selected as the most promising clone. In addition, NGS analysis was performed to complement this study which then revealed the specific enrichment attained by phage display selection. Then, C5 was successfully conjugated with SN-38 and its anticancer properties were proven for canine lymphoma. This study resulted in the discovery of an anti-cNHL antibody for ADC development, which was possible by combining innovative techniques of *in vivo* phage display with an immune library using lymphoma cells from canine patients, which then enabled the selection of highly specific antibodies for B-cell lymphoma. Moreover, by using rabbit derived VL sdAbs scaffolds, we obtained a potent ADC with a DAR of 1, by conjugating SN-38 with the free exposed Cys80 of the VL sdAb. This study resulted in the validation of a highly efficient approach towards the discovery and generation of new ADCs.

Due to the drug resistance issue, efforts have been made in the identification of novel payloads with different action mechanisms. One of the main challenges of ADCs is the low number of molecules that can be attached to the antibody. This issue makes the choice of the compound, and in particular, the choice of highly potent molecules even more important. Due to its promising potency characteristics, bacterial toxins have emerged as a potential payload

to join towards antibodies, resulting in a particular case of drug delivery system, known as an immunotoxin. One advantage of immunotoxins is the fact that they do not damage DNA when cells are killed, as its mechanism is related with the inhibition of protein synthesis. Immunotoxins have been displaying remarkable efficacy in hematological malignancies. The approval of moxetumomab pasudotox by FDA is one of the most successful examples. However, one of the major challenges of these molecules, when administered in patients is the off-target toxicity that leads to a poor safety profile. One of the most efficient ways to mitigate these effects is modulating the affinity and specificity of the immunotoxin in order to accurately target the tumor cell, causing the molecule to be active when in the target's site. All of these features can be achieved by having a highly selective and specific antibody to direct the molecule to the tumor's cell by using mechanisms to release the toxin only at the target site (Li et al. 2022).

Regarding what was previously described, we developed an immunotoxin using a rabbit-derived VL sdAb conjugated with a truncated form of PE38 in order to create a new immunotoxin for NHL treatment using the dog as an animal model, as described under chapter 3. For that purpose, we used recombinant DNA methods to fuse the sdAbs with the PE38 toxin. These methods were introduced in the third generation of immunotoxins, facilitating the fusion of antibody fragments to the truncated and deimmunized toxins via peptide linker. The antibody fragment that was used, VL C5 sdAb, was the same as the one used in the development of the ADC in Chapter 2. So, this VL sdAb was already validated as a suitable scaffold to specifically reach the tumoral cells of canine lymphoma. This allows the reduction of immunogenicity, elimination of heterogeneity and better tissue penetration due to the molecules reduced size. The PE38 form used in this study was the truncated one due to its reduced immunogenicity. Moreover, the release mechanism of this immunotoxin is activated only inside the cell. Domain II of the toxin contains a furin cleavage site, essential for toxin activation such that, when the furin, naturally present inside a cell, cleaves the toxin, it becomes active. In contrast, if the immunotoxin does not enter the cell, the toxin will not be activated, and no effect will occur. This, together with the specificity of sdAb towards canine lymphoma cells, makes this molecule less toxic. Later, the developed immunotoxin (C5-PE38) demonstrated to have an effect on cell death by inhibiting protein synthesis in canine lymphoma cells. Moreover, in a xenograft mouse model of canine lymphoma a fast elimination of the immunotoxin was verified avoiding undesired toxicity, and also verifying good tumor uptake. The obtained results revealed the potential of the C5-PE38 immunotoxin in killing tumor cells specifically, and the potential to eventually treat canine lymphoma. This work enabled the development of a new immunotoxin for the treatment of canine lymphoma, validating the PE38 toxin as a molecule for the treatment of dog-related tumors, and sdAbs as a suitable scaffold for the development of new immunotoxins. As far as we know, this was the

first report on using the PE38 toxin in dogs aiming to treat canine B-cell lymphoma. So, this opens up new perspectives for the introduction of new molecules in the veterinary field that can help in the treatment of other malignancies.

Beyond ADCs and immunotoxins, other drug delivery systems have gained prominence due to their promising outcomes, particularly, nanoparticles. Among nanoparticles, lipid-based systems are one of the most well-studied and are on the frontline for cancer therapy. In fact, the first approved liposome, Doxil, was aimed for ovarian cancer treatment, demonstrating the potential of liposomes in treating cancer. Throughout the years, other liposomal formulations were approved, including Vyxeos with indication for leukemia treatment. Since Doxil, several improvements have been made in this field in order to render liposomes even more specific towards tumor cells. Indeed, many studies have reported the success of preclinical immunoliposomes, and particularly the use of antibody fragments for liposome delivery (van der Meel et al. 2013; Miller et al. 2016; SynerGene Therapeutics, Inc. 2017; Swiss Group for Clinical Cancer Research 2021). One the other hand, the great advantages of liposomes lie on the fact that they can protect the drug and modify its pharmacokinetics. Furthermore, one of the biggest challenges of chemotherapeutic drugs are their narrow therapeutic index, often producing unpredictable effects. All of these challenges can be overcome by using a liposome system that entraps the drug and take it to the target. Thus, panobinostat, an HDAC inhibitor, was selected for this study. Panobinostat has a high antitumoral activity in canine lymphoma, however we know that this molecule is highly cytotoxic in the xenograft mouse model of canine lymphoma. This high *in vivo* cytotoxicity and the aim to reduce it was the reason for the development of a liposome system with the compound entrapped (Dias et al. 2018b). In light of this, in Chapter 4, we described the development of folate-targeted liposomes encapsulating panobinostat, and investigated their cytotoxicity properties against canine lymphoma, an animal model of hNHL. In this study, active targeting was attained by using folate, which has been showing its great potential in mediating tumor uptake of a variety of drugs (Kumar et al. 2019). In the course of this study, liposomes were successfully loaded with panobinostat. Our study validates liposomes as an effective cancer treatment that enhances the therapeutic potential of panobinostat, thus contributing to the treatment of canine lymphoma. In the future, our goal is to conjugate the folate-liposomes with C5 VL sdAb to obtain an immunoliposome highly specific towards canine B-cell lymphoma.

In summary, this thesis culminates in the development of three different therapeutic molecules and systems for treatment of canine lymphoma.

In conclusion, the use of sdAb-derived antibody libraries obtained from rabbits immunized with cells from canine lymphoma patients, combined with an innovative phage display selection in a xenograft mouse model, resulted in a front-runner combination of methodologies that allowed the discovery of highly specific sdAbs against canine lymphoma.

The results obtained validated this combination of techniques as a promising approach for the development of highly specific and potent ADCs. Moreover, this work offers new perspectives in the development of ADCs for cancer treatment, validating the canine model as a promising alternative for the study and development of new therapeutics to implement in the treatment of human lymphoma.

A new immunotoxin was developed by fusing a rabbit-derived sdAb as the targeting moiety with the PE38 toxin used as a payload. The results obtained validate PE38 toxin as a possible molecule for the treatment of dog-related tumors, and sdAbs as a suitable scaffold for the development of new immunotoxins. This opens new perspectives for the use of immunotoxins as a treatment for canine lymphoma, reinforcing the dog as a clinical model for the development of new therapeutic molecules for the treatment of human lymphoma.

In addition, to the best of our knowledge, our work is also the first study that reports the use of a liposome-based drug delivery system loaded with panobinostat for the treatment of canine lymphoma. Overall, these results validated liposome systems as effective cancer treatment modalities that significantly enhanced the anti-cancer therapeutic efficacy of panobinostat. Although this liposome-based drug delivery system presented strong anti-cancer activity on canine lymphoma cells, additional preclinical studies on a canine lymphoma murine model will be needed to evaluate its *in vivo* efficacy and safety, allowing its further progression towards clinical studies in canine patients. In conclusion, this work contributes for the development of panobinostat nanocarriers for the treatment of canine B-cell lymphoma as a predictive preclinical surrogate for human NHL, mutually benefiting both species and opening up perspectives in comparative oncology.

In conclusion, the work described in this thesis contributes to the understanding of the importance of using pet dogs as a model and how these animals can contribute with realistic perspectives for clinical translation in the field of immune-oncology. This provides a great example of how the One Health concept can be integrated into the development of new therapies not only for cancer, but also for other diseases that can also be a public health problem.

Undoubtedly, Humanity is going through an exciting time in cancer research with an unprecedented speed and innovation in both basic and clinical science and translational progress. This has resulted in an increasing number of therapeutic options that are increasingly effective, bringing a healthier and longer life expectancy for cancer patients. Moreover, a new era is beginning where personalized and precision medicine are key for the development of new approaches to face new challenges in the cancer field (Golan et al. 2017). With all the work developed throughout these years, we hope to have contributed to these extraordinary times where basic science meets clinical progress and all can work together for a more personalized and precise medicine for all cancer patients (including animals).

## References


Aguiar SI, Dias JNR, André AS, Silva ML, Martins D, Carrapiço B, Castanho M, Carriço J, Cavaco M, Gaspar MM, et al. 2021. Highly Specific Blood-Brain Barrier Transmigrating Single-Domain Antibodies Selected by an In Vivo Phage Display Screening. Pharmaceutics. 13(10):1598. doi:10.3390/pharmaceutics13101598.

Aires da Silva F, Corte-Real S, Goncalves J. 2008. Recombinant Antibodies as Therapeutic Agents: Pathways for Modeling New Biodrugs. BioDrugs. 22(5):301–314. doi:10.2165/00063030-200822050-00003.

Aires-Da-Silva F, Côrte-Real S, Freitas R, Lourenço S. 2014 May 8. Anti-tumor necrosis factor-alpha agents and uses thereof. Aplication No. PCTPT2012000035. WO2013043070A9.

Ait-Oudhia S, Mager D, Straubinger R. 2014. Application of Pharmacokinetic and Pharmacodynamic Analysis to the Development of Liposomal Formulations for Oncology. Pharmaceutics. 6(1):137–174. doi:10.3390/pharmaceutics6010137.

Akbari B, Farajnia S, Ahdi Khosroshahi S, Safari F, Yousefi M, Dariushnejad H, Rahbarnia L. 2017. Immunotoxins in cancer therapy: Review and update. International Reviews of Immunology. 36(4):207–219. doi:10.1080/08830185.2017.1284211.

Alfaleh MA, Alsaab HO, Mahmoud AB, Alkayyal AA, Jones ML, Mahler SM, Hashem AM. 2020. Phage Display Derived Monoclonal Antibodies: From Bench to Bedside. Front Immunol. 11:1986. doi:10.3389/fimmu.2020.01986.

André AS, Moutinho I, Dias JNR, Aires-da-Silva F. 2022. In vivo Phage Display: A promising selection strategy for the improvement of antibody targeting and drug delivery properties. Frontiers in Microbiology. 13. doi:10.3389/fmicb.2022.962124.

André AS, Dias JNR, Aguiar S, Nogueira S, Bule P, Carvalho JI, António JPM, Cavaco M, Neves V, Oliveira S, et al. 2023. Rabbit derived VL single-domains as promising scaffolds to generate antibody–drug conjugates. Sci Rep. 13(1):4837. doi:10.1038/s41598-023-31568-x.

André AS, Dias JNR, Aguiar SI, Leonardo A, Nogueira S, Amaral JD, Fernandes C, Gano L, Correia JDG, Cavaco M, et al. 2023. Panobinostat-loaded folate targeted liposomes as a promising drug delivery system for treatment of canine B-cell lymphoma. Frontiers in Veterinary Science. 10:1236136. doi:10.3389/fvets.2023.1236136.

Ansell SM. 2015. Non-Hodgkin Lymphoma: Diagnosis and Treatment. Mayo Clin Proc. 90(8):1152–1163. doi:10.1016/j.mayocp.2015.04.025.

Antignani A, FitzGerald D. 2013. Immunotoxins: The Role of the Toxin. Toxins. 5(8):1486–1502. doi:10.3390/toxins5081486.

António JPM, Carvalho JI, André AS, Dias JNR, Aguiar SI, Faustino H, Lopes RMRM, Veiros LF, Bernardes GJL, Silva FA, et al. 2021 Nov 5. Diazaborines Are a Versatile Platform to Develop ROS-Responsive Antibody Drug Conjugates**. Angew Chem Int Ed.:anie.202109835. doi:10.1002/anie.202109835.

Armitage JO, Gascoyne RD, Lunning MA, Cavalli F. 2017. Non-Hodgkin lymphoma. Lancet. 390(10091):298–310. doi:10.1016/S0140-6736(16)32407-2.

Assouline SE, Nielsen TH, Yu S, Alcaide M, Chong L, MacDonald D, Tosikyan A, Kukreti V, Kezouh A, Petrogiannis-Haliotis T, et al. 2016. Phase 2 study of panobinostat with or without

rituximab in relapsed diffuse large B-cell lymphoma. Blood. 128(2):185–194. doi:10.1182/blood-2016-02-699520.

Aubry OA, Spangler EA, Schleis SE, Smith AN. 2014. Evaluation of bone marrow aspirates from multiple sites for staging of canine lymphoma and mast cell tumours. Veterinary and Comparative Oncology. 12(1):58–66. doi:10.1111/j.1476-5829.2012.00331.x.

Ayyappan S, Maddocks K. 2019. Novel and emerging therapies for B cell lymphoma. J Hematol Oncol. 12:82. doi:10.1186/s13045-019-0752-3.

Bábíčková J, Tóthová Ľ, Boor P, Celec P. 2013. In vivo phage display — A discovery tool in molecular biomedicine. Biotechnology Advances. 31(8):1247–1259. doi:10.1016/j.biotechadv.2013.04.004.

Baek M, DiMaio F, Anishchenko I, Dauparas J, Ovchinnikov S, Lee GR, Wang J, Cong Q, Kinch LN, Schaeffer RD, et al. 2021. Accurate prediction of protein structures and interactions using a three-track neural network. Science. 373(6557):871–876. doi:10.1126/science.abj8754.

Barbas CF, Kang AS, Lerner RA, Benkovic SJ. 1991. Assembly of combinatorial antibody libraries on phage surfaces: the gene III site. Proc Natl Acad Sci U S A. 88(18):7978–7982. doi:10.1073/pnas.88.18.7978.

Barbas III CF, Burton DR, Scott JK, Silverman GJ. 2001. Phage Display: A Laboratory Manual. Cold Spring Harbor, NY: Cold Spring Harbor Laboratory Press.

Barenholz Y. 2012. Doxil®--the first FDA-approved nano-drug: lessons learned. J Control Release. 160(2):117–134. doi:10.1016/j.jconrel.2012.03.020.

Barenholz Y (Chezy). 2021. Doxil® — The First FDA-Approved Nano-Drug: From an Idea to a Product. In: Handbook of Harnessing Biomaterials in Nanomedicine. 2nd ed. Jenny Stanford Publishing. 66 p.

Beck A, Goetsch L, Dumontet C, Corvaïa N. 2017. Strategies and challenges for the next generation of antibody–drug conjugates. Nat Rev Drug Discov. 16(5):315–337. doi:10.1038/nrd.2016.268.

Behdani M, Zeinali S, Karimipour M, Khanahmad H, Schoonooghe S, Aslemarz A, Seyed N, Moazami-Godarzi R, Baniahmad F, Habibi-Anbouhi M, et al. 2013. Development of VEGFR2-specific Nanobody Pseudomonas exotoxin A conjugated to provide efficient inhibition of tumor cell growth. New Biotechnology. 30(2):205–209. doi:10.1016/j.nbt.2012.09.002.

Beltrán-Gracia E, López-Camacho A, Higuera-Ciapara I, Velázquez-Fernández JB, Vallejo-Cardona AA. 2019. Nanomedicine review: clinical developments in liposomal applications. Cancer Nanotechnology. 10(1):11. doi:10.1186/s12645-019-0055-y.

Bertino EM, Otterson GA. 2011. Romidepsin: a novel histone deacetylase inhibitor for cancer. Expert Opin Investig Drugs. 20(8):1151–1158. doi:10.1517/13543784.2011.594437.

Blackwood L, German AJ, Stell AJ, O'Neill T. 2004. Multicentric lymphoma in a dog after cyclosporine therapy. Journal of Small Animal Practice. 45(5):259–262. doi:10.1111/j.1748-5827.2004.tb00233.x.

Blackwood L, Sullivan M, Lawson H. 1997. Radiographic abnormalities in canine multicentric lymphoma: a review of 84 cases. J Small Anim Pract. 38(2):62–69. doi:10.1111/j.1748-5827.1997.tb02989.x.

Boerkamp KM, Teske E, Boon LR, Grinwis GCM, van den Bossche L, Rutteman GR. 2014. Estimated incidence rate and distribution of tumours in 4,653 cases of archival submissions derived from the Dutch golden retriever population. BMC Vet Res. 10:34. doi:10.1186/1746-6148-10-34.

Boschanski M, Krüger T, Karsten L, Falck G, Alam S, Gerlach M, Müller B, Müller KM, Sewald N, Dierks T. 2021. Site-Specific Conjugation Strategy for Dual Antibody–Drug Conjugates Using Aerobic Formylglycine-Generating Enzymes. Bioconjugate Chem. 32(6):1167–1174. doi:10.1021/acs.bioconjchem.1c00246.

Bowzyk Al-Naeeb A, Ajithkumar T, Behan S, Hodson DJ. 2018. Non-Hodgkin lymphoma. BMJ. 362. doi:10.1136/bmj.k3204. [accessed 2020 Mar 26]. http://www.bmj.com/lookup/doi/10.1136/bmj.k3204.

Bozzuto G, Molinari A. 2015. Liposomes as nanomedical devices. Int J Nanomedicine. 10:975–999. doi:10.2147/IJN.S68861.

Bradbury ARM, Marks JD. 2004. Antibodies from phage antibody libraries. Journal of Immunological Methods. 290(1–2):29–49. doi:10.1016/j.jim.2004.04.007.

Bray F, Ferlay J, Soerjomataram I, Siegel RL, Torre LA, Jemal A. 2018. Global cancer statistics 2018: GLOBOCAN estimates of incidence and mortality worldwide for 36 cancers in 185 countries. CA: A Cancer Journal for Clinicians. 68(6):394–424. doi:10.3322/caac.21492.

Bulbake U, Doppalapudi S, Kommineni N, Khan W. 2017. Liposomal Formulations in Clinical Use: An Updated Review. Pharmaceutics. 9(4):12. doi:10.3390/pharmaceutics9020012.

Burton JH, Garrett-Mayer E, Thamm DH. 2013. Evaluation of a 15-week CHOP protocol for the treatment of canine multicentric lymphoma. Vet Comp Oncol. 11(4):306–315. doi:10.1111/j.1476-5829.2012.00324.x.

Cal PMSD, Bernardes GJL, Gois PMP. 2014. Cysteine-Selective Reactions for Antibody Conjugation. Angewandte Chemie International Edition. 53(40):10585–10587. doi:10.1002/anie.201405702.

Cao L, Li Q, Tong Z, Xing Y, Xu K, Yijia Wang J, Li W, Zhao J, Zhao L, Hong Z. 2020. HER2-specific immunotoxins constructed based on single-domain antibodies and the improved toxin PE24X7. International Journal of Pharmaceutics. 574:118939. doi:10.1016/j.ijpharm.2019.118939.

Cao W, Zhou J, Wang Y, Zhu L. 2010. Synthesis and In Vitro Cancer Cell Targeting of Folate-Functionalized Biodegradable Amphiphilic Dendrimer-Like Star Polymers. Biomacromolecules. 11(12):3680–3687. doi:10.1021/bm101154r.

Carter PJ. 2016. Next generation antibody drugs: pursuit of the “high-hanging fruit.” Nat Rev Drug Discov. 17:197–223.

Chames P, Van Regenmortel M, Weiss E, Baty D. 2009. Therapeutic antibodies: successes, limitations and hopes for the future. British Journal of Pharmacology. 157(2):220–233. doi:10.1111/j.1476-5381.2009.00190.x.

Chau CH, Steeg PS, Figg WD. 2019. Antibody–drug conjugates for cancer. The Lancet. 394(10200):793–804. doi:10.1016/S0140-6736(19)31774-X.

Chaudhury A, Das S. 2015. Folate receptor targeted liposomes encapsulating anti-cancer drugs. Curr Pharm Biotechnol. 16(4):333–343. doi:10.2174/1389201016666150118135107.

Chaudhury A, Das S, Bunte RM, Chiu GNC. 2012. Potent therapeutic activity of folate receptor-targeted liposomal carboplatin in the localized treatment of intraperitoneally grown human ovarian tumor xenograft. Int J Nanomedicine. 7:739–751. doi:10.2147/IJN.S26172.

Chen T, Liu X, Hong H, Wei H. 2020. Novel single-domain antibodies against the EGFR domain III epitope exhibit the anti-tumor effect. J Transl Med. 18:376. doi:10.1186/s12967-020-02538-y.

Chi X, Li Y, Qiu X. 2020. V(D)J recombination, somatic hypermutation and class switch recombination of immunoglobulins: mechanism and regulation. Immunology. 160(3):233–247. doi:10.1111/imm.13176.

Chiou S-H, Chow K-C, Yang C-H, Chiang S-F, Lin C-H. 2005. Discovery of Epstein–Barr virus (EBV)-encoded RNA signal and EBV nuclear antigen leader protein DNA sequence in pet dogs. Journal of General Virology. 86(4):899–905. doi:10.1099/vir.0.80792-0.

Chun P. 2015. Histone deacetylase inhibitors in hematological malignancies and solid tumors. Arch Pharm Res. 38(6):933–949. doi:10.1007/s12272-015-0571-1.

Chun R, Garrett LD, Vail DM. 2000. Evaluation of a high-dose chemotherapy protocol with no maintenance therapy for dogs with lymphoma. J Vet Intern Med. 14(2):120–124. doi:10.1892/0891-6640(2000)014<0120:eoahcp>2.3.co;2.

Co S, Jo P, Jm L, Aj A, Mm G, C R. 2019. Current Trends in Cancer Nanotheranostics: Metallic, Polymeric, and Lipid-Based Systems. Pharmaceutics. 11(1). doi:10.3390/pharmaceutics11010022.

Coumans RGE, Ariaans GJA, Spijker HJ, Renart Verkerk P, Beusker PH, Kokke BPA, Schouten J, Blomenröhr M, van der Lee MMC, Groothuis PG, et al. 2020. A Platform for the Generation of Site-Specific Antibody–Drug Conjugates That Allows for Selective Reduction of Engineered Cysteines. Bioconjugate Chem. 31(9):2136–2146. doi:10.1021/acs.bioconjchem.0c00337.

Cunha-Santos C, Figueira TN, Borrego P, Oliveira SS, Rocha C, Couto A, Cantante C, Santos-Costa Q, Azevedo-Pereira JM, Fontes CMGA, et al. 2016. Development of synthetic light-chain antibodies as novel and potent HIV fusion inhibitors: AIDS. 30(11):1691–1701. doi:10.1097/QAD.0000000000001108.

Damle B, Tay L, Comereski C, Warner W, Kaul S. 2010. Influence of Immunogenicity on the Pharmacokinetics of BMS-191352, a *Pseudomonas* Exotoxin Immunoconjugate, in Rats and Dogs. Journal of Pharmacy and Pharmacology. 52(6):671–678. doi:10.1211/0022357001774345.

Damle NK, Frost P. 2003. Antibody-targeted chemotherapy with immunoconjugates of calicheamicin. Curr Opin Pharmacol. 3(4):386–390. doi:10.1016/s1471-4892(03)00083-3.

De Souza C, Ma Z, Lindstrom AR, Chatterji BP. 2020. Nanomaterials as potential transporters of HDAC inhibitors. Medicine in Drug Discovery. 6:100040. doi:10.1016/j.medidd.2020.100040.

Dennler P, Chiotellis A, Fischer E, Brégeon D, Belmant C, Gauthier L, Lhospice F, Romagne F, Schibli R. 2014. Transglutaminase-Based Chemo-Enzymatic Conjugation Approach Yields Homogeneous Antibody–Drug Conjugates. Bioconjugate Chem. 25(3):569–578. doi:10.1021/bc400574z.

DeVita VT, Chu E. 2008. A History of Cancer Chemotherapy. Cancer Res. 68(21):8643–8653. doi:10.1158/0008-5472.CAN-07-6611.

Dhillon S. 2018. Moxetumomab Pasudotox: First Global Approval. Drugs. 78(16):1763–1767. doi:10.1007/s40265-018-1000-9.

Dias Joana N.R., Aguiar SI, Pereira DM, André AS, Gano L, Correia JDG, Carrapiço B, Rütgen B, Malhó R, Peleteiro C, et al. 2018a. The histone deacetylase inhibitor panobinostat is a potent antitumor agent in canine diffuse large B-cell lymphoma. Oncotarget. 9(47). doi:10.18632/oncotarget.25580.

Dias JNR, Almeida A, André AS, Aguiar SI, Bule P, Nogueira S, Oliveira SS, Carrapiço B, Gil S, Tavares L, et al. 2022. Characterization of the canine CD20 as a therapeutic target for comparative passive immunotherapy. Sci Rep. 12(1):2678. doi:10.1038/s41598-022-06549-1.

Dias JNR, André AS, Aguiar SI, Gil S, Tavares L, Aires-da-Silva F. 2021. Immunotherapeutic Strategies for Canine Lymphoma: Changing the Odds Against Non-Hodgkin Lymphoma. Front Vet Sci. 8:621758. doi:10.3389/fvets.2021.621758.

Dias Joana N. R., André AS, Aguiar SI, Ministro J, Oliveira J, Peleteiro MC, Rütgen B, Gano L, Correia JDG, Oliveira SS, et al. 2018. Establishment of a bioluminescent canine B-cell lymphoma xenograft model for monitoring tumor progression and treatment response in preclinical studies. Richards KL, editor. PLoS one. 13(12):e0208147. doi:10.1371/journal.pone.0208147.

Dias JNR, Lopes M, Peleteiro C, Vicente G, Nunes T, Mateus L, Aires-da-Silva F, Tavares L, Gil S. 2019a. Canine multicentric lymphoma exhibits systemic and intratumoral cytokine dysregulation. Veterinary Immunology and Immunopathology. 218:109940. doi:10.1016/j.vetimm.2019.109940.

Dieffenbach M, Pastan I. 2020. Mechanisms of Resistance to Immunotoxins Containing Pseudomonas Exotoxin A in Cancer Therapy. Biomolecules. 10:12.

Ding B-S, Dziubla T, Shuvaev VV, Muro S, Muzykantov VR. 2006. Advanced Drug Delivery Systems That Target The Vascular Endothelium. Molecular Interventions. 6(2):98. doi:10.1124/mi.6.2.7.

Dominik PK, Kossiakoff AA. 2015. Chapter Eleven - Phage Display Selections for Affinity Reagents to Membrane Proteins in Nanodiscs. In: Shukla AK, editor. Methods in Enzymology. Vol. 557. Academic Press. (Membrane Proteins—Engineering, Purification and Crystallization). p. 219–245.

Dorn CR, Taylor DO, Schneider R. 1970. The epidemiology of canine leukemia and lymphoma. Bibl Haematol.(36):403–415. doi:10.1159/000391733.

Doronina SO, Toki BE, Torgov MY, Mendelsohn BA, Cerveny CG, Chace DF, DeBlanc RL, Gearing RP, Bovee TD, Siegall CB, et al. 2003. Development of potent monoclonal antibody auristatin conjugates for cancer therapy. Nat Biotechnol. 21(7):778–784. doi:10.1038/nbt832.

Duray E, Lejeune M, Baron F, Beguin Y, Devoogdt N, Krasniqi A, Lauwers Y, Zhao YJ, D'Huyvetter M, Dumoulin M, et al. 2021. A non-internalised CD38-binding radiolabelled single-domain antibody fragment to monitor and treat multiple myeloma. Journal of Hematology & Oncology. 14(1):183. doi:10.1186/s13045-021-01171-6.

Eckschlager T, Plch J, Stiborova M, Hrabeta J. 2017. Histone Deacetylase Inhibitors as Anticancer Drugs. Int J Mol Sci. 18(7):1414. doi:10.3390/ijms18071414.

Edwards DS, Henley WE, Harding EF, Dobson JM, Wood JLN. 2003. Breed incidence of lymphoma in a UK population of insured dogs. Vet Comp Oncol. 1(4):200–206. doi:10.1111/j.1476-5810.2003.00025.x.

Emmons C, Hunsicker LG. 1987. Muromonab-CD3 (Orthoclone OKT3): the first monoclonal antibody approved for therapeutic use. Iowa Med. 77(2):78–82.

Ernst T, Kessler M, Lautscham E, Willimzig L, Neiger R. 2016. [Multicentric lymphoma in 411 dogs - an epidemiological study]. Tierarztl Prax Ausg K Kleintiere Heimtiere. 44(4):245–251. doi:10.15654/TPK-150338.

Fan Y, Marioli M, Zhang K. 2021. Analytical characterization of liposomes and other lipid nanoparticles for drug delivery. Journal of Pharmaceutical and Biomedical Analysis. 192:113642. doi:10.1016/j.jpba.2020.113642.

Farber S, Diamond LK, Mercer RD, Sylvester RF, Wolff JA. 1948. Temporary Remissions in Acute Leukemia in Children Produced by Folic Acid Antagonist, 4-Aminopteroyl-Glutamic Acid (Aminopterin). New England Journal of Medicine. 238(23):787–793. doi:10.1056/NEJM194806032382301.

Ferlay J, Colombet M, Soerjomataram I, Parkin DM, Piñeros M, Znaor A, Bray F. 2021. Cancer statistics for the year 2020: An overview. International Journal of Cancer. 149(4):778–789. doi:10.1002/ijc.33588.

Ferreira M, Ogren M, Dias JNR, Silva M, Gil S, Tavares L, Aires-da-Silva F, Gaspar MM, Aguiar SI. 2021. Liposomes as Antibiotic Delivery Systems: A Promising Nanotechnological Strategy against Antimicrobial Resistance. Molecules. 26(7):2047. doi:10.3390/molecules26072047.

Ferry JA. 2006. Burkitt's Lymphoma: Clinicopathologic Features and Differential Diagnosis. The Oncologist. 11(4):375–383. doi:10.1634/theoncologist.11-4-375.

Fleming BD, Urban DJ, Hall MD, Longerich T, Greten TF, Pastan I, Ho M. 2020. Engineered Anti-GPC3 Immunotoxin, HN3-ABD-T20, Produces Regression in Mouse Liver Cancer Xenografts Through Prolonged Serum Retention. Hepatology. 71(5):1696–1711. doi:10.1002/hep.30949.

Flory AB, Rassnick KM, Stokol T, Scrivani PV, Erb HN. 2007. Stage Migration in Dogs with Lymphoma. Journal of Veterinary Internal Medicine. 21(5):1041–1047. doi:10.1111/j.1939-1676.2007.tb03062.x.

Francisco JA, Cerveny CG, Meyer DL, Mixan BJ, Klussman K, Chace DF, Rejniak SX, Gordon KA, DeBlanc R, Toki BE, et al. 2003. cAC10-vcMMAE, an anti-CD30-monomethyl auristatin E conjugate with potent and selective antitumor activity. Blood. 102(4):1458–1465. doi:10.1182/blood-2003-01-0039.

Frigerio M, Kyle AF. 2017. The Chemical Design and Synthesis of Linkers Used in Antibody Drug Conjugates. Curr Top Med Chem. 17(32):3393–3424. doi:10.2174/1568026618666180118155847.

Gabizon A, Dagan A, Goren D, Barenholz Y, Fuks Z. 1982. Liposomes as in vivo carriers of adriamycin: reduced cardiac uptake and preserved antitumor activity in mice. Cancer Res. 42(11):4734–4739.

Gabizon A, Chisin R, Amselem S, Druckmann S, Cohen R, Goren D, Fromer I, Peretz T, Sulkes A, Barenholz Y. 1991. Pharmacokinetic and imaging studies in patients receiving a

formulation of liposome-associated adriamycin. Br J Cancer. 64(6):1125–1132. doi:10.1038/bjc.1991.476.

Gabizon A, Catane R, Uziely B, Kaufman B, Safra T, Cohen R, Martin F, Huang A, Barenholz Y. 1994. Prolonged circulation time and enhanced accumulation in malignant exudates of doxorubicin encapsulated in polyethylene-glycol coated liposomes. Cancer Res. 54(4):987–992.

Gabizon A, Horowitz AT, Goren D, Tzemach D, Shmeeda H, Zalipsky S. 2003. In Vivo Fate of Folate-Targeted Polyethylene-Glycol Liposomes in Tumor-Bearing Mice. Clin Cancer Res. 9(15):6551–6559.

Gabizon A, Tzemach D, Gorin J, Mak L, Amitay Y, Shmeeda H, Zalipsky S. 2010. Improved therapeutic activity of folate-targeted liposomal doxorubicin in folate receptor-expressing tumor models. Cancer Chemother Pharmacol. 66(1):43–52. doi:10.1007/s00280-009-1132-4.

Garden OA, Volk SW, Mason NJ, Perry JA. 2018. Companion animals in comparative oncology: One Medicine in action. The Veterinary Journal. 240:6–13. doi:10.1016/j.tvjl.2018.08.008.

Gardner HL, Fenger JM, London CA. 2016. Dogs as a Model for Cancer. Annu Rev Anim Biosci. 4(1):199–222. doi:10.1146/annurev-animal-022114-110911.

Garrett LD, Thamm DH, Chun R, Dudley R, Vail DM. 2002. Evaluation of a 6-month chemotherapy protocol with no maintenance therapy for dogs with lymphoma. J Vet Intern Med. 16(6):704–709. doi:10.1892/0891-6640(2002)016<0704:eoacpw>2.3.co;2.

Gaspar MM, Boerman OC, Laverman P, Corvo ML, Storm G, Cruz MEM. 2007. Enzymosomes with surface-exposed superoxide dismutase: In vivo behaviour and therapeutic activity in a model of adjuvant arthritis. Journal of Controlled Release. 117(2):186–195. doi:10.1016/j.jconrel.2006.10.018.

Gaspar MM, Radomska A, Gobbo OL, Bakowsky U, Radomski MW, Ehrhardt C. 2012. Targeted Delivery of Transferrin-Conjugated Liposomes to an Orthotopic Model of Lung Cancer in Nude Rats. J Aerosol Med Pulm Drug Deliv. 25(6):310–318. doi:10.1089/jamp.2011.0928.

Gaspar MM, Calado S, Pereira J, Ferronha H, Correia I, Castro H, Tomás AM, Cruz MEM. 2015. Targeted delivery of paromomycin in murine infectious diseases through association to nano lipid systems. Nanomedicine. 11(7):1851–1860. doi:10.1016/j.nano.2015.06.008.

Gavazza A, Lubas G, Valori E, Gugliucci B. 2008. Retrospective survey of malignant lymphoma cases in the dog: clinical, therapeutical and prognostic features. Vet Res Commun. 32 Suppl 1:S291-293. doi:10.1007/s11259-008-9131-1.

Gébleux R, Wulhfard S, Casi G, Neri D. 2015. Antibody Format and Drug Release Rate Determine the Therapeutic Activity of Noninternalizing Antibody-Drug Conjugates. Mol Cancer Ther. 14(11):2606–2612. doi:10.1158/1535-7163.MCT-15-0480.

Global Cancer Observatory: Cancer Today. Lyon, France: International Agency for Research on Cancer. [accessed 2023 Feb 19]. http://gco.iarc.fr/today.

Glozak MA, Seto E. 2007. Histone deacetylases and cancer. Oncogene. 26(37):5420–5432. doi:10.1038/sj.onc.1210610.

Golan T, Milella M, Ackerstein A, Berger R. 2017. The changing face of clinical trials in the personalized medicine and immuno-oncology era: report from the international congress on clinical trials in Oncology & Hemato-Oncology (ICTO 2017). Journal of Experimental & Clinical Cancer Research. 36(1):192. doi:10.1186/s13046-017-0668-0.

Goncalves JMB, Silva FNCAD. 2008 Nov 13. Engineered rabbit antibody variable domains and uses thereof. Application No. PCT/PT2008/000018. WO2008136694A9.

Gorrini C, Harris IS, Mak TW. 2013. Modulation of oxidative stress as an anticancer strategy. Nat Rev Drug Discov. 12(12):931–947. doi:10.1038/nrd4002.

Gouveia Z, Carlos AR, Yuan X, Aires-da-Silva F, Stocker R, Maghzal GJ, Leal SS, Gomes CM, Todorovic S, Iranzo O, et al. 2017. Characterization of plasma labile heme in hemolytic conditions. FEBS J. 284(19):3278–3301. doi:10.1111/febs.14192.

Greenberg AS, Avila D, Hughes M, Hughes A, McKinney EC, Flajnik MF. 1995. A new antigen receptor gene family that undergoes rearrangement and extensive somatic diversification in sharks. Nature. 374(6518):168–173. doi:10.1038/374168a0.

Griffiths AD, Duncan AR. 1998. Strategies for selection of antibodies by phage display. Current Opinion in Biotechnology. 9(1):102–108. doi:10.1016/S0958-1669(98)80092-X.

Guimarães D, Cavaco-Paulo A, Nogueira E. 2021. Design of liposomes as drug delivery system for therapeutic applications. Int J Pharm. 601:120571. doi:10.1016/j.ijpharm.2021.120571.

Gustafson HH, Olshefsky A, Sylvestre M, Sellers DL, Pun SH. 2018. Current state of in vivo panning technologies: Designing specificity and affinity into the future of drug targeting. Adv Drug Deliv Rev. 130:39–49. doi:10.1016/j.addr.2018.06.015.

Hamamichi S, Fukuhara T, Hattori N. 2020. Immunotoxin Screening System: A Rapid and Direct Approach to Obtain Functional Antibodies with Internalization Capacities. Toxins. 12(10):658. doi:10.3390/toxins12100658.

Hamblett KJ, Senter PD, Chace DF, Sun MMC, Lenox J, Cerveny CG, Kissler KM, Bernhardt SX, Kopcha AK, Zabinski RF, et al. 2004. Effects of Drug Loading on the Antitumor Activity of a Monoclonal Antibody Drug Conjugate. Clin Cancer Res. 10(20):7063–7070. doi:10.1158/1078-0432.CCR-04-0789.

Hamers-Casterman C, Atarhouch T, Muyldermans S, Robinson G, Hammers C, Songa EB, Bendahman N, Hammers R. 1993. Naturally occurring antibodies devoid of light chains. Nature. 363(6428):446–448. doi:10.1038/363446a0.

Hauck ML. 2006. Phase I Trial of Doxorubicin-Containing Low Temperature Sensitive Liposomes in Spontaneous Canine Tumors. Clin Cancer Res. 12(13):4004–4010. doi:10.1158/1078-0432.CCR-06-0226.

Henry CJ, Buss MS, Hellstrom I, Hellstrom KE, Brewer WG, Bryan JN, Siegall CB. 2005. Clinical Evaluation of BR96 sFv-PE40 Immunotoxin Therapy in Canine Models of Spontaneously Occurring Invasive Carcinoma. :6.

Henry CJ, Bryan JN. 2013. Not Lost in Translation: How Study of Diseases in Our Pets Can Benefit Them and Us. Mo Med. 110(3):216–219.

Hoffbrand AV, Weir DG. 2001. The history of folic acid. Br J Haematol. 113(3):579–589. doi:10.1046/j.1365-2141.2001.02822.x.

Holliger P, Hudson PJ. 2005. Engineered antibody fragments and the rise of single domains. Nat Biotechnol. 23(9):1126–1136. doi:10.1038/nbt1142.

Holt LJ, Herring C, Jespers LS, Woolven BP, Tomlinson IM. 2003. Domain antibodies: proteins for therapy. Trends in Biotechnology. 21(11):484–490. doi:10.1016/j.tibtech.2003.08.007.

Hoogenboom H. 1997. Designing and optimizing library selection strategies for generating high-affinity antibodies. Trends in Biotechnology. 15(2):62–70. doi:10.1016/S0167-7799(97)84205-9.

Hoogenboom HR. 2002. Overview of Antibody Phage-Display Technology and Its Applications. In: O'Brien PM, Aitken R, editors. Antibody Phage Display: Methods and Protocols. Totowa, NJ: Humana Press. p. 1–37. https://doi.org/10.1385/1-59259-240-6:001.

Hoogenboom HR. 2005. Selecting and screening recombinant antibody libraries. Nat Biotechnol. 23(9):1105–1116. doi:10.1038/nbt1126.

Hua S, Wu S. 2013. The use of lipid-based nanocarriers for targeted pain therapies. Frontiers in Pharmacology. 4.

Huang S-H, Kozak P, Kim J, Habineza-Ndikuyeze G, Meade C, Gaurnier-Hausser A, Patel R, Robertson E, Mason NJ. 2012. Evidence of an oncogenic Gammaherpesvirus in domestic Dogs. Virology. 427(2):107–117. doi:10.1016/j.virol.2012.02.013.

Hwang WYK, Foote J. 2005. Immunogenicity of engineered antibodies. Methods. 36(1):3–10. doi:10.1016/j.ymeth.2005.01.001.

Iezzi ME, Policastro L, Werbajh S, Podhajcer O, Canziani GA. 2018. Single-Domain Antibodies and the Promise of Modular Targeting in Cancer Imaging and Treatment. Front Immunol. 9:273. doi:10.3389/fimmu.2018.00273.

Impellizeri JA, Howell K, McKeever KP, Crow SE. 2006. The role of rituximab in the treatment of canine lymphoma: An ex vivo evaluation. The Veterinary Journal. 171(3):556–558. doi:10.1016/j.tvjl.2005.03.005.

Inglut CT, Sorrin AJ, Kuruppu T, Vig S, Cicalo J, Ahmad H, Huang H-C. 2020. Immunological and Toxicological Considerations for the Design of Liposomes. Nanomaterials. 10(2):190. doi:10.3390/nano10020190.

Ishida T, Kirchmeier MJ, Moase EH, Zalipsky S, Allen TM. 2001. Targeted delivery and triggered release of liposomal doxorubicin enhances cytotoxicity against human B lymphoma cells. Biochimica et Biophysica Acta (BBA) - Biomembranes. 1515(2):144–158. doi:10.1016/S0005-2736(01)00409-6.

Ito D, Frantz AM, Modiano JF. 2014. Canine lymphoma as a comparative model for human non-Hodgkin lymphoma: recent progress and applications. Vet Immunol and Immunopathol. 159(3–4):192–201. doi:10.1016/j.vetimm.2014.02.016.

Ito D, Brewer S, Modiano JF, Beall MJ. 2015. Development of a novel anti-canine CD20 monoclonal antibody with diagnostic and therapeutic potential. Leukemia & Lymphoma. 56(1):219–225. doi:10.3109/10428194.2014.914193.

Jack S, Madhivanan K, Ramadesikan S, Subramanian S, Edwards II DF, Elzey BD, Dhawan D, McCluskey A, Kischuk EM, Loftis AR, et al. 2020. A novel, safe, fast and efficient treatment for Her2-positive and negative bladder cancer utilizing an EGF-anthrax toxin chimera. International Journal of Cancer. 146(2):449–460. doi:10.1002/ijc.32719.

Jensen NF, Agama K, Roy A, Smith DH, Pfister TD, Rømer MU, Zhang H-L, Doroshow JH, Knudsen BR, Stenvang J, et al. 2016. Characterization of DNA topoisomerase I in three SN-38 resistant human colon cancer cell lines reveals a new pair of resistance-associated mutations. J Exp Clin Cancer Res. 35:56. doi:10.1186/s13046-016-0335-x.

Jin S, Sun Y, Liang X, Gu X, Ning J, Xu Y, Chen S, Pan L. 2022. Emerging new therapeutic antibody derivatives for cancer treatment. Sig Transduct Target Ther. 7(1):1–28. doi:10.1038/s41392-021-00868-x.

Jolivet L, Ait Mohamed Amar I, Horiot C, Boursin F, Colas C, Letast S, Denevault-Sabourin C, Allard-Vannier E, Joubert N, Aubrey N. 2022. Intra-Domain Cysteines (IDC), a New Strategy for the Development of Original Antibody Fragment–Drug Conjugates (FDCs). Pharmaceutics. 14(8):1524. doi:10.3390/pharmaceutics14081524.

Jones ML, Alfaleh MA, Kumble S, Zhang S, Osborne GW, Yeh M, Arora N, Hou JJC, Howard CB, Chin DY, et al. 2016. Targeting membrane proteins for antibody discovery using phage display. Sci Rep. 6(1):26240. doi:10.1038/srep26240.

Joubert N, Beck A, Dumontet C, Denevault-Sabourin C. 2020. Antibody–Drug Conjugates: The Last Decade. Pharmaceuticals. 13(9):345.

Jubala CM, Wojcieszyn JW, Valli VEO, Getzy DM, Fosmire SP, Coffey D, Bellgrau D, Modiano JF. 2005. CD20 Expression in Normal Canine B Cells and in Canine non-Hodgkin Lymphoma. Vet Pathol. 42(4):468–476. doi:10.1354/vp.42-4-468.

Junutula JR, Raab H, Clark S, Bhakta S, Leipold DD, Weir S, Chen Y, Simpson M, Tsai SP, Dennis MS, et al. 2008. Site-specific conjugation of a cytotoxic drug to an antibody improves the therapeutic index. Nat Biotechnol. 26(8):925–932. doi:10.1038/nbt.1480.

Kabat EA, Wu TT, Perry HM, Foeller C, Gottesman KS. 1991. Sequences of Proteins of Immunological Interest. Bethesda, MD: NIH publication.

Kano R, Inoiue C, Okano H, Yamazaki J, Takahashi T, Watari T, Tokuriki M, Hasegawa A. 2005. Canine CD20 gene. Veterinary Immunology and Immunopathology. 108(3):265–268. doi:10.1016/j.vetimm.2005.05.011.

Kapoor M, Lee SL, Tyner KM. 2017. Liposomal Drug Product Development and Quality: Current US Experience and Perspective. AAPS J. 19(3):632–641. doi:10.1208/s12248-017-0049-9.

Keller ET. 1992. Immune-mediated disease as a risk factor for canine lymphoma. Cancer. 70(9):2334–2337. doi:10.1002/1097-0142(19921101)70:9<2334::aid-cncr2820700920>3.0.co;2-7.

Kelley LA, Mezulis S, Yates CM, Wass MN, Sternberg MJE. 2015. The Phyre2 web portal for protein modeling, prediction and analysis. Nat Protoc. 10(6):845–858. doi:10.1038/nprot.2015.053.

Kelly PN. 2018. The Cancer Immunotherapy Revolution. Science. 359(6382):1344–1345. doi:10.1126/science.359.6382.1344.

Khazaeli MB, Conry RM, LoBuglio AF. 1994. Human immune response to monoclonal antibodies. J Immunother Emphasis Tumor Immunol. 15(1):42–52. doi:10.1097/00002371-199401000-00006.

Kim CH, Axup JY, Schultz PG. 2013. Protein conjugation with genetically encoded unnatural amino acids. Current Opinion in Chemical Biology. 17(3):412–419. doi:10.1016/j.cbpa.2013.04.017.

Kim EG, Kim KM. 2015. Strategies and Advancement in Antibody-Drug Conjugate Optimization for Targeted Cancer Therapeutics. Biomol The. 23(6):493–509. doi:10.4062/biomolther.2015.116.

Kim J-S, Jun S-Y, Kim Y-S. 2020. Critical Issues in the Development of Immunotoxins for Anticancer Therapy. J Pharm Sci. 109(1):104–115. doi:10.1016/j.xphs.2019.10.037.

Kirsch MI, Hülseweh B, Nacke C, Rülker T, Schirrmann T, Marschall H-J, Hust M, Dübel S. 2008. Development of human antibody fragments using antibody phage display for the detection and diagnosis of Venezuelan equine encephalitis virus (VEEV). BMC Biotechnology. 8(1):66. doi:10.1186/1472-6750-8-66.

Köhler G, Milstein C. 1975. Continuous cultures of fused cells secreting antibody of predefined specificity. Nature. 256(5517):495–497. doi:10.1038/256495a0.

Koning GA, Storm G. 2003. Targeted drug delivery systems for the intracellular delivery of macromolecular drugs. Drug Discovery Today. 8(11):482–483. doi:10.1016/S1359-6446(03)02699-0.

Kraft JC, Freeling JP, Wang Z, Ho RJY. 2014. Emerging research and clinical development trends of liposome and lipid nanoparticle drug delivery systems. J Pharm Sci. 103(1):29–52. doi:10.1002/jps.23773.

Kreitman RJ, Pastan I. 2011. Antibody Fusion Proteins: Anti-CD22 Recombinant Immunotoxin Moxetumomab Pasudotox. Clin Cancer Res. 17(20):6398–6405. doi:10.1158/1078-0432.CCR-11-0487.

Kreitman RJ, Pastan I. 2020. Contextualizing the Use of Moxetumomab Pasudotox in the Treatment of Relapsed or Refractory Hairy Cell Leukemia. The Oncol. 25(1). doi:10.1634/theoncologist.2019-0370.

Kristensen P, Winter G. 1998. Proteolytic selection for protein folding using filamentous bacteriophages. Folding and Design. 3(5):321–328. doi:10.1016/S1359-0278(98)00044-3.

Kuan CT, Pai LH, Pastan I. 1995. Immunotoxins containing Pseudomonas exotoxin that target LeY damage human endothelial cells in an antibody-specific mode: relevance to vascular leak syndrome. Clin Cancer Res. 1(12):1589–1594.

Kügler J, Tomszak F, Frenzel A, Hust M. 2018. Construction of Human Immune and Naive scFv Libraries. In: Hust M, Lim TS, editors. Phage Display: Methods and Protocols. New York, NY: Springer New York. p. 3–24. https://doi.org/10.1007/978-1-4939-7447-4_1.

Kumar P, Huo P, Liu B. 2019. Formulation Strategies for Folate-Targeted Liposomes and Their Biomedical Applications. Pharmaceutics. 11(8):381. doi:10.3390/pharmaceutics11080381.

Laing EJ, Fitzpatrick PJ, Binnington AG, Norris AM, Mosseri A, Rider WD, Valli VE, Baur A. 1989. Half-body radiotherapy in the treatment of canine lymphoma. J Vet Intern Med. 3(2):102–108. doi:10.1111/j.1939-1676.1989.tb03087.x.

Leamon CP, Cooper SR, Hardee GE. 2003. Folate-liposome-mediated antisense oligodeoxynucleotide targeting to cancer cells: Evaluation in vitro and in vivo. Bioconjugate Chemistry. 14(4):738–747. doi:10.1021/bc020089t.

Lee H-Z, Kwitkowski VE, Del Valle PL, Ricci MS, Saber H, Habtemariam BA, Bullock J, Bloomquist E, Li Shen Y, Chen X-H, et al. 2015. FDA Approval: Belinostat for the Treatment of Patients with Relapsed or Refractory Peripheral T-cell Lymphoma. Clin Cancer Res. 21(12):2666–2670. doi:10.1158/1078-0432.CCR-14-3119.

Lehner R, Wang X, Marsch S, Hunziker P. 2013. Intelligent nanomaterials for medicine: Carrier platforms and targeting strategies in the context of clinical application. Nanomedicine: Nanotechnology, Biology and Medicine. 9(6):742–757. doi:10.1016/j.nano.2013.01.012.

Leshem Y, Pastan I. 2019. Pseudomonas Exotoxin Immunotoxins and Anti-Tumor Immunity: From Observations at the Patient's Bedside to Evaluation in Preclinical Models. Toxins. 11(1):20. doi:10.3390/toxins11010020.

Li M, Liu Z-S, Liu X-L, Hui Q, Lu S-Y, Qu L-L, Li Y-S, Zhou Y, Ren H-L, Hu P. 2017. Clinical targeting recombinant immunotoxins for cancer therapy. OTT. Volume 10:3645–3665. doi:10.2147/OTT.S134584.

Li M, Mei S, Yang Y, Shen Y, Chen L. 2022. Strategies to mitigate the on- and off-target toxicities of recombinant immunotoxins: an antibody engineering perspective. Antib Ther. 5(3):164–176. doi:10.1093/abt/tbac014.

Li N, Fu H, Hewitt SM, Dimitrov DS, Ho M. 2017. Therapeutically targeting glypican-2 via single-domain antibody-based chimeric antigen receptors and immunotoxins in neuroblastoma. Proc Natl Acad Sci USA. 114(32):E6623–E6631. doi:10.1073/pnas.1706055114.

Li T, Qi S, Unger M, Hou YN, Deng QW, Liu J, Lam CMC, Wang XW, Xin D, Zhang P, et al. 2016. Immuno-targeting the multifunctional CD38 using nanobody. Sci Rep. 6(1):27055. doi:10.1038/srep27055.

Li X, Zhang J, Wang D-K, Pan W-S. 2012. Preparation and in vitro properties of folate receptor targeting docetaxel-loaded amphiphilic copolymer-modified liposomes. Yaoxue Xuebao. 47(9):1219–1226.

Li X, Yang J, Rader C. 2014. Antibody conjugation via one and two C-terminal selenocysteines. Methods. 65(1):133–138. doi:10.1016/j.ymeth.2013.05.023.

Lindblad-Toh K, Wade CM, Mikkelsen TS, Karlsson EK, Jaffe DB, Kamal M, Clamp M, Chang JL, Kulbokas EJ, Zody MC, et al. 2005. Genome sequence, comparative analysis and haplotype structure of the domestic dog. Nature. 438(7069):803–819. doi:10.1038/nature04338.

Lipes BD, Chen Y-H, Ma H, Staats HF, Kenan DJ, Gunn MD. 2008. An Entirely Cell-Based System to Generate Single-Chain Antibodies against Cell Surface Receptors. Journal of Molecular Biology. 379(2):261–272. doi:10.1016/j.jmb.2008.03.072.

Liu P, Chen G, Zhang J. 2022. A Review of Liposomes as a Drug Delivery System: Current Status of Approved Products, Regulatory Environments, and Future Perspectives. Molecules. 27(4):1372. doi:10.3390/molecules27041372.

Lu J, Jiang F, Lu A, Zhang G. 2016. Linkers Having a Crucial Role in Antibody–Drug Conjugates. International Journal of Molecular Sciences. 17(4). doi:10.3390/ijms17040561.

Luiz H, Oliveira Pinho J, Gaspar MM. 2023. Advancing Medicine with Lipid-Based Nanosystems-The Successful Case of Liposomes. Biomedicines. 11(2):435. doi:10.3390/biomedicines11020435.

MacMillan KS, Boger DL. 2009. Fundamental relationships between structure, reactivity, and biological activity for the duocarmycins and CC-1065. J Med Chem. 52(19):5771–5780. doi:10.1021/jm9006214.

Maherani B, Arab-Tehrany E, R. Mozafari M, Gaiani C, Linder M. 2011. Liposomes: A Review of Manufacturing Techniques and Targeting Strategies. Current Nanoscience. 7(3):436–452. doi:10.2174/157341311795542453.

Maloney D, Liles T, Czerwinski D, Waldichuk C, Rosenberg J, Grillo-Lopez A, Levy R. 1994. Phase I clinical trial using escalating single-dose infusion of chimeric anti-CD20 monoclonal antibody (IDEC-C2B8) in patients with recurrent B-cell lymphoma. Blood. 84(8):2457–2466. doi:10.1182/blood.V84.8.2457.2457.

Mann BS, Johnson JR, Cohen MH, Justice R, Pazdur R. 2007. FDA Approval Summary: Vorinostat for Treatment of Advanced Primary Cutaneous T-Cell Lymphoma. The Oncologist. 12(10):1247–1252. doi:10.1634/theoncologist.12-10-1247.

Marconato L, Gelain ME, Comazzi S. 2013. The dog as a possible animal model for human non-Hodgkin lymphoma: a review: The dog as model for human non-Hodgkin lymphoma. Hematol Oncol. 31(1):1–9. doi:10.1002/hon.2017.

Marks JD, Hoogenboom HR, Bonnert TP, McCafferty J, Griffiths AD, Winter G. 1991. By-passing immunization. Journal of Molecular Biology. 222(3):581–597. doi:10.1016/0022-2836(91)90498-U.

Martini V, Melzi E, Comazzi S, Gelain ME. 2015. Peripheral blood abnormalities and bone marrow infiltration in canine large B-cell lymphoma: is there a link? Vet Comp Oncol. 13(2):117–123. doi:10.1111/vco.12024.

Maruani A, Smith MEB, Miranda E, Chester KA, Chudasama V, Caddick S. 2015. A plug-and-play approach to antibody-based therapeutics via a chemoselective dual click strategy. Nat Commun. 6(1):6645. doi:10.1038/ncomms7645.

Matsuda Y, Mendelsohn BA. 2021. Recent Advances in Drug-Antibody Ratio Determination of Antibody-Drug Conjugates. Chem Pharm Bull (Tokyo). 69(10):976–983. doi:10.1248/cpb.c21-00258.

Mayer LD, Bally MB, Hope MJ, Cullis PR. 1986. Techniques for encapsulating bioactive agents into liposomes. Chemistry and Physics of Lipids. 40(2):333–345. doi:10.1016/0009-3084(86)90077-0.

Maynard J, Georgiou G. 2000. Antibody Engineering. Annual Review of Biomedical Engineering. 2(1):339–376. doi:10.1146/annurev.bioeng.2.1.339.

Mazor R, Onda M, Pastan I. 2016. Immunogenicity of therapeutic recombinant immunotoxins. Immunol Rev. 270(1):152–164. doi:10.1111/imr.12390.

Mazor R, King EM, Pastan I. 2018. Strategies to Reduce the Immunogenicity of Recombinant Immunotoxins. The American Journal of Pathology. 188(8):1736–1743. doi:10.1016/j.ajpath.2018.04.016.

Mazor R, Pastan I. 2020. Immunogenicity of Immunotoxins Containing Pseudomonas Exotoxin A: Causes, Consequences, and Mitigation. Front Immunol. 11(1261). doi:10.3389/fimmu.2020.01261.

McCafferty J, Griffiths AD, Winter G, Chiswell DJ. 1990. Phage antibodies: filamentous phage displaying antibody variable domains. Nature. 348(6301):552–554. doi:10.1038/348552a0.

McCartney-Francis N, Skurla RM, Mage RG, Bernstein KE. 1984. Kappa-chain allotypes and isotypes in the rabbit: cDNA sequences of clones encoding b9 suggest an evolutionary pathway and possible role of the interdomain disulfide bond in quantitative allotype expression. Proc Natl Acad Sci U S A. 81(6):1794–1798. doi:10.1073/pnas.81.6.1794.

McDonagh CF, Turcott E, Westendorf L, Webster JB, Alley SC, Kim K, Andreyka J, Stone I, Hamblett KJ, Francisco JA, et al. 2006. Engineered antibody–drug conjugates with defined sites and stoichiometries of drug attachment. Protein Engineering, Design and Selection. 19(7):299–307. doi:10.1093/protein/gzl013.

van der Meel R, Vehmeijer LJC, Kok RJ, Storm G, van Gaal EVB. 2013. Ligand-targeted particulate nanomedicines undergoing clinical evaluation: Current status. Advanced Drug Delivery Reviews. 65(10):1284–1298. doi:10.1016/j.addr.2013.08.012.

Merlo DF, Rossi L, Pellegrino C, Ceppi M, Cardellino U, Capurro C, Ratto A, Sambucco PL, Sestito V, Tanara G, et al. 2008. Cancer incidence in pet dogs: findings of the Animal Tumor Registry of Genoa, Italy. J Vet Intern Med. 22(4):976–984. doi:10.1111/j.1939-1676.2008.0133.x.

Metselaar JM, Storm G. 2005. Liposomes in the treatment of inflammatory disorders. Expert Opinion on Drug Delivery. 2(3):465–476. doi:10.1517/17425247.2.3.465.

Miller K, Cortes J, Hurvitz SA, Krop IE, Tripathy D, Verma S, Riahi K, Reynolds JG, Wickham TJ, Molnar I, et al. 2016. HERMIONE: a randomized Phase 2 trial of MM-302 plus trastuzumab versus chemotherapy of physician's choice plus trastuzumab in patients with previously treated, anthracycline-naïve, HER2-positive, locally advanced/metastatic breast cancer. BMC Cancer. 16:352. doi:10.1186/s12885-016-2385-z.

Milman G, Smith KC, Erles K. 2011. Serological detection of Epstein-Barr virus infection in dogs and cats. Veterinary Microbiology. 150(1):15–20. doi:10.1016/j.vetmic.2010.12.013.

Mitchell HK, Snell EE, Williams RJ. 1941. THE CONCENTRATION OF "FOLIC ACID." J Am Chem Soc. 63(8):2284–2284. doi:10.1021/ja01853a512.

Molenaar TJM, Michon I, de Haas SAM, van Berkel TJC, Kuiper J, Biessen EAL. 2002. Uptake and Processing of Modified Bacteriophage M13 in Mice: Implications for Phage Display. Virology. 293(1):182–191. doi:10.1006/viro.2001.1254.

Monteiro N, Martins A, Reis RL, Neves NM. 2014. Liposomes in tissue engineering and regenerative medicine. Journal of The Royal Society Interface. 11(101):20140459. doi:10.1098/rsif.2014.0459.

Moreira JN, Gaspar R, Allen TM. 2001. Targeting Stealth liposomes in a murine model of human small cell lung cancer. Biochim Biophys Acta. 1515(2):167–176. doi:10.1016/s0005-2736(01)00411-4.

Morrison C. 2019. Nanobody approval gives domain antibodies a boost. Nat Rev Drug Discov. 18(7):485–487. doi:10.1038/d41573-019-00104-w.

Motta G, Cea M, Moran E, Carbone F, Augusti V, Patrone F, Nencioni A. 2011. Monoclonal Antibodies for Non-Hodgkin's Lymphoma: State of the Art and Perspectives. Journal of Immunology Research. 2010:e428253. doi:10.1155/2010/428253.

Müller AMS, Ihorst G, Mertelsmann R, Engelhardt M. 2005. Epidemiology of non-Hodgkin's lymphoma (NHL): trends, geographic distribution, and etiology. Ann Hematol. 84(1):1–12. doi:10.1007/s00277-004-0939-7.

Muyldermans S, Cambillau C, Wyns L. 2001. Recognition of antigens by single-domain antibody fragments: the superfluous luxury of paired domains. Trends Biochem Sci. 26(4):230–235. doi:10.1016/s0968-0004(01)01790-x.

Nagayama A, Ellisen LW, Chabner B, Bardia A. 2017. Antibody-Drug Conjugates for the Treatment of Solid Tumors: Clinical Experience and Latest Developments. Target Oncol. 12(6):719–739. doi:10.1007/s11523-017-0535-0.

Nessler I, Khera E, Vance S, Kopp A, Qiu Q, Keating TA, Abu-Yousif AO, Sandal T, Legg J, Thompson L, et al. 2020. Increased Tumor Penetration of Single-Domain Antibody–Drug Conjugates Improves *In Vivo* Efficacy in Prostate Cancer Models. Cancer Res. 80(6):1268–1278. doi:10.1158/0008-5472.CAN-19-2295.

Nissim A, Hoogenboom HR, Tomlinson IM, Flynn G, Midgley C, Lane D, Winter G. 1994. Antibody fragments from a 'single pot' phage display library as immunochemical reagents. The EMBO Journal. 13(3):692–698. doi:10.1002/j.1460-2075.1994.tb06308.x.

Noble GT, Stefanick JF, Ashley JD, Kiziltepe T, Bilgicer B. 2014. Ligand-targeted liposome design: challenges and fundamental considerations. Trends in Biotechnology. 32(1):32–45. doi:10.1016/j.tibtech.2013.09.007.

Nogueira E, Lager F, Le Roux D, Nogueira P, Freitas J, Charvet C, Renault G, Loureiro A, Almeida CR, Ohradanova-Repic A, et al. 2015. Enhancing Methotrexate Tolerance with Folate Tagged Liposomes in Arthritic Mice. J Biomed Nanotechnol. 11(12):2243–2252. doi:10.1166/jbn.2015.2170.

Northfelt DW, Martin FJ, Working P, Volberding PA, Russell J, Newman M, Amantea MA, Kaplan LD. 1996. Doxorubicin Encapsulated in Liposomes Containing Surface-Bound Polyethylene Glycol: Pharmacokinetics, Tumor Localization, and Safety in Patients with AIDS-Related Kaposi's Sarcoma. The Journal of Clinical Pharmacology. 36(1):55–63. doi:10.1002/j.1552-4604.1996.tb04152.x.

Naknaei P, Margiana R, Bokov DO, Abdelbasset WK, Kouhbanani MAJ, Varma RS, Marofi F, Jarahian M, Beheshtkhoo N. 2021. Liposomes: Structure, Biomedical Applications, and Stability Parameters With Emphasis on Cholesterol. Frontiers in bioengineering and biotechnology. 9. doi:10.3389/fbioe.2021.705886.

Pan XQ, Lee RJ. 2005. In vivo antitumor activity of folate receptor-targeted liposomal daunorubicin in a murine leukemia model. Anticancer Res. 25(1A):343–346.

Pande J, Szewczyk MM, Grover AK. 2010. Phage display: Concept, innovations, applications and future. Biotechnology Advances. 28(6):849–858. doi:10.1016/j.biotechadv.2010.07.004.

Panobinostat Approved for Multiple Myeloma. 2015 May 1. Cancer Discov. doi:10.1158/2159-8290.CD-NB2015-040. http://cancerdiscovery.aacrjournals.org/content/5/5/OF4.abstract.

Panowski S, Bhakta S, Raab H, Polakis P, Junutula JR. 2014. Site-specific antibody drug conjugates for cancer therapy. mAbs. 6(1):34–45. doi:10.4161/mabs.27022.

Paoloni M, Khanna C. 2008. Translation of new cancer treatments from pet dogs to humans. Nature Reviews Cancer. 8(2):147–156. doi:10.1038/nrc2273.

Park JS, Withers SS, Modiano JF, Kent MS, Chen M, Luna JI, Culp WTN, Sparger EE, Rebhun RB, Monjazeb AM, et al. 2016. Canine cancer immunotherapy studies: linking mouse and human. J Immunother Cancer. 4:97. doi:10.1186/s40425-016-0200-7.

Park JW, Hong K, Kirpotin DB, Meyer O, Papahadjopoulos D, Benz CC. 1997. Anti-HER2 immunoliposomes for targeted therapy of human tumors. Cancer Lett. 118(2):153–160. doi:10.1016/s0304-3835(97)00326-1.

Park JW, Kirpotin DB, Hong K, Shalaby R, Shao Y, Nielsen UB, Marks JD, Papahadjopoulos D, Benz CC. 2001. Tumor targeting using anti-her2 immunoliposomes. J Control Release. 74(1–3):95–113. doi:10.1016/s0168-3659(01)00315-7.

Park JW, Hong K, Kirpotin DB, Colbern G, Shalaby R, Baselga J, Shao Y, Nielsen UB, Marks JD, Moore D, et al. 2002. Anti-HER2 immunoliposomes: enhanced efficacy attributable to targeted delivery. Clin Cancer Res. 8(4):1172–1181.

Parray HA, Shukla S, Samal S, Shrivastava T, Ahmed S, Sharma C, Kumar R. 2020. Hybridoma technology a versatile method for isolation of monoclonal antibodies, its applicability across species, limitations, advancement and future perspectives. Int Immunopharmacol. 85:106639. doi:10.1016/j.intimp.2020.106639.

Pattni BS, Chupin VV, Torchilin VP. 2015. New Developments in Liposomal Drug Delivery. Chem Rev. 115(19):10938–10966. doi:10.1021/acs.chemrev.5b00046.

Perez HL, Cardarelli PM, Deshpande S, Gangwar S, Schroeder GM, Vite GD, Borzilleri RM. 2014. Antibody–drug conjugates: current status and future directions. Drug Discovery Today. 19(7):869–881. doi:10.1016/j.drudis.2013.11.004.

Pettersen EF, Goddard TD, Huang CC, Couch GS, Greenblatt DM, Meng EC, Ferrin TE. 2004. UCSF Chimera-A visualization system for exploratory research and analysis. J Comput Chem. 25(13):1605–1612. doi:10.1002/jcc.20084.

Piek CJ, Rutteman GR, Teske E. 1999. Evaluation of the results of a L-asparaginase-based continuous chemotherapy protocol versus a short doxorubicin-based induction chemotherapy protocol in dogs with malignant lymphoma. Vet Q. 21(2):44–49. doi:10.1080/01652176.1999.9694990.

Pinho JO, Amaral JD, Castro RE, Rodrigues CM, Casini A, Soveral G, Gaspar MM. 2019. Copper complex nanoformulations featuring highly promising therapeutic potential in murine melanoma models. Nanomedicine. 14(7):835–850. doi:10.2217/nnm-2018-0388.

Pinho JO, Matias M, Marques V, Eleutério C, Fernandes C, Gano L, Amaral JD, Mendes E, Perry MJ, Moreira JN, et al. 2023. Preclinical validation of a new hybrid molecule loaded in liposomes for melanoma management. Biomed Pharmacother. 157:114021. doi:10.1016/j.biopha.2022.114021.

Pinot M, Vanni S, Pagnotta S, Lacas-Gervais S, Payet L-A, Ferreira T, Gautier R, Goud B, Antonny B, Barelli H. 2014. Lipid cell biology. Polyunsaturated phospholipids facilitate membrane deformation and fission by endocytic proteins. Science. 345(6197):693–697. doi:10.1126/science.1255288.

Poletto S, Novo M, Paruzzo L, Frascione PMM, Vitolo U. 2022. Treatment strategies for patients with diffuse large B-cell lymphoma. Cancer Treat Rev. 110:102443. doi:10.1016/j.ctrv.2022.102443.

Pommier Y. 2013. Drugging Topoisomerases: Lessons and Challenges. ACS Chem Biol. 8(1):82–95. doi:10.1021/cb300648v.

Ponce F, Marchal T, Magnol JP, Turinelli V, Ledieu D, Bonnefont C, Pastor M, Delignette ML, Fournel-Fleury C. 2010. A Morphological Study of 608 Cases of Canine Malignant Lymphoma in France With a Focus on Comparative Similarities Between Canine and Human Lymphoma Morphology. Vet Pathol. 47(3):414–433. doi:10.1177/0300985810363902.

Popkov M, Mage RG, Alexander CB, Thundivalappil S, Barbas CF, Rader C. 2003. Rabbit Immune Repertoires as Sources for Therapeutic Monoclonal Antibodies: The Impact of Kappa Allotype-correlated Variation in Cysteine Content on Antibody Libraries Selected by Phage Display. J Mol Biol. 325(2):325–335. doi:10.1016/S0022-2836(02)01232-9.

Popkov M, Rader C, Barbas CF. 2004. Isolation of human prostate cancer cell reactive antibodies using phage display technology. Journal of Immunological Methods. 291(1):137–151. doi:10.1016/j.jim.2004.05.004.

Porrello A, Cardelli P, Spugnini EP. 2006. Oncology of companion animals as a model for humans. an overview of tumor histotypes. J Exp Clin Cancer Res. 25(1):97–105.

Presta LG. 2006. Engineering of therapeutic antibodies to minimize immunogenicity and optimize function. Adv Drug Deliv Rev. 58(5–6):640–656. doi:10.1016/j.addr.2006.01.026.

Priester WA, McKay FW. 1980. The occurrence of tumors in domestic animals. Natl Cancer Inst Monogr.(54):1–210.

Qiu L, Dong C, Kan X. 2018. Lymphoma-targeted treatment using a folic acid-decorated vincristine-loaded drug delivery system. Drug Des Devel Ther. 12:863–872. doi:10.2147/DDDT.S152420.

Raskin RE, Krehbiel JD. 1989. Prevalence of leukemic blood and bone marrow in dogs with multicentric lymphoma. J Am Vet Med Assoc. 194(10):1427–1429.

Rassnick KM, Bailey DB, Malone EK, Intile JL, Kiselow MA, Flory AB, Barlow LL, Balkman CE, Barnard SM, Waite AH. 2010. Comparison between L-CHOP and an L-CHOP protocol with interposed treatments of CCNU and MOPP (L-CHOP-CCNU-MOPP) for lymphoma in dogs. Vet Comp Oncol. 8(4):243–253. doi:10.1111/j.1476-5829.2010.00224.x.

Reddy JA, Abburi C, Hofland H, Howard SJ, Vlahov I, Wils P, Leamon CP. 2002. Folate-targeted, cationic liposome-mediated gene transfer into disseminated peritoneal tumors. Gene Ther. 9(22):1542–1550. doi:10.1038/sj.gt.3301833.

Richards KL, Suter SE. 2015. Man's best friend: what can pet dogs teach us about non-Hodgkin's lymphoma? Immunological Reviews. 263(1):173–191. doi:10.1111/imr.12238.

Ritchie M, Tchistiakova L, Scott N. 2013. Implications of receptor-mediated endocytosis and intracellular trafficking dynamics in the development of antibody drug conjugates. MAbs. 5(1):13–21. doi:10.4161/mabs.22854.

Rondot S, Koch J, Breitling F, Dübel S. 2001. A helper phage to improve single-chain antibody presentation in phage display. Nat Biotechnol. 19(1):75–78. doi:10.1038/83567.

Rossi G, Rossi M, Vitali CG, Fortuna D, Burroni D, Pancotto L, Capecchi S, Sozzi S, Renzoni G, Braca G, et al. 1999. A Conventional Beagle Dog Model for Acute and Chronic Infection with Helicobacter pylori. Infect Immun. 67(6):3112–3120.

Rütgen BC, Hammer SE, Gerner W, Christian M, de Arespacochaga AG, Willmann M, Kleiter M, Schwendenwein I, Saalmüller A. 2010. Establishment and characterization of a novel canine B-cell line derived from a spontaneously occurring diffuse large cell lymphoma. Leuk Res. 34(7):932–938. doi:10.1016/j.leukres.2010.01.021.

Rütgen BC, Willenbrock S, Reimann-Berg N, Walter I, Fuchs-Baumgartinger A, Wagner S, Kovacic B, Essler SE, Schwendenwein I, Nolte I, et al. 2012. Authentication of Primordial Characteristics of the CLBL-1 Cell Line Prove the Integrity of a Canine B-Cell Lymphoma in a Murine In Vivo Model. Singh SR, editor. PLoS ONE. 7(6):e40078. doi:10.1371/journal.pone.0040078.

Sapra P, Allen TM. 2003. Ligand-targeted liposomal anticancer drugs. Prog Lipid Res. 42(5):439–462. doi:10.1016/s0163-7827(03)00032-8.

Sawant RR, Torchilin VP. 2012. Challenges in Development of Targeted Liposomal Therapeutics. AAPS J. 14(2):303–315. doi:10.1208/s12248-012-9330-0.

Schiffman JD, Breen M. 2015. Comparative oncology: what dogs and other species can teach us about humans with cancer. Philos Trans R Soc Lond, B, Biol Sci. 370(1673):20140231. doi:10.1098/rstb.2014.0231.

Schneider DW, Heitner T, Alicke B, Light DR, McLean K, Satozawa N, Parry G, Yoo J, Lewis JS, Parry R. 2009. In Vivo Biodistribution, PET Imaging, and Tumor Accumulation of 86Y- and 111In-Antimindin/RG-1, Engineered Antibody Fragments in LNCaP Tumor–Bearing Nude Mice. The Journal of Nuclear Medicine.:9.

Sercombe L, Veerati T, Moheimani F, Wu SY, Sood AK, Hua S. 2015. Advances and Challenges of Liposome Assisted Drug Delivery. Front Pharmacol. 6. doi:10.3389/fphar.2015.00286.

Sermer D, Pasqualucci L, Wendel H-G, Melnick A, Younes A. 2019. Emerging epigenetic-modulating therapies in lymphoma. Nat Rev Clin Oncol. 16(8):494–507. doi:10.1038/s41571-019-0190-8.

Shah RR. 2019. Safety and Tolerability of Histone Deacetylase (HDAC) Inhibitors in Oncology. Drug Saf. 42(2):235–245. doi:10.1007/s40264-018-0773-9.

Shen B-Q, Xu K, Liu L, Raab H, Bhakta S, Kenrick M, Parsons-Reponte KL, Tien J, Yu S-F, Mai E, et al. 2012. Conjugation site modulates the in vivo stability and therapeutic activity of antibody-drug conjugates. Nat Biotechnol. 30(2):184–189. doi:10.1038/nbt.2108.

Shim MK, Yoon HY, Lee S, Jo MK, Park J, Kim J-H, Jeong SY, Kwon IC, Kim K. 2017. Caspase-3/-7-Specific Metabolic Precursor for Bioorthogonal Tracking of Tumor Apoptosis. Sci Rep. 7(1):16635. doi:10.1038/s41598-017-16653-2.

Sievers EL, Senter PD. 2013. Antibody-Drug Conjugates in Cancer Therapy. Annu Rev Med. 64(1):15–29. doi:10.1146/annurev-med-050311-201823.

Silva FA da, Santa-Marta M, Freitas-Vieira A, Mascarenhas P, Barahona I, Moniz-Pereira J, Gabuzda D, Goncalves J. 2004. Camelized Rabbit-derived VH Single-domain Intrabodies Against Vif Strongly Neutralize HIV-1 Infectivity. Journal of Molecular Biology. 340(3):525–542. doi:10.1016/j.jmb.2004.04.062.

Simon D, Nolte I, Eberle N, Abbrederis N, Killich M, Hirschberger J. 2006. Treatment of dogs with lymphoma using a 12-week, maintenance-free combination chemotherapy protocol. J Vet Intern Med. 20(4):948–954. doi:10.1892/0891-6640(2006)20[948:todwlu]2.0.co;2.

Smith GP. 1985. Filamentous Fusion Phage: Novel Expression Vectors That Display Cloned Antigens on the Virion Surface. Science. 228(4705):1315–1317. doi:10.1126/science.4001944.

Smith GP, Petrenko VA. 1997. Phage Display. Chem Rev. 97(2):391–410. doi:10.1021/cr960065d.

Soendergaard M, Newton-Northup JR, Deutscher SL. 2014. In vivo phage display selection of an ovarian cancer targeting peptide for SPECT/CT imaging. Am J Nucl Med Mol Imaging. 4(6):561–570.

Sokolova E, Guryev E, Yudintsev A, Vodeneev V, Deyev S, Balalaeva I. 2017. HER2-specific recombinant immunotoxin 4D5scFv-PE40 passes through retrograde trafficking route and forces cells to enter apoptosis. Oncotarget. 8(13):22048–22058. doi:10.18632/oncotarget.15833.

Sorenmo K, Samluk M, Clifford C, Baez J, Barrett JS, Poppenga R, Overley B, Skorupski K, Oberthaler K, Winkle TV, et al. 2007. Clinical and Pharmacokinetic Characteristics of Intracavitary Administration of Pegylated Liposomal Encapsulated Doxorubicin in Dogs with Splenic Hemangiosarcoma. J Vet Intern Med. 21:1347–1354.

Sorenmo K, Overley B, Krick E, Ferrara T, LaBlanc A, Shofer F. 2010. Outcome and toxicity associated with a dose-intensified, maintenance-free CHOP-based chemotherapy protocol in canine lymphoma: 130 cases. Vet Comp Oncol. 8(3):196–208. doi:10.1111/j.1476-5829.2010.00222.x.

Stark Y, Venet S, Schmid A. 2017. Whole Cell Panning with Phage Display. In: Tiller T, editor. Synthetic Antibodies: Methods and Protocols. New York, NY: Springer. (Methods in Molecular Biology). p. 67–91. [accessed 2022 Jun 3]. https://doi.org/10.1007/978-1-4939-6857-2_5.

Staudacher AH, Brown MP. 2017. Antibody drug conjugates and bystander killing: is antigen-dependent internalisation required? Br J Cancer. 117(12):1736–1742. doi:10.1038/bjc.2017.367.

Stegemann M, Denker S, Schmitt CA. 2022. DLBCL 1L-What to Expect beyond R-CHOP? Cancers (Basel). 14(6):1453. doi:10.3390/cancers14061453.

Stevens PJ, Sekido M, Lee RJ. 2004. Synthesis and Evaluation of A Hematoporphyrin Derivative in A Folate Receptor-targeted Solid-Lipid Nanoparticle Formulation. Anticancer Research. 24(1):161–165.

Sudimack JJ, Guo W, Tjarks W, Lee RJ. 2002. A novel pH-sensitive liposome formulation containing oleyl alcohol. Biochimica et Biophysica Acta (BBA) - Biomembranes. 1564(1):31–37. doi:10.1016/S0005-2736(02)00399-1.

Sung H, Ferlay J, Siegel RL, Laversanne M, Soerjomataram I, Jemal A, Bray F. 2021a. Global Cancer Statistics 2020: GLOBOCAN Estimates of Incidence and Mortality Worldwide for 36 Cancers in 185 Countries. CA: A Cancer Journal for Clinicians. 71(3):209–249. doi:10.3322/caac.21660.

Sur S, C. Fries A, W. Kinzler K, Zhou S, Vogelstein B. 2014. Remote loading of preencapsulated drugs into stealth liposomes. Proceedings of the National Academy of Sciences of the United States of America. 111(6). doi:10.1073/pnas.1324135111.

Swiss Group for Clinical Cancer Research. 2021. Anti-EGFR-immunoliposomes Loaded With Doxorubicin in Patients With Advanced Triple Negative EGFR Positive Breast Cancer - A

Multicenter Single Arm Phase II Trial. clinicaltrials.gov Report No.: NCT02833766. [accessed 2023 Feb 17]. https://clinicaltrials.gov/ct2/show/NCT02833766.

Syed YY. 2020. Sacituzumab Govitecan: First Approval. Drugs. 80(10):1019–1025. doi:10.1007/s40265-020-01337-5.

SynerGene Therapeutics, Inc. 2017. A Phase I Study of Systemic Gene Therapy With SGT-94 in Patients With Solid Tumors. clinicaltrials.gov Report No.: NCT01517464. [accessed 2023 Feb 17]. https://clinicaltrials.gov/ct2/show/NCT01517464.

Tan Y, Tian T, Liu W, Zhu Z, J. Yang C. 2016. Advance in phage display technology for bioanalysis. Biotechnology Journal. 11(6):732–745. doi:10.1002/biot.201500458.

Tang H, Liu Y, Yu Z, Sun M, Lin L, Liu W, Han Q, Wei M, Jin Y. 2019. The Analysis of Key Factors Related to ADCs Structural Design. Front Pharmacol. 10:373. doi:10.3389/fphar.2019.00373.

Tang J, Li J, Zhu X, Yu Y, Chen D, Yuan L, Gu Z, Zhang X, Qi L, Gong Z, et al. 2016. Novel CD7-specific nanobody-based immunotoxins potently enhanced apoptosis of CD7-positive malignant cells. Oncotarget. 7(23):34070–34083. doi:10.18632/oncotarget.8710.

Teske E, Rutteman GR, Kirpenstein J, Hirschberger J. 2011. A randomized controlled study into the efficacy and toxicity of pegylated liposome encapsulated doxorubicin as an adjuvant therapy in dogs with splenic haemangiosarcoma. Vet Comp Oncol. 9(4):283–289. doi:10.1111/j.1476-5829.2011.00266.x.

Thandra KC, Barsouk Adam, Saginala K, Padala SA, Barsouk Alexander, Rawla P. 2021. Epidemiology of Non-Hodgkin's Lymphoma. Medical Sciences. 9(1):5. doi:10.3390/medsci9010005.

Thorpe PE, Ross WCJ, Cumber AJ, Hinson CA, Edwards DC, Davies AJS. 1978. Toxicity of diphtheria toxin for lymphoblastoid cells is increased by conjugation to antilymphocytic globulin. Nature. 271(5647):752–755. doi:10.1038/271752a0.

Thorson JS, Sievers EL, Ahlert J, Shepard E, Whitwam RE, Onwueme KC, Ruppen M. 2000. Understanding and exploiting nature's chemical arsenal: the past, present and future of calicheamicin research. Curr Pharm Des. 6(18):1841–1879. doi:10.2174/1381612003398564.

Tilly H, Morschhauser F, Sehn LH, Friedberg JW, Trněný M, Sharman JP, Herbaux C, Burke JM, Matasar M, Rai S, et al. 2022. Polatuzumab Vedotin in Previously Untreated Diffuse Large B-Cell Lymphoma. N Engl J Med. 386(4):351–363. doi:10.1056/NEJMoa2115304.

Tomley FM, Armstrong SJ, Mahy BW, Owen LN. 1983. Reverse transcriptase activity and particles of retroviral density in cultured canine lymphosarcoma supernatants. Br J Cancer. 47(2):277–284.

Tong JTW, Harris PWR, Brimble MA, Kavianinia I. 2021. An Insight into FDA Approved Antibody-Drug Conjugates for Cancer Therapy. Molecules. 26(19):5847. doi:10.3390/molecules26195847.

Torchilin VP, Klibanov AL, Huang L, O'Donnell S, Nossiff ND, Khaw BA. 1992. Targeted accumulation of polyethylene glycol-coated immunoliposomes in infarcted rabbit myocardium. FASEB J. 6(9):2716–2719. doi:10.1096/fasebj.6.9.1612296.

Torchilin VP. 2010. Passive and active drug targeting: drug delivery to tumors as an example. Handb Exp Pharmacol.(197):3–53. doi:10.1007/978-3-642-00477-3_1.

Vail DM, Kravis LD, Cooley AJ, Chun R, MacEwen EG. 1997. Preclinical trial of doxorubicin entrapped in sterically stabilized liposomes in dogs with spontaneously arising malignant tumors. Cancer Chemother Pharmacol. 39(5):410–416. doi:10.1007/s002800050591.

Vail DM, Michels GM, Khanna C, Selting KA, London CA, Veterinary Cooperative Oncology Group. 2010. Response evaluation criteria for peripheral nodal lymphoma in dogs (v1.0)--a Veterinary Cooperative Oncology Group (VCOG) consensus document. Vet Comp Oncol. 8(1):28–37. doi:10.1111/j.1476-5829.2009.00200.x.

Vail DM, Thamm DH, Liptak JM. 2019. Hematopoietic Tumors. Withrow and MacEwen's Small Animal Clinical Oncology.:688–772. doi:10.1016/B978-0-323-59496-7.00033-5.

Vaughan A, Johnson JL, Williams LE. 2007. Impact of chemotherapeutic dose intensity and hematologic toxicity on first remission duration in dogs with lymphoma treated with a chemoradiotherapy protocol. J Vet Intern Med. 21(6):1332–1339. doi:10.1892/06-197.1.

Veleva AN, Nepal DB, Frederick CB, Schwab J, Lockyer P, Yuan H, Lalush DS, Patterson C. 2011. Efficient In Vivo Selection of a Novel Tumor-Associated Peptide from a Phage Display Library. Molecules. 16(1):900–914. doi:10.3390/molecules16010900.

Vezzali E, Parodi AL, Marcato PS, Bettini G. 2010. Histopathologic classification of 171 cases of canine and feline non-Hodgkin lymphoma according to the WHO. Veterinary and Comparative Oncology. 8(1):38–49. doi:10.1111/j.1476-5829.2009.00201.x.

Villamil JA, Henry CJ, Hahn AW, Bryan JN, Tyler JW, Caldwell CW. 2009. Hormonal and Sex Impact on the Epidemiology of Canine Lymphoma. J Cancer Epidemiol. 2009:591753. doi:10.1155/2009/591753.

Waldmann TA. 2003. Immunotherapy: past, present and future. Nat Med. 9(3):269–277. doi:10.1038/nm0303-269.

Wang C, Gao W, Feng M, Pastan I, Ho M. 2017. Construction of an immunotoxin, HN3-mPE24, targeting glypican-3 for liver cancer therapy. Oncotarget. 8(20):32450–32460. doi:10.18632/oncotarget.10592.

Wang L, Amphlett G, Blättler WA, Lambert JM, Zhang W. 2005. Structural characterization of the maytansinoid-monoclonal antibody immunoconjugate, huN901-DM1, by mass spectrometry. Protein Sci. 14(9):2436–2446. doi:10.1110/ps.051478705.

Wang L, Li L, Young KH. 2020. New agents and regimens for diffuse large B cell lymphoma. J Hematol Oncol. 13(1):175. doi:10.1186/s13045-020-01011-z.

Ward RL, Clark MA, Lees J, Hawkins NJ. 1996. Retrieval of human antibodies from phage-display libraries using enzymatic cleavage. Journal of Immunological Methods. 189(1):73–82. doi:10.1016/0022-1759(95)00231-6.

Weber J, Peng H, Rader C. 2017. From rabbit antibody repertoires to rabbit monoclonal antibodies. Exp Mol Med. 49:305. doi:10.1038/emm.2017.23.

Weiner GJ. 2015. Building better monoclonal antibody-based therapeutics. Nat Rev Cancer. 15(6):361–370. doi:10.1038/nrc3930.

Weldon JE, Pastan I. 2011. A guide to taming a toxin--recombinant immunotoxins constructed from Pseudomonas exotoxin A for the treatment of cancer. FEBS J. 278(23):4683–4700. doi:10.1111/j.1742-4658.2011.08182.x.

Winter G, Griffiths AD, Hawkins RE, Hoogenboom HR. 1994. Making antibodies by phage display technology. Annu Rev Immunol. 12:433–455. doi:10.1146/annurev.iy.12.040194.002245.

Wu AM, Senter PD. 2005. Arming antibodies: prospects and challenges for immunoconjugates. Nature Biotechnology. 23(9):1137–1146. doi:10.1038/nbt1141.

Wu J, Liu Q, Lee RJ. 2006. A folate receptor-targeted liposomal formulation for paclitaxel. International Journal of Pharmaceutics. 316(1):148–153. doi:10.1016/j.ijpharm.2006.02.027.

Wu Y, Li Q, Kong Y, Wang Z, Lei C, Li J, Ding L, Wang C, Cheng Y, Wei Y, et al. 2022. A highly stable human single-domain antibody-drug conjugate exhibits superior penetration and treatment of solid tumors. Molecular Therapy. 30(8):2785–2799. doi:10.1016/j.ymthe.2022.04.013.

Xu WS, Parmigiani RB, Marks PA. 2007. Histone deacetylase inhibitors: molecular mechanisms of action. Oncogene. 26(37):5541–5552. doi:10.1038/sj.onc.1210620.

Yang F-Y, Wang H-E, Liu R-S, Teng M-C, Li J-J, Lu M, Wei M-C, Wong T-T. 2012. Pharmacokinetic Analysis of 111In-Labeled Liposomal Doxorubicin in Murine Glioblastoma after Blood-Brain Barrier Disruption by Focused Ultrasound. PLOS ONE. 7(9):e45468. doi:10.1371/journal.pone.0045468.

Ye P, Zhang W, Yang T, Lu Y, Lu M, Gai Y, Ma X, Xiang G. 2014. Folate receptor-targeted liposomes enhanced the antitumor potency of imatinib through the combination of active targeting and molecular targeting. International Journal of Nanomedicine. 9(1):2167–2178. doi:10.2147/IJN.S60178.

Yu Y, Li J, Zhu X, Tang X, Bao Y, Sun X, Huang Y, Tian F, Liu X, Yang L. 2017. Humanized CD7 nanobody-based immunotoxins exhibit promising anti-T-cell acute lymphoblastic leukemia potential. IJN. Volume 12:1969–1983. doi:10.2147/IJN.S127575.

Zandvliet M. 2016. Canine lymphoma: a review. Veterinary Quarterly. 36(2):76–104. doi:10.1080/01652176.2016.1152633.

Zhang Z, Yao J. 2012. Preparation of Irinotecan-Loaded Folate-Targeted Liposome for Tumor Targeting Delivery and Its Antitumor Activity. AAPS PharmSciTech. 13(3):802–810. doi:10.1208/s12249-012-9776-5.

Zhou Q, Stefano JE, Manning C, Kyazike J, Chen B, Gianolio DA, Park A, Busch M, Bird J, Zheng X, et al. 2014. Site-Specific Antibody–Drug Conjugation through Glycoengineering. Bioconjugate Chem. 25(3):510–520. doi:10.1021/bc400505q.

Zhou Q, Kyazike J, Boudanova E, Drzyzga M, Honey D, Cost R, Hou L, Duffieux F, Brun M-P, Park A, et al. 2021. Site-Specific Antibody Conjugation to Engineered Double Cysteine Residues. Pharmaceuticals. 14(7):672. doi:10.3390/ph14070672.

Zylberberg C, Matosevic S. 2016. Pharmaceutical liposomal drug delivery: a review of new delivery systems and a look at the regulatory landscape. Drug Delivery. 23(9):3319–3329. doi:10.1080/10717544.2016.1177136.